

Sustainable Nanotechnology: Life Cycle Thinking in Gold Nanoparticle Production and Recycling

Paramjeet Pati

Dissertation submitted to the faculty of the Virginia Polytechnic Institute and State University in partial fulfillment of the requirements for the degree of

Doctor of Philosophy  
In  
Civil Engineering

Peter J. Vikesland (Chair)  
Sean P. McGinnis (Co-chair)  
Linsey C. Marr  
Amy Pruden  
Scott H. Renneckar

August 4, 2015  
Blacksburg, Virginia

Keywords: nanotechnology, LCA, recycling, gold, sustainability

# Sustainable Nanotechnology: Life Cycle Thinking in Gold Nanoparticle Production and Recycling

Paramjeet Pati

## ABSTRACT

Nanotechnology has enormous potential to transform a wide variety of sectors, e.g., energy, electronics, healthcare, and environmental sustainability. At the same time, there are concerns about the health and environmental impacts of nanotechnology and uncertainties about the fate and toxicity of nanomaterials. Life cycle assessment (LCA), a quantitative framework for evaluating the cumulative environmental impacts associated with all stages of a material or process, has emerged as a decision-support tool for analyzing the environmental burdens of nanotechnology. The objective of this research was to combine laboratory techniques with LCA modeling to reduce the life cycle impacts of gold nanoparticle (AuNP) production. The LCA studies were focused on three aspects of AuNP synthesis: 1) the use of bio-based ('green') reducing agents; 2) the potential for recycling gold from nanomaterial waste; and, 3) the reduction of the life cycle impacts of AuNP production by conducting the synthesis at reduced temperature. The LCA models developed for AuNPs can inform future nanotechnology-focused LCA studies. Comparative LCA showed that in some cases, the environmental impacts associated with green synthesis methods may be worse than those of conventional synthesis approaches. The main driver of the environmental burdens associated with AuNP synthesis is the large embodied energy of gold, and so-called green synthesis methods do not offset those impacts. In addition, the reaction yield, which is seldom reported in the literature for green synthesis of nanomaterials, was found to greatly influence the life cycle impacts of AuNP synthesis. Gold from nanomaterial waste was successfully recovered by using host-guest inclusion complex formation facilitated by  $\alpha$ -cyclodextrin. This recycling approach involved room temperature conditions and did not require the toxic cyanide or mercury commonly used in the selective recovery of gold. A major advantage offered by this approach for selective gold recovery over conventional approaches is that the recovery does not involve the use of toxic cyanide or mercury. To reduce the energy footprint of citrate-reduced AuNP synthesis, the synthesis was conducted at room temperature. LCA models showed significant reduction in the energy footprint. The findings of this research can inform future LCAs of other nanomaterials.

## DEDICATION

“The greatest obstacle to discovering the shape of the earth, the continents, and the oceans was not ignorance but the illusion of knowledge.”

**-Daniel J. Boorstin**

“One accurate measurement is worth a thousand expert opinions.”

**-Grace Hopper**

*“I am recycled cells  
I learn to like myself  
More with each iteration*

*I’m an experiment  
Each trial is a test  
Constant recalibration”*

**-Sarah Daly (Iterations) Metaphorest**

## ACKNOWLEDGEMENTS

My Ph.D. journey is dotted with the kindness, support and generosity of several mentors, colleagues and friends.

I owe my deepest gratitude to Dr. Peter Vikesland, my primary advisor, for his guidance, support and encouragement throughout my graduate studies at Virginia Tech. **Pete:** Thanks for pushing me to strive for high-quality work and for constantly raising the bar. You trusted me when I had grave doubts about myself and my seemingly insane research plans, and you gave me ample room to experiment with ideas and to pursue my own intuitions and research interests. I owe much of my growth as an independent researcher to the fecund research environment, the generous resources and the numerous opportunities you provided.

Dr. Sean McGinnis, my co-advisor, played a major role in helping me develop my life cycle thinking muscles and LCA modeling skills. **Dr. McGinnis:** Our many conversations about sustainability helped me refine my ideas about the many meanings and interpretations of the deceptively simple word *sustainable*. Those conversations also helped me develop a systems approach for thinking about the wicked complexities at the intersection of environmental sustainability, economics and ethics. I also appreciate your insights and advice about the nuts and bolts of teaching.

I would also like to thank my committee members Dr. Linsey Marr, Dr. Amy Pruden and Dr. Scott Rennekar for their ideas and suggestions, which gave this dissertation its final shape. I will continue to incorporate your recommendations as I move my research projects forward.

This research would not have been possible without the facilities and resources provided by the Department of Civil and Environmental Engineering (CEE), the Virginia Tech Center for Sustainable Nanotechnology (VTSuN), and the Nanoscale Characterization and Fabrication Laboratory (NCFL). I am especially grateful to Chris Winkler for his many hours of help at the NCFL. **Chris:** Thank you for your boatloads of patience, as I tried my inexperienced, shaky, and over-caffeinated hands at transmission electron microscopy. You made the NCFL inviting and TEM less frightening – even fun. On behalf of all the eager researchers who show up at the NCFL with samples, clueless about TEM but reassured that they have Chris to guide them - I thank you.

I owe a huge thanks to Julie Petruska, for sharing with me her encyclopedic knowledge of lab protocols and safety practices, and for helping me find obscure chemicals, lab equipment, and glassware. **Julie:** Thanks to your help and suggestions in designing experiments that involved aqua regia, hydrobromic acid and other unsavory chemicals, I successfully managed to not poison, dissolve or vaporize myself even once.

During my Ph.D., I got to work with and to mentor two amazing undergraduate researchers – Jennifer Kim and Leejoo Wi. **Jennifer and Lee:** By working with you, I have learnt so much about mentoring. Your hard work has helped me move multiple research projects forward. I wish you both the very best.

I was fortunate to be a part of the Environmental Nanoscience and Technology (ENT) Lab. In my fellow ENTs, I found an incredibly supportive group of friends and colleagues with whom I shared so many conversations, rants, and laughs.

**Andrea:** Thank you for all the thought-provoking conversations and brainstorming sessions about the role of ethics in engineering, the state of academia, the cultural lenses through which we view life... Thanks also for the *aloo paranthas*, rice and *dal* that kept me nourished and alive when I fell ill before the defense. *Bahut bahut dhanyavaad.*

**Virginia:** Thanks to you too for the many conversations and for having me in your team during the softball matches. With my hand-eye coordination (or lack of thereof), I did not have much to contribute in terms skills. But I had a lot of fun even as I stayed perpetually confused about the rules. You bring a special joy, and you should know that everyone in the lab thinks we should clone you and paradrop your clones all over the globe – the world will be a happier place.

**Nina:** Thanks for your initiative and commitment to VTSuN. You play multiple roles for VTSuN - the engine, the steering wheel, the navigation system, and sometimes all three simultaneously – and make it all seem annoyingly effortless. I am in awe at your efficiency, creativity, vision and execution, and am always inspired (and very jealous). VTSuN is lucky to have you.

**Weinan:** You have taught me so much about lab work, designing experiments, and thinking through research problems. It was a pleasure working with you and learning from you, and is an honor to have you as my colleague and friend.

Andrea, Nina, Ron, Matt (Chan), Matt (Hull), Becky, Hossein, Haoran, Marjorie, Virginia, and Weinan – it was a pleasure.

My project with Sheldon Masters on the role of ethics in environmental engineering education was one of the highlights of my Ph.D. experience. **Sheldon:** I could not have done it without you. Thanks for the many meals, conversations and lightbulb-in-the-head-switching-on moments.

I would also like to express my gratitude to Matthew Grice in the Graduate School for reviewing this dissertation draft for formatting issues during one of his busiest times in the year.

No amount of graduate training could have prepared me to handle my arch nemeses that have always worried, flummoxed and frustrated me – HokieMart and paperwork. I am deeply indebted to Beth Lucas (EWR) for helping me to navigate the maze of paperwork, solve fiendishly knotty HokieMart-related puzzles, and for alerting me to upcoming deadlines that would have blindsided and derailed me. I am also very grateful to Leigh Anne Byrd (formerly in CEE, currently in Pamplin College) for all her help with scheduling my preliminary and final exams, and for expediting the paperwork related to those. **Beth and Leigh Anne:** Thank you so much for always coming through.

My acceptance into the CEE Ph.D. program at Virginia Tech was made possible by the education, mentorship and nurturing guidance I received from Dr. Masten at Michigan State University. **Dr. Masten:** The lessons I learnt from you at MSU have always stayed with me. Not only lessons in thinking, reasoning, writing, and scientific rigor, but also lessons in resilience, kindness and humility that I picked up from you when you not looking, but were busy being resilient, kind and humble. Forever grateful.

A lot has changed in these last five years. Thankfully, as I made my way through the ebb and flow of temporary setbacks and lucky breaks, what remained unchanged was the reassuringly constant love and unwavering support of my family and friends in India. See you all soon.

Virginia Tech has been very kind to me. The chemistry-heavy ENT lab is where I met my wife, Carol. (What can I say? We literally had chemistry.) I can't say enough about the support, encouragement and the tireless cheerleading that Carol provided (teamed up with Lucy, our cat-like dog). So I won't. **Carol and Lucy:** We did it!

param

August 17<sup>th</sup>, 2015

# TABLE OF CONTENTS

Chapter 1 -----	1
Introduction -----	1
ATTRIBUTIONS-----	4
COMPLEMENTARY WORK-----	5
REFERENCE-----	7
Chapter 2 -----	10
Life cycle assessment of “green” nanoparticle synthesis methods-----	10
ABSTRACT -----	10
INTRODUCTION-----	11
MATERIALS AND METHODS-----	13
RESULTS-----	19
DISCUSSION -----	23
SUMMARIES-----	31
ACKNOWLEDGEMENTS -----	32
REFERENCES-----	33
Chapter 3 -----	40
Waste Not Want Not: Life Cycle Implications of Gold Recovery and Recycling from Nanowaste -----	40
ABSTRACT -----	40
INTRODUCTION-----	41
MATERIALS AND METHODS-----	43
-----	45
RESULTS AND DISCUSSION-----	45
ACKNOWLEDGEMENTS -----	52
REFERENCES-----	53
Chapter 4 -----	57
Bleeding from a Thousand Paper Cuts: Avoiding Dissipative Losses of Critical Elements by Recycling Nanomaterial Waste Streams -----	57
ABSTRACT -----	57
INTRODUCTION-----	58
RECYCLING CRITICAL MATERIALS -----	64

CHALLENGES AND CONSIDERATIONS IN RECYCLING NANOWASTE -----	67
POLICY INNOVATIONS -----	71
REFERENCES -----	73
Chapter 5 -----	87
Room Temperature Seed Mediated Growth of Gold Nanoparticles: Mechanistic Investigations and Life Cycle Assessment -----	87
ABSTRACT -----	87
INTRODUCTION -----	88
MATERIALS AND METHODS -----	90
RESULTS AND DISCUSSION -----	95
CONCLUSIONS -----	113
ACKNOWLEDGEMENTS -----	113
REFERENCES -----	114
Chapter 6 -----	121
Summary -----	121
REFERENCES -----	125
Appendix A -----	127
Supplementary materials for Chapter 2 -----	127
Life cycle assessment of “green” nanoparticle synthesis methods -----	127
COMPARATIVE LCA OF GREEN AND CONVENTIONAL SYNTHESIS METHODS FOR AuNPs -----	131
AuNP SYNTHESIS USING SPENT COFFEE AND BANANA PEEL EXTRACT -----	133
Appendix B -----	135
Supplementary materials for Chapter 3 -----	135
Waste Not Want Not: Life Cycle Implications of Gold Recovery and Recycling from Nanowaste -----	135
UNCERTAINTY ANALYSIS IN LCA -----	139
Appendix C -----	144
Supplementary materials for Chapter 4 -----	144
Bleeding from a Thousand Paper Cuts: Avoiding Dissipative Losses of Critical Elements by Recycling Nanomaterial Waste Streams -----	144
REFERENCES -----	148
Appendix D -----	155
Supplementary materials for Chapter 5 -----	155



Seed Mediated Growth of Gold Nanoparticles at Room Temperature: Mechanistic Investigation and Life Cycle Assessment -----	155
FORMATION OF GOLD NANOPlates AND NANORODS -----	160
UNCERTAINTY ANALYSIS -----	166
REFERENCES -----	168
Appendix E -----	169
Reprint Permission Letters -----	169

## LIST OF FIGURES

<b>Figure 2-1</b> - Life cycle stages of gold nanoparticles. The LCA models include processes from raw material extraction through nanoparticle synthesis. The impacts of reducing agents are included in <b>Part I</b> of the study, but excluded in <b>Part II</b> . (Purification steps have been ignored in all models).....	15
<b>Figure 2-2</b> - Environmental impacts of 1 mg AuNP synthesis using three conventional reducing agents (sodium borohydride, citrate and hydrazine) and two plant-derived reducing agents (soybean seed and sugarbeet pulp). <b>(a)</b> Cumulative energy demands, <b>(b)</b> Climate change potential and metal depletion potential, <b>(c)</b> Freshwater ecotoxicity and Agricultural land occupation. The results include the impact of gold salt, reducing agent, deionized water, tap water, glassware cleaning solvent and energy required for stirring and heating ( <b>Part I</b> ). Error bars in represent 95% confidence intervals for the combined uncertainties in the chloroauric acid and citric acid models, energy use and uncertainties in the EcoInvent unit processes. ....	21
<b>Figure 2-3</b> - Cumulative energy demands of 16 different AuNP synthesis methods. The results include the impact of gold salt, deionized water, tap water, glassware cleaning solvent and energy required for stirring and heating. The impacts of the reducing agents were excluded in this calculation (Part II). Error bars in represent 95% confidence intervals for the combined uncertainties in the chloroauric acid and citric acid models, energy use and uncertainties in the EcoInvent unit processes.....	23
<b>Figure 3-1</b> – <b>A</b> (Left) Schematic of the gold recovery and recycling process. <b>B</b> (Right) The repeating unit involving one $[K(OH_2)_6]^+$ cation, one $[AuBr_4]^-$ anion and two CD molecules. An additional $[AuBr_4]^-$ anion is shown to illustrate how the unit is bound to the next unit through hydrogen bonding. ....	45
<b>Figure 3-2</b> - <b>A</b> (top) Schematic of LCA model for AuNP synthesis and recycling, <b>B</b> (bottom) - Life cycle impacts of 10%-, 50%-, 90%- and no-recycle scenarios. ....	49
<b>Figure 4-1</b> - Novel method for recycling indium from secondary sources such as display screens of used electronics and spent solar cells. Reprinted (adapted) with permission from Zimmermann, Y.-S.; Niewersch, C.; Lenz, M.; Kül, Z. Z.; Corvini, P. F. X.; Schäffer, A.; Wintgens, T., <i>Recycling of Indium From CIGS Photovoltaic Cells: Potential of Combining Acid-</i>	

*Resistant Nanofiltration with Liquid–Liquid Extraction*. Environmental Science & Technology 2014. Copyright (2014) American Chemical Society..... 64

**Figure 4-2** - Lab-on-chip devices as potential sources of recyclable critical materials. These devices may be discarded after a single use, and hence contribute to dissipative losses if they are not recycled. This figure shows a paper-based device for colorimetric detection of NADH in a microliter-scale sample in less than 4 min. The device consists of an upper plastic cover layer with a hole exposing the test zone, a wax-circled gold nanoparticle (AuNP) coated paper with a cotton absorbent layer. The detection time was < 4 minutes. Reprinted (adapted) with permission from Liang, P.; Yu, H.; Guntupalli, B.; Xiao, Y., *Paper-Based Device for Rapid Visualization of NADH Based on Dissolution of Gold Nanoparticles*. ACS Appl. Mater. Interfaces 2015.

Copyright (2015) American Chemical Society..... 66

**Figure 4-3** - Material values (y-axis), material mixing (x-axis) and recycling rates (areas of individual circles) for products. Larger circles imply higher recycling rates. Products with no circles are assumed to have recycling rates of zero. The material mixing, denoted by  $H$ , is the average number of binary separation steps required to extract any material from the mixture, and is higher for complex products. As seen from this figure, products with high recycling rates are clustered in the upper left corner, and the products with the very low recycling rates are in the lower right. This trend is particularly sharp for products with  $H > 0.5$ , where the recycling rates range from 66 to 96% in the upper left, and from 0 to 11% in the lower right. The authors of the original work marked the transition zone between them with a line labeled “apparent recycling boundary”. Similar modeling approaches for nano-enabled products can help in identifying the more recyclable products. This information can help in making decision when prioritizing the use of critical materials in specific products. Reprinted (adapted) with permission from Dahmus, J. B.; Gutowski, T. G., *What Gets Recycled: An Information Theory Based Model for Product Recycling*. Environmental Science & Technology 2007. Copyright (2007) American Chemical Society..... 69

**Figure 5-1** - TEM micrographs of seed nanoparticles synthesized by (A) pH controlled method and (B) w/o pH control; (C) TEM size distributions from both methods; (D) Normalized absorption spectra and hydrodynamic size distribution by intensity (Inset) of two seed

suspensions with (black lines) and w/o pH controlled (red lines) procedures. Suspensions were diluted 3× and 9× for UV-vis and DLS measurements, respectively. .... 96

**Figure 5-2** - TEM images of room temperature seed-mediated AuNPs of different sizes (aspect ratio): A) 24.0±6.1 nm (AR: 1.15±0.17), B) 37.1±4.6 nm (AR: 1.15±0.11), C) 46.0±4.6 nm (AR: 1.34±0.14), D) 57.6±4.5 nm (AR: 1.14±0.06), E) 69.6±11.8 nm (AR: 1.13±0.07), F) 82.5±14.0 nm (AR: 1.13±0.07), G) 92.4±11.4 nm (AR: 1.15±0.11), H) 100±11.4 nm (AR: 1.11±0.11), I) 111.0±8.3 nm (AR: 1.11±0.09). Inset: histograms of diameters as determined by NIH ImageJ software..... 101

**Figure 5-3** - Seed mediated growth for AuNPs (C) with mixed solution of HAuCl<sub>4</sub> (0.254 mM), Au seeds (5.35×10<sup>10</sup> particle/ml), and Na<sub>3</sub>Ctr (0.17 mM) at room temperature. TEM images of particles obtained at different growth times..... 103

**Scheme 5-1** - Reactions among Au seeds, citrate and AuCl<sub>4</sub><sup>-</sup> after initial mixing ..... 106

**Figure 5-4** - (A) Size distribution by intensity, (B) mean diameter of peak 1 (located in the range of 10 – 100 nm in A) and (C) UV-vis absorption spectra obtained at different time stages of seed growth synthesis of AuNPs..... 108

**Figure 5-5** – Time-dependent Au<sup>III</sup> and Au level in supernatant by UV-vis (squares) and ICP-MS (triangles). Inset: corresponding UV absorption spectra. Dash black line is the spectrum of the initial Au<sup>III</sup> solution. Prior to the UV-vis measurement, all AuNP suspensions were diluted 2× with deionized water. .... 110

**Figure 5-6** - SERS spectra of MGITC (20 nM) adsorbed on room temperature and 100 °C seed mediated AuNPs under 633 nm excitation. MGITC-AuNPs were prepared by quickly adding ≈1.5 μL of 14 μM MGITC solution to 1 mL AuNP suspension (5.4×10<sup>10</sup> particle/mL). .... 111

**Figure A 1** - The effect of different gold sources on the cumulative energy demand for citrate-reduced AuNPs. (RoW: Rest of the world. RoW-a: Rest of the world (precious metals from electronic scrap.) Error bars represent 95% confidence intervals for the combined uncertainties in the chloroauric acid and citric acid models, energy use and uncertainties in the EcoInvent unit processes. .... 132

**Figure A 2** - Heterodispersity in AuNP synthesis using plant-derived chemicals. **A)** and **B)** AuNPs prepared using tea **C)** AuNPs prepared using coffee and banana peel extract at 80° C. 133

**Figure B 1** - Powder X-ray diffraction of recovered gold. The highlighted peaks correspond to gold peaks. The unidentified peaks are presumably due to impurities. XRD measurements were performed on a Rigaku MiniFlex II instrument (Rigaku Americas, The Woodlands, TX, USA).  
..... 135

**Figure B 2** - UV-vis spectra of recovered gold chloride and chloroauric acid standard. All measurements were using a Cary 5000 UV-Vis-NIR spectrophotometer (Agilent, Santa Clara, CA). All samples were scanned in quartz cuvettes (Starna, model# 1-Q-10) with 10 mm path length..... 136

**Figure B 3** - Crystal structure information from SAED measurements confirms that the recovered precipitate is gold. TEM image shows highly aggregated citrate-reduced AuNPs produced by this approach. The existence of ‘throats’ between individual AuNPs provides evidence of AuNP coalescence. All TEM and SAED measurements were performed on a JEOL 2100 (JEOL, Peabody, MA, USA) ..... 137

**Figure B 4** - (Left) The overlapping error bars for 95% confidence intervals should not be interpreted as statistically insignificant differences, because these LCA models involve correlated uncertainties. (Right) The majority of the Monte Carlo simulations showed that 90%-recycle scenario has lower impact than no-recycle scenario in terms of metal depletion, toxicity and eutrophication..... 140

**Figure B 5** - Uncertainty analysis for 90% recycle scenario vs. no-recycle scenario..... 141

**Figure B 6** - Uncertainty analysis for 50% recycle scenario vs. no-recycle scenario..... 142

**Figure B 7** - Uncertainty analysis for 10% recycle scenario vs. no-recycle scenario..... 143

**Figure D 1** - Energy flows (cumulative energy demand) of 1 mg AuNP synthesis at 100 °C. (Flow lines show individual contributions of different inputs.) ..... 157

**Figure D 2** - Energy flows (cumulative energy demand) for 1 mg AuNP synthesis at room temperature. (Flow lines show individual contributions of different inputs.) ..... 158

**Figure D 3** - pH value at room temperature against the concentration ratio of Na<sub>3</sub>Ctr and Au<sup>III</sup> for a fixed 1 mM Au<sup>III</sup> concentration..... 159

**Figure D 4** - The standard reduction potential ( $E^0$ ) for  $Au^{III} \rightarrow Au^0$  for the gold solution species  $AuCl_x(OH)_{4-x}$  ( $x=0-4$ ).  $E^0$  was calculated using the Nernst equation of  $\Delta G^0 = -nFE^0$ , where Gibbs free energy ( $\Delta G^0$ ) of  $AuCl_x(OH)_{4-x}$  ( $x=0-4$ ) was reported by Machesky et al.<sup>1</sup> ..... 160

**Figure D 5** - Seed mediated growth with mixed solution of  $\text{HAuCl}_4$  (0.254 mM), Au seeds ( $3.3 \times 10^9$  particles/mL), and  $\text{Na}_3\text{Ctr}$  (0.17 mM) at room temperature. (A) optical images, (B) absorption spectra and (C) hydrodynamic diameter of growth solutions in different times. .... 161

**Figure D 6** - (A) Size distributions by intensity (DLS) and (B) absorption spectra of a set of seeded growth prepared samples with increased size and shifted SPR. .... 162

**Figure D 7** - UV absorption spectra of  $[\text{AuCl}_4]^-$  (0.127mM, black solid line),  $\text{Na}_3\text{Ctr}$  (0.088 mM, red line) and the mixture of same volume of  $[\text{AuCl}_4]^-$  and  $\text{Na}_3\text{Ctr}$  with final concentrations of 0.127 mM and 0.088 mM respectively (green line). Blue line is expected spectrum for the mixture based upon the combination of the spectra for  $[\text{AuCl}_4]^-$  and  $\text{Na}_3\text{Ctr}$ . .... 163

**Figure D 8** - Comparison of UV absorbance between supernatant from a completely reacted Au solution and a simulation mixture of HCl and NaCl. The final concentrations of HCl and NaCl are based on the stoichiometry of equation 11..... 164

**Figure D 9** - TEM images of seed mediated 46 nm AuNPs produced at room temperature (A) and at 100 °C (B)..... 165

**Figure D 10**- Cumulative energy demand (CED), marine eutrophication and water depletion for 1 mg of 46 nm AuNP synthesis at 100 °C vs. room temperature. AuNP synthesis at room temperature has lower environmental impacts than synthesis under boiling conditions..... 165

**Figure D 11** - The percentage of 1000 Monte Carlo simulations showing that across all impact categories, most simulations show that the environmental impacts for room temperature AuNP synthesis are lower than those for synthesis under boiling conditions. .... 167

## LIST OF TABLES

<b>Table 2-1-</b> Environmental impacts of three conventional reducing agents (sodium borohydride, citrate and hydrazine) and two bio-based reducing agents (soybean seed and sugarbeet pulp). The environmental impacts of unit mass of conventional reducing agents are greater than those of the plant-derived reducing agents. The impacts of soybean seeds per mg AuNP, however, are greater than those of the conventional reducing agents. These results highlight that “green” chemicals can have substantial environmental impacts that may be comparable or even worse than the impacts of conventional reducing agents.....	20
<b>Table 2-2</b> - Challenges in green nano-synthesis and in conducting LCAs for nanotechnologies	28
<b>Table 5-1</b> - Sizes, concentrations, zeta-potentials, and optical properties of seeded AuNPs.....	100
<b>Table 5-2</b> - Cumulative energy demand (CED) for AuNP synthesis at room temperature vs. boiling conditions. The CEDs for AuNP syntheses at room temperature and under boiling conditions are 1.25 MJ and 1.54 MJ respectively.....	112
<b>Table A 1</b> - Environmental impacts across all impact categories for 1 mg AuNP synthesized using borohydride, citrate, hydrazine, soybean seeds and sugarbeet pulp. (The errors show 95% interval. The source of the error in each case is the combined effect of the uncertainty due to energy use and gold salt (chloroauric acid) model.).....	128
<b>Table A 2</b> - AuNP morphology, reaction conditions, CEDs for the different synthesis methods (assuming 100% reaction yield).....	129
<b>Table A 3</b> - AuNP reaction conditions, Freshwater Ecotoxicity and Agricultural Land Occupation for the different synthesis methods.....	130
<b>Table B 1</b> - Life cycle inventories for custom defined chemicals AuNP synthesis and recovery steps.....	138
<b>Table B 2</b> - Life cycle inventories for AuNP synthesis steps.....	138
<b>Table B 3</b> - Life cycle inventories for AuNP recovery steps to treat 1 mg of gold nanowaste..	139
<b>Table C 1</b> - Recycling approaches for critical materials.....	144
<b>Table D 1</b> - Volumes (V) of nanopure water, HAuCl <sub>4</sub> , seed suspension, and trisodium citrate (Ctr) used in the seed-mediated synthesis of the different sized nanoparticles. ....	155
<b>Table D 2</b> - Inputs for 1 mg of the following custom-defined processes in SimaPro: a) Chloroauric acid, b) Trosodium citrate, and c) AuNP ‘seeds’ .....	156

**Table D 3** - Inputs for 1 mg of seed-mediated, citrate reduced AuNPs synthesized under boiling conditions ..... 157

**Table D 4** - Inputs for 1 mg of seed-mediated, citrate reduced AuNPs synthesized at room temperature ..... 158

**Table D 5** - The percentage of nanoplates and nanorods in AuNP sample D – I. .... 161



# Chapter 1

## Introduction

In recent years, sustainability has been much discussed by the media, in scientific communities, by businesses and the general public. The quest for increased energy efficiency and sustainable use of resources has led to the emergence of promising new developments, one of which is nanotechnology. The novel properties of nanomaterials have the potential to usher in transformative technological revolutions. At the same time, there are concerns about the health and environmental impacts of nanotechnology. Many promising nanotechnologies rely on the use of high-value, critical raw materials and often involve energy-intensive production processes, and the use of toxic chemicals. Life cycle assessment (LCA) has emerged as a potential decision-support tool for analyzing the sustainability of nanotechnology and evaluating the uncertainties therein.

LCA is a methodological framework for environmental assessment. When used in its broadest scope, LCA helps in estimating the cradle-to-grave environmental impacts attributable to the life cycle of a product or process. Environmental assessment within an LCA framework is done by defining a system boundary for a product or a process, and defining a baseline (referred to as *functional unit*) for comparison. For example, in an LCA study for determining whether glass bottles or aluminum cans would serve as the better packaging material for beverages, an appropriate functional unit may be liters of the packaged beverage. After defining the system boundary and functional unit, an inventory of material and energy flows (inputs), as well as emissions and waste flows (outputs) relevant to the defined system are compiled. All input and output flows are calculated in relation to the functional unit. Next, the inventory results

are aggregated and translated into more environmentally relevant information through life cycle impact assessment. For example, CO<sub>2</sub> emissions are translated into global warming potential. With regards to impact assessment, it is important to note that converting material and energy flows (e.g., kg of CO<sub>2</sub> emitted or MJ of electrical energy consumed) into relevant environmental impacts (global warming potential) necessarily involves some weighting. A variety of impacts such as climate change, stratospheric ozone depletion, smog formation, ecotoxicity, eutrophication, acidification, resource depletion, water footprint, land use, etc. are considered under life cycle impacts assessment. LCA has been used in various applications and at a wide range of scales, (e.g., estimating product footprints in the pulp and paper,<sup>1-3</sup> dairy,<sup>4,5</sup> meat,<sup>6</sup> polymer,<sup>7</sup> metal<sup>8</sup> and biofuel<sup>9-11</sup> industries; comparing the environmental impacts of recycling vs. incineration,<sup>12</sup> and; estimating the global warming potentials of using hand dryers vs. paper towels in restrooms.<sup>13</sup> In addition to environmental impacts, LCA framework can also be used to analyze economic<sup>14</sup> and social<sup>15,16</sup> aspects of technologies, regulations and policies.

In recent years, LCA has also been used to estimate the environmental impacts of nanomaterial production, e.g., carbon nanotubes (CNTs),<sup>17</sup> starch nanocrystals,<sup>18</sup> nanocellulose,<sup>19</sup> and silver nanoparticles.<sup>20</sup> Several studies have explored the life cycle considerations in the development of novel nano-enabled products (e.g., clothing<sup>21,22</sup> and bandages<sup>23</sup> embedded with silver nanoparticles; lithium-ion batteries containing CNTs;<sup>24</sup> and, thin film solar cells employing nano-crystalline silicon materials).<sup>25</sup> Furthermore, life cycle approaches have also been applied to study the end-of-life treatment of nanomaterials.<sup>26-28</sup>

The research presented in this dissertation combines LCA modeling with laboratory techniques to explore the life cycle impacts of gold nanoparticle (AuNP) production and recycling. Three key aspects of gold nanoparticle (AuNP) synthesis are analyzed from a life

cycle perspective: 1) the use of bio-based ('green') reducing agents; 2) the potential for recycling gold from nanomaterial waste; and, 3) the reduction of the life cycle impacts of AuNP production by conducting the synthesis at reduced temperature.

Chapter 2 is focused on the LCA of 'green' synthesis approaches for AuNPs. Several bio-based chemicals (e.g., extracts from plant leaves) can be used to reduce Au(III) to Au(0) during AuNP synthesis. These chemicals are milder and less toxic compared to commonly used conventional ('synthetic') reducing agents (e.g., hydrazine or sodium borohydride). Synthesis methods that employ bio-based chemicals as substitutes for harsher chemicals are often labeled as *green*, and are considered to be more sustainable than conventional synthesis approaches. However, the environmental impacts of the purportedly green methods have not been studied from a life cycle perspective. A comparative, cradle-to-gate LCA of green vs. conventional methods for AuNP synthesis is presented in Chapter 2. (The results of this study were published in *Environmental Engineering Science*.)<sup>29</sup>

The results reported in Chapter 2 showed that a substantial portion of the life cycle impacts of AuNP synthesis are associated with the mining and refining of gold, and substituting toxic reducing agents (e.g., hydrazine) with bio-based alternatives does not reduce those environmental impacts. A major hurdle in mitigating the environmental impacts of AuNP synthesis is tied with the use of gold. One potential solution is to recycle gold from nanomaterial waste streams. In Chapter 3, a method for selective recovery and recycling of gold from AuNP waste is presented along with the LCA of the overall process. A manuscript based on this chapter is currently in preparation.

In addition to gold, several critical materials (e.g., platinum group elements and rare earth elements) are integral to the development of next-generation nanotechnologies. These critical

materials are being increasingly used in a variety of nano-enabled applications, e.g., lab-on-chip technologies, point-of-care devices and wearable electronics. Without robust strategies to recover and recycle these resource-limited critical materials from nanomaterial waste streams and discarded nano-enabled products, dissipative losses from their material flow cycles can pose supply risks in the future. Chapter 4 reviews the challenges and opportunities regarding the recycling of critical materials in nanowaste. A manuscript based on this chapter is currently in preparation.

A third consideration in life cycle issues with AuNP synthesis, besides bio-based reagents (Chapter 2) and recycling (Chapter 3 and 4), is energy use. One of the most commonly used AuNP synthesis methods involves the reduction of Au(III) to Au(0) using citrate under boiling conditions. In Chapter 5, the feasibility of conducting the same synthesis at room temperature and the potential reductions in life cycle impact are explored. This chapter has been accepted for publication in *Environmental Science: Nano*.

The key findings from the studies reported in this dissertation are summarized in Chapter 6. Additional discussions in Chapter 6 include: limitations in applying the methodology of LCA to nanotechnology; challenges in choosing a functional unit for comparing nanomaterial production and the performance of nano-enabled products; uncertainties in the estimates of nanomaterial production, release and exposure; and lack of nano-specific toxicity information in the life cycle impact assessment of nanotechnologies.

## **ATTRIBUTIONS**

**Dr. Peter Vikesland** is the primary research advisor for my research projects and chair of the Ph.D. dissertation committee. Dr. Vikesland provided guidance for experimental design and data interpretation related to laboratory studies on AuNP synthesis and gold recycling. Dr.

Vikesland also provided valuable suggestions and feedback in the preparation of the manuscripts presented in the aforementioned chapters.

**Dr. Sean McGinnis** is the co-advisor for this research and co-chair of the Ph.D. dissertation committee. Dr. McGinnis provided valuable guidance in developing and trouble-shooting LCA models, and in preparing the manuscripts presented in Chapters 2, 3 and 4.

**Dr. Weinan Leng** is the first author for the manuscript on AuNP synthesis at room temperature (Chapter 5). Dr. Leng designed and conducted all the experiments and developed much of the original draft for that manuscript. I developed the LCA models and assisted Dr. Leng in writing and editing the final manuscript for submission. During the peer-review process, I helped in responding to the reviewers' comments. I also assisted in the data interpretation, provided additional supplementary material from the LCA models for the manuscript and helped in re-drafting substantial portions of the manuscript for resubmission.

## COMPLEMENTARY WORK

In addition to the manuscripts included in this dissertation, the results of these research projects were presented at the conferences listed below. An additional presentation on AuNP recycling (Chapter 3) and critical material sustainability (Chapter 4) will be presented at the American Chemical Society's National Conference in August 2015.

- **Pati, P.**, Vikesland, P.J., and McGinnis, S., Precious metal and rare earth element recovery from waste streams: Technical developments and life cycle considerations of recovering and recycling gold from nanomaterial waste streams American Chemical Society Fall Meeting, August 16-20, 2015, Boston, MA (*Abstract accepted*)
- **Pati, P.**, Vikesland, P.J., and McGinnis, S., Sustainable nanotechnology: Life cycle considerations in green synthesis of nanomaterials and precious metal recovery from nanomaterial waste streams, Association of Environmental Engineering and Science Professors (AEESP), June 13-16, 2015, New Haven, CT

- **Pati, P.**, Vikesland, P.J., and McGinnis, S., Waste Not Want Not: Life Cycle Implications for Precious Metal Recovery from Nanowaste, International Symposium on Sustainable Systems and Technology (ISSST), May 18-20, 2015, Dearborn, MI
- **Pati, P.**, Vikesland, P.J., and McGinnis, S., Life Cycle Assessment of Cerium Dioxide Nanoparticle-based Fuel Additives, Sustainable Nanotechnology Organization Conference, November 2-4, 2014, Boston, MA
- **Pati, P.**, Vikesland, P.J., and McGinnis, S., Precious Metal Recovery from Nanowaste for Sustainable Nanotechnology: Current Challenges and Life Cycle Considerations, Sustainable Nanotechnology Organization Conference, November 2-4, 2014, Boston, MA
- **Pati, P.**, Vikesland, P.J., and McGinnis, S., Life Cycle Assessment of Nanotechnology: Environmental Impacts of Nanomaterial Production and Precious Metal Recovery from Nanowaste, American Chemical Society Fall Meeting, August 10-14, 2014, San Francisco, CA
- **Pati, P.**, Vikesland, P.J., and McGinnis, S., Incorporating Life Cycle Thinking into Green Synthesis of Nanomaterials American Chemical Society Spring Meeting, March 16-20, 2014, Dallas, TX
- **Pati, P.**, Vikesland, P.J., and McGinnis, S., Assessing 'Green' Synthesis Processes for Nanoparticle Synthesis through a Life Cycle Perspective, Sustainable Nanotechnology Organization Conference, November 3-5, 2013, Santa Barbara, CA
- **Pati, P.**, Vikesland, P.J., and McGinnis, S., Evaluating 'Green' Synthesis Processes for Nanoparticles through a Life Cycle Perspective, American Centre for Life Cycle Assessment (ACLCA), October 1-3, 2013, Orlando, FL (Poster presentation)
- **Pati, P.**, Vikesland, P.J., and McGinnis, S., Gate-to-Gate Life Cycle Assessment of Gold Nanoparticle Synthesis Process, Sustainable Nanotechnology Organization Conference, November 4-6, 2012, Arlington, VA

## REFERENCE

1. Lopes, E.; Dias, A.; Arroja, L.; Capela, I.; Pereira, F., Application of Life Cycle Assessment to the Portuguese Pulp and Paper Industry. *Journal of Cleaner Production* **2003**, *11*, (1), 51-59.
2. Muñoz, I.; Rieradevall, J.; Torrades, F.; Peral, J.; Domènech, X., Environmental assessment of different advanced oxidation processes applied to a bleaching Kraft mill effluent. *Chemosphere* **2006**, *62*, (1), 9-16.
3. González-García, S.; Hospido, A.; Moreira, M. T.; Romero, J.; Feijoo, G., Environmental Impact Assessment of Total Chlorine Free Pulp from Eucalyptus Globulus in Spain. *Journal of Cleaner Production* **2009**, *17*, (11), 1010-1016.
4. Eide, M., Life Cycle Assessment (LCA) of Industrial Milk Production. *The International Journal of Life Cycle Assessment* **2002**, *7*, (2), 115-126.
5. Thomassen, M. A.; van Calker, K. J.; Smits, M. C. J.; Iepema, G. L.; de Boer, I. J. M., Life Cycle Assessment of Conventional and Organic Milk Production in the Netherlands. *Agricultural Systems* **2008**, *96*, (1-3), 95-107.
6. Cederberg, C.; Stadig, M., System Expansion and Allocation in Life Cycle Assessment of Milk and Beef Production. *The International Journal of Life Cycle Assessment* **2003**, *8*, (6), 350-356.
7. Vink, E. T. H.; Rábago, K. R.; Glassner, D. A.; Gruber, P. R., Applications of Life Cycle Assessment to Natureworks™ Polylactide (PLA) Production. *Polymer Degradation and Stability* **2003**, *80*, (3), 403-419.
8. Eckelman, M. J., Facility-level energy and greenhouse gas life-cycle assessment of the global nickel industry. *Resources, Conservation and Recycling* **2010**, *54*, (4), 256-266.
9. Tilman, D.; Hill, J.; Lehman, C., Carbon-Negative Biofuels from Low-Input High-Diversity Grassland Biomass. *Science* **2006**, *314*, (5805), 1598-1600.
10. Sander, K.; Murthy, G. S., Life Cycle Analysis of Algae Biodiesel. *Int. J. Life Cycle Assess.* **2010**, *15*, (7), 704-714.
11. Collet, P.; Helias, A.; Lardon, L.; Ras, M.; Goy, R.-A.; Steyer, J.-P., Life-Cycle Assessment of Microalgae Culture Coupled to Biogas Production. *Bioresource Technology* **2011**, *102*, (1), 207-214.
12. Finnveden, G.; Ekvall, T., Life-cycle assessment as a decision-support tool - the case of recycling versus incineration of paper. *Resour. Conserv. Recycl.* **1998**, *24*, (3-4), 235-256.
13. Greener Dryer Better: LCA of Hand Dryers vs. Paper Towels. <http://www.treehugger.com/clean-technology/greener-dryer-better-lca-of-hand-dryers-vs-paper-towels.html>

14. Weidema, B. P., The integration of economic and social aspects in life cycle impact assessment. *The International Journal of Life Cycle Assessment* **2006**, *11*, 89-96.
15. Aparcana, S.; Salhofer, S., Application of a methodology for the social life cycle assessment of recycling systems in low income countries: three Peruvian case studies. *The International Journal of Life Cycle Assessment* **2013**, *18*, (5), 1116-1128.
16. Aparcana, S.; Salhofer, S., Development of a social impact assessment methodology for recycling systems in low-income countries. *The International Journal of Life Cycle Assessment* **2013**, *18*, (5), 1106-1115.
17. Healy, M. L.; Dahlben, L. J.; Isaacs, J. A., Environmental Assessment of Single-Walled Carbon Nanotube Processes. *Journal of Industrial Ecology* **2008**, *12*, (3), 376-393.
18. LeCorre, D.; Hohenthal, C.; Dufresne, A.; Bras, J., Comparative Sustainability Assessment of Starch Nanocrystals. *J Polym Environ* **2013**, *21*, (1), 71-80.
19. Li, Q.; McGinnis, S.; Sydnor, C.; Wong, A.; Renneckar, S., Nanocellulose Life Cycle Assessment. *ACS Sustainable Chem. Eng.* **2013**, *1*, (8), 919-928.
20. Pourzahedi, L.; Eckelman, M. J., Comparative Life Cycle Assessment of Silver Nanoparticle Synthesis Routes. *Environ. Sci.: Nano* **2015**.
21. Meyer, D.; Curran, M.; Gonzalez, M., An examination of silver nanoparticles in socks using screening-level life cycle assessment. *Journal of Nanoparticle Research* **2011**, *13*, (1), 147-156.
22. Walser, T.; Demou, E.; Lang, D. J.; Hellweg, S., Prospective Environmental Life Cycle Assessment of Nanosilver T-Shirts. *Environmental Science & Technology* **2011**, *45*, (10), 4570-4578.
23. Pourzahedi, L.; Eckelman, M. J., Environmental Life Cycle Assessment of Nanosilver-Enabled Bandages. *Environmental Science & Technology* **2014**.
24. Kushnir, D.; Sandén, B. A., Multi-Level Energy Analysis of Emerging Technologies: A Case Study in New Materials for Lithium Ion Batteries. *Journal of Cleaner Production* **2011**, *19*, (13), 1405-1416.
25. Weil, M., Consideration of the Precautionary Principle – the Responsible Development of Nano Technologies. In *Glocalized Solutions for Sustainability in Manufacturing*, Hesselbach, J.; Herrmann, C., Eds. Springer Berlin Heidelberg: 2011; pp 185-188.
26. Olapiriyakul, S.; Caudill, R. J., Thermodynamic Analysis to Assess the Environmental Impact of End-of-life Recovery Processing for Nanotechnology Products. *Environmental Science & Technology* **2009**, *43*, (21), 8140-8146.
27. Walser, T.; Limbach, L. K.; Brogioli, R.; Erismann, E.; Flamigni, L.; Hattendorf, B.; Juchli, M.; Krumeich, F.; Ludwig, C.; Prikopsky, K.; Rossier, M.; Saner, D.; Sigg, A.; Hellweg, S.; Günther, D.;



Stark, W. J., Persistence of engineered nanoparticles in a municipal solid-waste incineration plant. *Nature Nanotechnology* **2012**, 7, (8), 520-524.

28. Walser, T.; Gottschalk, F., Stochastic fate analysis of engineered nanoparticles in incineration plants. *Journal of Cleaner Production* **2014**, 80, 241-251.

29. Pati, P.; McGinnis, S.; Vikesland, P. J., Life Cycle Assessment of “Green” Nanoparticle Synthesis Methods. *Environmental Engineering Science* **2014**.

## Chapter 2

### Life cycle assessment of “green” nanoparticle synthesis methods

*Paramjeet Pati<sup>1,2,3</sup>, Sean McGinnis<sup>2,4</sup>, and Peter J. Vikesland<sup>1,2,3</sup>\**

<sup>1</sup>Department of Civil and Environmental Engineering, Virginia Tech, Blacksburg, Virginia

<sup>2</sup>Virginia Tech Institute of Critical Technology and Applied Science (ICTAS) Sustainable Nanotechnology Center (VTSuN), Blacksburg, Virginia

<sup>3</sup>Center for the Environmental Implications of Nanotechnology (CEINT), Duke University, Durham, North Carolina

<sup>4</sup>Department of Materials Science and Engineering and Virginia Tech Green Engineering Program, Virginia Tech, Blacksburg, Virginia

\*Corresponding author. Phone: (540) 231-3568, Email: [pvikes@vt.edu](mailto:pvikes@vt.edu)

***Environmental Engineering Science* 31.7 (2014): 410-420**

**DOI: 10.1089/ees.2013.0444.**

Reprinted (adapted) with permission from Mary Ann Liebert, Inc.

#### **ABSTRACT**

In recent years, ‘green’ nanomaterial synthesis methods that rely upon natural alternatives to industrial chemicals have been increasingly studied. Although the feasibility of synthesizing nanoparticles using phytochemicals, carbohydrates, and other biomolecules is well established, the environmental burdens of these synthesis processes have not been critically evaluated from a life cycle perspective. The environmental impacts of nanotechnologies may potentially be reduced by applying green chemistry principles. However, doing so without evaluating the life cycle impacts of the processes may be misleading; merely replacing a conventional chemical with a natural or renewable alternative may not reduce environmental impacts. To explore this

issue, we conducted a comparative, screening-level life cycle assessment (LCA) of gold nanoparticle (AuNP) synthesis using three conventional reducing agents and thirteen green reducing agents. We found that a substantial portion of the energy footprint of AuNP synthesis is due to the embodied energy in gold. As a result of this embodied energy, even green AuNP synthesis methods have significant environmental impacts that are highly dependent upon reaction times and yields. Our results show that LCA can elucidate the different environmental impacts of AuNP synthesis processes, help in choosing processes with reduced life cycle impacts and directing decisions for future research and data collection efforts. We also discuss some challenges in conducting LCAs for nanotechnologies and highlight some major gaps in the green nano-synthesis literature that limit the comparability of reported green synthesis protocols. This research shows that screening-level LCAs can direct nanotechnology research towards more environmentally sustainable paths.

**Keywords:** green synthesis, life cycle assessment, sustainability, nanotechnology, gold, LCA, AuNP

## **INTRODUCTION**

In recent years, the scientific community has focused on the application of nanotechnology for sustainable development<sup>1</sup>, energy efficiency<sup>2,3</sup> and effective pollution control and reduction through the development of novel nano-based environmental monitoring<sup>4-6</sup>, environmental remediation<sup>7-9</sup> and numerous other applications. However, the potential for nanotechnology to address many systemic issues related to global sustainability should be weighed against uncertainties related to the environmental and health effects of nanomaterials<sup>10</sup>. Nanomaterial

syntheses often rely upon multi-step, multi-solvent, manufacturing methods with inherent sustainability challenges due to their reliance on limited resource materials. Moreover, energy intensive manufacturing processes<sup>11,12</sup> and the potentially hazardous impacts of the nanomaterials themselves<sup>13,14</sup> lead to additional questions about the environmental impacts of these processes<sup>15</sup>.

Gold nanoparticles (AuNPs) are one class of nanomaterial that is receiving significant attention for their potential capacity to address many societal problems<sup>16,17</sup>. A substantial challenge to the sustainable development of gold-based nanotechnologies is the limited supply of the raw material. Gold ore grades have declined over the last decade<sup>19</sup>, the cost of extracting gold has steadily increased<sup>20</sup>, and there are concerns about having surpassed peak gold<sup>21</sup>. The current demand of gold for nanotechnology-based application may be small compared to other demands (e.g., jewelry<sup>22</sup>). Nonetheless, given the rapid growth of the nanotechnology industry<sup>23,24</sup>, the market share of gold-based nanotechnologies can be expected to increase. It is therefore important to investigate the efficiencies of the AuNP manufacturing processes that use gold as an input.

The application of green chemistry principles may potentially help in reducing the environmental impacts associated with nanotechnology. A common approach towards green nanotechnology is to use phytochemicals from plant extracts, carbohydrates, and biomolecules as reducing and capping agents for nanoparticle synthesis (**Table 2-1**). Throughout this paper we use the term '*green*' to refer to the nanoparticle synthesis methods that use plant-derived or bio-based chemicals. When making the case for plant-derived reducing agents, the intuitive argument often employed is that natural reductants are less toxic than synthetic ones. However, simply replacing an industrial chemical with a renewable source may not mitigate the environmental

impacts of products that have high embodied energy (e.g., precious metal nanoparticles) or those that require energy-intensive production processes. The production of plant-derived reducing agents will require use of fertilizers, pesticides, freshwater, fossil fuels, etc., which can have significant environmental impacts<sup>25,26</sup>. It is therefore prudent to weigh desirable qualities of renewable chemicals (e.g., increased biodegradability, non-toxicity etc.) against these upstream impacts, when proposing green nano-synthesis approaches in place of conventional ones. Life cycle assessment (LCA) is one such quantitative framework that can be used for evaluating the cumulative environmental impacts associated with all stages of a material – from the extraction of raw materials through the end-of-life<sup>27</sup>.

In this paper, we present a screening-level, comparative LCA of thirteen previously reported green methods for AuNP synthesis<sup>28-39</sup> and three conventional methods that use citrate, sodium borohydride and hydrazine as reductants<sup>40-43</sup>. We also discuss some specific data gaps in extant green nano-synthesis studies. Lastly, we highlight some of the broader challenges in conducting LCAs for nanotechnologies.

## **MATERIALS AND METHODS**

We constructed cradle-to-gate AuNP synthesis models using SimaPro (8.0.1) for comparative LCA of three conventional AuNP synthesis methods and thirteen green synthesis methods previously described in the peer-reviewed literature. The functional unit used in each of these LCA models is 1 mg of AuNP synthesized by each method. These LCA models include processes from raw material extraction and processing through the synthesis of the nanoparticles (as shown by the dotted box in **Figure 2-1**). In this study, as discussed later, purification steps (centrifugation, dialysis, etc.) were excluded. For the purpose of this study, we did not model

recycling streams since it is not common practice to capture AuNP waste streams in laboratory scale synthesis. Waste products from the syntheses were not included in these models since disposal practices vary widely by lab and location.

AuNPs from citrate reduction (cit-AuNPs) were prepared in the laboratory. The material and energy inventory for the citrate-based synthesis was characterized using measured data from our laboratory. These laboratory measurements allow assumptions to be made for the other synthesis models for which some key inventory information was not available. Cit-AuNPs of  $\approx 15$  nm diameter were prepared by modifying previously reported synthesis procedures<sup>40,41</sup>. In brief, 10 mL of 38.8 mM trisodium citrate (Sigma-Aldrich) was added to 100 mL of 1 mM chloroauric acid (Sigma-Aldrich) at 100 °C. AuNPs were formed within 1 minute. Boiling was stopped after 5 minutes and the reaction solution was stirred for an additional 10 minutes. The AuNP suspension was then filtered through a 0.22  $\mu\text{m}$  polytetrafluoroethylene filter and centrifuged in 15 mL Amicon Ultracell-30K centrifuge filters at  $5000 \times g$  for 10 minutes (Thermo Scientific Sorvall Legend X1R). The concentration of remnant dissolved gold ion in the filtrate was determined by ICP-MS using standard method 3125-B<sup>45</sup> as discussed elsewhere<sup>46</sup>. All experiments were performed in triplicate. The energy required for stirring and heating during cit-AuNP synthesis was measured using a Watts Up energy meter (Model: PRO).

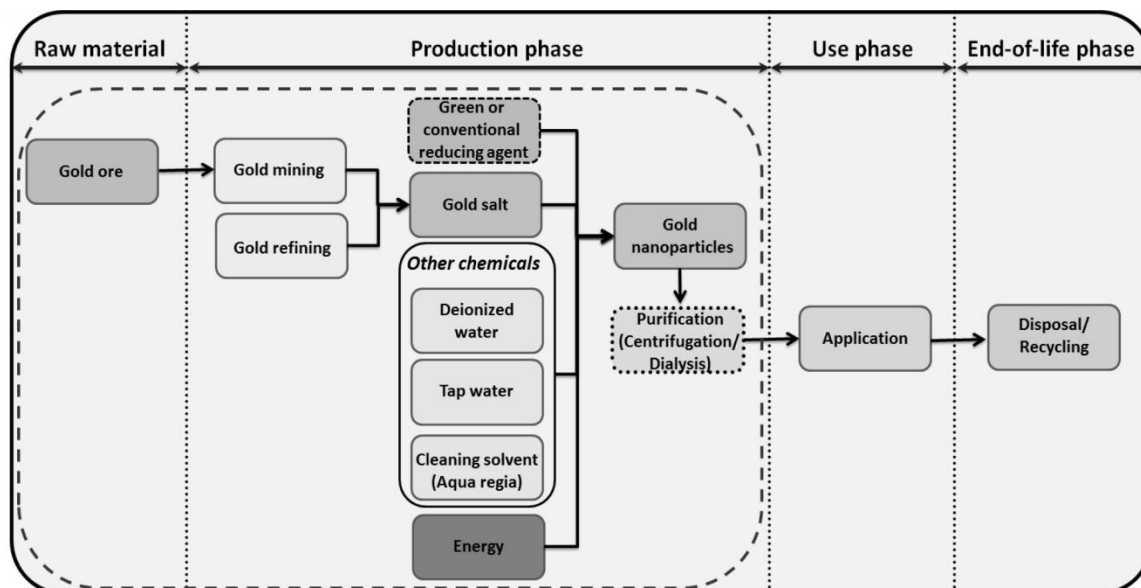


**Figure 2-1** - Life cycle stages of gold nanoparticles. The LCA models include processes from raw material extraction through nanoparticle synthesis. The impacts of reducing agents are included in **Part I** of the study, but excluded in **Part II**. (Purification steps have been ignored in all models).

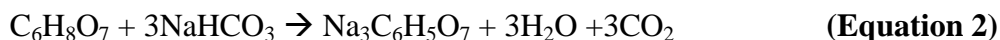
We assumed that the same amounts of tap water, deionized water and cleaning solvents were used in all synthesis protocols, and based those estimates on the actual amounts required for cit-AuNP synthesis in the laboratory. These inputs account for a small fraction of the life cycle impacts of the overall synthesis process, as seen from the results in **Table A2 and A3**. Differences in the impacts due to uncertainties in the actual amounts used are likely to be negligible. The energy requirement inventories were obtained from direct measurements in the laboratory and information in the peer-reviewed literature about the synthesis methods and instrument wattage used in the thirteen green synthesis methods. Instrument specifications were not reported for some processes (e.g., heating and stirring); the energy demands for those processes were estimated based upon similar measurements for our cit-AuNP production experiments. (We therefore ignored any differences in the wattage of specific equipment used in

each study). This estimation approach is justified because the bench-top heater and stirrer we used for the cit-AuNP synthesis process are reasonably representative of the laboratory scale instruments used by most research laboratories. The average medium-voltage electricity mix for the US Northeast Power Coordinating Council was used to model energy use. The uncertainty for energy use was modeled as a uniform distribution with the maximum and minimum values being  $\pm 20\%$  of the calculated energy use as per measurements performed in our laboratory.

The inventory for chemical precursors used in these syntheses was modeled using the EcoInvent database<sup>47</sup> (version 3.01). Because chloroauric acid was not found in any LCA inventory databases we built a custom-defined ‘chloroauric acid’ (HAuCl<sub>4</sub>) process in SimaPro using gold, chlorine, and hydrochloric acid as inputs based on the stoichiometric relation<sup>48</sup>



Similarly, we modeled trisodium citrate as a custom process based on the following equation, using citric acid and sodium bicarbonate from the EcoInvent 3 database.



We assumed a reaction yield of 80% for both equations (1 and 2). In our uncertainty analysis, we assumed a uniform distribution with a minimum of 70% and a maximum 95% reaction yield. These assumptions are reasonable based on industrial yield values used to model chemical processes<sup>49</sup>.

Life cycle impact assessment (LCIA) was done using the Cumulative Energy Demand (CED) method version 1.08<sup>47,50</sup> and ReCiPe version 1.08<sup>51</sup>. The former method estimates all embodied and direct energy use for materials and processes in the syntheses to give a detailed energy footprint across the life cycle. The latter method considers the life cycle impacts across a



broader range of environmental impact categories and is an updated method combining the CML and EcoIndicator assessment methods. The ReCiPe impact assessment was done using midpoints and the hierarchist (H) perspective with European normalization. All uncertainty analyses were performed using Monte-Carlo simulations for 2000 runs. The uncertainty analyses include the uncertainties in the custom-defined chloroauric acid and citric acid, energy use as well as the uncertainties in the unit processes in EcoInvent used in our LCA models. Further details of the LCA models and impact assessments are described in **Part I** and **Part II** below.

**Part I:** In the first part of this study, we compared the cradle-to-gate impacts of two green AuNP synthesis methods (that used soybean seeds and sugarbeet pulp) with three conventional AuNP synthesis methods (that used citrate, sodium borohydride and hydrazine). Except for sodium citrate, the remaining four reducing agents were available in the EcoInvent database. For the LCA models with hydrazine as reductant, the stabilizer poly(vinyl)pyrrolidone was excluded as it is not available in the LCA databases.

For cit-AuNPs we determined the yield to be >99.9% using ICP-MS. All subsequent calculations for cit-AuNPs were performed using a reaction yield of 100%. The reaction yields for sodium borohydride, hydrazine, soybean seed and sugarbeet pulp were assumed to be 100%, as best case scenarios. The inventory used to compare the five AuNP synthesis methods included the metal precursor (chloroauric acid), reducing agent, deionized water, tap water, cleaning solvents and the energy required for heating and stirring. The energy demands for each of the five syntheses were calculated using the CED impact assessment method. We used the ReCiPe Midpoint method to investigate how the five different reducing agents affect the environmental impact of the synthesis process across different impact categories. The results from four impact categories: i) climate change potential, ii) metal depletion potential, iii) agricultural land

occupation, and iv) freshwater ecotoxicity – are presented in **Figure 2-2**. The results of all impact categories are tabulated in **Table A1**. Except for Agricultural Land Occupation, the environmental impacts associated with our five test reducing agents were found to be at least  $10^2$ × smaller than the overall impacts of AuNP synthesis. Based upon these findings, we expanded our study to incorporate other green synthesis approaches, while excluding the reducing agents from the LCA models, as detailed in **Part II** of the study.

**Part II:** In the second part of the study, we performed a comparative LCA study of sixteen different AuNP synthesis methods, including the five methods analyzed in Part I. The additional synthesis methods compared in Part II represent a wide variety of green synthesis approaches and reaction conditions, and are therefore of interest from a comparative LCA standpoint. We excluded the reducing agents from the inventory, as the plant-derived reducing agents in most of these studies are not available in the existing LCA databases. As noted previously, the exclusion of the reductants from the LCA models should have little impact on the final results. The cumulative energy demands for three different reaction yield scenarios were calculated using the CED method (**Figure 2-3**).

The reaction yield for citrate was assumed to be 100% (based on our ICP-MS results). The reaction yields in the case of sodium borohydride and hydrazine were also assumed to be 100%, given that they are strong reducing agents. For the green reductants cypress leaf<sup>34</sup> and grape pomace<sup>28</sup>, the reaction yields were reported in the literature to be 94% and 80%, respectively. For the remaining reductants, the reaction yields were not reported and we thus simulated three different reaction yield scenarios: 50% yield, 75% yield, and 100% yield when calculating the environmental impacts. These choices for reaction yield scenarios are reasonable based on the yields for metallic NP synthesis reported in the literature<sup>52,53</sup>. The values reported in **Table A2**

and **A3** (*Appendix A*) are based on the best-case scenario (100% yield) for the studies in which reaction yields were not reported.

## RESULTS

**Figure 2-2** shows the environmental impacts of production of 1 mg AuNP by different reducing agents based on the processes modeled in **Part I**. The purposes of **Part I** of the study were to ascertain: i) whether the five reducing agents contributed significantly to the overall environmental impact of AuNP synthesis, and ii) whether the green synthesis methods (involving soybean seed and sugarbeet pulp) reduced the overall environmental impacts of the synthesis, when compared to the processes involving sodium borohydride, citrate and hydrazine. To facilitate these comparisons, the impacts of the reducing agents alone are presented in **Table 2-1**.

**Table 2-1-** Environmental impacts of three conventional reducing agents (sodium borohydride, citrate and hydrazine) and two bio-based reducing agents (soybean seed and sugarbeet pulp). The environmental impacts of unit mass of conventional reducing agents are greater than those of the plant-derived reducing agents. The impacts of soybean seeds per mg AuNP, however, are greater than those of the conventional reducing agents. These results highlight that “green” chemicals can have substantial environmental impacts that may be comparable or even worse than the impacts of conventional reducing agents.

<b>Environmental impacts of 1 mg of reducing agents</b>					
<b>Reducing agent</b>	<b>Cumulative Energy demand (MJ)</b>	<b>Climate change potential (kg CO<sub>2</sub> equivalent)</b>	<b>Metal depletion potential (kg Fe equivalent)</b>	<b>Agricultural land occupation (m<sup>2</sup>.year)</b>	<b>Freshwater ecotoxicity (kg 1,4-dichlorobenzene equivalent)</b>
sodium borohydride	$4.63 \times 10^{-4}$	$2.87 \times 10^{-5}$	$1.36 \times 10^{-6}$	$5.95 \times 10^{-7}$	$2.49 \times 10^{-9}$
citrate	$3.88 \times 10^{-5}$	$3.40 \times 10^{-6}$	$2.19 \times 10^{-7}$	$6.92 \times 10^{-7}$	$3.03 \times 10^{-9}$
hydrazine	$1.57 \times 10^{-4}$	$1.03 \times 10^{-5}$	$8.49 \times 10^{-7}$	$2.86 \times 10^{-7}$	$1.14 \times 10^{-6}$
soybean seeds	$6.75 \times 10^{-6}$	$8.94 \times 10^{-7}$	$5.03 \times 10^{-8}$	$4.10 \times 10^{-6}$	$2.22 \times 10^{-10}$
sugarbeet pulp	$6.51 \times 10^{-7}$	$4.16 \times 10^{-8}$	$2.64 \times 10^{-9}$	$6.76 \times 10^{-10}$	$6.46 \times 10^{-12}$
<b>Environmental impacts of reducing agents required per mg of AuNP</b>					
<b>Reducing agent</b>	<b>Cumulative Energy demand (MJ)</b>	<b>Climate change potential (kg CO<sub>2</sub> equivalent)</b>	<b>Metal depletion potential (kg Fe equivalent)</b>	<b>Agricultural land occupation (m<sup>2</sup>.year)</b>	<b>Freshwater ecotoxicity (kg 1,4-dichlorobenzene equivalent)</b>
sodium borohydride	$1.17 \times 10^{-3}$	$7.28 \times 10^{-5}$	$3.46 \times 10^{-6}$	$1.51 \times 10^{-6}$	$6.31 \times 10^{-9}$
citrate	$1.97 \times 10^{-4}$	$3.40 \times 10^{-6}$	$2.19 \times 10^{-7}$	$6.92 \times 10^{-7}$	$3.03 \times 10^{-9}$
hydrazine	$2.56 \times 10^{-5}$	$1.68 \times 10^{-6}$	$1.38 \times 10^{-7}$	$4.65 \times 10^{-8}$	$1.86 \times 10^{-7}$
soybean seeds	$5.59 \times 10^{-5}$	$4.54 \times 10^{-4}$	$2.55 \times 10^{-5}$	$2.08 \times 10^{-3}$	$1.13 \times 10^{-7}$
sugarbeet pulp	$3.43 \times 10^{-3}$	$3.57 \times 10^{-6}$	$2.27 \times 10^{-7}$	$5.81 \times 10^{-8}$	$5.55 \times 10^{-10}$

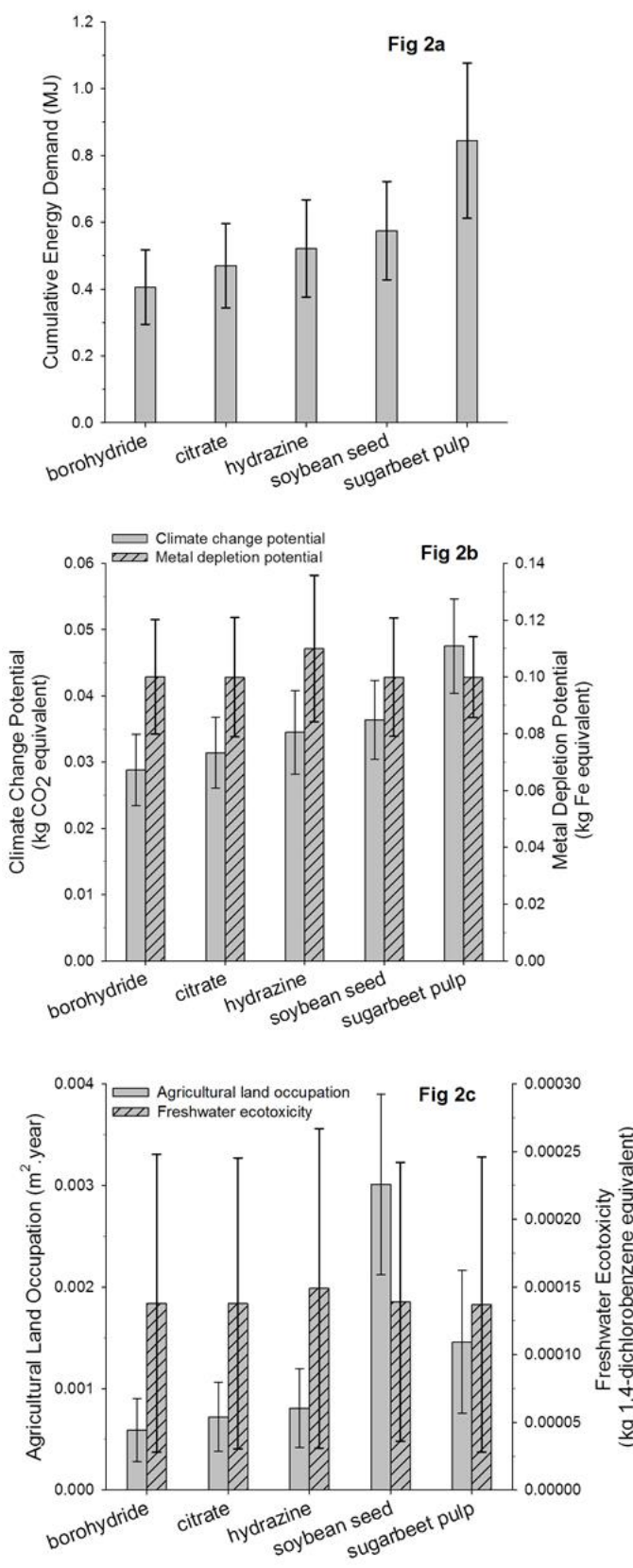


**Figure 2-2** - Environmental impacts of 1 mg AuNP synthesis using three conventional reducing agents (sodium borohydride, citrate and hydrazine) and two plant-derived reducing agents (soybean seed and sugarbeet pulp). **(a)** Cumulative energy demands, **(b)** Climate change potential and metal depletion potential, **(c)** Freshwater ecotoxicity and Agricultural land occupation. The results include the impact of gold salt, reducing agent, deionized water, tap water, glassware cleaning solvent and energy required for stirring and heating **(Part I)**. Error bars in represent 95% confidence intervals for the combined uncertainties in the chloroauric acid and citric acid models, energy use and uncertainties in the EcoInvent unit processes.

**Figure 2-2a** shows the cumulative energy demand (CED) of the five AuNP synthesis methods based on the CED impact assessment method. The environmental impacts of the AuNP synthesis methods across four impact categories (climate change, metal depletion, agricultural land occupation and freshwater ecotoxicity) are presented in **Figures 2-2b** and **2-2c**. All error bars in **Figures 2-2 and 2-3** represent 95% confidence intervals for the combined uncertainties in the chloroauric acid and citric acid models (Equation 1 and 2), energy use and uncertainties in the EcoInvent unit processes.

Plant derived reductants (soybean seeds, sugarbeet pulp) can have environmental impacts that are one to six orders of magnitude smaller when compared to strong reducing agents (sodium borohydride, hydrazine; **Table 2-1**). However, we observe that by substituting conventional reducing agents with plant derived chemicals, the overall environmental impact of the AuNP synthesis processes may not be mitigated. Based on the energy requirements for the laboratory scale synthesis, the cumulative energy demands of AuNP synthesis actually increase when using green reducing agents (**Figure 2-2a**).

A key motivation behind the use of plant-derived reductants is to mitigate the toxicity of conventional reducing agents (such as sodium borohydride or hydrazine). Although some green reducing agents may be non-toxic compared to stronger, conventional reducing agents, they do not diminish the overall toxicity when the cradle-to-gate impacts of the AuNPs are considered (as demonstrated by the freshwater toxicity results in **Figure 2-2c**). As discussed later, some environmental impacts may actually worsen when using plant derived reductants (e.g., agricultural land use (**Figure 2-2c**), freshwater eutrophication (**Table A2**)).

The results of **Part II** of the study are presented in **Figure 2-3**. Importantly, our LCA analysis indicates the actual energy footprint for green reducing agents can be even higher than that for conventional reducing agents if the reaction yields are low. Conducting such LCA studies requires accurate estimations of reaction yields; it is important to note that reaction yields are seldom reported in the literature.

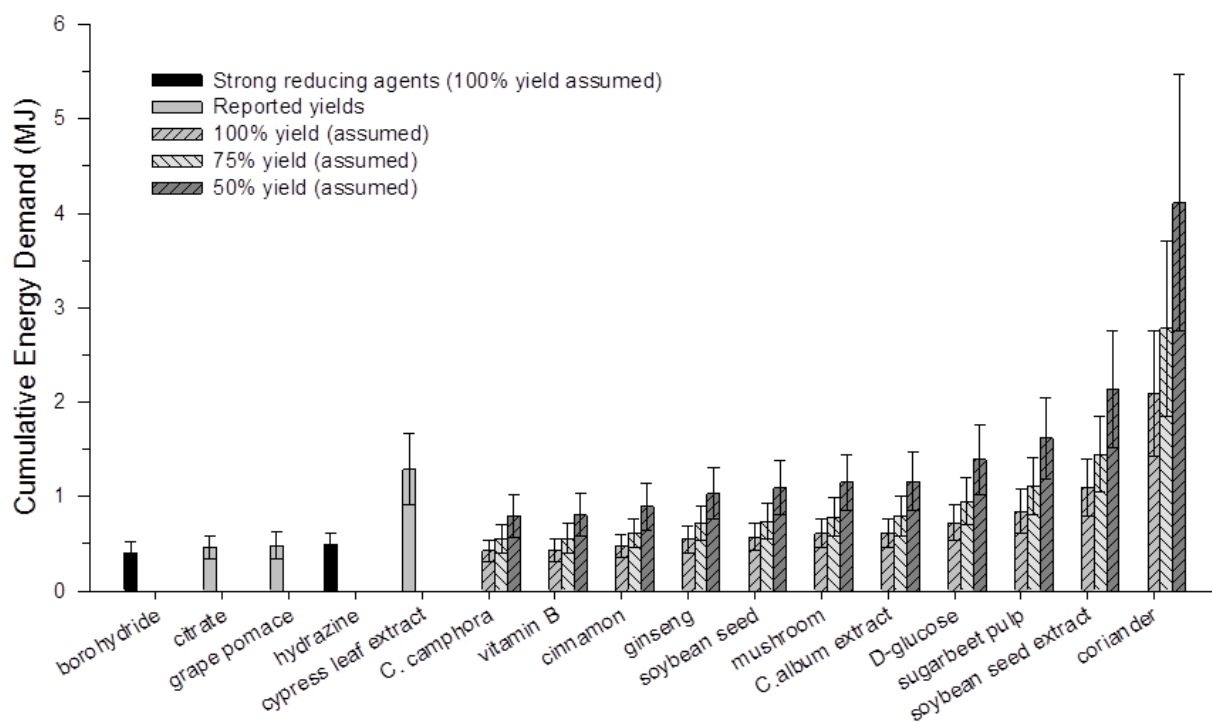


**Figure 2-3** - Cumulative energy demands of 16 different AuNP synthesis methods. The results include the impact of gold salt, deionized water, tap water, glassware cleaning solvent and energy required for stirring and heating. The impacts of the reducing agents were excluded in this calculation (Part II). Error bars in represent 95% confidence intervals for the combined uncertainties in the chloroauric acid and citric acid models, energy use and uncertainties in the EcoInvent unit processes.

## DISCUSSION

**Comparative Life Cycle Assessment.** The motivation for this screening-level, comparative LCA was to estimate the environmental impacts of AuNPs synthesized through different green

synthesis methods. Out of potentially 77 different AuNP green synthesis procedures published in the peer-reviewed literature (Web of Science, 2014), we focused on thirteen studies for our analysis (**Table A2**). These studies represent a wide variety of green routes for AuNP synthesis - using plant extracts<sup>29,31,34</sup>, edible food<sup>35,37,39</sup>, waste products<sup>28,38</sup>, synthetically prepared purified reductants (e.g., Vitamin B<sub>2</sub>, D-glucose)<sup>33,36</sup>, as well as processes that used microwave<sup>28</sup>, sonication<sup>32</sup>. These studies also cover a range of reaction conditions and times.

As mentioned earlier, in **Part I** of this study, we compared the environmental impacts of three conventional AuNP synthesis methods with two green synthesis methods for which inventory data was available in the EcoInvent database. On a unit mass basis, strong reducing agents (e.g., sodium borohydride and hydrazine) have environmental impacts that are 10<sup>1</sup>-10<sup>6</sup> greater than those of plant-derived reducing agents (**Table 2-1**). However, as shown in **Table 2-1**, **Figure 2-2**, and **Table A1**, we find that replacing a toxic reducing agent (e.g., hydrazine) with a plant-derived reductant may not reduce the environmental impact of the overall synthesis process. Even in the best case scenario (assumed yield of 100%), the CEDs for green synthesis methods were higher than for conventional methods due to their longer reaction times, which required higher energy for stirring (**Figure 2-2a**). Climate change potentials for the synthesis methods (**Figure 2-2b**) followed the same trend as CEDs (**Figure 2-2a**). This similarity can be attributed to the fact that greenhouse gas (GHG) emissions are primarily due to fossil fuel use in upstream processes that are accounted for in the CEDs. Given that 100% reaction yields were assumed for all five syntheses, the metal depletion potential differed by about 10% (**Figure 2-2b**). The impact of a synthesis process on metal depletion potential will typically scale with reaction yield. In **Figure 2-2c**, we compare the environmental impacts of toxic reductants (hydrazine and sodium borohydride) and plant-derived chemicals in terms of freshwater



ecotoxicity and agricultural land occupation. Considering that plant-derived reductants are used to displace toxic reducing agents (e.g., hydrazine), it is interesting to note that the freshwater toxicity of the soybean seed and sugarbeet pulp methods are only about 10% lower than that of the hydrazine process. These results show that in some cases, the life cycle impacts of a bio-based AuNP synthesis method may be comparable to those of toxic chemical-based method. Thus, while intuitively it may seem that replacing a toxic chemical with a plant-derived chemical would make a process more benign, the actual gains from this switch may be marginal from a life cycle perspective. Moreover, this switch may exacerbate the environmental impacts in another impact category (e.g., agricultural land occupation, **Figure 2-2c**).

We note that the reducing agents were excluded from the LCA models in **Part II**. This step was taken primarily because those chemicals are not available in current LCA databases. We emphasize, however, that except for Agricultural Land Occupation, the impacts associated with the reducing agents in **Part I** were negligible compared to the overall impact of AuNP synthesis. Therefore, these exclusions are unlikely to change the overall life cycle impacts of the AuNP syntheses significantly.

A key insight gained from our analysis of the variety of green synthesis approaches in Part II was that a substantial part of the overall impact of a given synthesis can be associated with heating, stirring and sonication (**Table A2 and A3**). Moreover, as shown in **Figure 2-3**, the CED of a given synthesis process is strongly dependent on the reaction yield. This calculation illustrates how a LCA framework can be used to compare the energy footprints of synthesis processes with reported reaction yields (e.g., grape pomace vs. cypress leaf extract), as well as to compare bio-based synthesis processes with conventional processes (e.g., citrate reduction). Reaction yields are seldom reported in the literature. The results in **Figure 2-3** highlight the need

for reporting reaction yields to facilitate comparison of environmental impacts of nanoparticle synthesis processes.

A substantial part of the energy footprint in the AuNP synthesis is associated with the use of gold salt, and is primarily attributed to the mining and refining processes for conversion of bulk gold from a mineral deposit into gold salt. The energy and environmental impacts of mining and refining are embedded into most metal-based nanotechnologies and therefore should be accounted for when referring to a nanomaterial or its application as green. Country-specific and process-specific differences in mining and refinery of gold also play a role in the overall environmental impact of gold-based nanotechnologies (**Figure A1**). Such insight can only be gained by doing a holistic, life cycle evaluation of purported green nanotechnologies. LCAs can also help in assessing the environmental impacts and cost-effectiveness of recycling nanomaterials and nanocomposites that contain precious metals. Additional discussion of the results from Part II of the study is presented in Appendix A.

***Challenges in green synthesis of nanomaterials.*** Most extant bio-based nanoparticle syntheses use renewable chemicals and mild reaction conditions. Achieving tightly controlled nanoparticle synthesis to obtain uniform size and morphology is, however, still a challenge (**Table A2** and **Figure A2**). A deeper, mechanistic understanding of these synthesis reactions is required to provide design rules<sup>55</sup> for production of tightly controlled sizes and shapes of nanoparticles and to improve their overall quality<sup>56,57</sup>. The extreme variability in the composition and concentration of phytochemicals in different plant extracts presents another challenge, making it difficult to establish tightly controlled, reproducible synthesis protocols. Impurities in bio-based reductants can affect the stability of the surface moieties of AuNPs as well as their colloidal stability. Heterodispersity in terms of NP size and morphology or colloidal instability

can lead to unpredictable and non-ideal properties<sup>58,59</sup> and may limit the use of the final products during the use-phase.

Owing to this heterodispersity, energy-intensive purification steps (e.g., cryo-centrifugation or ultracentrifugation) may be required after synthesis<sup>60</sup>. Post-synthesis purification steps can increase the environmental impact of the overall synthesis process. Downstream applications would determine the appropriate purification steps. Since this study is focused on the synthesis process only, we did not consider purification steps. We note that post-synthesis purification steps may typically decrease the final AuNP yield, thereby further increasing the environmental impact of the AuNPs.

***Challenges in LCAs of nanotechnologies.*** Previous studies<sup>61-64</sup> identified the lack of nano-specific characterization factors (CFs) as a major hurdle in conducting LCAs for nanotechnologies. For example, silver nanoparticles are suggested to be more toxic than AuNPs<sup>65,66</sup> – a crucial property that is not accounted for when estimating life cycle impacts using CEDs alone. This limitation, however, exists in the case of other impact assessment methods as well. Because of the lack of scientific data, nano-specific CFs have not been incorporated into the current impact assessment methods (e.g., Eco-Indicator 99, TRACI 2.0, ReCiPe etc.) that consider a broader spectrum of environmental impacts. Using impact assessment methods without nano-specific CFs for LCAs may provide an incomplete picture of the life cycle impacts of nanomaterials. The challenges in green synthesis of nanomaterials and conducting LCAs of nanotechnologies are summarized in **Table 2-2**.

**Table 2-2 - Challenges in green nano-synthesis and in conducting LCAs for nanotechnologies**

<b><u>Challenges in green nano-synthesis:</u></b>	<b><u>Challenges in nano-LCA:</u></b>
<p>If green nanoparticle synthesis protocols are expected to replace conventional processes then it must meet the following criteria:</p> <ol style="list-style-type: none"><li>i) Use of benign, sustainably sourced chemicals (Anastas and Warner, 2000)</li><li>ii) Mild reaction conditions (i.e., temperatures and pressures close to ambient) (Anastas and Warner, 2000)</li><li>iii) High reaction yields with short reaction times (Hutchison, 2008)</li><li>iv) Tight control of NP size and morphology</li><li>v) The capacity to reproducibly produce monodisperse, stable nanoparticle suspensions.</li><li>vi) The amenability of the synthesized NPs for desired surface functionalization and bio-based applications.</li></ol>	<p>For life cycle approaches to be embedded into nano-industries and regulations the following must be addressed:</p> <ol style="list-style-type: none"><li>i) Building comprehensive life cycle inventories for nanomaterials (Bauer <i>et al.</i>, 2008; Gavankar <i>et al.</i>, 2012).</li><li>ii) Establish the actual amounts of nanomaterial releases (or potential for release) into different environmental matrices, pertinent to global and local environments (Keller and Lazareva, 2013; Keller <i>et al.</i>, 2013; Meyer <i>et al.</i>, 2009).</li><li>iii) Build consensus-based (Hauschild <i>et al.</i>, 2008), characterization factors (Bare, 2011; Rosenbaum <i>et al.</i>, 2008) for nano-specific impacts.</li><li>iv) Incorporate nano-specific information into the existing LCIA and software.</li><li>v) Foster industry-government and industry-academia partnerships to make confidential business information (CBI) related to nano-based products easily accessible for LCAs.</li></ol>

The results presented in **Figure 2-3** highlight the importance of yield on the environmental impact of different synthesis processes. Compared to conventional syntheses that employ strong reducing agents, green synthesis methods that use milder bio-based reductants may involve longer reaction times. Reaction yields may also be lower when milder bio-based reductants are used. Purification steps required for potentially heterodisperse AuNPs synthesized using a mixture of phytochemicals may further reduce the yield. In such cases, additional steps may be necessary to improve the reaction yields of green synthesis methods.

Although yield influences all environmental impacts of a synthesis process, there are other factors that should also be considered when choosing the best route for AuNP synthesis. Colloidal stability, amenability for surface functionalization and future modifications, monodispersity, tightly tunable size control, biocompatibility – these are all important factors that should be taken into account when choosing a synthesis process. It may be that a low yield reaction might actually be better suited for some specific nanomaterial synthesis, based on the aforementioned criteria. Nonetheless, reaction yields are important when using a high value synthetic chemical – a purified salt of a precious metal – to make nanoparticles, and should be calculated when reporting any green synthesis protocol. Although mass does not capture the properties or the novelty of a new technology and is not based on *function*, previous studies have shown that it is useful as a ‘baseline’<sup>67-72</sup>. If we know how much of the *interim* product (e.g., AuNPs) needs to be incorporated into a product to achieve a certain function, the results of a mass-based study can be later converted into a functional unit representative of the application during the use phase<sup>73</sup>. Based on the scope and objective of this study, a mass-based functional unit is appropriate<sup>74</sup>.

***Challenges in scale-up of laboratory-scale LCAs.*** The performance of industrial scale technologies is often more efficient compared to laboratory- or pilot-scale equipment<sup>75</sup>. With higher reaction yields, recycling of reagents and efficient equipment, the CED for unit mass of AuNPs produced at the industrial scale may be much lower than those predicted by bench-scale, screening-level LCAs<sup>72</sup>, which may not accurately predict environmental burdens upon scale up<sup>76</sup>. Therefore, the results of our lab-scale study cannot be directly extrapolated to estimate scaled up impacts. Modeling scale-up scenarios based on laboratory scale studies is likely to introduce additional uncertainty, especially for emerging technologies<sup>77</sup>. Full-scale LCAs are too

time- and resource-consuming to conduct at the research and development stage of novel products and processes<sup>63,78,79</sup>. Instead, by using secondary data and with appropriate assumptions and sensitivity analysis, screening-level LCAs can highlight the life cycle environmental impacts, and are therefore more suitable for emerging technologies<sup>80</sup>. In the case of nano-manufacturing, the proprietary nature of the processes and the evolving production methodologies hinder development of such comprehensive LCAs<sup>62,81</sup>. Based on the rapid growth and proliferation of nanotechnology, it is in the interest of the industry to provide life cycle inventories. Doing so will help in the development of more robust nano-LCA models and thereby address concerns of the environmental impacts associated with nano-based products. Meanwhile, due to the lack of industrial-scale process data, some simplification in nano-LCA studies is unavoidable<sup>82</sup>. Nonetheless, a life cycle approach using laboratory scale studies can help in decision-directing for future research and data collection<sup>68</sup>.

Despite some limitations in the present study as discussed above, our results show that screening-level LCAs can be a valuable tool for comparing the environmental impacts of emerging nano-synthesis methods. By incorporating green chemistry concepts as well as life cycle thinking into nanotechnology, we can usher this rapidly growing field along paths that are environmentally sustainable rather than those which might inadvertently shift the environmental burden from one part of the process to another. Using plant-derived chemicals (especially from plant-based waste or byproducts<sup>28,83</sup>) for nanoparticle production and implementing such processes into industrial-scale nano-manufacturing holds great promise for achieving this goal, but should be done while considering synthesis efficiencies and overall life cycle impacts.

The results of this study do not suggest that conventional nano-synthesis methods are superior to green synthesis methods or vice-versa. Indeed, for biomedical applications of AuNPs, plant-

derived reactants may be preferred over toxic reductants (e.g., hydrazine or sodium borohydride) to ensure that the AuNPs are biocompatible. In contrast, for AuNP applications that require tightly controlled size and morphology, well-established and tunable conventional synthesis methods may serve better than green methods. Moreover, choosing a particular synthesis method also requires deliberate value-judgments for assigning weights to different impacts. Which is more important: freshwater ecotoxicity or agricultural land occupation?

## **SUMMARIES**

The present approach to making nano-synthesis more environmentally benign focuses on reducing the use of toxic chemicals (e.g., hydrazine) and replacing them with bio-based chemicals. However, doing so without clear metrics to evaluate the environmental sustainability of a green synthesis process from an environmental perspective will only provide a partial, superficial, and at times an ineffective solution to address the complex, ‘wicked’ problems<sup>84</sup> of sustainability. We therefore need to think about environmental sustainability not just in terms of renewable inputs and benign processes, but from a broader life-cycle perspective. In this study, we compared the energy footprint of laboratory-scale green synthesis processes with the conventional methods, from a life cycle perspective. We found that reaction yield is a key parameter in determining the CED of a synthesis process, and is especially important in the case of nanotechnologies based on resource-limited raw materials (e.g., gold). Our results show that screening-level LCAs of green AuNP synthesis methods are helpful for comparing their environmental footprints and facilitating decisions regarding environmentally benign synthesis route. The nanomaterials production industry is still in its infancy; by incorporating life cycle thinking into nanotechnology, we have the opportunity to proactively direct its future course along more environmentally sustainable paths.

## **ACKNOWLEDGEMENTS**

This material is based upon work supported by the National Science Foundation (NSF) and the Environmental Protection Agency (EPA) under NSF Cooperative Agreement EF-0830093, Center for the Environmental Implications of NanoTechnology (CEINT). Additional support from the Virginia Tech graduate school for P.P. is gratefully acknowledged. Nanoparticle characterization was conducted using the facilities of the ICTAS Nanoscale Characterization and Fabrication Laboratory (NCFL). The efforts of Jennifer Kim in the green synthesis of AuNPs, and Chris Winkler and in the collection of TEM images are much appreciated. We are also grateful to the three anonymous reviewers who helped us make this manuscript better through their comments and suggestions.

---

### **Author Disclosure Statement:**

The authors declare no competing financial interests.



## REFERENCES

1. Diallo, M.; Brinker, C. J., Nanotechnology for Sustainability: Environment, Water, Food, Minerals, and Climate. In *Nanotechnology Research Directions for Societal Needs in 2020*, Springer Netherlands: 2011; pp 221-259.
2. Smith, G. B.; Granqvist, C. G.; Lakhtakia, A., Green Nanotechnology: Solutions for Sustainability and Energy in the Built Environment. *Journal of Nanophotonics* **2011**, 5, (1), 050201-050201.
3. Wang, Z. L.; Wu, W., Nanotechnology-enabled energy harvesting for self-powered micro-/nanosystems. *Angewandte Chemie - International Edition* **2012**, 51, (47), 11700-11721.
4. Rule, K. L.; Vikesland, P. J., Surface-Enhanced Resonance Raman Spectroscopy for the Rapid Detection of *Cryptosporidium parvum* and *Giardia lamblia*. *Environmental Science & Technology* **2009**, 43, (4), 1147-1152.
5. Vikesland, P. J.; Wigginton, K. R., Nanomaterial Enabled Biosensors for Pathogen Monitoring - A Review. *Environmental Science & Technology* **2010**, 44, (10), 3656-3669.
6. Fan, Q. L.; Liu, X. F.; Miao, L. K.; Jiang, X.; Ma, Y. W.; Huang, W., Highly Sensitive Fluorometric Hg(2+) Biosensor with a Mercury(II)-Specific Oligonucleotide (MSO) Probe and Water-Soluble Graphene Oxide (WSGO). *Chinese Journal of Chemistry* **2011**, 29, (5), 1031-1035.
7. Karn, B.; Kuiken, T.; Otto, M., Nanotechnology and in Situ Remediation: A Review of the Benefits and Potential Risks. *Environmental Health Perspectives* **2009**, 117, (12), 1813-1831.
8. Puddu, V.; Choi, H.; Dionysiou, D. D.; Puma, G. L., TiO<sub>2</sub> photocatalyst for indoor air remediation: Influence of crystallinity, crystal phase, and UV radiation intensity on trichloroethylene degradation. *Applied Catalysis B: Environmental* **2010**, 94, (3-4), 211-218.
9. Zhang, D.; Wei, S.; Kaila, C.; Su, X.; Wu, J.; Karki, A. B.; Young, D. P.; Guo, Z., Carbon-stabilized iron nanoparticles for environmental remediation. *Nanoscale* **2010**, 2, (6), 917-919.
10. Lowry, G. V.; Hotze, E. M.; Bernhardt, E. S.; Dionysiou, D. D.; Pedersen, J. A.; Wiesner, M. R.; Xing, B., Environmental Occurrences, Behavior, Fate, and Ecological Effects of Nanomaterials: An Introduction to the Special Series. *Journal of Environmental Quality* **2010**, 39, (6), 1867-74.
11. Kushnir, D.; Sandén, B. A., Energy Requirements of Carbon Nanoparticle Production. *Journal of Industrial Ecology* **2008**, 12, (3), 360-375.
12. Kushnir, D.; Sandén, B. A., Multi-Level Energy Analysis of Emerging Technologies: A Case Study in New Materials for Lithium Ion Batteries. *Journal of Cleaner Production* **2011**, 19, (13), 1405-1416.

13. Oberdörster, E., Manufactured nanomaterials (fullerenes, C60) induce oxidative stress in the brain of juvenile largemouth bass. *Environmental Health Perspectives* **2004**, *112*, (10), 1058-1062.
14. Oberdörster, G., Safety Assessment for Nanotechnology and Nanomedicine: Concepts of Nanotoxicology. *Journal of Internal Medicine* **2010**, *267*, (1), 89-105.
15. Helland, A.; Kastenholz, H., Development of nanotechnology in light of sustainability. *Journal of Cleaner Production* **2008**, *16*, (8–9), 885-888.
16. Lohse, S. E.; Murphy, C. J., Applications of colloidal inorganic nanoparticles: from medicine to energy. *Journal of the American Chemical Society* **2012**, *134*, (38), 15607-20.
17. Dreaden, E. C.; Alkilany, A. M.; Huang, X.; Murphy, C. J.; El-Sayed, M. A., The golden age: gold nanoparticles for biomedicine. *Chemical Society Reviews* **2012**, *41*, (7), 2740-2779.
18. cientifica.com Nanotechnology for Drug Delivery: Global Market for Nanocarriers. <http://www.cientifica.com/research/market-reports/nanotechnology-for-drug-delivery-global-market-for-nanocarriers/>
19. Mudd, G. M., Global trends in gold mining: Towards quantifying environmental and resource sustainability. *Resources Policy* **2007**, *32*, (1–2), 42-56.
20. Schodde, R. In *Recent trends in gold discovery*, NewGenGold Conference, 2011/11/22/23, 2011; 2011.
21. Kerr, R. A., Is the World Tottering on the Precipice of Peak Gold? *Science* **2012**, *335*, (6072), 1038-1039.
22. Starr, M.; Tran, K., Determinants of the physical demand for gold: Evidence from panel data. *The World Economy* **2008**, *31*, (3), 416-436.
23. Wiek, A.; Gasser, L.; Siegrist, M., Systemic scenarios of nanotechnology: Sustainable governance of emerging technologies. *Futures* **2009**, *41*, (5), 284-300.
24. Roco, M. C., The long view of nanotechnology development: the National Nanotechnology Initiative at 10 years. In *Nanotechnology Research Directions for Societal Needs in 2020*, Springer: 2011; pp 1-28.
25. Avraamides, M.; Fatta, D., Resource consumption and emissions from olive oil production: a life cycle inventory case study in Cyprus. *Journal of Cleaner Production* **2008**, *16*, (7), 809-821.
26. Hayashi, K.; Makino, N.; Shobatake, K.; Hokazono, S., Influence of scenario uncertainty in agricultural inputs on life cycle greenhouse gas emissions from agricultural production systems: the case of chemical fertilizers in Japan. *Journal of Cleaner Production* **2013**.

27. Guinée, J. B.; Heijungs, R.; Huppes, G.; Zamagni, A.; Masoni, P.; Buonamici, R.; Ekvall, T.; Rydberg, T., Life Cycle Assessment: Past, Present, and Future†. *Environmental Science & Technology* **2011**, *45*, (1), 90-96.
28. Baruwati, B.; Varma, R. S., High value products from waste: grape pomace extract: A three-in-one package for the synthesis of metal nanoparticles. *ChemSusChem* **2009**, *2*, (11), 1041-4.
29. Chanda, N.; Shukla, R.; Zambre, A.; Mekapothula, S.; Kulkarni, R.; Katti, K.; Bhattacharyya, K.; Fent, G.; Casteel, S.; Boote, E.; Viator, J.; Upendran, A.; Kannan, R.; Katti, K., An Effective Strategy for the Synthesis of Biocompatible Gold Nanoparticles Using Cinnamon Phytochemicals for Phantom CT Imaging and Photoacoustic Detection of Cancerous Cells. *Pharmaceutical Research* **2011**, *28*, (2), 279-291.
30. Dwivedi, A. D.; Gopal, K., Biosynthesis of silver and gold nanoparticles using *Chenopodium album* leaf extract. *Colloids and Surfaces A: Physicochemical and Engineering Aspects* **2010**, *369*, (1-3), 27-33.
31. Huang, J.; Li, Q.; Sun, D.; Lu, Y.; Su, Y.; Yang, X.; Wang, H.; Wang, Y.; Shao, W.; He, N.; Hong, J.; Chen, C., Biosynthesis of silver and gold nanoparticles by novel sundried *Cinnamomum camphora* leaf. *Nanotechnology* **2007**, *18*, (10), 105104.
32. Leonard, K.; Ahmmad, B.; Okamura, H.; Kurawaki, J., In situ green synthesis of biocompatible ginseng capped gold nanoparticles with remarkable stability. *Colloids and surfaces. B, Biointerfaces* **2011**, *82*, (2), 391-6.
33. Nadagouda, M. N.; Varma, R. S., Green and controlled synthesis of gold and platinum nanomaterials using vitamin B2: density-assisted self-assembly of nanospheres, wires and rods. *Green Chemistry* **2006**, *8*, (6), 516-518.
34. Noruzi, M.; Zare, D.; Davoodi, D., A rapid biosynthesis route for the preparation of gold nanoparticles by aqueous extract of cypress leaves at room temperature. *Spectrochimica acta. Part A, Molecular and biomolecular spectroscopy* **2012**, *94*, 84-8.
35. Philip, D., Biosynthesis of Au, Ag and Au-Ag nanoparticles using edible mushroom extract. *Spectrochimica acta. Part A, Molecular and biomolecular spectroscopy* **2009**, *73*, (2), 374-81.
36. Raveendran, P.; Fu, J.; Wallen, S. L., A simple and “green” method for the synthesis of Au, Ag, and Au–Ag alloy nanoparticles. *Green Chemistry* **2006**, *8*, (1), 34-38.
37. Narayanan, K. B.; Sakthivel, N., Coriander leaf mediated biosynthesis of gold nanoparticles. *Materials Letters* **2008**, *62*, (30), 4588-4590.
38. Castro, L.; Blázquez, M. L.; Muñoz, J. A.; González, F.; García-Balboa, C.; Ballester, A., Biosynthesis of gold nanowires using sugar beet pulp. *Process Biochemistry* **2011**, *46*, (5), 1076-1082.

39. Shukla, R.; Nune, S. K.; Chanda, N.; Katti, K.; Mekapothula, S.; Kulkarni, R. R.; Welshons, W. V.; Kannan, R.; Katti, K. V., Soybeans as a Phytochemical Reservoir for the Production and Stabilization of Biocompatible Gold Nanoparticles. *Small* **2008**, *4*, (9), 1425-1436.
40. Turkevich, J.; Stevenson, P. C.; Hillier, J., A study of the nucleation and growth processes in the synthesis of colloidal gold. *Discuss. Faraday Soc.* **1951**, *11*, 55-75.
41. Frens, G., Controlled Nucleation for the Regulation of the Particle Size in Monodisperse Gold Suspensions. *Nature* **1973**, *241*, (105), 20-22.
42. Low, A.; Bansal, V., A visual tutorial on the synthesis of gold nanoparticles. *Biomed Imaging Interv J* **2010**, *6*, (1).
43. Jeong, G. H.; Lee, Y. W.; Kim, M.; Han, S. W., High-yield synthesis of multi-branched gold nanoparticles and their surface-enhanced Raman scattering properties. *Journal of colloid and interface science* **2009**, *329*, (1), 97-102.
44. Viswanathan, S.; Radecka, H.; Radecki, J., Electrochemical biosensor for pesticides based on acetylcholinesterase immobilized on polyaniline deposited on vertically assembled carbon nanotubes wrapped with ssDNA. *Biosensors and Bioelectronics* **2009**, *24*, (9), 2772-2777.
45. APHA, American Public Health Association, American Water Works Association, and Water Environment Federation. *Standard Methods for the Examination of Water and Wastewater*. **1998**.
46. Hull, M. S.; Chaurand, P.; Rose, J.; Auffan, M.; Bottero, J.-Y.; Jones, J. C.; Schultz, I. R.; Vikesland, P. J., Filter-Feeding Bivalves Store and Biodeposit Colloidally Stable Gold Nanoparticles. *Environmental Science & Technology* **2011**, *45*, (15), 6592-6599.
47. Frischknecht, R.; Jungbluth, N.; Althaus, H.-J.; Doka, G.; Dones, R.; Heck, T.; Hellweg, S.; Hirschler, R.; Nemecek, T.; Rebitzer, G., The ecoinvent database: Overview and methodological framework (7 pp). *The International Journal of Life Cycle Assessment* **2005**, *10*, (1), 3-9.
48. Holleman, A. F.; Wiberg, N.; Wiberg, E., *Inorganic Chemistry*. 1 ed.; Academic Press: New York, 2001; p 1924.
49. Hessel, V.; Renken, A.; Schouten, J. C.; Yoshida, J.-i., *Micro Process Engineering: A Comprehensive Handbook*. John Wiley & Sons: 2009; p 1413.
50. Frischknecht, R.; Jungbluth, N.; Althaus, H. J.; Bauer, C.; Doka, G.; Dones, R.; Hirschler, R.; Hellweg, S.; Humbert, S.; Köllner, T. *Implementation of life cycle impact assessment methods*; 3; EcoInvent Report: 2007, 2007.
51. Goedkoop, M.; Heijungs, R.; Huijbregts, M.; De Schryver, A.; Struijs, J.; van Zelm, R., ReCiPe 2008. A life cycle impact assessment method which comprises harmonised category indicators at the midpoint and the endpoint level **2009**, 1.

52. Sung, K.-M.; Mosley, D. W.; Peelle, B. R.; Zhang, S.; Jacobson, J. M., Synthesis of Monofunctionalized Gold Nanoparticles by Fmoc Solid-Phase Reactions. *Journal of the American Chemical Society* **2004**, *126*, (16), 5064-5065.
53. Garcia-Martinez, J. C.; Lezutekong, R.; Crooks, R. M., Dendrimer-Encapsulated Pd Nanoparticles as Aqueous, Room-Temperature Catalysts for the Stille Reaction. *Journal of the American Chemical Society* **2005**, *127*, (14), 5097-5103.
54. webofknowledge.com Web of Science Results, Topic=(green synthesis) AND Topic=(gold nano).  
[http://apps.webofknowledge.com/summary.do?SID=3B4UaJdXOgp1utltqIe&product=WOS&qid=1&search\\_mode=GeneralSearch](http://apps.webofknowledge.com/summary.do?SID=3B4UaJdXOgp1utltqIe&product=WOS&qid=1&search_mode=GeneralSearch)
55. Langille, M. R.; Personick, M. L.; Zhang, J.; Mirkin, C. A., Defining Rules for the Shape Evolution of Gold Nanoparticles. *Journal of the American Chemical Society* **2012**, *134*, (35), 14542-14554.
56. Das, S. K.; Marsili, E., A green chemical approach for the synthesis of gold nanoparticles: characterization and mechanistic aspect. *Rev Environ Sci Biotechnol* **2010**, *9*, (3), 199-204.
57. Warner, J. C.; Cannon, A. S.; Dye, K. M., Green chemistry. *Environmental Impact Assessment Review* **2004**, *24*, (7-8), 775-799.
58. Green, A. A.; Hersam, M. C., Emerging Methods for Producing Monodisperse Graphene Dispersions. *The journal of physical chemistry letters* **2010**, *1*, (2), 544-549.
59. Tsai, D. H.; Cho, T. J.; DelRio, F. W.; Taurozzi, J.; Zachariah, M. R.; Hackley, V. A., Hydrodynamic fractionation of finite size gold nanoparticle clusters. *Journal of the American Chemical Society* **2011**, *133*, (23), 8884-7.
60. Anctil, A.; Babbitt, C. W.; Raffaele, R. P.; Landi, B. J., Material and Energy Intensity of Fullerene Production. *Environmental science & technology* **2011**, *45*, (6), 2353-2359.
61. Bauer, C.; Buchgeister, J.; Hischer, R.; Poganietz, W. R.; Schebek, L.; Warsen, J., Towards a framework for life cycle thinking in the assessment of nanotechnology. *Journal of Cleaner Production* **2008**, *16*, (8-9), 910-926.
62. Gavankar, S.; Suh, S.; Keller, A., Life cycle assessment at nanoscale: review and recommendations. *The International Journal of Life Cycle Assessment* **2012**, *17*, (3), 295-303.
63. Hetherington, A. C.; Borrion, A. L.; Griffiths, O. G.; McManus, M. C., Use of LCA as a Development Tool within Early Research: Challenges and Issues Across Different Sectors. *The International Journal of Life Cycle Assessment* **2014**, 1-14.

64. Kim, H. C.; Fthenakis, V., Life Cycle Energy and Climate Change Implications of Nanotechnologies. *Journal of Industrial Ecology* **2013**, *17*, (4), 528-541.
65. Lapresta-Fernández, A.; Fernández, A.; Blasco, J., Nanoecotoxicity effects of engineered silver and gold nanoparticles in aquatic organisms. *TrAC Trends in Analytical Chemistry* **2012**, *32*, 40-59.
66. Bar-Ilan, O.; Albrecht, R. M.; Fako, V. E.; Furgeson, D. Y., Toxicity assessments of multisized gold and silver nanoparticles in zebrafish embryos. *Small* **2009**, *5*, (16), 1897-910.
67. Osterwalder, N.; Capello, C.; Hungerbühler, K.; Stark, W. J., Energy Consumption During Nanoparticle Production: How Economic is Dry Synthesis? *Journal of Nanoparticle Research* **2006**, *8*, (1), 1-9.
68. Joshi, S., Can Nanotechnology Improve the Sustainability of Biobased Products? *Journal of Industrial Ecology* **2008**, *12*, (3), 474-489.
69. Deorsola, F. A.; Russo, N.; Blengini, G. A.; Fino, D., Synthesis, characterization and environmental assessment of nanosized MoS<sub>2</sub> particles for lubricants applications. *Chemical Engineering Journal* **2012**, 195–196, 1-6.
70. LeCorre, D.; Hohenthal, C.; Dufresne, A.; Bras, J., Comparative Sustainability Assessment of Starch Nanocrystals. *J Polym Environ* **2013**, *21*, (1), 71-80.
71. Li, Q.; McGinnis, S.; Sydnor, C.; Wong, A.; Rennekar, S., Nanocellulose Life Cycle Assessment. *ACS Sustainable Chem. Eng.* **2013**, *1*, (8), 919-928.
72. Gao, T.; Jelle, B. P.; Sandberg, L. I.; Gustavsen, A., Monodisperse hollow silica nanospheres for nano insulation materials: Synthesis, characterization, and life cycle assessment. *ACS applied materials & interfaces* **2013**, *5*, (3), 761-7.
73. Wender, B. A.; Seager, T. P. In *Towards prospective life cycle assessment: Single wall carbon nanotubes for lithium-ion batteries*, 2011 IEEE International Symposium on Sustainable Systems and Technology (ISSST), 2011/05//, 2011; 2011; pp 1-4.
74. Hischer, R.; Walser, T., Life Cycle Assessment of Engineered Nanomaterials: State of the Art and Strategies to Overcome Existing Gaps. *Science of The Total Environment* **2012**, *425*, 271-282.
75. Frischknecht, R.; Büsser, S.; Krewitt, W., Environmental Assessment of Future Technologies: How to Trim LCA to Fit This Goal? *The International Journal of Life Cycle Assessment* **2009**, *14*, (6), 584-588.
76. Shibasaki, M.; Fischer, M.; Barthel, L., Effects on Life Cycle Assessment — Scale Up of Processes. In *Advances in Life Cycle Engineering for Sustainable Manufacturing Businesses*, Takata, S.; Umeda, Y., Eds. Springer London: 2007; pp 377-381.
77. Levin, M., *Pharmaceutical Process Scale-Up*. CRC Press: 2001; p 589.

78. Koller, G.; Fischer, U.; Hungerbühler, K., Assessing Safety, Health, and Environmental Impact Early during Process Development. *Industrial & Engineering Chemistry Research* **2000**, *39*, (4), 960-972.
79. Tufvesson, L. M.; Tufvesson, P.; Woodley, J. M.; Börjesson, P., Life cycle assessment in green chemistry: overview of key parameters and methodological concerns. *The International Journal of Life Cycle Assessment* **2013**, *18*, (2), 431-444.
80. Meyer, D. E.; Curran, M. A.; Gonzalez, M. A., An examination of silver nanoparticles in socks using screening-level life cycle assessment. *Journal of Nanoparticle Research* **2010**, *13*, (1), 147-156.
81. Eckelman, M. J.; Mauter, M. S.; Isaacs, J. A.; Elimelech, M., New perspectives on nanomaterial aquatic ecotoxicity: production impacts exceed direct exposure impacts for carbon nanotubes. *Environmental science & technology* **2012**, *46*, (5), 2902-10.
82. Kunnari, E.; Valkama, J.; Keskinen, M.; Mansikkamäki, P., Environmental evaluation of new technology: printed electronics case study. *Journal of Cleaner Production* **2009**, *17*, (9), 791-799.
83. Bankar, A.; Joshi, B.; Kumar, A. R.; Zinjarde, S., Banana peel extract mediated synthesis of gold nanoparticles. *Colloids and surfaces. B, Biointerfaces* **2010**, *80*, (1), 45-50.
84. Seager, T.; Selinger, E.; Wiek, A., Sustainable Engineering Science for Resolving Wicked Problems. *J Agric Environ Ethics* **2012**, *25*, (4), 467-484.

## Chapter 3

# Waste Not Want Not: Life Cycle Implications of Gold Recovery and Recycling from Nanowaste

*Paramjeet Pati,<sup>1,2,3</sup> Sean McGinnis,<sup>2,4</sup> and Peter J. Vikesland<sup>1,2,3\*</sup>*

<sup>1</sup>Civil and Environmental Engineering, Virginia Tech

<sup>2</sup>Virginia Tech Institute of Critical Technology and Applied Science (ICTAS) Sustainable Nanotechnology Center (VTSuN)

<sup>3</sup>Center for the Environmental Implications of Nanotechnology (CEINT), Duke University

<sup>4</sup>Department of Material Science and Engineering, Virginia Tech

\*Corresponding author. Phone: (540) 231-3568, Email: [pvikes@vt.edu](mailto:pvikes@vt.edu)

### ABSTRACT

Commercial-scale application of nanotechnology is rapidly increasing. Enhanced production of nanomaterials and nano-enabled products and their resultant disposal lead to concomitant increases in the volume of nanomaterial wastes (i.e., *nanowaste*). Many nanotechnologies employ resource-limited materials, such as precious metals and rare earth elements, which ultimately end up as nanowaste. To make nanotechnology more sustainable it is essential to develop strategies to recover high-value, resource-limited materials from nanowaste. To address this complex issue, we developed laboratory-scale methods to recover nanowaste gold. To this end,  $\alpha$ -cyclodextrin facilitated host-guest inclusion complex formation involving second-sphere coordination of  $[\text{AuBr}_4]^-$  and  $[\text{K}(\text{OH}_2)_6]^+$  was used for gold recovery and the recovered gold was then used to produce new nanoparticles. To quantify the environmental impacts of this gold recycling process we produced life cycle assessments to compare nanoparticulate gold production scenarios with and without recycling. The LCA results indicate that recovery and recycling of gold from nanowaste can significantly reduce the environmental impacts of gold



nanoparticle synthesis. Besides facilitating gold recovery from nanowaste, this research also has the potential to improve current waste management practices and inform future nanowaste management policies.

## INTRODUCTION

There has been rapid growth in the number of nanomaterial-based consumer products in recent years, resulting in a concomitant increase in waste streams containing nanomaterials (e.g., *nanowaste*). Several nanotechnologies depend on resource-limited precious metals and rare earth elements (REEs). Supply risks related to these critical raw materials will one day threaten the sustainable growth of nano-industries. In light of the declining global reserves of high-value metals,<sup>1-3</sup> the recovery and recycling of critical materials is of paramount importance. Current waste treatment practices do not have specific provisions for nanomaterials,<sup>4</sup> and uncertainties regarding end-of-life scenarios currently hinder the formulation of regulations for nanomaterial waste management and resource recovery from waste streams.<sup>5</sup>

Conventional metal recovery methods (e.g., solvent extraction,<sup>6</sup> ion-exchange,<sup>7</sup> electrolysis,<sup>8</sup> plasma technology,<sup>9</sup> and microbiological methods<sup>10,11</sup>) offer strategies for recovering high-value metals and REEs from nanowaste. The diversity and complexity of nanowaste, however, make it difficult to develop universally applicable methods for waste management.<sup>12</sup> Fortunately, recent studies have developed novel approaches to metal recovery that may address these challenges. Nano-SnO<sub>2</sub> was recovered from industrial electroplating waste sludge using the selective crystallization and growth of acid-soluble amorphous SnO<sub>2</sub> into acid-insoluble SnO<sub>2</sub> nanowires<sup>13</sup>. In another study, adsorption-induced crystallization of uranium rich nanocrystals was used for uranyl enrichment.<sup>14</sup> Thermo-reversible liquid-liquid phase transition<sup>12</sup> and cloud

point extraction<sup>15-18</sup> also hold promise for the successful separation and recovery of critical, high-value and resource-limited materials from nanowaste. One such critical raw material is gold.

The concentration of gold in the continental crust is estimated to be about 1.5 µg/kg.<sup>19</sup> Gold ore grades have declined over the last decade;<sup>20</sup> the cost of extracting gold has steadily increased<sup>21</sup> and there are concerns about having reached peak gold.<sup>22</sup> The current demand for gold by nanotechnology-based applications is small compared to other demands (e.g., jewelry<sup>23</sup>). Nonetheless, given the rapid growth of the nanotechnology industry,<sup>24,25</sup> the market share for gold-based nanotechnologies is expected to increase exponentially. In the future, a limited supply of the raw material may pose a substantial challenge to the development of gold-based nanotechnologies. Therefore, novel approaches for gold recovery from waste streams are being actively researched today.<sup>16,26,27</sup> Recently, Liu *et al.*<sup>26</sup> reported one approach to recover gold using  $\alpha$ -cyclodextrin ( $\alpha$ -CD). This method involves the formation of a host-guest inclusion complex involving tetrabromoaurate anion [AuBr<sub>4</sub>]<sup>-</sup>,  $\alpha$ -CD, and hexaquo potassium cation [K(OH<sub>2</sub>)<sub>6</sub>]<sup>+</sup>, followed by rapid co-precipitation at room temperature. This method has been reported to have high separation efficiencies (>75%) and recovery yields (> 90%), and unlike traditional methods for selective gold recovery, does not involve the use of toxic cyanide<sup>28</sup> or mercury.<sup>29</sup> In this study, we investigated the applicability of such an approach for the recovery of gold from nanowaste, and analyzed the life cycle impacts of the process.

Life cycle assessment (LCA) is a quantitative framework used to evaluate the cumulative environmental impacts associated with all stages of a material – from the extraction of raw materials (‘cradle’) through the end-of-life (‘grave’).<sup>30</sup> Technical innovations that are suggested to make nanotechnology more sustainable must be analyzed within an LCA framework to identify potential hidden environmental burdens. For example, the use of benign reagents during

nanomaterial synthesis, while intuitively ‘green’, can have significant life cycle impacts.<sup>31</sup> Similarly, novel methods for nanowaste recycling may involve hidden environmental costs that can only be identified through development of comprehensive LCAs. For example, a new method for recovery of gold from sewage sludge ash was recently reported,<sup>27</sup> claiming that the method “eliminates the need for water” in the recovery process. However, the process involves temperatures of ~800 °C for optimum gold recovery. High temperature processes typically have substantial water footprints because they involve considerable fuel consumption and generally employ high-pressure steam. Any reduction in direct water use during material recovery may be negated by such indirect water uses. We therefore need to analyze the environmental burdens from a life cycle perspective when developing new nanowaste management strategies. By coupling novel recycling approaches with LCA modeling, we can develop next-generation closed-loop processes for sustainable nanotechnology. For these reasons we conducted an LCA study for the  $\alpha$ -CD-facilitated gold-recovery process and analyzed the life cycle impacts of different nanowaste recycling scenarios.

## **MATERIALS AND METHODS**

***Selective gold recovery by  $\alpha$ -CD.*** We prepared simulated nanowaste comprised of citrate-reduced gold nanoparticles (AuNPs).<sup>32</sup> The simulated nanowaste suspension was precipitated by adding KCl and was then dissolved using a 3:1 v:v mixture of HBr and HNO<sub>3</sub>. HBr was employed to ensure that gold was present as the square planar complex AuBr<sub>4</sub><sup>-</sup>. The pH of the resultant clear red solution was adjusted to ~5 using KOH. Assuming that all the gold originally in the AuNP suspension was precipitated and redissolved in the HBr-HNO<sub>3</sub> mixture, we added a calculated mass of  $\alpha$ -CD sufficient to achieve a 2:1 molar ratio of gold: $\alpha$ -CD. Almost

immediately the clear red solution became turbid. After 30 minutes, the reaction mixture was filtered through a 0.22  $\mu\text{m}$  PTFE filter. The retentate was then resuspended in deionized water by sonication, which yielded a clear brown solution. An aliquot of 50 mM of sodium metabisulfite ( $\text{Na}_2\text{S}_2\text{O}_5$ ) was then added to precipitate and recover gold. The exact volume of 50 mM  $\text{Na}_2\text{S}_2\text{O}_5$  required was based on the amount of gold originally present in the simulated nanowaste. The percent recovery of gold for three samples was determined by inductively coupled plasma mass spectrometry (ICP-MS) using standard method 3125-B.<sup>33</sup>

The solid precipitate obtained after adding  $\text{Na}_2\text{S}_2\text{O}_5$  was recovered by filtration, analyzed using powder X-ray diffraction (XRD) (**Figure B1**, *Appendix B*), and then dissolved in aqua regia. The yellow solution was boiled to remove  $\text{HNO}_3$  (observed as brown nitrogen dioxide gas leaving the flask), while adding HCl intermittently. Boiling was stopped after ebullition of brown gas concluded. The final solution was analyzed by UV-vis spectroscopy (**Figure B2**) and used to synthesize new citrate-reduced AuNPs. The AuNPs were characterized for size and chemical composition using high resolution transmission electron microscopy (TEM) and selected area electron diffraction (SAED) (**Figure B3**). The overall recovery process is summarized in **Figure 3-1A**.

**LCA modeling.** We constructed LCA models using SimaPro 8. The functional unit for our study was 1 mg of AuNP. The inventory for chemical precursors used in the AuNP synthesis and gold recovery was modeled using the EcoInvent 3.0 database.<sup>34</sup> The energy use during AuNP synthesis and gold recycling was recorded for LCA model development. Energy use uncertainty was modeled as described elsewhere<sup>31</sup>. Life cycle impact assessment (LCIA) was done using the ReCiPe method<sup>35</sup> (version 1.08), using midpoints and the hierarchist (H) perspective with European normalization. Uncertainty analyses were performed using Monte-Carlo simulations

for 1000 runs. Four scenarios were simulated for 0%, 10%, 50%, and 90% recovery of gold from nanowaste. In these four scenarios, all of the recovered gold was assumed to be recycled to make new AuNPs, and the unrecovered gold along with other chemicals was simulated as hazardous waste for incineration. The inventories are presented in **Table B1, B2 and B3** (*Appendix B*).

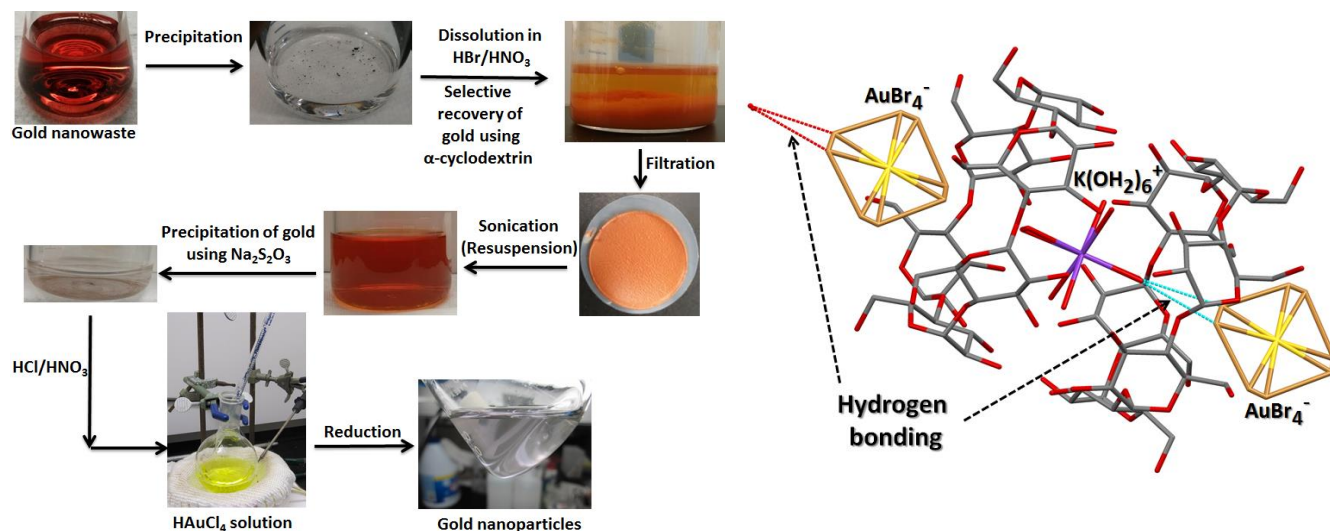


**Figure 3-1** – **A** (Left) Schematic of the gold recovery and recycling process. **B** (Right) The repeating unit involving one [K(OH<sub>2</sub>)<sub>6</sub>]<sup>+</sup> cation, one [AuBr<sub>4</sub>]<sup>-</sup> anion and two CD molecules. An additional [AuBr<sub>4</sub>]<sup>-</sup> anion is shown to illustrate how the unit is bound to the next unit through hydrogen bonding.

## RESULTS AND DISCUSSION

*Selective recovery of gold using α-CD.* Host-guest inclusion complexes involving cyclodextrin (host) and metal ions (guest) have been reported to form rod- and chain-like nanoscale supramolecular assemblies.<sup>36,37</sup> These inclusion complexes form when water molecules are displaced from the cyclodextrin cavity by more hydrophobic guest molecules, thus resulting in energetically favorable reduced ring-strain.<sup>38</sup> The selective recovery of gold using α-CD is made possible by the perfect molecular recognition between [AuBr<sub>4</sub>]<sup>-</sup> and α-CD, causing square planar [AuBr<sub>4</sub>]<sup>-</sup> to orient axially with respect to the α-CD channel.<sup>26</sup> Moreover, the cavity between two α-CD molecules is ideally suited to accommodate the octahedral [K(OH<sub>2</sub>)<sub>6</sub>]<sup>+</sup> ion,

thereby restricting its solvation by water molecules in the bulk solution. The specific orientation of the  $[\text{AuBr}_4]^-$  ion and the favorable location of  $[\text{K}(\text{OH}_2)_6]^+$  within the  $\alpha$ -CD dimer facilitates second-sphere coordination between  $[\text{K}(\text{OH}_2)_6]^+$  and  $[\text{AuBr}_4]^-$ . A rod-shaped nanostructure forms due to the equatorial  $[\text{C}-\text{H}\cdots\text{Br}-\text{Au}]$  hydrogen bonds between  $\alpha$ -CD and  $[\text{AuBr}_4]^-$ , and axial  $[\text{O}-\text{H}\cdots\text{Br}-\text{Au}]$  hydrogen bonds between  $[\text{K}(\text{OH}_2)_6]^+$  and  $[\text{AuBr}_4]^-$ . Individual rods bind to each other radially due to hydrogen bonding, forming a supramolecular assembly that ultimately precipitates due to colloidal instability.<sup>26</sup> Each unit of this assembly is comprised of an  $[\text{AuBr}_4]^-$  anion and an  $\alpha$ -CD dimer enclosing a  $[\text{K}(\text{OH}_2)_6]^+$  cation (**Figure 3-1B**).

The superstructure shown in **Figure 3-1B** does not form in the case of  $\beta$ - or  $\gamma$ -CD due to the unfavorable cavity size of the CD dimer. The second-sphere coordination is highly specific to  $[\text{AuBr}_4]^-$ . Other gold complexes (e.g.,  $[\text{AuCl}_4]^-$ ) or square planar anions of other metals, (e.g.,  $[\text{PtBr}_4]^-$  or  $[\text{PdBr}_4]^-$ ) cannot form the rod-like assembly.<sup>26</sup> Therefore this method is highly suitable for selective recovery of gold from mixed nanowaste.

The gold contained within the precipitated superstructure can be isolated by  $\text{Na}_2\text{S}_2\text{O}_5$  reduction. XRD analysis of the reduced precipitate confirmed that it contained gold along with some unidentified peaks that indicate impurities. UV-vis spectroscopy of this precipitate following dissolution in aqua regia showed that the absorbance spectrum closely matches that of chloroauric acid. ICP-MS analysis showed that the percent recoveries of gold for the three samples were 59.6%, 60.2% and 77.4%. We synthesized citrate-reduced AuNPs using this recovered gold. The AuNPs were, however, colloiddally unstable and coalesced soon after synthesis, presumably due to as yet unidentified impurities in the recovered gold. Nonetheless, the d-spacings in the diffraction patterns confirmed that the nanoparticles were AuNPs (**Figure B3**).

Nanowaste from laboratories is a complex matrix with extremely low concentrations of gold. Several parameters need to be precisely controlled for optimum recovery. For example, the co-precipitation of the rod-like supramolecular assembly is pH-dependent. In the pH range 2.5–5.9, most of the  $[\text{AuBr}_4]^-$  is bound through complexation and associated with the supramolecular assembly; the residual concentration of  $[\text{AuBr}_4]^-$  in the reaction mixture is lowest in this pH range.<sup>26</sup> Therefore, the maximum recovery of gold occurs within this pH range. Depending on the pH (and the residual concentration of  $[\text{AuBr}_4]^-$ ), the moles of  $\alpha$ -CD required for optimum recovery will vary. Consequently, depending on the concentration of gold recovered in the resuspended retentate, the moles of  $\text{Na}_2\text{S}_2\text{O}_5$  needed to precipitate and recover gold will also vary. With this information, the recovery process can be optimized for higher yields and greater purity of the recovered gold.

***LCA of AuNP recycling process.*** A schematic of the LCA models for this study are shown in **Figure 3-2A**. The life cycle impacts of four different gold recycling scenarios (0%, 10%, 50% and 90% recycling) show that recycling can significantly reduce the environmental impacts of AuNP synthesis across several impact categories. The normalized impact assessment results show that the most important impact categories are freshwater and marine eutrophication, freshwater and marine ecotoxicity, human toxicity and metal depletion. **Figure 3-2B** shows the environmental impacts in the categories of metal depletion, freshwater ecotoxicity, human toxicity and fossil fuel depletion. Scenarios involving recycling outperform the no-recycle scenario in most cases (as confirmed by uncertainty analysis; **Figure B4, B5, B6 and B7**), except for climate change potential, fossil fuel depletion and water depletion. However, based on the normalized impact assessment results, the environmental burdens of recycle scenarios in these

three impact categories were found to be negligible when compared to the benefits of recycling in other impact categories.



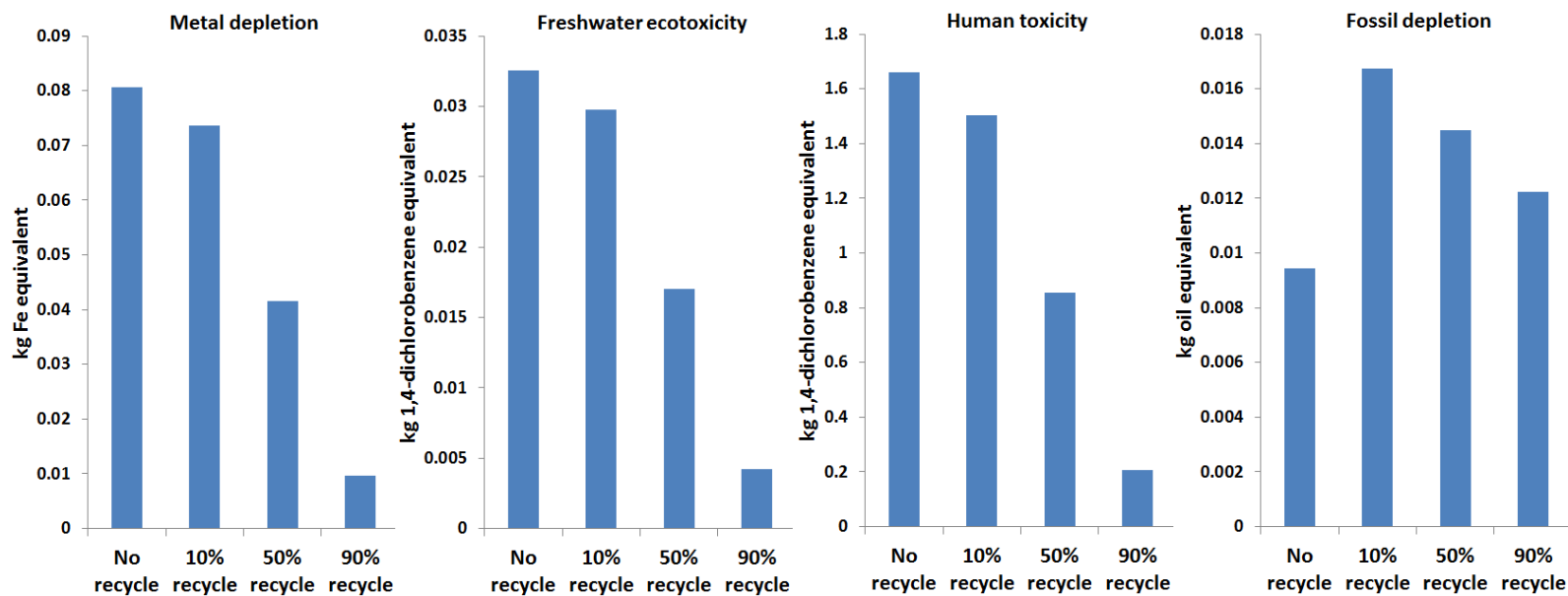
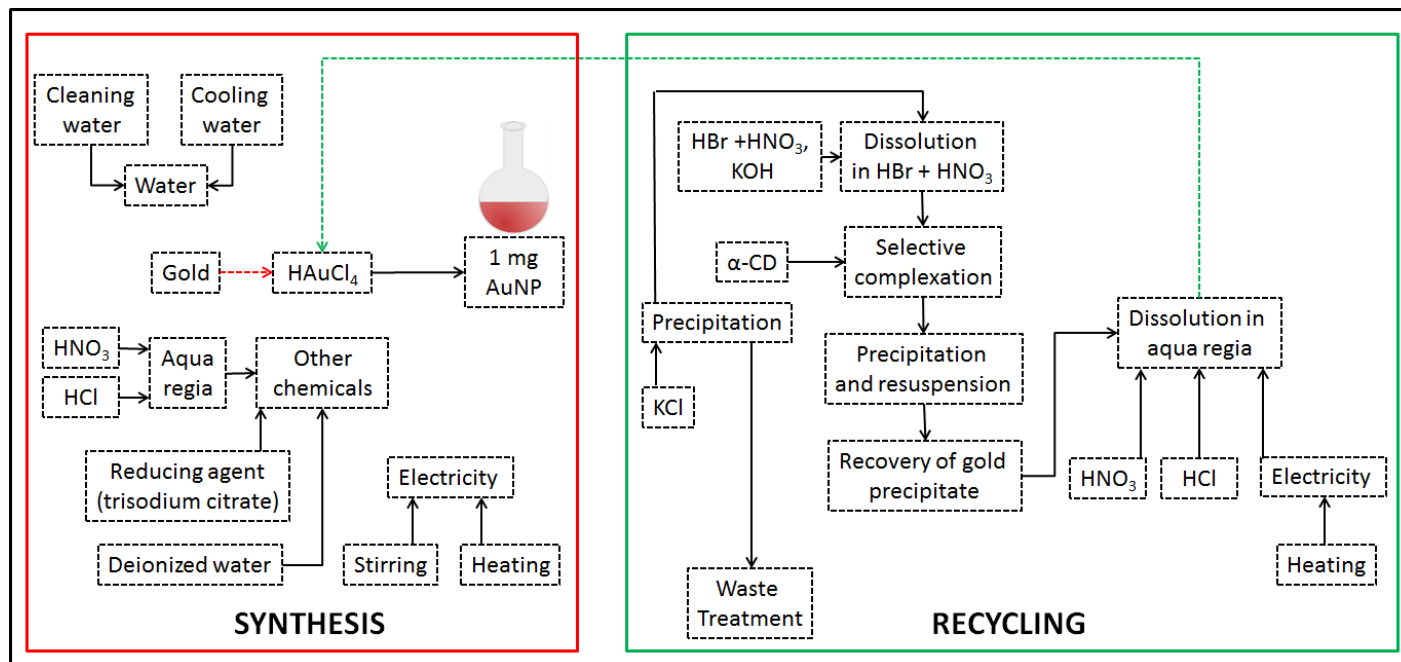


**Figure 3-2 - A** (top) Schematic of LCA model for AuNP synthesis and recycling, **B** (bottom) - Life cycle impacts of 10%-, 50%-, 90%- and no-recycle scenarios.

The high fossil fuel depletion in the recycle scenarios is due to inefficiencies in the laboratory-scale boil-off of HNO<sub>3</sub>. Currently, the dissolution of every batch of recovered gold in aqua regia and subsequent boiling are done in parallel. The energy footprint of this boiling step can be substantially reduced by first dissolving several batches of recovered gold in aqua regia and then boiling off HNO<sub>3</sub> in a single step. Further analysis of scale-up scenarios may indicate additional reductions to the energy footprint.

**Broader impacts.** With increased nanomaterial production, their waste flows will increase as well, along with the demand for raw materials. A substantial part of the increased raw material demand can be met by utilizing waste flow streams through closed-loop recycling within nano-manufacturing infrastructures. Recycling strategies such as the one we present in this paper can help mitigate the supply risk of critical raw materials in the future.<sup>39</sup> Recently there has been a surge in research on recovery and recycling of precious metals and REEs from anthropogenic waste streams<sup>40</sup> (e.g., cell- phones,<sup>41</sup> hard drives,<sup>42</sup> printed circuit boards,<sup>43</sup> liquid crystal displays,<sup>44</sup> used fluorescent lamps,<sup>45</sup> sewage sludge ash<sup>27</sup>) as well as the natural environment (e.g., seawater<sup>46</sup>). However, we must analyze recycling approaches from a life cycle perspective to identify unanticipated environmental burdens. Caballero-Guzman *et al.*<sup>47</sup> reported that current recycling approaches do not significantly increase the incorporation of recycled nanomaterials in new products or applications. LCA models can help us analyze how effectively we incorporate recovered materials into the supply chain. The novelty of our study lies in the combination of LCA modeling with an innovative approach for selective gold recovery.

As mentioned earlier, the rod-like superstructure involved in the selective recovery of gold does not form in the case of other square planar tetrahalides (e.g., [PtBr<sub>4</sub>]<sup>-</sup> or [PdBr<sub>4</sub>]<sup>-</sup>)<sup>26</sup> because the second-sphere coordination is specific to [AuBr<sub>4</sub>]<sup>-</sup>. This method can therefore be applied for

selective recovery of gold from mixed nanowaste. Although this study focused on closed-loop recycling of gold for AuNP synthesis, the separation technique can also be applied for separation, pre-concentration and open-loop recycling of gold. Moreover using this method, we can recover gold not only from nanowaste (e.g., nanoparticulate gold in spent point-of-use sensors and medical devices, bulk gold from e-waste etc.), but also from other waste streams that contain gold (e.g., e-waste). Given the growing concerns about e-waste management<sup>48</sup> and the urgent need to establish best practices<sup>49</sup>, this novel approach for recovering gold is especially important. By recovering precious metals and REEs from waste streams, we can reduce the adverse impacts of mining metals and REEs, mitigate the environmental burdens of toxic waste, decrease the cost of critical raw material procurement and improve the resilience of material supply chain.<sup>50</sup>

Current end-of-life treatment facilities may not be well-suited to handle nanowaste, because nanomaterials may differ significantly in their properties (e.g., specific heat capacities, melting temperatures etc.) compared to their corresponding bulk materials. For example, current high temperature metal recovery processes used for battery recycling may be inadequate for nano-enabled lithium ion batteries. The nanomaterials in those batteries may require smelting temperatures that are significantly higher than current operating conditions, resulting in higher energy consumptions and overall emissions.<sup>51</sup> In such cases, thermodynamic analysis based on life cycle approaches can help inform the modifications that current waste management facilities need to make when dealing with nanowaste. The life cycle considerations highlighted in this study are therefore integral to the development of future nanowaste management.

To ensure that nanotechnologies based on critical elements are sustainable in the future, we must incorporate recovery, recycling and life cycle thinking into nano-manufacturing and

nanowaste management from inception. Extant environmental regulations, however, do not address the specific challenges associated with managing nanowaste. There are no well-established practices for recovery of precious metals in nanowaste generated in laboratories. Meanwhile, universities and research laboratories rely on in-house policies for collection and disposal of nanowaste.<sup>52</sup> The results of this study are therefore timely, and can address this key gap in nanowaste management and material recovery, as well as inform future waste management policies.

## **ACKNOWLEDGEMENTS**

This work was supported by grants from the Virginia Tech Graduate School (Sustainable Nanotechnology Interdisciplinary Graduate Education Program), the Virginia Tech Institute of Critical Technology and Applied Science (ICTAS), and NSF Award CBET-1133746. Nanoparticle characterization was conducted using the facilities of the ICTAS Nanoscale Characterization and Fabrication Laboratory (NCFL). The efforts of Jennifer Kim and Leejoo Wi in gold recovery experiments, and Chris Winkler in the collection of TEM images are much appreciated. We are also grateful to Jeffrey Parks for conducting the ICP-MS analyses.

## REFERENCES

1. van Vuuren, D. P.; Strengers, B. J.; De Vries, H. J. M., Long-term perspectives on world metal use—a system-dynamics model. *Resources Policy* **1999**, *25*, (4), 239-255.
2. Gordon, R. B.; Bertram, M.; Graedel, T. E., Metal stocks and sustainability. *Proceedings of the National Academy of Sciences of the United States of America* **2006**, *103*, (5), 1209-1214.
3. Busch, J.; Steinberger, J. K.; Dawson, D. A.; Purnell, P.; Roelich, K., Managing Critical Materials with a Technology-Specific Stocks and Flows Model. *Environmental Science & Technology* **2013**.
4. Breggin, L.; Pendergrass, J. PEN 10 - Where Does the Nano Go? End-of-Life Regulation of Nanotechnologies. <http://www.wilsoncenter.org/publication/pen-10-where-does-the-nano-go-end-life-regulation-nanotechnologies>
5. Musee, N., Nanowastes and the environment: Potential new waste management paradigm. *Environment International* **2011**, *37*, (1), 112-128.
6. Shibayama, A.; Takasaki, Y.; Haga, K.; Umeda, H.; Sasaki, A.; Takahashi, K. In *Metal recovery from effluent water of metallurgical refining processes by cementation and solvent extraction*, 2009, 2009; GDMB-Informationsgesellschaft: 2009; pp 375-384.
7. Badawy, N.; Rabah, M. A.; Hasan, R., Separation of some heavy metal species from electroplating rinsing solutions by ion exchange resin. *International Journal of Environment and Waste Management* **2013**, *12*, (1), 33-51.
8. Zhang, L.; Qiu, L. X.; Xi, X. L.; Ma, L. W.; Zhang, L. W.; Wang, Z. H.; Zhou, J. F. In *Recovery of copper from waste printed circuit boards by suspension electrolysis*, 2013, 2013; Trans Tech Publications Ltd: 2013; pp 452-455.
9. Gomez, E.; Rani, D. A.; Cheeseman, C. R.; Deegan, D.; Wise, M.; Boccaccini, A. R., Thermal plasma technology for the treatment of wastes: A critical review. *Journal of Hazardous Materials* **2009**, *161*, (2–3), 614-626.
10. Gadd, G. M., Bioremediation potential of microbial mechanisms of metal mobilization and immobilization. *Current Opinion in Biotechnology* **2000**, *11*, (3), 271-279.
11. Volesky, B., Detoxification of metal-bearing effluents: biosorption for the next century. *Hydrometallurgy* **2001**, *59*, (2–3), 203-216.
12. Myakonkaya, O.; Guibert, C. m.; Eastoe, J.; Grillo, I., Recovery of Nanoparticles Made Easy. *Langmuir* **2010**, *26*, (6), 3794-3797.

13. Zhuang, Z.; Xu, X.; Wang, Y.; Wang, Y.; Huang, F.; Lin, Z., Treatment of nanowaste via fast crystal growth: With recycling of nano-SnO<sub>2</sub> from electroplating sludge as a study case. *Journal of Hazardous Materials* **2012**, *211–212*, 414-419.
14. Chen, Z.; Zhuang, Z.; Cao, Q.; Pan, X.; Guan, X.; Lin, Z., Adsorption-Induced Crystallization of U-Rich Nanocrystals on Nano-Mg(OH)<sub>2</sub> and the Aqueous Uranyl Enrichment. *ACS Appl. Mater. Interfaces* **2013**.
15. Liu, J.-f.; Chao, J.-b.; Liu, R.; Tan, Z.-q.; Yin, Y.-g.; Wu, Y.; Jiang, G.-b., Cloud Point Extraction as an Advantageous Preconcentration Approach for Analysis of Trace Silver Nanoparticles in Environmental Waters. *Analytical Chemistry* **2009**, *81*, (15), 6496-6502.
16. Liu, J.-f.; Liu, R.; Yin, Y.-g.; Jiang, G.-b., Triton X-114 based cloud point extraction: a thermoreversible approach for separation/concentration and dispersion of nanomaterials in the aqueous phase. *Chemical Communications* **2009**, (12), 1514-1516.
17. Mustafina, A. R.; Elistratova, J. G.; Bochkova, O. D.; Burilov, V. A.; Fedorenko, S. V.; Konovalov, A. I.; Soloveva, S. Y., Temperature induced phase separation of luminescent silica nanoparticles in Triton X-100 solutions. *Journal of Colloid and Interface Science* **2011**, *354*, (2), 644-649.
18. Nazar, M. F.; Shah, S. S.; Eastoe, J.; Khan, A. M.; Shah, A., Separation and recycling of nanoparticles using cloud point extraction with non-ionic surfactant mixtures. *Journal of Colloid and Interface Science* **2011**, *363*, (2), 490-496.
19. Frimmel, H. E., Earth's continental crustal gold endowment. *Earth and Planetary Science Letters* **2008**, *267*, (1–2), 45-55.
20. Mudd, G. M., Global trends in gold mining: Towards quantifying environmental and resource sustainability. *Resources Policy* **2007**, *32*, (1–2), 42-56.
21. Schodde, R. In *Recent trends in gold discovery*, NewGenGold Conference, 2011/11/22/23, 2011; 2011.
22. Kerr, R. A., Is the World Tottering on the Precipice of Peak Gold? *Science* **2012**, *335*, (6072), 1038-1039.
23. Starr, M.; Tran, K., Determinants of the physical demand for gold: Evidence from panel data. *The World Economy* **2008**, *31*, (3), 416-436.
24. Roco, M.; Mirkin, C.; Hersam, M., Nanotechnology research directions for societal needs in 2020: summary of international study. *Journal of Nanoparticle Research* **2011**, *13*, (3), 897-919.
25. Wiek, A.; Gasser, L.; Siegrist, M., Systemic scenarios of nanotechnology: Sustainable governance of emerging technologies. *Futures* **2009**, *41*, (5), 284-300.

26. Liu, Z.; Frascioni, M.; Lei, J.; Brown, Z. J.; Zhu, Z.; Cao, D.; Iehl, J.; Liu, G.; Fahrenbach, A. C.; Botros, Y. Y.; Farha, O. K.; Hupp, J. T.; Mirkin, C. A.; Fraser Stoddart, J., Selective isolation of gold facilitated by second-sphere coordination with  $\alpha$ -cyclodextrin. *Nature Communications* **2013**, *4*.
27. Kakumazaki, J.; Kato, T.; Sugawara, K., Recovery of Gold from Incinerated Sewage Sludge Ash by Chlorination. *ACS Sustainable Chem. Eng.* **2014**.
28. Stenson, J., Disaster management as a tool for sustainable development: a case study of cyanide leaching in the gold mining industry. *Journal of Cleaner Production* **2006**, *14*, (3–4), 230-233.
29. Malm, O., Gold Mining as a Source of Mercury Exposure in the Brazilian Amazon. *Environmental Research* **1998**, *77*, (2), 73-78.
30. Guinée, J. B.; Heijungs, R.; Huppes, G.; Zamagni, A.; Masoni, P.; Buonamici, R.; Ekvall, T.; Rydberg, T., Life Cycle Assessment: Past, Present, and Future†. *Environmental Science & Technology* **2011**, *45*, (1), 90-96.
31. Pati, P.; McGinnis, S.; Vikesland, P. J., Life Cycle Assessment of “Green” Nanoparticle Synthesis Methods. *Environmental Engineering Science* **2014**.
32. Frens, G., Controlled Nucleation for the Regulation of the Particle Size in Monodisperse Gold Suspensions. *Nature* **1973**, *241*, (105), 20-22.
33. APHA, American Public Health Association, American Water Works Association, and Water Environment Federation. *Standard Methods for the Examination of Water and Wastewater*. **1998**.
34. Frischknecht, R.; Jungbluth, N.; Althaus, H.-J.; Doka, G.; Dones, R.; Heck, T.; Hellweg, S.; Hischer, R.; Nemecek, T.; Rebitzer, G., The ecoinvent database: Overview and methodological framework (7 pp). *The International Journal of Life Cycle Assessment* **2005**, *10*, (1), 3-9.
35. Goedkoop, M.; Heijungs, R.; Huijbregts, M.; De Schryver, A.; Struijs, J.; van Zelm, R., ReCiPe 2008. *A life cycle impact assessment method which comprises harmonised category indicators at the midpoint and the endpoint level* **2009**, *1*.
36. Liu, Y.; Li; Zhang, H.-Y.; Zhao, Y.-L.; Wu, X., Bis(pseudopolyrotaxane)s Possessing Copper(II) Ions Formed by Different Polymer Chains and Bis( $\beta$ -cyclodextrin)s Bridged with a 2,2'-Bipyridine-4,4'-Dicarboxy Tether. *Macromolecules* **2002**, *35*, (27), 9934-9938.
37. Liu, Y.; Zhao, Y.-L.; Zhang, H.-Y.; Song, H.-B., Polymeric Rotaxane Constructed from the Inclusion Complex of  $\beta$ -Cyclodextrin and 4,4'-Dipyridine by Coordination with Nickel(II) Ions. *Angewandte Chemie International Edition* **2003**, *42*, (28), 3260-3263.
38. Szejtli, J., Introduction and General Overview of Cyclodextrin Chemistry. *Chemical Reviews* **1998**, *98*, (5), 1743-1754.

39. Rademaker, J. H.; Kleijn, R.; Yang, Y., Recycling as a Strategy against Rare Earth Element Criticality: A Systemic Evaluation of the Potential Yield of NdFeB Magnet Recycling. *Environmental Science & Technology* **2013**.
40. Tan, Q.; Li, J., Recycling Metals from Wastes: A Novel Application of Mechanochemistry. *Environmental Science & Technology* **2015**, *49*, (10), 5849-5861.
41. Navazo, J. M. V.; Méndez, G. V.; Peiró, L. T., Material flow analysis and energy requirements of mobile phone material recovery processes. *The International Journal of Life Cycle Assessment*, 1-13.
42. Sprecher, B.; Kleijn, R.; Kramer, G. J., Recycling Potential of Neodymium: The Case of Computer Hard Disk Drives. *Environmental Science & Technology* **2014**.
43. Wang, J.; Xu, Z., Disposing and Recycling Waste Printed Circuit Boards: Disconnecting, Resource Recovery, and Pollution Control. *Environmental Science & Technology* **2014**.
44. Zeng, X.; Wang, F.; Sun, X.; Li, J., Recycling Indium from Scraped Glass of Liquid Crystal Display: Process Optimizing and Mechanism Exploring. *ACS Sustainable Chem. Eng.* **2015**.
45. Yang, F.; Kubota, F.; Baba, Y.; Kamiya, N.; Goto, M., Selective extraction and recovery of rare earth metals from phosphor powders in waste fluorescent lamps using an ionic liquid system. *Journal of Hazardous Materials* **2013**, *254-255*, (1), 79-88.
46. Diallo, M. S.; Kotte, M. R.; Cho, M., Mining Critical Metals and Elements from Seawater: Opportunities and Challenges. *Environmental Science & Technology* **2015**.
47. Caballero-Guzman, A.; Sun, T.; Nowack, B., Flows of engineered nanomaterials through the recycling process in Switzerland. *Waste Management*.
48. Zhang, K.; Schnoor, J. L.; Zeng, E. Y., E-Waste Recycling: Where Does It Go from Here? *Environmental Science & Technology* **2012**, *46*, (20), 10861-10867.
49. Li, J.; Zeng, X.; Chen, M.; Ogunseitan, O. A.; Stevels, A., "Control-Alt-Delete": Rebooting Solutions for the E-Waste Problem. *Environmental Science & Technology* **2015**, *49*, (12), 7095-7108.
50. Sprecher, B.; Daigo, I.; Murakami, S.; Kleijn, R.; Vos, M.; Kramer, G. J., Framework for Resilience in Material Supply Chains, With a Case Study from the 2010 Rare Earth Crisis. *Environmental Science & Technology* **2015**, *49*, (11), 6740-6750.
51. Olapiriyakul, S.; Caudill, R. J., Thermodynamic Analysis to Assess the Environmental Impact of End-of-life Recovery Processing for Nanotechnology Products. *Environmental Science & Technology* **2009**, *43*, (21), 8140-8146.
52. Hallock, M. F.; Greenley, P.; DiBerardinis, L.; Kallin, D., Potential risks of nanomaterials and how to safely handle materials of uncertain toxicity. *Journal of Chemical Health and Safety* **2009**, *16*, (1), 16-23.



## Chapter 4

# Bleeding from a Thousand Paper Cuts: Avoiding Dissipative Losses of Critical Elements by Recycling Nanomaterial Waste Streams

*Paramjeet Pati,<sup>1,2,3</sup> Sean McGinnis,<sup>2,4</sup> and Peter J. Vikesland<sup>1,2,3\*</sup>*

<sup>1</sup>Civil and Environmental Engineering, Virginia Tech

<sup>2</sup>Virginia Tech Institute of Critical Technology and Applied Science (ICTAS) Sustainable Nanotechnology Center (VTSuN)

<sup>3</sup>Center for the Environmental Implications of Nanotechnology (CEINT), Duke University

<sup>4</sup>Department of Material Science and Engineering, Virginia Tech

\*Corresponding author. Phone: (540) 231-3568, Email: [pvikes@vt.edu](mailto:pvikes@vt.edu)

### ABSTRACT

Critical materials such as precious metals and rare earth elements are integral to the development of new technologies. However, uncertainties about the future availability of critical materials raise questions about the sustainable growth and development of promising technologies. Nanotechnology is one such technology that relies on critical materials. Commercial-scale applications of nanotechnology are on the rise today. The rapid proliferation of nanotechnology into electronics, consumer products and lab-on-chip applications suggests that the demand for critical materials in the nano-manufacturing industry will continue to increase. Given the potential supply risks associated with critical materials, their recovery from waste streams is of paramount importance. Without early incorporation of recycling strategies into nano-manufacturing practices, critical materials in nanomaterial waste streams and discarded nano-enabled products will result in dissipative losses from the material cycle. It is therefore essential to develop strategies to recover high-value, resource-limited materials from nanowaste. In this review, we discuss some key challenges related to recycling; highlight recent

developments in selective recovery of precious metals and rare earths; and, identify opportunities for using waste streams as secondary sources of critical materials.

## INTRODUCTION

Critical elements such as noble metals, platinum group elements (PGMs) and rare earth elements (REEs) wield great influence over societal prosperity and environmental sustainability. In our interconnected world, a nation's prosperity depends on successfully developing, adopting and implementing novel technologies. These technologies in turn are intimately tied to the reliable supply of several noble metals, PGMs and REEs. Our planet's endowment of these critical elements, however, is finite. Uncertainties about their availability loom large as our desire for sustainable growth and development clashes with the realities of our limited resources and their unsustainable consumption. A business-as-usual approach threatens the continued development of next-generation technologies. Nanotechnology is one such promising technology that strongly depends on high-value, critical elements. Recent studies have estimated dramatic increases in the demand for REEs required for emerging green technologies.<sup>1</sup> Poised today for exponential growth, nanotechnology's demand for high purity critical elements will similarly increase in the near future.

*Nanotechnology powered by critical materials.* Nanotechnology is an *enabling* technology with enormous potential to transform a wide variety of sectors, e.g., energy, electronics, transportation, healthcare, pharmaceuticals, environmental monitoring, and national security. Much of the promise of nanotechnology for revolutionary and transformative improvements lies in the unique properties of critical materials that impart novel optical, photothermal and catalytic properties<sup>2-4</sup> when used as nanoparticles or as dopants in nanocomposites.<sup>5-10</sup> For example,

nanocomposites comprised of indium oxide nanoparticles and carbon nanotubes showed superior sensitivity for ammonia gas sensing at room temperature, thus offering an improvement over conventional ammonia gas sensors, which have limited maximum sensitivity and require high operating temperatures.<sup>11</sup> Besides ammonia, indium oxide nanoparticles can also be used as gas sensors for carbon monoxide and nitrogen dioxide.<sup>12</sup> Terbium-doped CdS and ZnO nanoparticles have been reported to exhibit enhanced luminescence,<sup>10,13,14</sup> and terbium nanoparticles when used as biolabels for DNA assays, showed a 100-fold increase in detection sensitivity<sup>15</sup>. Slow oxygen reduction reaction (ORR) kinetics on platinum catalysts is currently a key limiting factor in the energy conversion efficiency of membrane fuel cells.<sup>16</sup> Tantalum nanoparticles can help overcome this limitation as they have been shown to enhance the ORR kinetics.<sup>17</sup>

Nano-sized yttrium iron garnets (YIG)<sup>18</sup> and yttrium aluminum garnets (YAG)<sup>19</sup> are used for developing new magneto-optical devices. Nano-structured palladium- and yttrium-doped ZrO<sub>2</sub> electrodes<sup>18</sup> have been developed as cathodes of intermediate temperature solid oxide fuel cells (IT-SOFCs).<sup>9</sup> Europium nanoparticles were also used as nano-labels in the successful detection and bio-imaging of *Giardia lamblia* in environmental water samples.<sup>20</sup> Other applications of critical material-based environmental monitoring tool are thorium-enabled nanocomposites used in ion-selective membrane electrodes for mercury detection.<sup>21</sup> Luminescent properties of neodymium ion in combination with nanocrystals (e.g., CaTiO<sub>3</sub> nanocrystals<sup>22</sup>) hold promise for advanced photonic applications. Neodymium doped NaYF<sub>4</sub> nanoparticles used as optical temperature sensors.<sup>23</sup> Nanoparticles doped with neodymium hold promise as sub-tissue optical probes because the emission band spectrum of neodymium overlaps with the transparency windows of human tissues (e.g., neodymium-doped LaF<sub>3</sub> core/shell nanoparticles).<sup>24</sup>

The rapid progress made in developing novel nano-enabled devices and their current growth trends<sup>25,26</sup> hint at a future where most of the devices we will have may be in some ways have enhanced functionality. Be it smarter credit cards,<sup>27,28</sup> biometrics,<sup>29</sup> batteries,<sup>30</sup> light emitting diodes,<sup>31,32</sup> or antimicrobial clothing,<sup>33</sup> nanotechnology is poised to permeate every aspect of our daily lives. Miniaturized, multifunctional, and smart devices with enhanced sensitivity and ultra-low power consumption will soon find their way into our homes, desks, and pockets. Bottom-up nano-manufacturing through self-assembly offers unique advantages. Nanoscale memory architectures based on self-assembly allow for substantial miniaturization in nanoelectronics<sup>34,35</sup> due to high packing density and superior performance while consuming less power. Moreover, these nano-enabled devices themselves may be powered by wearable nanogenerators<sup>36</sup> and human-interactive photodetectors<sup>37</sup> made possible by critical materials such as gallium and indium. Other examples of critical materials in nanotechnologies include europium<sup>38</sup> and yttrium<sup>39,40</sup> in anti-reflective displays; silver in photovoltaics,<sup>41</sup> photocatalytic systems<sup>42</sup> and organic light emitting diodes;<sup>32</sup> samarium and praseodymium in photocatalytic systems;<sup>43</sup> gadolinium in multicolor displays;<sup>44</sup> ruthenium in solar cells;<sup>45-47</sup> gold in nano-enabled environmental monitoring;<sup>48,49</sup> platinum in fuel cells,<sup>3,50</sup> palladium in gas sensing,<sup>51</sup> gallium in optoelectronics;<sup>52</sup> europium in drug-delivery<sup>53</sup> and bio-imaging;<sup>7,20</sup> indium in in-vivo bio-imaging;<sup>54</sup> germanium<sup>55,56</sup> and tellurium<sup>57</sup> in chip-technologies for nanoelectronics; terbium in bioassays<sup>15</sup> and fingerprint detection technologies;<sup>58</sup> and dysprosium in white LEDs;<sup>59,60</sup> tantalum in biomedical applications;<sup>61</sup> and neodymium in permanent magnets,<sup>62</sup> optical temperature sensing<sup>23</sup> and sub-tissue thermal imaging.<sup>24</sup>

***Sustainability of nanotechnologies dependent on critical materials.*** Sustainability has emerged as a design criterion in nano-manufacturing.<sup>63-65</sup> Discussions on the sustainability of

nanotechnologies have mostly been focused on environmental implications and applications. Nanotechnology's dependence on critical elements and the recycling of noble metals, rare earth elements and platinum group metals from nanomaterial waste streams has been relatively underexplored. The realization of nanotechnology's enormous potential is integrally tied to the reliable supply of high-purity critical materials in the future. We therefore need rigorous book-keeping of material flows of critical elements used in various nanotechnologies and quantify the uncertainties therein.

Combined with the planet's growing population and the upward mobility and buying power of consumers, the demand for nano-enabled products and applications will continue to increase. These factors, combined with the rapid proliferation of nanotechnology into electronics, consumer products, point-of-care applications in medicine and environmental monitoring etc. indicate that use for critical materials for the nano-industry will grow rapidly. Dependence on imports, price fluctuations and supply risks of critical materials will threaten the in-house development and commercialization of next-generation, transdisciplinary nano-bio-info-cogno technologies,<sup>66,67</sup> as well as the ability to participate in the growing global nanotechnology economy. Therefore, dynamic material flow analyses of critical materials used in nanotechnology are urgently required.

***Material flows in nanotechnology.*** The material flows of bulk metals (e.g., lithium,<sup>68</sup> aluminum,<sup>69,70</sup> nickel,<sup>71</sup> copper,<sup>72,73</sup> and silver<sup>74</sup>) and rare earth elements<sup>75</sup> have been reported. Other studies have focused on material flows related to specific products (e.g., cellphones,<sup>76</sup> hard-drives, waste electrical and electronic components (WEEE),<sup>77-79</sup> display screens,<sup>80</sup> passenger cars<sup>81</sup> etc.), Several researchers have raised concerns about the unsustainable use of metals.<sup>82-86</sup> With the declining global reserves of high-value metals,<sup>72,87,88</sup> the recovery and

recycling of precious metals and rare earth elements is of paramount importance. Nanotechnology relies heavily on the reliable supplies of critical materials that are limited in resource and are becoming increasingly difficult to mine. For example, gold ore grades have declined over the last decade,<sup>89</sup> the cost of extracting gold has steadily increased,<sup>90</sup> and there are concerns about having surpassed peak gold.<sup>82</sup> Although nanomaterials have been part of regional and global material cycles for many years, their flows have only recently started to be quantified.<sup>91-99</sup> The initial focus of nanomaterial flows has been on the health and environmental implications of nanomaterials in treated waste streams, and dissipative losses of critical materials have not received as much attention. Initial estimations of nanomaterial mass flows involve large uncertainties and require further research for developing dynamic material flow models, with a special focus in critical materials. The inventory data for many nanotechnologies is proprietary, and initial estimates of nanotechnology-related material flows have largely relied on stochastic analysis and modeling<sup>94,99,100</sup> instead of primary (measured) data. Nonetheless, recent studies on nanomaterial release suggest that residual nanomaterials in the treated waste may be released into the environment,<sup>93,101,102</sup> which might contribute to dissipative losses of critical materials. Due to the data and knowledge gaps, industries and policy-makers may meet challenges related to nanomaterial waste flows reactively rather than proactively,<sup>103</sup> thus making it difficult to form long-term policies for producing, trading and recycling critical materials. Determining nanomaterial waste flows is therefore an urgent research need, especially with regard to dissipative losses of critical materials.

Nanomaterials may be found in a variety of waste streams, e.g., silver nanoparticles in wastewater after leaching from antimicrobial textiles,<sup>104,105</sup> or carbon nanotubes (in lithium-ion batteries)<sup>106</sup> in battery recycling smelters. Recycling strategies will therefore need to be tailored

for specific waste streams and nanomaterials of interest. Before discussing potential recycle approaches for waste streams containing nanomaterials, it is important to understand that some waste streams may be more amenable for separation, concentration and recycling than others, and that information should guide product design to embrace recyclability. For example, TiO<sub>2</sub> nanoparticles in toothpaste<sup>107</sup> or gold nanoparticles in skin cream<sup>108</sup> are likely to contribute minor dissipative losses<sup>109</sup> of titanium and gold from their respective anthropogenic metal cycles, thus evading recycle. These dissipative losses may be substantial over time because they will scale with access and buying power of a growing population. On the other hand, critical materials in some nano-enabled products, e.g., indium tin oxide nanoparticles in display screens or LEDs<sup>31</sup> may be more amenable for selective recovery made possible by pre-processing steps (i.e., disassembly and separation) followed by selective absorption of indium chloro complex onto anion exchange resin after acid leaching,<sup>110</sup> or by nanofiltration combined with liquid-liquid extraction (**Figure 4-1**).<sup>111</sup> Although display screens are not designed with easy recyclability of indium in mind, modular construction of display screens can make separation of parts from used display screens easier and recovery of indium possible, compared to separating titanium from used toothpaste. It is also important to note that at the end of the use-phase or during the end-of-life phase, the critical material in nano-enabled product may no longer be nanoparticulate, and may no longer exhibit the novel ('enabling') properties, and traditional recycling approaches may be applicable. Nonetheless, a robust quantitative assessment of critical material flows would help in identifying potential dissipative losses.

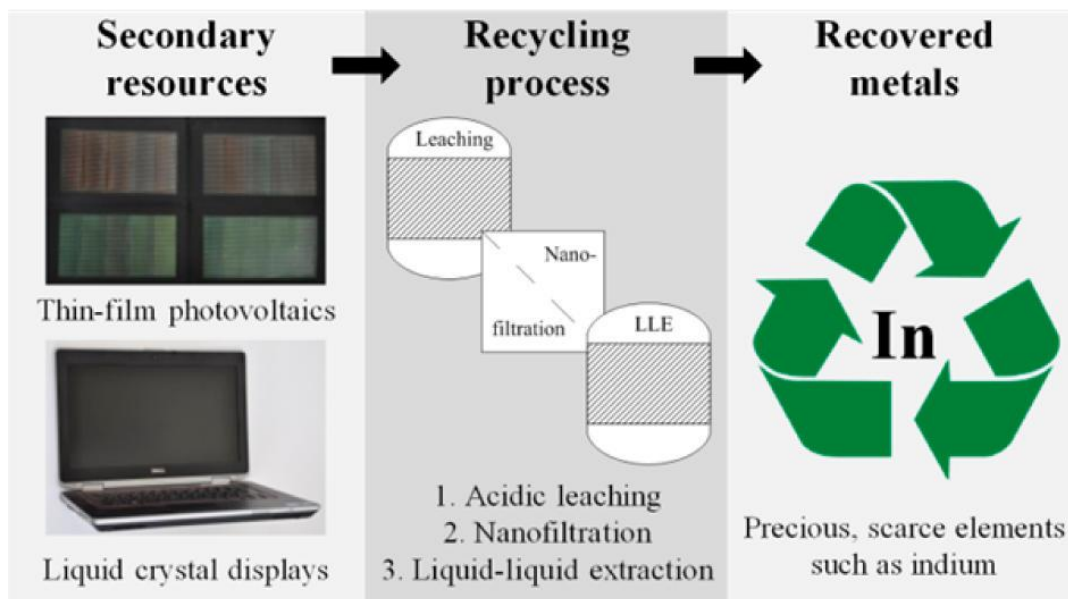


**Figure 4-1** - Novel method for recycling indium from secondary sources such as display screens of used electronics and spent solar cells. Reprinted (adapted) with permission from Zimmermann, Y.-S.; Niewersch, C.; Lenz, M.; Kül, Z. Z.; Corvini, P. F. X.; Schäffer, A.; Wintgens, T., *Recycling of Indium From CIGS Photovoltaic Cells: Potential of Combining Acid-Resistant Nanofiltration with Liquid-Liquid Extraction*. Environmental Science & Technology 2014. Copyright (2014) American Chemical Society.

## RECYCLING CRITICAL MATERIALS

In addition to quantifying industry-specific, regional and global flows of critical materials used in nanotechnology, recovery and recycling strategies must be integrated into nanomanufacturing from the start. A variety of approaches for recovering critical materials from conventional waste streams have been reported, which can inform future recycling strategies for nanomaterial wastes. Examples of critical material recovery include cloud point extraction<sup>112</sup>, selective complexation<sup>113</sup>, and magnetic recovery<sup>114</sup> (gold); Smopex<sup>®</sup> metal scavenging<sup>115</sup>, bioreduction<sup>116,117</sup> and biosorption<sup>118</sup> (palladium); pyrometallurgical recovery<sup>119</sup> and anion



exchange<sup>110</sup> (indium); selective acid leaching followed solvent extraction and precipitation<sup>120</sup> (neodymium); hydrometallurgical recovery from waste sludge<sup>121</sup> (dysprosium); and selective extraction using ionic liquids<sup>122</sup> (europium). Additional separation and recovery approaches are listed in **Table C1** (*Appendix C*).

Recent studies have reported novel approaches for recovering high-value materials from nanomaterial wastes. Nano-SnO<sub>2</sub> was selectively recovered from industrial electroplating waste sludge using the selective crystallization and growth of acid-soluble amorphous SnO<sub>2</sub> into acid-insoluble SnO<sub>2</sub> nanowires.<sup>123</sup> Adsorption-induced crystallization of uranium rich nanocrystals was used for uranyl enrichment.<sup>124</sup> Thermo-reversible liquid-liquid phase transition<sup>125</sup> and cloud point extraction<sup>126-129</sup> also hold promise for the successful separation and recovery of critical materials from nanowaste. Waste treatment facilities can employ metal detection, sequestration and removal approaches borrowed from water treatment and environmental contaminant detection and analysis techniques.<sup>126,130-133</sup> Trace metal separation methods can be employed to recover critical materials using recently reported novel chemistries.<sup>113,126,133,134</sup> Pairing these new recovery approaches with appropriate nanomaterial waste streams can help design anthropogenic nanomaterial flows with recycling built into the process flow.

An example of future nano-enabled application of critical materials in mass-produced consumer products is smart clothing.<sup>135,136</sup> Wearable technologies that combine electronic textiles<sup>137,138</sup> with wearable nanoelectronics<sup>35,56,139</sup> and nanogenerators<sup>30,36</sup> can have wide-ranging applications. Nanopiezoelectronics and sensors<sup>140</sup> integrated into smart fabrics can open up new ways of biomonitoring (e.g., heart rate, electrocardiogram (ECG) measurements, breathing rates etc.) and replace traditional adhesive based electrodes used in hospitals and ambulances. Nano-enabled smart fabrics can be used to develop miniaturized, low-cost wearable

assistive to technologies for people with disabilities. Athletic clothing made from e-textiles and nanoelectronics can be used as personal fitness trackers. Miniaturization offered by nanoelectronics can allow for new ways of integrating wireless communication devices and audio-video players with smart fabrics. Given the popularity of consumer electronics today (e.g., cellphones and MP3 players) it is not difficult to imagine the potential mass adoption of these wearable technologies driven by both functionality and fashion.

Other examples of nano-enabled products that can be paired with appropriate novel recycling methods are lab-on-chip<sup>141-145</sup> and point-of-care<sup>146-148</sup> devices that rely on critical materials, e.g., gold and silver (**Figure 4-2**).

These devices may use extremely small amounts of critical materials, but may be mass-produced and find large-scale applications in diagnostics<sup>149,150</sup> and environmental monitoring.<sup>48,151,152</sup> When combined with wearable electronics augmented with wireless communication technologies, these point-of-care devices can assist in early detection and warning of contagious outbreaks<sup>153</sup>. It is important to note that these point-of-care devices might often be discarded after a single-use. If material recovery is not planned ahead for these devices, they can contribute

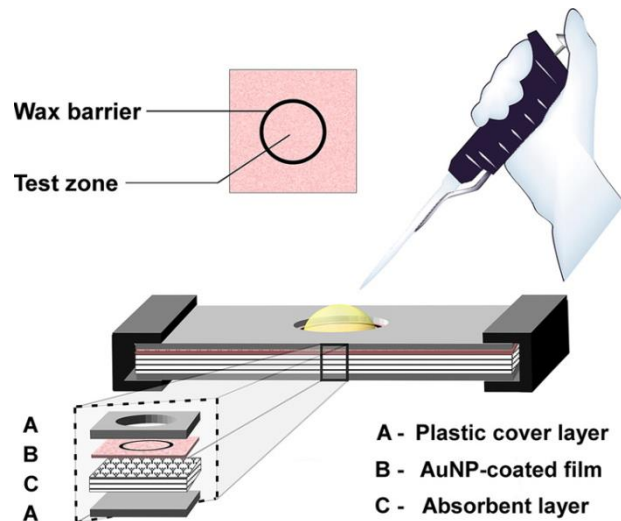


**Figure 4-2** - Lab-on-chip devices as potential sources of recyclable critical materials. These devices may be discarded after a single use, and hence contribute to dissipative losses if they are not recycled. This figure shows a paper-based device for colorimetric detection of NADH in a microliter-scale sample in less than 4 min. The device consists of an upper plastic cover layer with a hole exposing the test zone, a wax-circled gold nanoparticle (AuNP) coated paper with a cotton absorbent layer. The detection time was < 4 minutes. Reprinted (adapted) with permission from Liang, P.; Yu, H.; Guntupalli, B.; Xiao, Y., *Paper-Based Device for Rapid Visualization of NADH Based on Dissolution of Gold Nanoparticles*. ACS Appl. Mater. Interfaces 2015. Copyright (2015) American Chemical Society.

substantial dissipative losses over time. Therefore, the disposal of such nano-enabled products must necessarily involve selective recovery and recycling strategies.

Conventional recycling methods, however, have some drawbacks. For example, pyrometallurgical methods require high temperatures and are energy-intensive. Similarly, selective acid leaching and solvent extraction involve strong acids and toxic solvents, generating large amounts of hazardous chemical wastes which pose substantial health and environmental risks. Moreover, when applying these recycling approaches to nanomaterial wastes, we face some unique challenges. The dilute quantities of critical elements and their high degree of mixing in a complex matrix of different nanomaterial wastes hinder selective recovery and recycling. Current waste management approaches and treatment facilities may be inadequate for treating nanowaste, because nanomaterials may have significantly different physicochemical properties compared to bulk materials. For example, nano-enabled lithium ion batteries may require much higher smelting temperatures compared to current operating conditions.<sup>154</sup> Therefore thermodynamic analyses,<sup>154,155</sup> information theory<sup>156</sup> and life cycle approaches<sup>157</sup> are needed to inform the modifications that current waste management facilities need to make when dealing with nanowaste, as well as to inform next-generation waste treatment strategies. Without proper analysis of the life cycle and thermodynamic considerations, recovery approaches may not significantly increase the incorporation of recycled nanomaterials in new products or applications.<sup>102</sup>

## **CHALLENGES AND CONSIDERATIONS IN RECYCLING NANOWASTE**

When developing recycling strategies for nanomaterial waste streams, it is important to note recyclability has not been a core focus of product design paradigms. In fact, product design has increasingly shifted towards using less recyclable materials.<sup>156</sup> Three key factors make recycling

critical elements from nanomaterial waste streams challenging: high degree of mixing, miniaturization and dilution. For recycling to be profitable, the financial gains from obtaining the recycled material should exceed the cost of interim steps (separation, collection, processing). Modern products have a higher degree of mixing of critical raw materials, making separation increasingly difficult (**Figure 4-3**), thereby raising the cost of these interim steps. Miniaturization of modern products (e.g., laptop computers) also decreases the value of the recycled material *per unit* (i.e., per laptop),<sup>156</sup> which further diminishes the economic incentives for recycling. Also, critical materials may form a small fraction of the overall nanomaterial waste stream, and from a thermodynamic standpoint, the work required to separate a critical material from a mixture monotonically increases as the mixture becomes more dilute.<sup>155</sup> These three factors (i.e., degree of mixing, miniaturization, and dilution) must therefore be considered when developing strategies and policies for recycling nanomaterial waste streams.

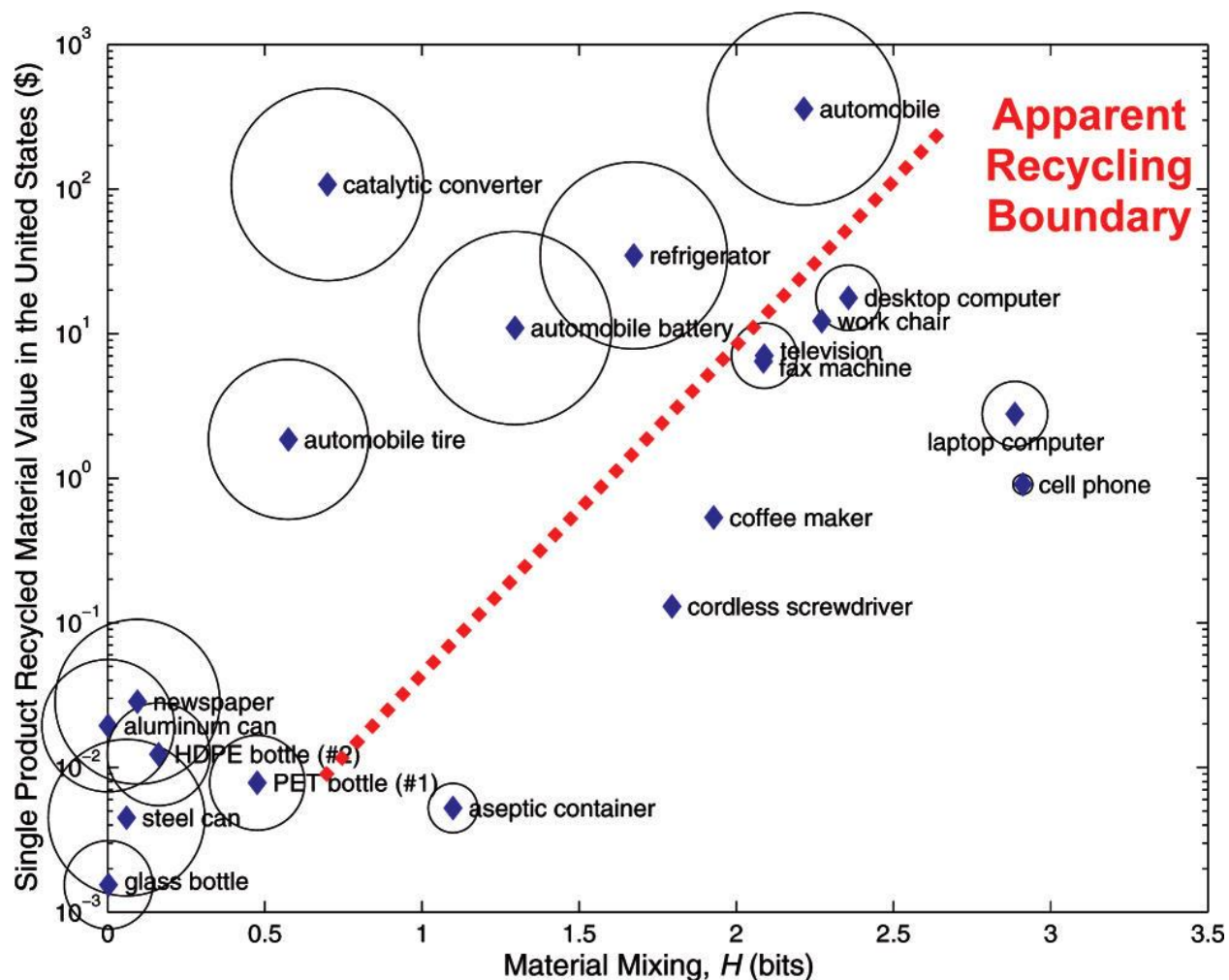


**Figure 4-3** - Material values (y-axis), material mixing (x-axis) and recycling rates (areas of individual circles) for products. Larger circles imply higher recycling rates. Products with no circles are assumed to have recycling rates of zero. The material mixing, denoted by  $H$ , is the average number of binary separation steps required to extract any material from the mixture, and is higher for complex products. As seen from this figure, products with high recycling rates are clustered in the upper left corner, and the products with the very low recycling rates are in the lower right. This trend is particularly sharp for products with  $H > 0.5$ , where the recycling rates range from 66 to 96% in the upper left, and from 0 to 11% in the lower right. The authors of the original work marked the transition zone between them with a line labeled “apparent recycling boundary”. Similar modeling approaches for nano-enabled products can help in identifying the more recyclable products. This information can help in making decision when prioritizing the use of critical materials in specific products. Reprinted (adapted) with permission from Dahmus, J. B.; Gutowski, T. G., *What Gets Recycled: An Information Theory Based Model for Product Recycling*. Environmental Science & Technology 2007. Copyright (2007) American Chemical Society.

The heterogeneity of waste containing nano-enabled products is another complication. Material flows interweave. The mining, refining and recycling of earth-abundant metals, noble metals, platinum group metals and rare earths are interconnected, and the challenges in their production and recycling cannot be considered independently of each other<sup>158</sup>. Similarly, in the case of nano-enabled products, critical elements may be considered as co-products or even impurities if the recycling is focused on extracting other components in the waste mixture. For example, in the case of smart clothing, the nanoelectronics can hinder the recyclability of the textiles<sup>138</sup> by being dispersed as a contaminant in the heterogeneous mixture. Nonetheless, innovations in separation techniques in the end-of-life phase of nano-enabled products can help circumvent this issue.<sup>159</sup>

Intersecting and interwoven material flows must be taken into account when making decisions for implementing recycling strategies for nanowaste. As mentioned earlier, data gaps and uncertainties can make such decision-making reactive instead of proactive. To inform decisions on recycling, a key research need is to develop dynamic material flow models<sup>73</sup> for individual materials as well as for specific technologies.<sup>88</sup> Such models will help identify intentional sinks (e.g., landfills) of critical materials used in nanotechnology and unintentional dissipative releases (e.g., residuals released during incineration), and will link those anthropogenic material flows with natural cycles when possible. Knowledge of such material flows will aid in choosing current environmental and anthropogenic sinks that can best serve as secondary sources of critical materials.<sup>71</sup>

In addition to the novel recycling methods mentioned earlier, another technological solution for reducing nanotechnology's dependence on critical materials is to find substitutes. For example, carbon nanotubes and silver nanowires hold promise as potential substitutes for indium

tin oxide, which is widely used in touch screens. Other efforts to seek alternatives include the Heusler Alloy Replacement for Iridium (HARFIR) initiative<sup>160</sup>, Recyval-Nano<sup>161</sup> and NOVACAM<sup>162</sup>. Substitution strategies, however, have limits<sup>163</sup> at least in the short-to-medium term. Current efforts to substitute critical materials with more earth-abundant alternatives or renewable materials hold promise for the future. In the meantime, however, we will continue to rely on critical materials to allow the novel substitution technologies to mature.

## **POLICY INNOVATIONS**

In addition to technological solutions, we need proactive policy innovations to ensure that critical material-dependent nanotechnologies are sustainable. Extended producer responsibility for several consumer products and landfill bans for electronic waste are examples successful policies that favor recycling. Policy measures can also help set up material flow cycles that keep critical elements in circulation within specific nanotechnology-based industries or economies, e.g., platinum leasing programs for fuel cells.<sup>164</sup> Policies must also ensure that critical materials are employed for *critical* needs, and for uses that are most the amenable for recycling. For example, knowing that gold, silver, and platinum are scarce elements, is it justified to use these critical materials in cosmetics?<sup>108,165</sup> Finally, policy-makers should also identify latent demand for nano-enabled products and services, and safeguard against potential macroeconomic rebound effects that may undermine the sustainability of critical elements despite increases in material use efficiency.<sup>166</sup>

As we begin searching our seas,<sup>167</sup> ocean floors,<sup>168</sup> and neighboring asteroids<sup>169-171</sup> for critical materials, it is important that we also avoid losing them via unintentional and avoidable dissipative routes. A close scrutiny of innovation trends and technological developments will help in identifying how to best integrate waste preventative strategies at this early phase of

nanotechnology. Current product design practices, consumer behavior, inadequate recycling technologies and the limitations on separation imposed by thermodynamics contribute to low rates of recycling.<sup>172,173</sup> In addition, low recycling rates of critical materials have been attributed to high dissipative losses along their life cycle,<sup>174</sup> during which they can be lost in use phase and may get mixed with other material flows, which can make separation and recovery difficult. Such dissipative losses in recycling have been identified before,<sup>175,176</sup> but recycling nanomaterials presents new challenges.<sup>154,172,177</sup> Policy innovations, recycle-friendly product designs, novel methods for recycling combined with dynamic material flow analyses, thermodynamic modeling and life cycle assessments can help in minimizing dissipative losses of critical materials used in nanotechnologies. To effectively tackle the challenges in recycling critical materials from nanomaterial waste, technological innovations must be complemented with appropriate environmental and societal metrics, market strategies, economic incentives and novel entrepreneurial initiatives. It is therefore necessary to address these issues through an interdisciplinary framework, global stewardship efforts and a collective vision.



## REFERENCES

1. Alonso, E.; Sherman, A. M.; Wallington, T. J.; Everson, M. P.; Field, F. R.; Roth, R.; Kirchain, R. E., Evaluating Rare Earth Element Availability: A Case with Revolutionary Demand from Clean Technologies. *Environmental Science & Technology* **2012**, *46*, (6), 3406-3414.
2. Jain, P. K.; Huang, X.; El-Sayed, I. H.; El-Sayed, M. A., Noble Metals on the Nanoscale: Optical and Photothermal Properties and Some Applications in Imaging, Sensing, Biology, and Medicine. *Accounts of Chemical Research* **2008**, *41*, (12), 1578-1586.
3. Chen, J.; Lim, B.; Lee, E. P.; Xia, Y., Shape-controlled synthesis of platinum nanocrystals for catalytic and electrocatalytic applications. *Nano Today* **2009**, *4*, (1), 81-95.
4. Guo, S.; Wang, E., Noble metal nanomaterials: Controllable synthesis and application in fuel cells and analytical sensors. *Nano Today* **2011**, *6*, (3), 240-264.
5. Mauser, N.; Piatkowski, D.; Mancabelli, T.; Nyk, M.; Mackowski, S.; Hartschuh, A., Tip Enhancement of Upconversion Photoluminescence from Rare Earth Ion Doped Nanocrystals. *ACS Nano* **2015**.
6. Bocker, C.; Herrmann, A.; Loch, P.; Rüssel, C., The nano-crystallization and fluorescence of terbium doped Na<sub>2</sub>O/K<sub>2</sub>O/CaO/CaF<sub>2</sub>/Al<sub>2</sub>O<sub>3</sub>/SiO<sub>2</sub> glasses. *J. Mater. Chem. C* **2015**, *3*, (10), 2274-2281.
7. Casanova, D.; Bouzigues, C.; Nguyễn, T.-L.; Ramodiharilafy, R. O.; Bouzahir-Sima, L.; Gacoin, T.; Boilot, J.-P.; Tharaux, P.-L.; Alexandrou, A., Single europium-doped nanoparticles measure temporal pattern of reactive oxygen species production inside cells. *Nature Nanotechnology* **2009**, *4*, (9), 581-585.
8. Jung, J. H.; Bae, D. R.; Lee, S. J.; Han, S. W.; Lim, J. M.; Kang, D. M., Au-doped magnetic silica nanotube for binding of cysteine-containing proteins. *Chemistry of Materials* **2008**, *20*, (12), 3809-3813.
9. Liang, F.; Chen, J.; Cheng, J.; Jiang, S. P.; He, T.; Pu, J.; Li, J., Novel nano-structured Pd+yttrium doped ZrO<sub>2</sub> cathodes for intermediate temperature solid oxide fuel cells. *Electrochemistry Communications* **2008**, *10*, (1), 42-46.
10. Liu, S.-M.; Liu, F.-Q.; Wang, Z.-G., Relaxation of carriers in terbium-doped ZnO nanoparticles. *Chemical Physics Letters* **2001**, *343*, (5-6), 489-492.
11. Du, N.; Zhang, H.; Chen, B. D.; Ma, X. Y.; Liu, Z. H.; Wu, J. B.; Yang, D. R., Porous Indium Oxide Nanotubes: Layer-by-Layer Assembly on Carbon-Nanotube Templates and Application for Room-Temperature NH<sub>3</sub> Gas Sensors. *Advanced Materials* **2007**, *19*, (12), 1641-1645.
12. Soulantica, K.; Erades, L.; Sauvan, M.; Senocq, F.; Maisonnat, A.; Chaudret, B., Synthesis of Indium and Indium Oxide Nanoparticles from Indium Cyclopentadienyl Precursor and Their Application for Gas Sensing. *Advanced Functional Materials* **2003**, *13*, (7), 553-557.

13. Wakefield, G.; Keron, H. A.; Dobson, P. J.; Hutchison, J. L., Structural and optical properties of terbium oxide nanoparticles. *Journal of Physics and Chemistry of Solids* **1999**, *60*, (4), 503-508.
14. Reisfeld, R.; Gaft, M.; Saridarov, T.; Panczer, G.; Zelner, M., Nanoparticles of cadmium sulfide with europium and terbium in zirconia films having intensified luminescence. *Materials Letters* **2000**, *45*, (3-4), 154-156.
15. Chen, Y.; Chi, Y.; Wen, H.; Lu, Z., Sensitized Luminescent Terbium Nanoparticles: Preparation and Time-Resolved Fluorescence Assay for DNA. *Analytical Chemistry* **2007**, *79*, (3), 960-965.
16. Wang, B., Recent development of non-platinum catalysts for oxygen reduction reaction. *Journal of Power Sources* **2005**, *152*, 1-15.
17. Chisaka, M.; Ishihara, A.; Uehara, N.; Matsumoto, M.; Imai, H.; Ota, K.-i., Nano-TaOxNy Particles Synthesized from Oxy-tantalum Phthalocyanine: How to Prepare Precursors to Enhance the Oxygen Reduction Reaction Activity after Ammonia Pyrolysis. *J. Mater. Chem. A* **2015**.
18. Kuroda, C. S.; Kim, T. Y.; Hirano, T.; Yoshida, K.; Namikawa, T.; Yamazaki, Y., Preparation of nano-sized Bi-YIG particles for micro optics applications. *Electrochimica Acta* **1999**, *44*, (21-22), 3921-3925.
19. Xu, G.; Zhang, X.; He, W.; Liu, H.; Li, H., The study of surfactant application on synthesis of YAG nano-sized powders. *Powder Technology* **2006**, *163*, (3), 202-205.
20. Wu, J.; Ye, Z.; Wang, G.; Jin, D.; Yuan, J.; Guan, Y.; Piper, J., Visible-light-sensitized highly luminescent europium nanoparticles: preparation and application for time-gated luminescence bioimaging. *Journal of Materials Chemistry* **2009**, *19*, (9), 1258-1264.
21. Khan, A. A.; Khan, A.; Inamuddin, Preparation and characterization of a new organic-inorganic nano-composite poly-o-toluidine Th(IV) phosphate: Its analytical applications as cation-exchanger and in making ion-selective electrode. *Talanta* **2007**, *72*, (2), 699-710.
22. Lemański, K.; Gağor, A.; Kurnatowska, M.; Pązik, R.; Dereń, P. J., Spectroscopic properties of Nd<sup>3+</sup> ions in nano-perovskite CaTiO<sub>3</sub>. *Journal of Solid State Chemistry* **2011**, *184*, (10), 2713-2718.
23. Wawrzynczyk, D.; Bednarkiewicz, A.; Nyk, M.; Strek, W.; Samoc, M., Neodymium(III) doped fluoride nanoparticles as non-contact optical temperature sensors. *Nanoscale* **2012**, *4*, (22), 6959-6961.
24. Rocha, U.; Jacinto da Silva, C.; Ferreira Silva, W.; Guedes, I.; Benayas, A.; Martínez Maestro, L.; Acosta Elias, M.; Bovero, E.; van Veggel, F. C. J. M.; García Solé, J. A.; Jaque, D., Subtissue Thermal Sensing Based on Neodymium-Doped LaF<sub>3</sub> Nanoparticles. *ACS Nano* **2013**, *7*, (2), 1188-1199.
25. Chen, H.; Roco, M. C.; Li, X.; Lin, Y., Trends in nanotechnology patents. *Nature Nanotechnology* **2008**, *3*, (3), 123-125.

26. Hobson, D. W., Commercialization of nanotechnology. *Wiley Interdisciplinary Reviews: Nanomedicine and Nanobiotechnology* **2009**, *1*, (2), 189-202.
27. Rippen, M.; Braunstein, H.; Nelson, C.; Schuck, C.; Guillaud, P.; Blott, P. In *Interactive Multitask Credit Card Technology*, 2007, 2007; IEEE: 2007; pp 1-5.
28. Brown, K. D.; Pariseau, D. K.; Chatelain, D. Automated payment card fraud detection and location. US7543739 B2, 2009/06/09/, 2009.
29. Lyshevski, M. A.; Lyshevski, S. E. In *Optoelectromagnetic nanocrystals and microoptoelectromechanical systems*, 4th IEEE Conference on Nanotechnology, 2004, 2004/08//, 2004; 2004; pp 406-409.
30. Hu, Y.; Lin, L.; Zhang, Y.; Wang, Z. L., Replacing a Battery by a Nanogenerator with 20 V Output. *Advanced Materials* **2012**, *24*, (1), 110-114.
31. Kang, M. G.; Guo, L. J., Nanoimprinted Semitransparent Metal Electrodes and Their Application in Organic Light-Emitting Diodes. *Advanced Materials* **2007**, *19*, (10), 1391-1396.
32. Lee, S.-M.; Chae, J.-S.; Kim, D.-Y.; Choi, K. C., Plasmonic nanomeshes as large-area, low-resistive transparent electrodes and their application to ITO-free organic light-emitting diodes. *Organic Electronics* **2014**, *15*, (11), 3354-3361.
33. Dastjerdi, R.; Montazer, M., A review on the application of inorganic nano-structured materials in the modification of textiles: Focus on anti-microbial properties. *Colloids and Surfaces B: Biointerfaces* **2010**, *79*, (1), 5-18.
34. Lu, W.; Lieber, C. M., Nanoelectronics from the bottom up. *Nature Materials* **2007**, *6*, (11), 841-850.
35. Yu, B.; Meyyappan, M., Nanotechnology: Role in emerging nanoelectronics. *Solid-State Electron.* **2006**, *50*, (4), 536-544.
36. Zhu, G.; Bai, P.; Chen, J.; Lin Wang, Z., Power-generating shoe insole based on triboelectric nanogenerators for self-powered consumer electronics. *Nano Energy* **2013**, *2*, (5), 688-692.
37. Peng, L.; Hu, L.; Fang, X., Energy Harvesting for Nanostructured Self-Powered Photodetectors. *Advanced Functional Materials* **2014**, *24*, (18), 2591-2610.
38. Lim, G. S.; Kim, H.; Chang, J. Y., Laser highlighting on a flat panel display coated with a double-layered anti-reflection film containing a europium(III) complex. *J. Mater. Chem. C* **2014**, *2*, (47), 10184-10188.
39. Tanaka, S.; Fujihara, S., Design and Fabrication of Luminescent Antireflective Sol–Gel Coatings with a Bi-Layer Structure. *International Journal of Applied Ceramic Technology* **2011**, *8*, (5), 1001-1009.

40. Tanaka, S.; Fujihara, S., Luminescent Antireflective Coatings with Disordered Surface Nanostructures Fabricated by Liquid Processes. *Langmuir* **2011**, *27*, (6), 2929-2935.
41. Zhang, C.; Zhao, D.; Gu, D.; Kim, H.; Ling, T.; Wu, Y.-K. R.; Guo, L. J., An Ultrathin, Smooth, and Low-Loss Al-Doped Ag Film and Its Application as a Transparent Electrode in Organic Photovoltaics. *Advanced Materials* **2014**, *26*, (32), 5696-5701.
42. Tan, C. F.; Ong, W. L.; Ho, G. W., Self-Biased Hybrid Piezoelectric-Photoelectrochemical Cell with Photocatalytic Functionalities. *ACS Nano* **2015**.
43. Xu, A.-W.; Gao, Y.; Liu, H.-Q., The Preparation, Characterization, and their Photocatalytic Activities of Rare-Earth-Doped TiO<sub>2</sub> Nanoparticles. *Journal of Catalysis* **2002**, *207*, (2), 151-157.
44. Lee, B.-I.; Lee, E.-s.; Byeon, S.-H., Assembly of Layered Rare-Earth Hydroxide Nanosheets and SiO<sub>2</sub> Nanoparticles to Fabricate Multifunctional Transparent Films Capable of Combinatorial Color Generation. *Advanced Functional Materials* **2012**, *22*, (17), 3562-3569.
45. Mor, G. K.; Shankar, K.; Paulose, M.; Varghese, O. K.; Grimes, C. A., Use of Highly-Ordered TiO<sub>2</sub> Nanotube Arrays in Dye-Sensitized Solar Cells. *Nano Letters* **2006**, *6*, (2), 215-218.
46. Gao, F.; Wang, Y.; Shi, D.; Zhang, J.; Wang, M.; Jing, X.; Humphry-Baker, R.; Wang, P.; Zakeeruddin, S. M.; Grätzel, M., Enhance the Optical Absorptivity of Nanocrystalline TiO<sub>2</sub> Film with High Molar Extinction Coefficient Ruthenium Sensitizers for High Performance Dye-Sensitized Solar Cells. *Journal of the American Chemical Society* **2008**, *130*, (32), 10720-10728.
47. Chen, C.-Y.; Wang, M.; Li, J.-Y.; Pootrakulchote, N.; Alibabaei, L.; Ngoc-le, C.-h.; Decoppet, J.-D.; Tsai, J.-H.; Grätzel, C.; Wu, C.-G.; Zakeeruddin, S. M.; Grätzel, M., Highly Efficient Light-Harvesting Ruthenium Sensitizer for Thin-Film Dye-Sensitized Solar Cells. *ACS Nano* **2009**, *3*, (10), 3103-3109.
48. Vikesland, P. J.; Wigginton, K. R., Nanomaterial Enabled Biosensors for Pathogen Monitoring - A Review. *Environmental Science & Technology* **2010**, *44*, (10), 3656-3669.
49. Wigginton, K. R.; Vikesland, P. J., Gold-coated polycarbonate membrane filter for pathogen concentration and SERS-based detection. *Analyst* **2010**, *135*, (6), 1320-1326.
50. Dimitriadis, S.; Nomikou, N.; McHale, A. P., Pt-based electro-catalytic materials derived from biosorption processes and their exploitation in fuel cell technology. *Biotechnology Letters* **2007**, *29*, (4), 545-551.
51. Tittl, A.; Mai, P.; Taubert, R.; Dregely, D.; Liu, N.; Giessen, H., Palladium-Based Plasmonic Perfect Absorber in the Visible Wavelength Range and Its Application to Hydrogen Sensing. *Nano Letters* **2011**, *11*, (10), 4366-4369.

52. Goldberger, J.; He, R.; Zhang, Y.; Lee, S.; Yan, H.; Choi, H.-J.; Yang, P., Single-crystal gallium nitride nanotubes. *Nature* **2003**, *422*, (6932), 599-602.
53. Chen, F.; Zhu, Y.-J.; Zhang, K.-H.; Wu, J.; Wang, K.-W.; Tang, Q.-L.; Mo, X.-M., Europium-doped amorphous calcium phosphate porous nanospheres: preparation and application as luminescent drug carriers. *Nanoscale research letters* **2011**, *6*, (67), 1-9.
54. Zimmer, J. P.; Kim, S.-W.; Ohnishi, S.; Tanaka, E.; Frangioni, J. V.; Bawendi, M. G., Size Series of Small Indium Arsenide–Zinc Selenide Core–Shell Nanocrystals and Their Application to In Vivo Imaging. *Journal of the American Chemical Society* **2006**, *128*, (8), 2526-2527.
55. Lee, S.-H.; Jung, Y.; Agarwal, R., Highly scalable non-volatile and ultra-low-power phase-change nanowire memory. *Nature Nanotechnology* **2007**, *2*, (10), 626-630.
56. Yu, B.; Sun, X. H.; Calebotta, G. A.; Dholakia, G. R.; Meyyappan, M., One-dimensional Germanium Nanowires for Future Electronics. *J Clust Sci* **2006**, *17*, (4), 579-597.
57. Yu, D.; Wu, J.; Gu, Q.; Park, H., Germanium Telluride Nanowires and Nanohelices with Memory-Switching Behavior. *Journal of the American Chemical Society* **2006**, *128*, (25), 8148-8149.
58. Saif, M., Synthesis of down conversion, high luminescent nano-phosphor materials based on new developed  $\text{Ln}^{3+}:\text{Y}_2\text{Zr}_2\text{O}_7/\text{SiO}_2$  for latent fingerprint application. *Journal of Luminescence* **2013**, *135*, 187-195.
59. Ye, R.; Cui, Z.; Hua, Y.; Deng, D.; Zhao, S.; Li, C.; Xu, S.,  $\text{Eu}^{2+}/\text{Dy}^{3+}$  co-doped white light emission glass ceramics under UV light excitation. *Journal of Non-Crystalline Solids* **2011**, *357*, (11–13), 2282-2285.
60. Haritha, P.; Martín, I. R.; Linganna, K.; Monteseuro, V.; Babu, P.; León-Luis, S. F.; Jayasankar, C. K.; Rodríguez-Mendoza, U. R.; Lavín, V.; Venkatramu, V., Optimizing white light luminescence in  $\text{Dy}^{3+}$ -doped  $\text{Lu}_3\text{Ga}_5\text{O}_{12}$  nano-garnets. *Journal of Applied Physics* **2014**, *116*, (17).
61. Maccauro, G.; Iommetti, P. R.; Muratori, F.; Raffaelli, L.; Manicone, P. F.; Fabbriani, C., An overview about biomedical applications of micron and nano size tantalum. *Recent Pat Biotechnol* **2009**, *3*, (3), 157-165.
62. Brown, D.; Ma, B.-M.; Chen, Z., Developments in the processing and properties of NdFeB-type permanent magnets. *Journal of Magnetism and Magnetic Materials* **2002**, *248*, (3), 432-440.
63. Murphy, C. J., Sustainability as an emerging design criterion in nanoparticle synthesis and applications. *J. Mater. Chem.* **2008**, *18*, (19), 2173-2176.
64. Dahl, J. A.; Maddux, B. L. S.; Hutchison, J. E., Toward Greener Nanosynthesis. *Chemical Reviews* **2007**, *107*, (6), 2228-2269.

65. Hutchison, J. E., Greener Nanoscience: A Proactive Approach to Advancing Applications and Reducing Implications of Nanotechnology. *ACS Nano* **2008**, *2*, (3), 395-402.
66. Canton, J., NBIC Convergent Technologies and the Innovation Economy: Challenges and Opportunities for the 21st Century. In *Managing nano-bio-info-cogno innovations*, Bainbridge, W. S.; Roco, M. C., Eds. Springer Netherlands: 2006; pp 33-45.
67. Roco, M. C., Science and Technology Integration for Increased Human Potential and Societal Outcomes. *Annals of the New York Academy of Sciences* **2004**, *1013*, (1), 1-16.
68. Yaksic, A.; Tilton, J. E., Using the cumulative availability curve to assess the threat of mineral depletion: The case of lithium. *Resources Policy* **2009**, *34*, (4), 185-194.
69. Chen, W.-Q., Recycling Rates of Aluminum in the United States. *Journal of Industrial Ecology* **2013**, *17*, (6), 926-938.
70. Liu, G.; Müller, D. B., Mapping the Global Journey of Anthropogenic Aluminum: A Trade-Linked Multilevel Material Flow Analysis. *Environmental Science & Technology* **2013**.
71. Eckelman, M. J.; Reck, B. K.; Graedel, T. E., Exploring the Global Journey of Nickel with Markov Chain Models. *Journal of Industrial Ecology* **2012**, *16*, (3), 334-342.
72. Gordon, R. B.; Bertram, M.; Graedel, T. E., Metal stocks and sustainability. *Proceedings of the National Academy of Sciences of the United States of America* **2006**, *103*, (5), 1209-1214.
73. Glöser, S.; Soulier, M.; Tercero Espinoza, L. A., Dynamic Analysis of Global Copper Flows. Global Stocks, Postconsumer Material Flows, Recycling Indicators, and Uncertainty Evaluation. *Environmental Science & Technology* **2013**, *47*, (12), 6564-6572.
74. Gsodam, P.; Lassnig, M.; Kreuzeder, A.; Mrotzek, M., The Austrian silver cycle: A material flow analysis. *Resources, Conservation and Recycling* **2014**, *88*, 76-84.
75. Du, X.; Graedel, T. E., Uncovering the Global Life Cycles of the Rare Earth Elements. *Sci. Rep.* **2011**, *1*.
76. Navazo, J. M. V.; Méndez, G. V.; Peiró, L. T., Material flow analysis and energy requirements of mobile phone material recovery processes. *The International Journal of Life Cycle Assessment*, 1-13.
77. Hischer, R.; Wäger, P.; Gauglhofer, J., Does WEEE recycling make sense from an environmental perspective?: The environmental impacts of the Swiss take-back and recycling systems for waste electrical and electronic equipment (WEEE). *Environmental Impact Assessment Review* **2005**, *25*, (5), 525-539.
78. Chancerel, P.; Meskers, C. E. M.; Hagelüken, C.; Rotter, V. S., Assessment of Precious Metal Flows During Preprocessing of Waste Electrical and Electronic Equipment. *Journal of Industrial Ecology* **2009**, *13*, (5), 791-810.

79. Wäger, P. A.; Hischer, R.; Eugster, M., Environmental impacts of the Swiss collection and recovery systems for Waste Electrical and Electronic Equipment (WEEE): A follow-up. *Science of The Total Environment* **2011**, *409*, (10), 1746-1756.
80. Nakajima, K.; Yokoyama, K.; Nakano, K.; Nagasaka, T., Substance Flow Analysis of Indium for Flat Panel Displays in Japan. *Materials Transactions* **2007**, *48*, (9), 2365-2369.
81. Widmer, R.; Du, X.; Haag, O.; Restrepo, E.; Wäger, P. A., Scarce Metals in Conventional Passenger Vehicles and End-of-Life Vehicle Shredder Output. *Environmental Science & Technology* **2015**.
82. Kerr, R. A., Is the World Tottering on the Precipice of Peak Gold? *Science* **2012**, *335*, (6072), 1038-1039.
83. Graedel, T. E., On the Future Availability of the Energy Metals. *Annual Review of Materials Research* **2011**, *41*, (1), 323-335.
84. Graedel, T. e.; Erdmann, L., Will metal scarcity impede routine industrial use? *MRS Bulletin* **2012**, *37*, (04), 325-331.
85. Kerr, R. A., The Coming Copper Peak. *Science* **2014**, *343*, (6172), 722-724.
86. Tilton, J. E., *On Borrowed Time: Assessing the Threat of Mineral Depletion*. Routledge: 2010; p 168.
87. van Vuuren, D. P.; Strengers, B. J.; De Vries, H. J. M., Long-term perspectives on world metal use—a system-dynamics model. *Resources Policy* **1999**, *25*, (4), 239-255.
88. Busch, J.; Steinberger, J. K.; Dawson, D. A.; Purnell, P.; Roelich, K., Managing Critical Materials with a Technology-Specific Stocks and Flows Model. *Environmental Science & Technology* **2013**.
89. Mudd, G. M., Global trends in gold mining: Towards quantifying environmental and resource sustainability. *Resources Policy* **2007**, *32*, (1–2), 42-56.
90. Schodde, R. In *Recent trends in gold discovery*, NewGenGold Conference, 2011/11/22/23, 2011; 2011.
91. Keller, A. A.; Lazareva, A., Predicted Releases of Engineered Nanomaterials: From Global to Regional to Local. *Environ. Sci. Technol. Lett.* **2013**.
92. Keller, A. A.; McFerran, S.; Lazareva, A.; Suh, S., Global life cycle releases of engineered nanomaterials. *Journal of Nanoparticle Research* **2013**, *15*, (6), 1-17.
93. Gottschalk, F.; Nowack, B., The Release of Engineered Nanomaterials to the Environment. *Journal of Environmental Monitoring* **2011**, *13*, (5).

94. Gottschalk, F.; Sonderer, T.; Scholz, R. W.; Nowack, B., Modeled Environmental Concentrations of Engineered Nanomaterials (TiO<sub>2</sub>, ZnO, Ag, CNT, Fullerenes) for Different Regions. *Environ. Sci. Technol.* **2009**, *43*, (24), 9216-9222.
95. Gottschalk, F.; Sun, T.; Nowack, B., Environmental concentrations of engineered nanomaterials: Review of modeling and analytical studies. *Environmental Pollution*.
96. Mueller, N. C.; Nowack, B., Exposure Modeling of Engineered Nanoparticles in the Environment. *Environ. Sci. Technol.* **2008**, *42*, (12), 4447-4453.
97. Nowack, B.; David, R. M.; Fissan, H.; Morris, H.; Shatkin, J. A.; Stintz, M.; Zepp, R.; Brouwer, D., Potential release scenarios for carbon nanotubes used in composites. *Environment International* **2013**, *59*, 1-11.
98. Piccinno, F.; Gottschalk, F.; Seeger, S.; Nowack, B., Industrial production quantities and uses of ten engineered nanomaterials in Europe and the world. *Journal of Nanoparticle Research* **2012**, *14*, (9), 1-11.
99. Sun, T. Y.; Gottschalk, F.; Hungerbühler, K.; Nowack, B., Comprehensive probabilistic modelling of environmental emissions of engineered nanomaterials. *Environmental Pollution* **2014**, *185*, 69-76.
100. Walser, T.; Gottschalk, F., Stochastic fate analysis of engineered nanoparticles in incineration plants. *Journal of Cleaner Production* **2014**, *80*, 241-251.
101. Walser, T.; Limbach, L. K.; Brogioli, R.; Erismann, E.; Flamigni, L.; Hattendorf, B.; Juchli, M.; Krumeich, F.; Ludwig, C.; Prikopsky, K.; Rossier, M.; Saner, D.; Sigg, A.; Hellweg, S.; Günther, D.; Stark, W. J., Persistence of engineered nanoparticles in a municipal solid-waste incineration plant. *Nature Nanotechnology* **2012**, *7*, (8), 520-524.
102. Caballero-Guzman, A.; Sun, T.; Nowack, B., Flows of engineered nanomaterials through the recycling process in Switzerland. *Waste Management*.
103. Musee, N., Nanowastes and the environment: Potential new waste management paradigm. *Environment International* **2011**, *37*, (1), 112-128.
104. Lorenz, C.; Windler, L.; von Goetz, N.; Lehmann, R. P.; Schuppler, M.; Hungerbühler, K.; Heuberger, M.; Nowack, B., Characterization of Silver Release from Commercially Available Functional (nano)textiles. *Chemosphere* **2012**, *89*, (7), 817-824.
105. Walser, T.; Demou, E.; Lang, D. J.; Hellweg, S., Prospective Environmental Life Cycle Assessment of Nanosilver T-Shirts. *Environmental Science & Technology* **2011**, *45*, (10), 4570-4578.



106. Zhang, Q.; Huang, J.-Q.; Qian, W.-Z.; Zhang, Y.-Y.; Wei, F., The Road for Nanomaterials Industry: A Review of Carbon Nanotube Production, Post-Treatment, and Bulk Applications for Composites and Energy Storage. *Small* **2013**, *9*, (8), 1237-1265.
107. Weir, A.; Westerhoff, P.; Fabricius, L.; Hristovski, K.; von Goetz, N., Titanium Dioxide Nanoparticles in Food and Personal Care Products. *Environmental Science & Technology* **2012**, *46*, (4), 2242-2250.
108. Chantecaille 'Nano Gold' Energizing Cream | Nordstrom. <http://shop.nordstrom.com/s/chantecaille-nano-gold-energizing-cream/3102982?origin=related-3102982-0-0-2>
109. Ciacci, L.; Reck, B. K.; Nassar, N. T.; Graedel, T. E., Lost by Design. *Environmental Science & Technology* **2015**.
110. Tsujiguchi, M., Indium Recovery and Recycling from an LCD Panel. In *Design for Innovative Value Towards a Sustainable Society*, Matsumoto, D. M.; Umeda, P. Y.; Masui, D. K.; Fukushige, D. S., Eds. Springer Netherlands: 2012; pp 743-746.
111. Zimmermann, Y.-S.; Niewersch, C.; Lenz, M.; Kül, Z. Z.; Corvini, P. F. X.; Schäffer, A.; Wintgens, T., Recycling of Indium From CIGS Photovoltaic Cells: Potential of Combining Acid-Resistant Nanofiltration with Liquid–Liquid Extraction. *Environmental Science & Technology* **2014**.
112. Akita, S.; Rovira, M.; Sastre, A. M.; Takeuchi, H., Cloud-Point Extraction of Gold(III) with Nonionic Surfactant—Fundamental Studies and Application to Gold Recovery from Printed Substrate. *Separation Science and Technology* **1998**, *33*, (14), 2159-2177.
113. Liu, Z.; Frascioni, M.; Lei, J.; Brown, Z. J.; Zhu, Z.; Cao, D.; Iehl, J.; Liu, G.; Fahrenbach, A. C.; Botros, Y. Y.; Farha, O. K.; Hupp, J. T.; Mirkin, C. A.; Fraser Stoddart, J., Selective isolation of gold facilitated by second-sphere coordination with  $\alpha$ -cyclodextrin. *Nature Communications* **2013**, *4*.
114. Oliveira, R. L.; Kiyohara, P. K.; Rossi, L. M., High performance magnetic separation of gold nanoparticles for catalytic oxidation of alcohols. *Green Chemistry* **2010**, *12*, (1), 144-149.
115. Phillips, S.; Kauppinen, P., Final Analysis: The Use of Metal Scavengers for Recovery of Palladium Catalyst from Solution. *Platinum Metals Review* **2010**, *54*, (1), 69-70.
116. Yong, P.; Farr, J. P. G.; Harris, I. R.; Macaskie, L. E., Palladium recovery by immobilized cells of *Desulfovibrio desulfuricans* using hydrogen as the electron donor in a novel electrobioreactor. *Biotechnology Letters* **2002**, *24*, (3), 205-212.
117. Yong, P.; Paterson-Beedle, M.; Mikheenko, I. P.; Macaskie, L. E., From bio-mineralisation to fuel cells: biomanufacture of Pt and Pd nanocrystals for fuel cell electrode catalyst. *Biotechnology Letters* **2007**, *29*, (4), 539-544.

118. Dodson, J. R.; Parker, H. L.; García, A. M.; Hicken, A.; Asemave, K.; Farmer, T. J.; He, H.; Clark, J. H.; Hunt, A. J., Bio-derived materials as a green route for precious & critical metal recovery and re-use. *Green Chemistry* **2015**.
119. Terakado, O.; Saeki, T.; Irizato, R.; Hirasawa, M., Pyrometallurgical Recovery of Indium from Dental Metal Recycling Sludge by Chlorination Treatment with Ammonium Chloride. *Materials Transactions* **2010**, *51*, (6), 1136-1140.
120. Hoogerstraete, T. V.; Blanpain, B.; Gerven, T. V.; Binnemans, K., From NdFeB magnets towards the rare-earth oxides: a recycling process consuming only oxalic acid. *RSC Adv.* **2014**, *4*, (109), 64099-64111.
121. Rabatho, J. P.; Tongamp, W.; Takasaki, Y.; Haga, K.; Shibayama, A., Recovery of Nd and Dy from rare earth magnetic waste sludge by hydrometallurgical process. *J Mater Cycles Waste Manag* **2012**, *15*, (2), 171-178.
122. Rout, A.; Venkatesan, K. A.; Srinivasan, T. G.; Vasudeva Rao, P. R., Ionic liquid extractants in molecular diluents: Extraction behavior of europium (III) in quaternary ammonium-based ionic liquids. *Separation and Purification Technology* **2012**, *95*, 26-31.
123. Zhuang, Z.; Xu, X.; Wang, Y.; Wang, Y.; Huang, F.; Lin, Z., Treatment of nanowaste via fast crystal growth: With recycling of nano-SnO<sub>2</sub> from electroplating sludge as a study case. *Journal of Hazardous Materials* **2012**, *211–212*, 414-419.
124. Chen, Z.; Zhuang, Z.; Cao, Q.; Pan, X.; Guan, X.; Lin, Z., Adsorption-Induced Crystallization of U-Rich Nanocrystals on Nano-Mg(OH)<sub>2</sub> and the Aqueous Uranyl Enrichment. *ACS Appl. Mater. Interfaces* **2013**.
125. Myakonkaya, O.; Guibert, C. m.; Eastoe, J.; Grillo, I., Recovery of Nanoparticles Made Easy. *Langmuir* **2010**, *26*, (6), 3794-3797.
126. Liu, J.-f.; Chao, J.-b.; Liu, R.; Tan, Z.-q.; Yin, Y.-g.; Wu, Y.; Jiang, G.-b., Cloud Point Extraction as an Advantageous Preconcentration Approach for Analysis of Trace Silver Nanoparticles in Environmental Waters. *Analytical Chemistry* **2009**, *81*, (15), 6496-6502.
127. Liu, J.-f.; Liu, R.; Yin, Y.-g.; Jiang, G.-b., Triton X-114 based cloud point extraction: a thermoreversible approach for separation/concentration and dispersion of nanomaterials in the aqueous phase. *Chemical Communications* **2009**, (12), 1514-1516.
128. Mustafina, A. R.; Elistratova, J. G.; Bochkova, O. D.; Burilov, V. A.; Fedorenko, S. V.; Konovalov, A. I.; Soloveva, S. Y., Temperature induced phase separation of luminescent silica nanoparticles in Triton X-100 solutions. *Journal of Colloid and Interface Science* **2011**, *354*, (2), 644-649.

129. Nazar, M. F.; Shah, S. S.; Eastoe, J.; Khan, A. M.; Shah, A., Separation and recycling of nanoparticles using cloud point extraction with non-ionic surfactant mixtures. *Journal of Colloid and Interface Science* **2011**, *363*, (2), 490-496.
130. Admassie, S.; Elfving, A.; Skallberg, A.; Inganäs, O., Extracting metal ions from water with redox active biopolymer electrodes. *Environ. Sci.: Water Res. Technol.* **2015**.
131. Li, C.; Zhuang, Z.; Huang, F.; Wu, Z.; Hong, Y.; Lin, Z., Recycling Rare Earth Elements from Industrial Wastewater with Flowerlike Nano-Mg(OH)<sub>2</sub>. *ACS Appl. Mater. Interfaces* **2013**, *5*, (19), 9719-9725.
132. Majedi, S. M.; Lee, H. K.; Kelly, B. C., Chemometric Analytical Approach for the Cloud Point Extraction and Inductively Coupled Plasma Mass Spectrometric Determination of Zinc Oxide Nanoparticles in Water Samples. *Analytical Chemistry* **2012**, *84*, (15), 6546-6552.
133. Tsogas, G. Z.; Giokas, D. L.; Vlessidis, A. G., Ultratrace Determination of Silver, Gold, and Iron Oxide Nanoparticles by Micelle Mediated Preconcentration/Selective Back-Extraction Coupled with Flow Injection Chemiluminescence Detection. *Analytical Chemistry* **2014**, *86*, (7), 3484-3492.
134. Bogart, J. A.; Lippincott, C. A.; Carroll, P. J.; Schelter, E. J., An Operationally Simple Method for Separating the Rare-Earth Elements Neodymium and Dysprosium. *Angewandte Chemie International Edition* **2015**, *54*, (28), 8222-8225.
135. Sawhney, A. P. S.; Condon, B.; Singh, K. V.; Pang, S. S.; Li, G.; Hui, D., Modern Applications of Nanotechnology in Textiles. *Textile Research Journal* **2008**, *78*, (8), 731-739.
136. Cho, G.; Lee, S.; Cho, J., Review and Reappraisal of Smart Clothing. *International Journal of Human-Computer Interaction* **2009**, *25*, (6), 582-617.
137. Shim, B. S.; Chen, W.; Doty, C.; Xu, C.; Kotov, N. A., Smart Electronic Yarns and Wearable Fabrics for Human Biomonitoring made by Carbon Nanotube Coating with Polyelectrolytes. *Nano Letters* **2008**, *8*, (12), 4151-4157.
138. Köhler, A. R.; Hilty, L. M.; Bakker, C., Prospective Impacts of Electronic Textiles on Recycling and Disposal. *Journal of Industrial Ecology* **2011**, *15*, (4), 496-511.
139. Wu, W.; Pan, C.; Zhang, Y.; Wen, X.; Wang, Z. L., Piezotronics and piezo-phototronics – From single nanodevices to array of devices and then to integrated functional system. *Nano Today* **2013**, *8*, (6), 619-642.
140. Wang, Z. L. In *Top emerging technologies for self-powered nanosystems: nanogenerators and nanopiezotronics*, 2010/01//, 2010; IEEE: 2010; pp 63-64.
141. Gaster, R. S.; Hall, D. A.; Wang, S. X., nanoLAB: An ultraportable, handheld diagnostic laboratory for global health. *Lab on a Chip* **2011**, *11*, (5), 950-956.

142. Chan, K.; Ng, T. B., Isolation and Detection of Proteins with Nano-Particles and Microchips for Analyzing Proteomes on a Large Scale Basis. *Protein and Peptide Letters* **2011**, *18*, (4), 423-433.
143. Englebienne, P.; Van Hoonacker, A.; Verhas, M., Surface plasmon resonance: principles, methods and applications in biomedical sciences. *Spectroscopy-an International Journal* **2003**, *17*, (2-3), 255-273.
144. Grow, A. E.; Wood, L. L.; Claycomb, J. L.; Thompson, P. A., New biochip technology for label-free detection of pathogens and their toxins. *Journal of Microbiological Methods* **2003**, *53*, (2), 221-233.
145. Liu, X.; Mwangi, M.; Li, X.; O'Brien, M.; Whitesides, G. M., Paper-based piezoresistive MEMS sensors. *Lab on a Chip* **2011**, *11*, (13), 2189-2196.
146. Lahr, R. H.; Wallace, G. C.; Vikesland, P. J., Raman Characterization of Nanoparticle Transport in Microfluidic Paper-Based Analytical Devices ( $\mu$ PADs). *ACS Appl. Mater. Interfaces* **2015**, *7*, (17), 9139-9146.
147. Torabi, S. F.; Lu, Y., Small-molecule diagnostics based on functional DNA nanotechnology: a dipstick test for mercury. *Faraday Discussions* **2011**, *149*, 125-135.
148. Liang, P.; Yu, H.; Guntupalli, B.; Xiao, Y., Paper-Based Device for Rapid Visualization of NADH Based on Dissolution of Gold Nanoparticles. *ACS Appl. Mater. Interfaces* **2015**.
149. Jain, K. K., Applications of Nanobiotechnology in Clinical Diagnostics. *Clinical Chemistry* **2007**, *53*, (11), 2002-2009.
150. Song, S. P.; Yan, J.; Pan, D.; Zhu, C. F.; Wang, L. H.; Fan, C. H., A Gold Nanoparticle-Based Microfluidic Protein Chip for Tumor Markers. *Journal of Nanoscience and Nanotechnology* **2009**, *9*, (2), 1194-1197.
151. Halvorson, R. A.; Vikesland, P. J., Surface-Enhanced Raman Spectroscopy (SERS) for Environmental Analyses. *Environmental Science & Technology* **2010**, *44*, (20), 7749-7755.
152. Rule, K. L.; Vikesland, P. J., Surface-Enhanced Resonance Raman Spectroscopy for the Rapid Detection of *Cryptosporidium parvum* and *Giardia lamblia*. *Environmental Science & Technology* **2009**, *43*, (4), 1147-1152.
153. Christakis, N. A.; Fowler, J. H., Social Network Sensors for Early Detection of Contagious Outbreaks. *PLoS ONE* **2010**, *5*, (9), e12948.
154. Olapiriyakul, S.; Caudill, R. J., Thermodynamic Analysis to Assess the Environmental Impact of End-of-life Recovery Processing for Nanotechnology Products. *Environmental Science & Technology* **2009**, *43*, (21), 8140-8146.
155. Gutowski, T. G. In *Thermodynamics and recycling: A review*, 2008, 2008; 2008; pp 321-32.

156. Dahmus, J. B.; Gutowski, T. G., What Gets Recycled: An Information Theory Based Model for Product Recycling. *Environmental Science & Technology* **2007**, *41*, (21), 7543-7550.
157. Finnveden, G.; Ekvall, T., Life-cycle assessment as a decision-support tool - the case of recycling versus incineration of paper. *Resour. Conserv. Recycl.* **1998**, *24*, (3-4), 235-256.
158. Nuss, P.; Eckelman, M. J., Life Cycle Assessment of Metals: A Scientific Synthesis. *PLoS ONE* **2014**, *9*, (7).
159. Zhang, X.; Guan, J.; Guo, Y.; Yan, X.; Yuan, H.; Xu, J.; Guo, J.; Zhou, Y.; Su, R.; Guo, Z., Selective Desoldering Separation of Tin–Lead Alloy for Dismantling of Electronic Components from Printed Circuit Boards. *ACS Sustainable Chem. Eng.* **2015**.
160. HARFIR | 'Heusler Alloy Replacement for Iridium' R&D project. <http://www.harfir.eu/>
161. Recyval-Nano. [http://www.recyval-nano.eu/web/content/42\\_Technical-description](http://www.recyval-nano.eu/web/content/42_Technical-description)
162. NOVACAM - Developing catalysts using non-critical elements designed to unlock the potential of biomass. <http://novacam.wpengine.com/project-summary/>  
<http://novacam.eu/project-summary/>
163. Ayres, R. U., On the practical limits to substitution. *Ecological Economics* **2007**, *61*, (1), 115-128.
164. Kromer, M. A.; Joseck, F.; Rhodes, T.; Guernsey, M.; Marcinkoski, J., Evaluation of a platinum leasing program for fuel cell vehicles. *International Journal of Hydrogen Energy* **2009**, *34*, (19), 8276-8288.
165. Platinum Silver Nanocolloid Milky Essence | Boosters | DHC | The Japanese Skincare and Makeup Experts | DHC. <http://www.dhccare.com/platinum-silver-nanocolloid-milky-essence>
166. Grepperud, S.; Rasmussen, I., A general equilibrium assessment of rebound effects. *Energy Economics* **2004**, *26*, (2), 261-282.
167. Diallo, M. S.; Kotte, M. R.; Cho, M., Mining Critical Metals and Elements from Seawater: Opportunities and Challenges. *Environmental Science & Technology* **2015**.
168. Kato, Y.; Fujinaga, K.; Nakamura, K.; Takaya, Y.; Kitamura, K.; Ohta, J.; Toda, R.; Nakashima, T.; Iwamori, H., Deep-sea mud in the Pacific Ocean as a potential resource for rare-earth elements. *Nature Geosci* **2011**, *4*, (8), 535-539.
169. Lewicki, C.; Diamandis, P.; Anderson, E.; Voorhees, C.; Mycroft, F., Planetary Resources—The Asteroid Mining Company. *New Space* **2013**, *1*, (2), 105-108.
170. Sonter, M. J., The technical and economic feasibility of mining the near-earth asteroids. *Acta Astronautica* **1997**, *41*, (4–10), 637-647.

171. Slezak, M., Space miners hope to build first off-Earth economy. *New Scientist* **2013**, *217*, (2906), 8-10.
172. Reck, B. K.; Graedel, T. E., Challenges in Metal Recycling. *Science* **2012**, *337*, (6095), 690-695.
173. Bartl, A., Moving from recycling to waste prevention: A review of barriers and enables. *Waste Manag Res* **2014**, *32*, (9 suppl), 3-18.
174. Zimmermann, T.; Gößling-Reisemann, S., Critical materials and dissipative losses: A screening study. *Science of The Total Environment* **2013**, *461–462*, 774-780.
175. Ayres, R. U., Metals recycling: economic and environmental implications. *Resources, Conservation and Recycling* **1997**, *21*, (3), 145-173.
176. Tilton, J. E., The future of recycling. *Resources Policy* **1999**, *25*, (3), 197-204.
177. Asmatulu, E.; Twomey, J.; Overcash, M., Life cycle and nano-products: end-of-life assessment. *Journal of Nanoparticle Research* **2012**, *14*, (3), 1-8.

## Chapter 5

# Room Temperature Seed Mediated Growth of Gold Nanoparticles: Mechanistic Investigations and Life Cycle Assessment

Weinan Leng, Paramjeet Pati, and Peter J Vikesland \*

Department of Civil and Environmental Engineering, Virginia Polytechnic Institute and State University, 418 Durham Hall, Blacksburg, VA 24060-0246

\*Corresponding author e-mail address: [pvikes@vt.edu](mailto:pvikes@vt.edu)

### (Room Temperature Seed Mediated Growth of Gold Nanoparticles: Mechanistic Investigations and Life Cycle Assessment)

Weinan Leng, Paramjeet Pati and Peter Vikesland, *Environ. Sci.: Nano*, 2015,

DOI: 10.1039/C5EN00026B

Adapted from *Environmental Science: Nano* with permission from The Royal Society of Chemistry)

### ABSTRACT

In this study, we report the first room temperature seed-mediated synthesis of gold nanoparticles (AuNPs) in the presence of citrate and gold salt. In contrast to citrate-reduction in boiling water, these mild reaction conditions provide expanded capacity to probe the mechanism of seed-mediated growth following gold salt addition. Moreover, comparative life cycle assessment indicates significant reductions in the environmental impacts for the room temperature synthesis. For this study, highly uniform gold seeds with Z-average diameter of  $17.7 \pm 0.8$  nm and a polydispersity index of  $0.03 \pm 0.01$  were prepared by a pH controlled protocol. We investigated the AuNP growth mechanism via time resolved UV-vis spectroscopy, dynamic light scattering, and transmission electron microscopy. This study indicates that citrate and its oxidation byproduct acetone dicarboxylate serve to bridge and gather Au(III) ions around gold nanoparticle seeds in the initial growth step.

## INTRODUCTION

Nanotechnology holds immense promise for its capacity to address many societal problems. A key challenge in exploiting the novel properties of nanomaterials is in the synthesis of nanoparticles with precisely controlled sizes and morphologies. In addition, nanomaterial synthesis may involve multi-step, multi-solvent, energy intensive manufacturing processes<sup>1, 2</sup> which may be associated with significant environmental impacts. Recently there have been increased efforts 1) to develop design principles to synthesize highly monodisperse nanoparticles<sup>3, 4</sup> and 2) to incorporate the principles of green chemistry into nanomaterial synthesis.<sup>5-7</sup> In this paper we present a novel approach for the seeded growth of gold nanoparticles (AuNPs) at room temperature and compare its life cycle impacts with those of previously reported methods<sup>8,9</sup> that require high-temperature boiling.

AuNPs and their conjugates are particularly versatile nanomaterials.<sup>10-12</sup> Exhibiting low toxicity in biological systems,<sup>13-15</sup> AuNPs conjugated with drugs and peptides have been used to modulate pharmacokinetics and drug delivery, thus allowing for specific targeting of cancer cells and organelles.<sup>16-21</sup> The physical properties of AuNPs (e.g., color, localized surface plasmon resonance (LSPR), electrical conductivity, etc.) are significantly enhanced when they are functionalized with appropriate metal or organic groups.<sup>22</sup> For example, aggregation induced changes in plasmon response can be coupled with colorimetric detection mechanisms to establish rapid analyte detection.<sup>13, 23-27</sup> Such methods are promising in that they entail very simple sample handling procedures, minimum instrumental investment, and can be carried out in the field using portable devices.

The nanoscale properties of AuNPs are size- and shape-dependent,<sup>11, 28</sup> and thus there has been an extensive effort to control AuNP size, shape, and surface composition while



simultaneously maintaining narrow size distributions.<sup>11, 29-32</sup> The synthesis of gold nanoparticles by trisodium citrate ( $\text{Na}_3\text{Ctr}$ ) mediated reduction of aqueous chloroauric acid ( $\text{HAuCl}_4$ )<sup>8, 9</sup>, is one of the most widely used AuNP synthesis strategies. This synthesis approach, involving rapid addition of  $\text{Na}_3\text{Ctr}$  into a hot aqueous solution of  $\text{HAuCl}_4$ , has been modified and optimized over many decades.<sup>31, 33-35</sup> In this synthesis  $\text{Na}_3\text{Ctr}$  simultaneously acts as (i) reducing agent (driving the reduction of  $\text{Au}^{\text{III}}$  to  $\text{Au}^0$ ),<sup>9, 33, 36, 37</sup> (ii) capping agent (electrostatically stabilizing the AuNP colloidal solution),<sup>37-39</sup> and (iii) pH mediator (modifying the reactivity of Au species involved in the reaction).<sup>31</sup>

Room temperature syntheses of noble metal nanoparticles involving synthetic surfactant<sup>40</sup> and bio-based reductants and capping agents<sup>41</sup> have been previously reported. Seed-mediated growth of AuNPs has been shown to be especially effective in producing highly monodisperse AuNPs<sup>42, 43</sup>. In this work, however, we discuss what we believe to be the first effort to examine seed-mediated AuNP growth in the presence of citrate and gold salt at room temperature. Highly uniform and reproducible gold seeds were prepared for seed-mediated growth using a pH-controlled protocol. By inoculating the growth medium with a controlled number of gold seeds, the particles produced via this approach have sizes varying from 20-110 nm with the final size dependent on the number of seeds and the total concentration of gold ions in the growth solution. Given the room temperature conditions, this seeded growth synthesis approach adheres to Principle 6 of the Green Chemistry Principles<sup>44</sup> (Design for Energy Efficiency), which recommends using ambient temperature and pressure when possible. The longer reaction times also offer new opportunities to probe the reaction mechanism and study the evolution of AuNP size and morphology.

Sustainability has been identified as an emerging design criterion in nanomaterial synthesis.<sup>3</sup> Incorporating green chemistry and engineering principles into nanoscience has been suggested as a proactive approach to mitigate the environmental impacts of nanotechnology.<sup>5, 6</sup> However, green synthesis approaches for nanoparticle production may have unintended environmental impacts.<sup>45</sup> Life cycle assessment (LCA) is being increasingly used to study the environmental impacts of different nanotechnologies<sup>46-50</sup> to assess tradeoffs and identify environmental hotspots therein. For example, are reductions in the energy footprint of the AuNP synthesis process due to the milder room temperature conditions substantially larger than any increase in the energy use due to longer reaction times? To investigate this issue, we conducted an LCA study to compare the environmental impacts of the AuNP synthesis at room temperature as well as under boiling conditions.

## **MATERIALS AND METHODS**

**Materials.** Gold(III) chloride trihydrate ( $\text{HAuCl}_4 \cdot 3\text{H}_2\text{O}$ ) and trisodium citrate dihydrate ( $\text{Na}_3\text{Citr} \cdot 2\text{H}_2\text{O}$ ) were purchased from Sigma-Aldrich (St. Louis, MO) at the highest purity grade available. Deionized water (18 M $\Omega$ -cm) was used for all preparations. All glassware was cleaned in a bath of freshly prepared aqua regia ( $\text{HCl}/\text{HNO}_3$ , 3:1 v/v) and then rinsed thoroughly with deionized water prior to use. All reagent solutions were filtered through a 0.2  $\mu\text{m}$  polycarbonate membrane prior to their use in AuNP synthesis.

**AuNP seed preparation.** Gold nanoparticles of  $\approx 14$  nm diameter were synthesized according to Frens *et al.*<sup>8</sup> with a slight modification for size and monodispersity control.<sup>31</sup> This synthesis involves chemical reduction of  $\text{AuCl}_4^-$  at pH 6.2–6.5 by dissolved  $\text{Na}_3\text{Citr}$  at 100 °C. In brief, 100 mL of 1 mM  $\text{HAuCl}_4$  containing 200  $\mu\text{L}$  of 1 M NaOH was prepared in a 250-mL

flask equipped with a condenser. The solution was brought to boil while being stirred with a PTFE-coated magnetic stir-bar and 10 mL of 38.8 mM Na<sub>3</sub>Ctr was rapidly added. The reaction was allowed to proceed until the solution attained a wine red color. After 15 min of reaction, the reflux system was shut down and deionized water was added to the AuNP seed suspension to bring the final volume to ≈100 mL. ‘Room temperature synthesis’ refers to seed-mediated growth of AuNPs, and not the synthesis of AuNP seeds. We note that citrate-stabilized AuNP seeds may be synthesized by other methods that may or may not involve elevated temperatures.

***Seed-mediated AuNP growth at room temperature.*** Growth reactions (40 mL final volume) were performed in a 100-mL Erlenmeyer flask. Briefly, a variable volume aliquot of seed suspension ( $N = 6.54 \times 10^{12}$  particles/mL) and 227  $\mu$ L of 44.7 mM HAuCl<sub>4</sub>·3H<sub>2</sub>O were added to the flask with water. Subsequently, a 176  $\mu$ L aliquot of 38.8 mM Na<sub>3</sub>Ctr·2H<sub>2</sub>O was added to the flask under constant stirring. In these syntheses the only variable was the initial AuNP seed concentration (**Table D1, Appendix D**).

***AuNP characterization.*** UV–vis spectra were acquired using a Cary 5000 UV-vis-NIR spectrophotometer. AuNP suspensions were placed in 1 cm sample cells and spectra between 400-800 nm were acquired at room temperature. For the time-dependent measurements of the seeded growth experiments, solutions were removed and samples were probed within 2 min of reductant addition. At the same time, an aliquot of suspension was frozen at -20 °C. At this temperature the suspended nanoparticles precipitated out of the suspension. The thawed solution was centrifuged at 10000  $\times$  g for 10 min, and the supernatant was used for UV-vis and ICP-MS analysis.

Gold nanoparticles were visualized using a Zeiss 10CA transmission electron microscope equipped with an AMT Advantage GR/HR-B CCD Camera System. Sample aliquots of 3  $\mu$ L

were drop-cast onto carbon-coated 100-mesh copper grids (Electron Microscopy Sciences. After 5 minutes, the drop was wicked away using filter paper. The sample was rinsed three times by inverting the TEM grid onto a drop of water and left in contact with water for 5 seconds, finally allow the grid to dry face up. TEM images of the as prepared AuNPs were used for size distribution measurements. For each sample, the dimensions of >60 particles were quantified using NIH ImageJ software (version 1.44). Electrophoretic mobility and intensity based particle size distributions and hydrodynamic diameter were determined with a Zetasizer NanoZS instrument (Malvern Instruments, UK) with a 173° scattering angle at a temperature of 25 °C. A refractive index of 1.35 and an absorption value of 0.01 were used for the AuNPs.<sup>51</sup> Raman experiments were performed using a WITec alpha500R (Ulm, Germany). A 10× Olympus objective (NA=0.3) was used to focus a 633 nm laser into a 2-mm flow cell. The Raman signal was collected in 5 minutes with 30s of integration time.

***Size and concentration calculation of AuNPs.*** (1) *Size and concentration of Au seeds.* The average size of the gold seeds was calculated via TEM analysis. A TEM image of seeds synthesized via the pH controlled method is shown in **Figure 5-1**. Using ImageJ software, the average nanoparticle diameter ( $d_{seed}$ ) was determined to be  $13.9 \pm 0.5$  nm. Assuming a spherical particle and a reaction yield of 100%,<sup>45</sup> the number density of gold seeds ( $N_{seed} = 6.75 \times 10^{12}$  particles/mL) was calculated based upon the known initial concentration of gold  $c_{Au}$  (mol/L).<sup>52</sup>

$$N_{seed} = \frac{6 \times 10^{21} c_{Au} M}{\pi \rho_{Au} d_{seed}^3} \quad (1)$$

where  $\rho$  is the density for gold ( $19.3 \text{ g/cm}^3$ ) and  $M$  is the atomic weight of gold ( $197 \text{ g/mol}$ ). A similar concentration of  $6.54 \times 10^{12}$  particles/mL was calculated based upon the absorbance of the particle suspension at 450 nm ( $A_{450}$ ) using the method reported by Haiss *et al.*<sup>53</sup>

$$N_{seed} = \frac{A_{450} \times 10^{14}}{d_{seed}^2 \left[ -0.295 + 1.36 \exp\left(-\left(\frac{d_{seed} - 96.8}{78.2}\right)^2\right) \right]} \quad (2)$$

Given the similarity of these values and due to the possibility of overestimating the gold nanoparticle concentration following filtration, a  $N_{seed}$  value of  $6.54 \times 10^{12}$  particles/mL as determined using the Haiss equation was used in all calculations.

(2) *Size and concentration of seed mediated AuNPs.*

Assuming that (a) all of the gold precursor is consumed during the reaction, (b) the resultant AuNPs are spherical in shape, and (c) gold reduction and nanoparticle growth take place without nucleation of new ‘seed’ particles, the effective size of the grown particles can be quantitatively predicted.<sup>54</sup>

$$d_{AuNP}^3 = d_{seed}^3 + \frac{6 \times 10^{21} m_{Au}}{\pi \rho_{Au} n_{seed}} \quad (3)$$

Where  $m_{Au}$  and  $n_{seed}$  are the Au mass (g) and the number of seed particles present during seed mediated growth. The number density of AuNPs ( $N_{AuNP}$ ) is simply  $n_{seed}$  divided by the total volume (V) of the AuNP solution,

$$N_{AuNP} = \frac{n_{seed}}{V} \quad (4)$$

The molar concentration of the AuNP solutions was then calculated by dividing the number density of particles by Avogadro's constant ( $6.022 \times 10^{23}$ ).

***Life cycle assessment (LCA) of AuNP synthesis methods.*** LCA is a quantitative framework used to evaluate the cumulative environmental impacts associated with all stages of a material – from raw material extraction through the end-of-life.<sup>55</sup> We conducted a cradle-to-gate comparative LCA of seeded-AuNP growth at room temperature and under boiling conditions. Our LCA models consider processes from raw material extraction (“cradle”) and processing through the synthesis of the nanoparticles (“gate”). The functional unit is 1 mg of AuNP synthesized by each approach. The LCA models exclude purification steps and synthesis waste

products. Furthermore, we did not consider recycle streams since it is not common practice to capture AuNP waste streams in laboratory scale synthesis.

The material and energy inventories for the AuNP synthesis were built using measured data from our laboratory. The average medium-voltage electricity mix for the US Northeast Power Coordinating Council was used to model energy use. The uncertainty for energy use was modeled as a uniform distribution with the maximum and minimum values being  $\pm 20\%$  of the calculated energy use as per measurements performed in our laboratory. LCA models were constructed using SimaPro (version 8.0.4). The inventory for chemical precursors used in these syntheses was modeled using the EcoInvent database<sup>56</sup> (version 3.01).

Gold(III) chloride and sodium citrate were not found in the LCA inventory databases. Therefore, the synthesis of these two chemicals were modeled as custom-built processes using appropriate assumptions for yield and uncertainties as discussed elsewhere.<sup>57</sup> Life cycle impact assessment (LCIA) was done using the Cumulative Energy Demand (CED) method<sup>56, 58</sup> (version 1.09) and the ReCiPe MidPoint method (version 1.11), using midpoints and the hierarchist (H) perspective with European normalization. CED estimates the embodied and direct energy use for materials and processes in the syntheses and gives a detailed energy footprint. The ReCiPe impact assessment method estimates life cycle impacts across a broad range of impact categories (e.g., climate change, freshwater eutrophication, marine ecotoxicity, etc.). All uncertainty analyses were performed using Monte-Carlo simulations for 1000 runs. The uncertainty analyses include the uncertainties in the custom-defined processes in SimaPro, energy use in lab equipment and the unit processes in EcoInvent used in our LCA models. **Figures D1 and D2** show the chemicals and processes considered in the LCA models. The life cycle inventories are shown in **Table D2, D3 and D4**.

## RESULTS AND DISCUSSION

***Monodisperse AuNP seed production.*** Highly uniform and reproducible AuNP seeds were prepared via citrate reduction both with and without pH adjustment. In the traditional Turkevich/Frens' approach, nanoparticle size, nanoparticle polydispersity, and the overall reaction mechanism are determined by the solution pH set by  $[\text{Na}_3\text{Ctr}]$ .<sup>31</sup> Unfortunately, as the  $\text{Na}_3\text{Ctr}/\text{HAuCl}_4$  ratio increases from 0 to 30 there is an increase in solution pH from 2.8 to 6.8 (**Figure D3, Appendix D**). Over this pH range,  $\text{AuCl}_4^-$  undergoes pH-dependent hydrolysis to produce  $[\text{AuCl}_x(\text{OH})_{4-x}]^-$  ( $x=0-4$ ) complexes.<sup>59</sup> Due to the electron withdrawing capacity of the hydroxyl ligand increased gold ion hydroxylation results in a decrease in standard reduction potential (**Figure D4, Appendix D**).<sup>31, 60, 61</sup> Past studies have shown that the final AuNP size can be tuned by changing the solution pH due to this effect<sup>31, 60</sup>

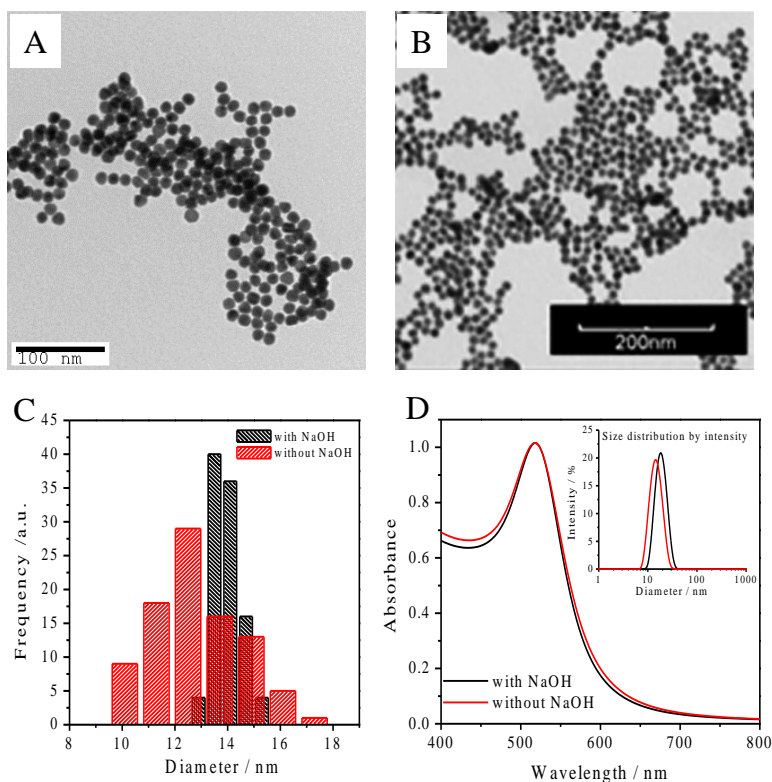


**Figure 5-1** - TEM micrographs of seed nanoparticles synthesized by (A) pH controlled method and (B) w/o pH control; (C) TEM size distributions from both methods; (D) Normalized absorption spectra and hydrodynamic size distribution by intensity (Inset) of two seed suspensions with (black lines) and w/o pH controlled (red lines) procedures. Suspensions were diluted 3× and 9× for UV-vis and DLS measurements, respectively.

Addition of  $\text{Na}_3\text{Cit}$  without pH control causes the solution pH to increase above 6.2 during the latter stages of AuNP synthesis. This change converts highly reactive  $\text{AuCl}_3(\text{OH})^-$  into less reactive complexes of  $\text{AuCl}_x(\text{OH})_{4-x}$  ( $x=0-2$ ), and the reaction pathway consists of a single nucleation-growth step.<sup>31, 61</sup> Tight control of nanoparticle size is challenging under these conditions because growth and nucleation occur simultaneously during the early stages of  $\text{Na}_3\text{Cit}$  addition (i.e., when the  $\text{pH} < 6.2$ ). To address this issue during seed preparation we set the solution pH to a value of  $\approx 6.4$  by addition of 200  $\mu\text{L}$  of 1 M NaOH to the reaction solution.

**Figure 5-1A** shows a typical TEM micrograph for seed nanoparticles synthesized using our pH controlled synthetic protocol. The nanoparticles are highly monodisperse with a pseudo-



spherical diameter of  $13.9 \pm 0.5$  nm and an average aspect ratio (AR) of  $1.06 \pm 0.04$ . We also calculated average particle diameters using Haiss' equation (11) (with  $B_1=3.00$  and  $B_2=2.20$ ),<sup>53</sup> based on the UV-vis spectra of the AuNP seeds. This particle diameter ( $13.6 \pm 0.7$  nm) closely matched the average particle size obtained from TEM measurements ( $13.9 \pm 0.5$  nm). The size distribution of 3.6% coincides with a highly reproducible DLS Z-average diameter and polydispersity index (PDI),  $17.7 \pm 0.8$  nm and  $0.03 \pm 0.01$ , respectively, for twelve replicate batches. Particles synthesized without pH control (i.e., without adding NaOH) were also characterized (as illustrated in **Figure 5-1**). For this synthesis, the pH value of 5.6 at the beginning of reaction was set by the  $\text{Na}_3\text{Ct}/\text{HAuCl}_4$  ratio alone (**Figure D3, Appendix D**). Compared with the pH controlled synthesis, an immediate color change ( $< 1$  min) of the reaction suspension was observed following  $\text{Na}_3\text{Ct}$  injection, while the pH controlled reaction required 2-3 min to see a similar color change, thus indicating faster nucleation and growth due to the higher reactivity of the gold complexes at elevated pH (**Figure D4, Appendix D**). Although **Figure 5-1D** shows the two syntheses have very similar LSPR  $\lambda_{\text{max}}$  (517.9 nm for non pH controlled particles, 518.5 nm for pH controlled particles), the hydrodynamic diameter and TEM diameter of the nanoparticle increased from 15.2 nm to 17.7 nm and from 12.9 nm to 13.9 nm respectively as the pH increased from 5.6 to 6.4. Consistent with the broader TEM size distribution (**Figure 5-1C**) and absorption peak width at half maximum<sup>62</sup> of the LSPR band (**Figure 5-1D**), a larger PDI of 0.19 was obtained for the non-pH controlled particles along with a 17% error between the particle size determined based upon the TEM measurements (12.9 nm of) and the size calculated using the Haiss equation (10.7 nm). As the initial  $\text{Au}^{\text{III}}$  concentration and the  $\text{Na}_3\text{Ct}/\text{HAuCl}_4$  ratio were both fixed for the two seed synthesis approaches, this finding

is consistent with the previous observation that AuNP size and monodispersity of gold nanocrystals are strongly dependent on the initial pH of the reaction medium.<sup>31</sup>

**Room temperature seeded growth of AuNPs.** Because of the rapid reaction kinetics at 100 °C it is necessary to keep Au<sup>III</sup> and the reductant apart during seed-mediated growth<sup>63</sup> and the order and speed of reagent addition strongly affect the final size and polydispersity of the nanoparticles.<sup>62</sup> To achieve improved nanoparticle homogeneity, we hypothesized that seeded growth could be carried out at room temperature – and could simply be initiated following addition of seed nanoparticles to premixed solutions of Au<sup>III</sup> and reductant (or alternatively the introduction of Au<sup>III</sup> to a mixture of reductant and seeds). As illustrated herein, such an outcome can be accomplished when the rate constant for surface mediated growth is significantly greater than the rate constant for nucleation – a condition that occurs at room temperature. As shown in **Figure 5-2**, by inoculating the growth medium with a controlled number of gold seeds, the particles produced via this approach have sizes varying from 20-110 nm with the final size dependent on the number of seeds and the total concentration of gold ions in the growth solution. A majority of the NPs produced by this approach are quasi-spherical in shape, although nanocrystal triangles and rods also form in low yield in the larger nanoparticle (>70 nm) preparations (Supporting Information). Ignoring the presence of the non-spherical particles, the average diameters and concentrations of the particles were determined and are tabulated in **Table 5-1**. For this calculation, we assumed that all of the particles exhibit spherical geometries. However, as illustrated in **Figure 5-2** this assumption becomes increasingly incorrect for the larger nanomaterial sizes. We note that the similarity in particle size determined experimentally and predicted using equation (3) suggests that nucleation of small nanoparticles does not occur,

thus indicating that the final concentration of AuNPs correlates well with the initial number of AuNP seeds.

**Table 5-1** - Sizes, concentrations, zeta-potentials, and optical properties of seeded AuNPs

AuNP	SPR peak (nm)	Concentration (NPs/mL) <sup>a</sup>	Mean $\xi$ potential (mV)	Diameter of AuNP (nm)		
				Calculated <sup>b</sup>	TEM <sup>c</sup>	Z-average/PDI (DLS)
A	525.9		-40.5±1.2	22.7	24.0±6.1	25.9/0.193
B	533.9		-40.2±0.7	34.2	37.1±4.6	25.0/0.53
C	536.5	5.5×10 <sup>11</sup> 1.3×10 <sup>11</sup>	-38.7±1.1	45.7	46.0±4.6	31.2/0.502
D	537.2	5.4×10 <sup>10</sup> 2.7×10 <sup>10</sup>	-40.7±1.6	57.1	57.6±4.5	45.9/0.314
E	541.2	1.6×10 <sup>10</sup>	-42.7±0.5	68.6	69.6±11.8	61.2/0.239
F	551.9	9.7×10 <sup>9</sup> 6.5×10 <sup>9</sup>	-43.5±0.6	80.0	82.5±14.0	79.2/0.162
G	561.2	4.6×10 <sup>9</sup> 3.3×10 <sup>9</sup>	-44.4±1.5	91.4	92.4±11.4	89.7/0.148
H	569.9		-42.2±2.7	102.9	100.0±11.4	97.8/0.113
I	581.9		-46.6±1.4	114.3	111.0±8.3	105.8/0.114

<sup>a</sup>Theoretical concentration of seeded AuNPs based upon the seed concentration and assuming that all gold salt precursors are reduced to gold atoms that condense onto the seed particle surface;

<sup>b</sup>Particle sizes as determined using Eq 3 for a seed concentration of 6.54×10<sup>12</sup> particles / mL.

<sup>c</sup>For the particles with one dimension elongated, the sizes are overestimated by  $[(AR)^{1/6} - 1] \times 100\%$ . (where AR is the aspect ratio of the elongated particle).

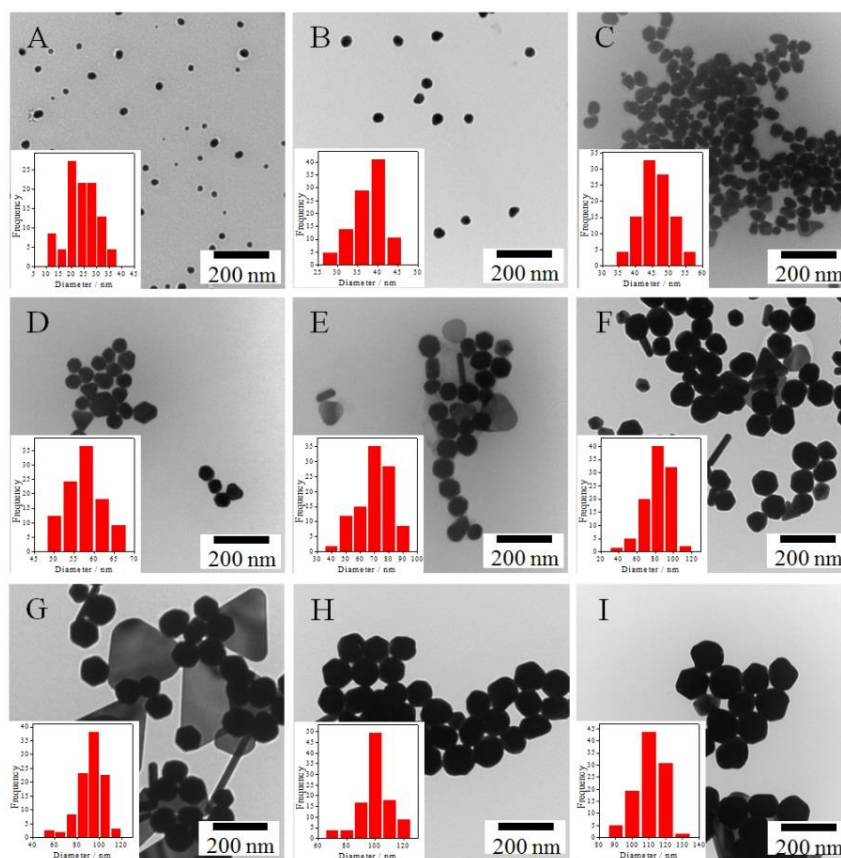


**Figure 5-2** - TEM images of room temperature seed-mediated AuNPs of different sizes (aspect ratio): A)  $24.0 \pm 6.1$  nm (AR:  $1.15 \pm 0.17$ ), B)  $37.1 \pm 4.6$  nm (AR:  $1.15 \pm 0.11$ ), C)  $46.0 \pm 4.6$  nm (AR:  $1.34 \pm 0.14$ ), D)  $57.6 \pm 4.5$  nm (AR:  $1.14 \pm 0.06$ ), E)  $69.6 \pm 11.8$  nm (AR:  $1.13 \pm 0.07$ ), F)  $82.5 \pm 14.0$  nm (AR:  $1.13 \pm 0.07$ ), G)  $92.4 \pm 11.4$  nm (AR:  $1.15 \pm 0.11$ ), H)  $100 \pm 11.4$  nm (AR:  $1.11 \pm 0.11$ ), I)  $111.0 \pm 8.3$  nm (AR:  $1.11 \pm 0.09$ ). Inset: histograms of diameters as determined by NIH ImageJ software.

As indicated in **Table 5-1** and **Figure D6A (Appendix D)**, we determined the hydrodynamic diameter and size distribution of the AuNPs using DLS. The extreme sensitivity of the scattered signal to changes in the radius ( $R$ ) of the scattering objects (scattered intensity  $\propto R^6$ ),<sup>64</sup> enables DLS to detect the presence of even small numbers of aggregates in NP dispersions. The seeded AuNPs in our work are not true spheres and should be described as ovoid with one dimension elongated relative to the other. The effects of rotational diffusion result in the appearance of a false peak in a size range of about 5-10 nm during DLS measurement for size distribution by

intensity.<sup>65</sup> This artifact causes the hydrodynamic size determined by DLS to be smaller than the TEM determined core size, a result consistent with production of AuNPs by seed-mediated growth at 100 °C.<sup>66,67</sup>

Gold nanoparticles display colors and LSPR bands in the visible spectral region that are dependent upon NP size and shape.<sup>11,68,69</sup> The origin of the LSPR band is the coherent excitation of free conduction electrons due to polarization induced by the electric field of the incident light. A change in the absorbance or wavelength of the LSPR band provides a measure of particle size, shape, as well as aggregation state. UV-vis measurements were obtained to provide additional characterization of the nanoparticle properties. In **Figure D6B (Appendix D)**, we provide both optical images and normalized UV-vis spectra for AuNPs of different sizes. For nanoparticle diameters between 14 and 120 nm, the color exhibits a smooth transition from dark red to pink and ultimately to yellowish brown. As expected,<sup>70</sup> the LSPR wavelength is dependent on the nanoparticle size, as evinced by the increase of the maximum absorbance wavelength ( $\lambda_{\text{max}}$ ) from 518 to 582 nm for nanoparticles of increasing size. This red shift is accompanied by the broadening of the LSPR band in the long wavelength region. This broadening may be due to an increase in polydispersity,<sup>71</sup> particle agglomeration,<sup>31</sup> or a combination of both processes. Samples left at room temperature in the dark often agglomerated and precipitated, but could be easily re-suspended by shaking or sonication. Such storage exhibited no effect on nanoparticle stability.

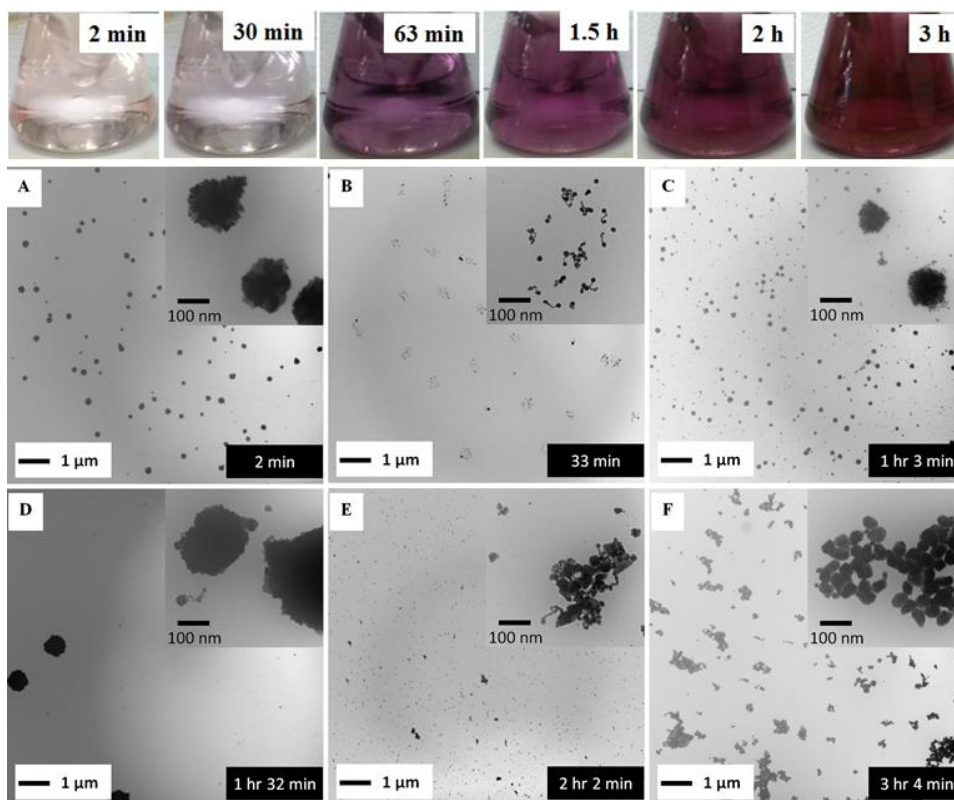
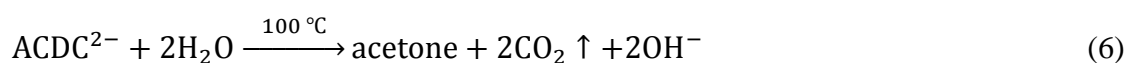
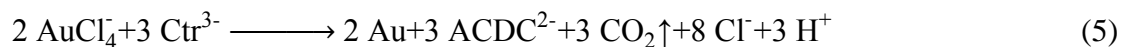
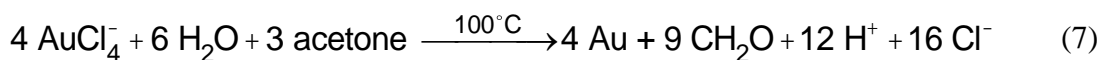


**Figure 5-3** - Seed mediated growth for AuNPs (C) with mixed solution of  $\text{HAuCl}_4$  (0.254 mM), Au seeds ( $5.35 \times 10^{10}$  particle/ml), and  $\text{Na}_3\text{Ctr}$  (0.17 mM) at room temperature. TEM images of particles obtained at different growth times.

**Monitoring seed-mediated AuNP growth process.** During AuNP synthesis,  $\text{Ctr}^{3-}$  is oxidized to acetone dicarboxylate ( $\text{ACDC}^{2-}$ ; eqn. 5), a ligand that complexes  $\text{Au}^{\text{III}}$ , thus facilitating nanoparticle growth. Following nanoparticle nucleation,  $\text{ACDC}^{2-}$  is thought to be rapidly degraded to acetate at the synthesis temperature of  $\approx 100^\circ\text{C}$ .<sup>9</sup>



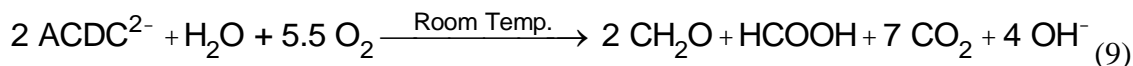
Past studies suggest that ACDC<sup>2-</sup> or its degradation products take part in additional redox reactions when the Na<sub>3</sub>Ctr /HAuCl<sub>4</sub> ratio is less than 1.5.<sup>62</sup> Of particular relevance is a model developed based upon the kinetics of the AuNP formation which suggests that acetone or other carboxylate byproducts formed by the degradation of ACDC<sup>2-</sup> (eqn. 6) reduce auric chloride and lead to its complete conversion to Au<sup>0</sup> (eqn. 7).<sup>9,39</sup>



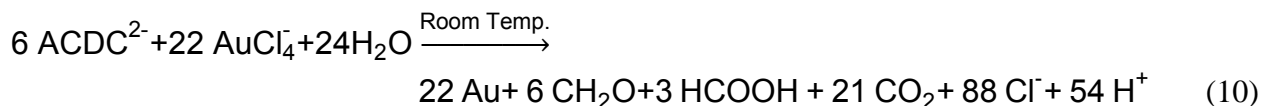
Summing up equations 5-7 and correcting for the reaction stoichiometry provides the following:



This model, however, does not consider the effects of temperature on ACDC<sup>2-</sup> degradation. At room temperature it is known that ACDC<sup>2-</sup> undergoes slow oxidation in the presence of oxygen.<sup>72</sup>

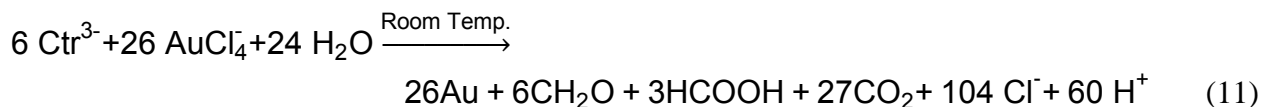


We speculate the following similar reaction occurs preferentially in the presence of Au<sup>III</sup>:



By summing up equations 5 and 10, the reaction stoichiometry in equation 11 indicates that

1 mol of citrate can reduce > 4 mol of HAuCl<sub>4</sub>.



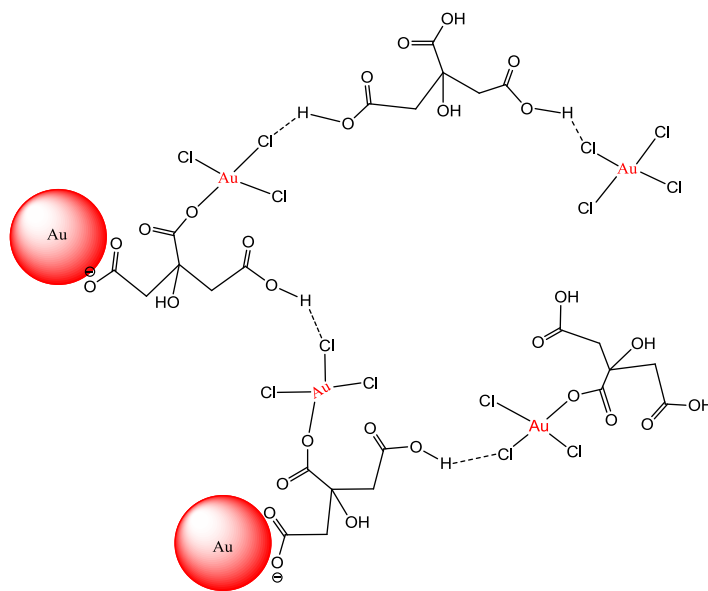
We note that both Ctr<sup>3-</sup> and ACDC<sup>2-</sup> are carboxylates and that any byproducts of their oxidation, reduction, or degradation are likely to contain carboxylate groups.<sup>73</sup> Therefore, the carboxylate moiety is a likely means of interaction agent with the AuNP surface regardless of the exact species involved in AuNP capping.<sup>74, 75</sup>



As noted previously, room temperature reaction conditions slow the AuNP synthesis reaction, thus allowing for improved opportunities to characterize the seeded growth process. At room temperature, the suspension color changed very slowly, but followed a similar sequence as the traditional process at elevated temperature (i.e., from pale pink (seeds), to dark blue, to purple). **Figure 5-3** shows typical TEM images for different growth times for seed mediated AuNPs prepared at a Na<sub>3</sub>Ctr/HAuCl<sub>4</sub> ratio of 0.67 and a seed concentration of  $5.35 \times 10^{10}$  particles/mL (this corresponds to the ‘Type C’ AuNPs in **Table 5-1**). As shown in **Figure D7 (Appendix D)**, the UV absorption of Na<sub>3</sub>Ctr decreases dramatically following Au<sup>III</sup> addition, thus indicating its rapid coordination with Au<sup>III</sup>. In this synthesis, Na<sub>3</sub>Ctr facilitates coordination of Au<sup>III</sup> ions around the AuNP seeds. This coordination involves fast ligand exchange between the carboxylates and chlorine ions within the AuCl<sub>x</sub>(OH)<sub>4-x</sub> complexes.<sup>37</sup>

Previous studies suggest that the mode of interaction between Na<sub>3</sub>Ct and AuNPs/Au ions is likely through a bidentate bridging mode or via unidentate or chelate modes.<sup>39, 76-78</sup> As shown in **Figure 5-3A**, within 2 minutes of mixing the AuNP seeds with Na<sub>3</sub>Ctr and HAuCl<sub>4</sub> we observed formation of large (> 100 nm) weakly associated clusters that consist of large numbers of AuNP seeds. These images are very similar to the large fluffy clusters observed by Chow and Zukoski in the early stage of AuNP synthesis at 60 °C.<sup>35</sup> Some of these crystallites may have formed following the drying of the suspension on the TEM grid. Nonetheless, this result suggests that carboxylates bound to the seed surface and present in the growth medium enhance the association between AuNP seeds and Au<sup>III</sup> ions (Scheme 1). After 30 minutes the clusters are no longer observed and have broken apart due to the continued reaction between the carboxylates and Au<sup>III</sup> and the suspension exhibits a light blue color. **Figure 5-3B** shows irregular gold nanowires together with aggregates at this growth stage, a result similar to the observations by Ji

*et al.*<sup>31</sup> and Pei *et al.*<sup>79</sup> for nanoparticles produced using Frens' method.<sup>8</sup> After 1 hour, the gold nanowires form fluffy spherical networks (diameter  $\approx$  100 nm; **Figure 5-3C**). In **Figure 5-3C** (inset), some irregular gold nanowires remain isolated from the larger network. As the reaction proceeds, however, the network continues to grow in size (**Figure 5-3D**). Similar trends in the AuNP synthesis progress at elevated temperatures have been reported by previous researchers.<sup>35</sup> After two hours, the fluffy network breaks apart into smaller segments (**Figure 5-3E**). Ultimately, as the color of the reaction suspension changes color to purple-red, spherical nanoparticles with diameter of 30-40 nm cleave off of the nanowires (**Figure 5-3F**). At the conclusion of the reaction, evinced by the unchanging particle diameter (**Figure 5-4B**) and LSPR peak (**Figure 5-4C**), the suspension attains a purple-red color and well-defined particles of 46 nm diameter are observed (**Figure 5-2C**).



**Scheme 5-1** - Reactions among Au seeds, citrate and  $\text{AuCl}_4^-$  after initial mixing.

Aliquots of the reaction suspensions were also extracted and monitored by DLS and UV-Vis to further characterize the particle growth process depicted in **Figure 5-3**. **Figure 5-4A** illustrates

the intensity weighted hydrodynamic size distributions determined by DLS at different growth stages. In addition to the peak for the seeded particles in the region of 10-100 nm, a small size distribution peak was detected after 1 hour of growth. This peak can be explained as a result of the formation of non-spherical particles with one dimension elongated relative to the other. The effects of rotational diffusion result in the appearance of a false peak in a size range of about 5-10 nm during DLS measurement.<sup>65</sup> The presence of this peak is also consistent with the TEM results in **Figure 5-3 C-F** that show that there is a small proportion of particles with sizes less than 10 nm. The mean diameter of the major peak located between 10–100 nm increased dramatically (**Figure 5-4B**) within an hour of Na<sub>3</sub>Ctr addition and then stabilized at ≈57 nm after 3 hours. The latter phenomenon agrees with the TEM result in **Figure 5-3F**, which shows that at this point the reaction progress has neared completion of the “cleave” process. Interestingly, there is no evidence in either **Figure 5-4A** or **5-4B** of spherical networks with size in excess of 100 nm, which suggests that the large networks may have formed during TEM sample preparation. Capillary drying forces are well known to result in enhanced nanoparticle association following drop drying.<sup>80</sup> The association between solution phase Au<sup>III</sup> and the AuNPs is reflected in the absorption spectra in **Figure 5-4C**. There was a broad absorption at wavelengths > 600 nm that increased in magnitude as time increased from t=2 min to t=92 min. This phase of the particle size evolution corresponds to **Figure 5-3 A-D**, during which the AuNPs form fluffy networks. The broadening of the LSPR peak in the region > 600 nm (**Figure 5-4C**) and the increased absorbance at 700 nm (**Figure 5-4C inset**) corresponds to these fluffy networks. After 92 minutes, a sharp red-shift in the LSPR peak was observed (**Figure 5-4C**), which has been referred to as “turnover” in the literature<sup>81</sup>. The “turnover” point at t=92 min supports the structure/size change from **Figure 5-3D** to **5-3E**, during which the fluffy networked

structure gave way to discrete AuNPs, which also corresponds to the decreased absorbance at 700 nm (**Figure 5-4C inset**).

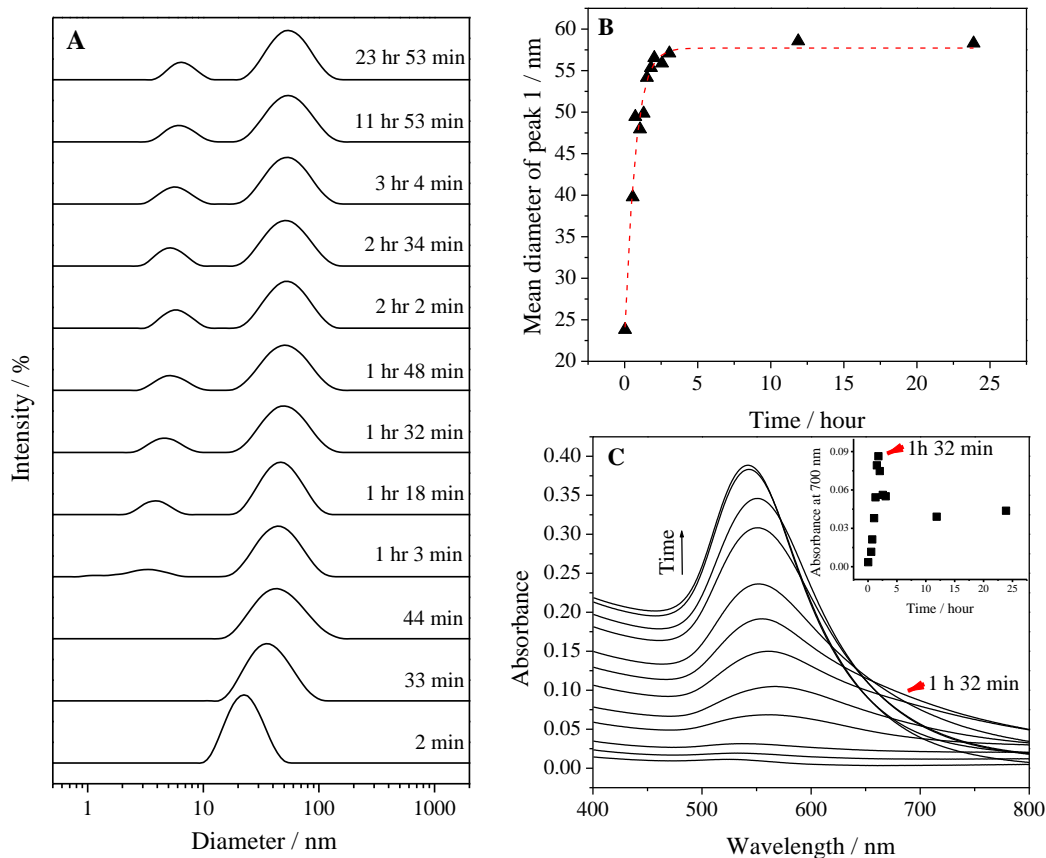


**Figure 5-4** - (A) Size distribution by intensity, (B) mean diameter of peak 1 (located in the range of 10 – 100 nm in A) and (C) UV-vis absorption spectra obtained at different time stages of seed growth synthesis of AuNPs.

Reaction supernatants separated by centrifugation at each reaction time were analyzed by UV-vis spectroscopy and ICP-MS. As shown in **Figure 5-5**, the absorbance at  $\approx 218$  nm, which corresponds to unreacted  $\text{Au}^{\text{III}}$ ,<sup>82</sup> decreases rapidly after the initial mixing of the reagents, stabilizes for approximately 30 minutes, and then decreases linearly with time. Compared to the initial  $\text{Au}^{\text{III}}$  peak intensity at 218 nm,  $\approx 30\%$  of  $\text{Au}^{\text{III}}$  was reduced after the initial mixing of the reagents. A total of  $\approx 93\%$  Au was detected by ICP-MS in the reaction supernatant, which may

include the intermediate reduced product of Au<sup>III</sup> or very small AuNPs. Such a result is consistent with rapid coordination between the carboxylates and Au<sup>III</sup> and association of these complexes with the Au seeds (i.e., the clusters of seeds and Au<sup>III</sup> shown in **Figure 5-3A**). The Au<sup>III</sup> concentration was then stable for next 30 minutes. Such a result suggests that the initial oxidation-reduction reaction only takes place in the clusters shown in **Figure 5-3A** and Scheme 1, which is consistent with the change from **Figure 5-3A** to **5-3B**. After the initial 30 minutes of reaction, the concentration of both Au<sup>III</sup> and total Au in the supernatant began to decrease linearly and a total reaction time of  $\approx 5$  hours was observed. We used UV-vis spectroscopy to verify that the AuNP growth reaction proceeded according to equation 11. A mixture of HCl and NaCl with relative concentrations based upon the stoichiometry of equation 11 was prepared to compare the UV absorption of supernatant of the reaction solution after 5 hours reaction. A perfect match of the spectra shown in **Figure D8 (Appendix D)** provides evidence that the stoichiometry of the room temperature seed mediated growth process is reasonably described by equation 11. Moreover, no residual gold chloride ion was detected in the UV-vis spectrum of the supernatant. As has been previously reported<sup>31</sup>, residual gold ion can be detected in the UV-vis spectra. The absence of this peak in the final UV-vis spectra suggests that there was no residual gold ion. For this reason a 100% reaction yield was assumed, which was also verified by the ICP-MS results in **Figure 5-5**. To the best of our knowledge this is the first time a reaction stoichiometry has been developed for room-temperature seed-mediated AuNP synthesis.

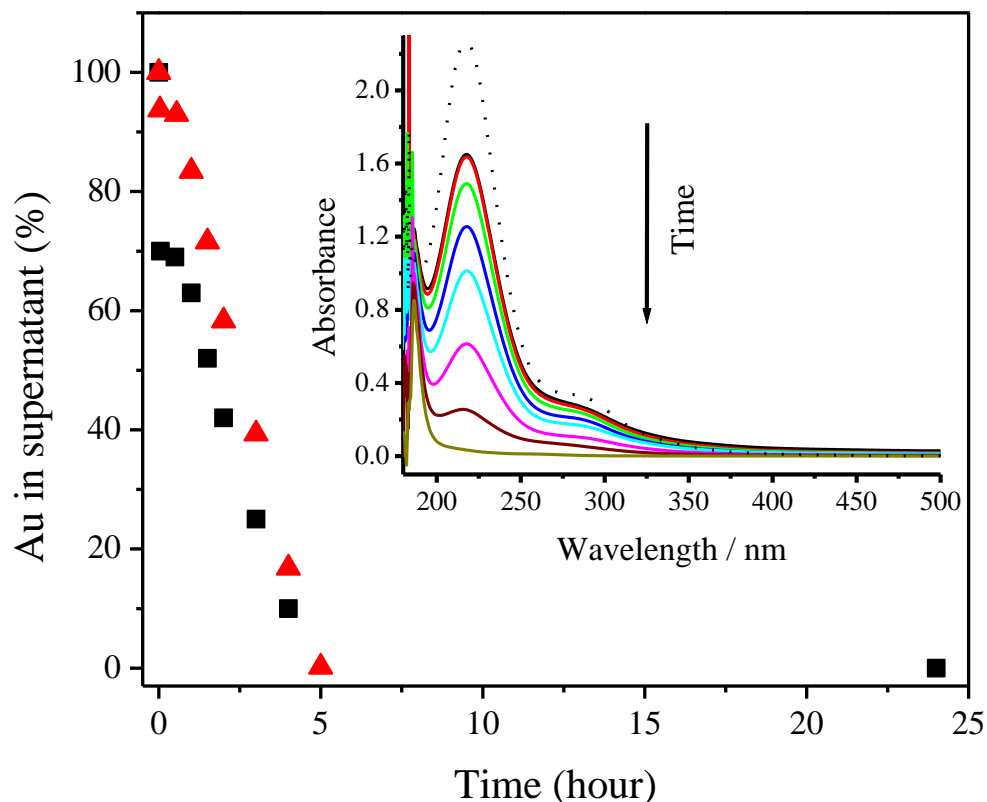


**Figure 5-5** – Time-dependent Au<sup>III</sup> and Au level in supernatant by UV-vis (squares) and ICP-MS (triangles). Inset: corresponding UV absorption spectra. Dash black line is the spectrum of the initial AuIII solution. Prior to the UV-vis measurement, all AuNP suspensions were diluted 2× with deionized water.

*Evaluation of room temperature seeded AuNPs.* The as-prepared AuNPs exhibit exceptional colloidal stability and can be stored at room temperature over several months in spite of their slow agglomeration. The nanoparticles could be easily re-suspended by shaking or sonication. This result suggests these particles can be favorably employed for SERS applications. **Figure 5-6** gives the comparison of surface Raman enhancement of MGITC adsorbed on seed mediated 46 nm AuNPs produced at room temperature and those produced at 100 °C (**Figure D9, Appendix D**). Importantly, the AuNPs prepared at room temperature exhibit a 2× greater

Raman enhancement than AuNPs prepared at 100 °C. We attribute this enhancement to the greater surface roughness of the room temperature AuNPs.<sup>83</sup>

The particles with edges, corners or branches (e.g., nanorods, nanostars) were stable at low temperatures, but are likely to transform into more thermodynamically stable shapes (spheres) if sufficient thermal energy were provided for atomic reorganization. The particles prepared at room temperature had more edges and corners than 100 °C prepared particles, as shown by TEM images (**Figure D9, Appendix D**). Due to the same concentration and volume of AuNPs, the surface area of the resulting particles at room temperature will be larger than those synthesized at 100°C, which explains increased surface roughness compared to AuNPs prepared at 100°C.

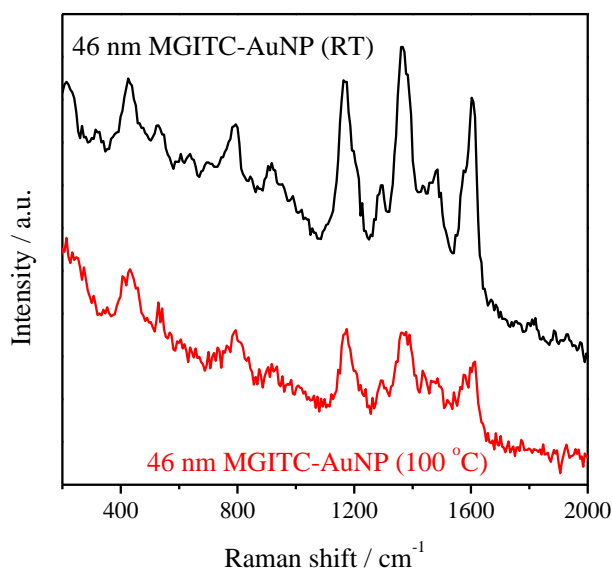


**Figure 5-6** - SERS spectra of MGITC (20 nM) adsorbed on room temperature and 100 °C seed mediated AuNPs under 633 nm excitation. MGITC-AuNPs were prepared by quickly adding  $\approx 1.5 \mu\text{L}$  of 14  $\mu\text{M}$  MGITC solution to 1 mL AuNP suspension ( $5.4 \times 10^{10}$  particle/mL).

**Comparative LCA.** The cumulative energy demand (CED) of the AuNP synthesis methods from the LCA models are presented in **Table 5-2**. The results show that despite the longer

reaction time, AuNP synthesis at room temperature has lower CED than synthesis under boiling conditions. The trend of the other impacts across different impact categories matches that of the CED (**Figure D10, Appendix D**). This result is expected as CED has been shown to correlate well to other environmental impact methods (e.g., EcoIndicator, EcoScarcity, etc.).<sup>84</sup> This observation is understandable because the use of fossil fuels (included in CED) is a dominant driver of many environmental impacts.<sup>85</sup>

Uncertainty analysis shows that the differences in the environmental impacts for AuNP synthesis at room temperature and under boiling conditions are statistically significant (**Figure D11, Appendix D**). Although laboratory-scale room temperature synthesis does seem to reduce the energy footprint of AuNP synthesis (compared to the conventional approach at higher temperatures), further studies on scale-up scenarios are recommended, since the environmental footprints are likely to be influenced by yield, energy efficiencies and the available energy sources and fuel-mixes.<sup>86, 87</sup> Conventional scale-up of boilers and generators has been shown to follow a power law relationship.<sup>88, 89</sup> However, similar relationships for scaling up have not been established for nanoparticle synthesis. Longer reaction times in pilot-scale and commercial-scale setups will involve additional

**Table 5-2** - Cumulative energy demand (CED) for AuNP synthesis at room temperature vs. boiling conditions. The CEDs for AuNP syntheses at room temperature and under boiling conditions are 1.25 MJ and 1.54 MJ respectively.

Synthesis at room temperature		
Material and energy inputs	Cumulative energy demand (MJ)	% contribution
Chloroauric acid	$4.07 \times 10^{-1}$	32.59%
Deionized water	$8.31 \times 10^{-3}$	0.67%
Aqua regia	$5.67 \times 10^{-2}$	4.54%
AuNP 'seeds'	$1.60 \times 10^{-2}$	1.28%
Sodium hydroxide	$5.27 \times 10^{-7}$	$4.22 \times 10^{-5}\%$
Trisodium citrate	$5.12 \times 10^{-6}$	$4.10 \times 10^{-4}\%$
Stirring	$7.61 \times 10^{-1}$	60.93%
<b>Total</b>	<b><math>1.25 \times 10^0</math></b>	<b>100.00%</b>

Synthesis under boiling conditions		
Material and energy inputs	Cumulative energy demand (MJ)	% contribution
Chloroauric acid	$4.07 \times 10^{-1}$	26.48%
DI water	$8.31 \times 10^{-3}$	0.54%
Tap water	$1.67 \times 10^{-4}$	0.01%
Aqua regia	$5.67 \times 10^{-2}$	3.69%
AuNP 'seeds'	$1.60 \times 10^{-2}$	1.04%
Sodium hydroxide	$5.27 \times 10^{-7}$	$3.43 \times 10^{-5}\%$
Trisodium citrate	$5.12 \times 10^{-6}$	$3.33 \times 10^{-4}\%$
Heating	$9.73 \times 10^{-1}$	63.29%
Stirring	$7.61 \times 10^{-2}$	4.95%
<b>Total</b>	<b><math>1.54 \times 10^0</math></b>	<b>100.00%</b>



energy demands (e.g., lighting, heat ventilation, air-conditioning etc.) which should also be considered in scale up scenarios. The role of regional variability in the energy and water footprints should also be factored into future decisions about nanomaterials industry siting and resource allocation.

## **CONCLUSIONS**

A simple room temperature seed mediated preparation route for AuNPs has been demonstrated. Tunability of the AuNP diameter was achieved by simply varying the number concentration of seeds under mild environmental conditions. Such a result shows a promising colorimetric assay using the size-dependent optical property. The continuous surface plasmon oscillations associated with this broad spectral feature gives them broad selection in the future SERS applications. Our reported AuNP synthesis approach helps decrease the rate of AuNP growth due to the milder (room temperature) conditions, thus providing increased opportunities to study a very complicated reaction mechanism. Moreover, this method shows significant reductions in the cradle-to-gate life cycle impacts compared to the previously reported methods that employed boiling conditions.

## **ACKNOWLEDGEMENTS**

This work was supported by grants from the Virginia Tech Graduate School (Sustainable Nanotechnology Interdisciplinary Graduate Education Program), the Virginia Tech Institute of Critical Technology and Applied Science (ICTAS), and NSF Award CBET-1133746.

## REFERENCES

1. Kushnir, D.; Sandén, B. A., Multi-Level Energy Analysis of Emerging Technologies: A Case Study in New Materials for Lithium Ion Batteries. *Journal of Cleaner Production* **2011**, *19*, (13), 1405-1416.
2. Kushnir, D.; Sandén, B. A., Energy Requirements of Carbon Nanoparticle Production. *Journal of Industrial Ecology* **2008**, *12*, (3), 360-375.
3. Murphy, C. J., Sustainability as an emerging design criterion in nanoparticle synthesis and applications. *J. Mater. Chem.* **2008**, *18*, (19), 2173-2176.
4. Grzelczak, M.; Pérez-Juste, J.; Mulvaney, P.; Liz-Marzán, L. M., Shape control in gold nanoparticle synthesis. *Chemical Society Reviews* **2008**, *37*, (9), 1783-1791.
5. Dahl, J. A.; Maddux, B. L. S.; Hutchison, J. E., Toward Greener Nanosynthesis. *Chemical Reviews* **2007**, *107*, (6), 2228-2269.
6. Hutchison, J. E., Greener Nanoscience: A Proactive Approach to Advancing Applications and Reducing Implications of Nanotechnology. *ACS Nano* **2008**, *2*, (3), 395-402.
7. McKenzie, L. C.; Hutchison, J. E., Green nanoscience. *Chimica oggi* **2004**, *22*, (9), 30-33.
8. Frens, G., Controlled Nucleation for the Regulation of the Particle Size in Monodisperse Gold Suspensions. *Nature* **1973**, *241*, (105), 20-22.
9. Turkevich, J.; Stevenson, P. C.; Hillier, J., The nucleation and growth processes in the synthesis of colloidal gold. *Discuss. Faraday Soc.* **1951**, *No. 11*, 55-75.
10. Kogan, M. J.; Bastus, N. G.; Amigo, R.; Grillo-Bosch, D.; Araya, E.; Turiel, A.; Labarta, A.; Giralt, E.; Puentes, V. F., Nanoparticle-Mediated Local and Remote Manipulation of Protein Aggregation. *Nano Letters* **2006**, *6*, (1), 110-115.
11. Daniel, M.-C.; Astruc, D., Gold Nanoparticles: Assembly, Supramolecular Chemistry, Quantum-Size-Related Properties, and Applications toward Biology, Catalysis, and Nanotechnology. *Chemical Reviews (Washington, DC, United States)* **2004**, *104*, (1), 293-346.
12. Bastus, N. G.; Sanchez-Tillo, E.; Pujals, S.; Farrera, C.; Lopez, C.; Giralt, E.; Celada, A.; Lloberas, J.; Puentes, V., Homogeneous Conjugation of Peptides onto Gold Nanoparticles Enhances Macrophage Response. *ACS Nano* **2009**, *3*, (6), 1335-1344.
13. Connor, E. E.; Mwamuka, J.; Gole, A.; Murphy, C. J.; Wyatt, M. D., Gold nanoparticles are taken up by human cells but do not cause acute cytotoxicity. *Small* **2005**, *1*, (3), 325-327.
14. Chen, Y.-S.; Hung, Y.-C.; Liao, I.; Huang, G. S., Assessment of the in vivo toxicity of gold nanoparticles. *Nanoscale Research Letters* **2009**, *4*, (8), 858-864.

15. Hauck, T. S.; Ghazani, A. A.; Chan, W. C. W., Assessing the effect of surface chemistry on gold nanorod uptake, toxicity, and gene expression in mammalian cells. *Small* **2008**, *4*, (1), 153-159.
16. Brown, S. D.; Nativo, P.; Smith, J.-A.; Stirling, D.; Edwards, P. R.; Venugopal, B.; Flint, D. J.; Plumb, J. A.; Graham, D.; Wheate, N. J., Gold Nanoparticles for the Improved Anticancer Drug Delivery of the Active Component of Oxaliplatin. *Journal of the American Chemical Society* **2010**, *132*, (13), 4678-4684.
17. Bhattacharyya, S.; Bhattacharya, R.; Curley, S.; McNiven, M. A.; Mukherjee, P., Nanoconjugation modulates the trafficking and mechanism of antibody induced receptor endocytosis. *Proceedings of the National Academy of Sciences of the United States of America* **2010**, *107*, (33), 14541-14546, S14541/1-S14541/8.
18. Tkachenko, A. G.; Xie, H.; Coleman, D.; Glomm, W.; Ryan, J.; Anderson, M. F.; Franzen, S.; Feldheim, D. L., Multifunctional gold nanoparticle-peptide complexes for nuclear targeting. *Journal of the American Chemical Society* **2003**, *125*, (16), 4700-4701.
19. Kang, B.; Mackey, M. A.; El-Sayed, M. A., Nuclear Targeting of Gold Nanoparticles in Cancer Cells Induces DNA Damage, Causing Cytokinesis Arrest and Apoptosis. *Journal of the American Chemical Society* **2010**, *132*, (5), 1517-1519.
20. Oh, E.-K.; Delehanty, J. B.; Sapsford, K. E.; Susumu, K.; Goswami, R.; Blanco-Canosa, J. B.; Dawson, P. E.; Granek, J.; Shoff, M.; Zhang, Q.; Goering, P. L.; Huston, A.; Medintz, I. L., Cellular Uptake and Fate of PEGylated Gold Nanoparticles Is Dependent on Both Cell-Penetration Peptides and Particle Size. *ACS Nano* **2011**, *5*, (8), 6434-6448.
21. Paciotti, G. F.; Kingston, D. G. I.; Tamarkin, L., Colloidal gold nanoparticles: a novel nanoparticle platform for developing multifunctional tumor-targeted drug delivery vectors. *Drug Development Research* **2006**, *67*, (1), 47-54.
22. Upadhyayula, V. K. K., Functionalized gold nanoparticle supported sensory mechanisms applied in detection of chemical and biological threat agents: A review. *Analytica Chimica Acta* **2012**, *715*, 1-18.
23. Wang, J., Nanomaterial-based amplified transduction of biomolecular interactions. *Small* **2005**, *1*, (11), 1036-1043.
24. He, P.; Shen, L.; Liu, R.; Luo, Z.; Li, Z., Direct Detection of N2-Agonists by Use of Gold Nanoparticle-Based Colorimetric Assays. *Analytical Chemistry (Washington, DC, United States)* **2012**, *83*, (18), 6988-6995.
25. Pellegrino, T.; Kudera, S.; Liedl, T.; Javier, A. M.; Manna, L.; Parak, W. J., On the development of colloidal nanoparticles towards multifunctional structures and their possible use for biological applications. *Small* **2005**, *1*, (1), 48-63.

26. Scampicchio, M.; Wang, J.; Blasco, A. J.; Arribas, A. S.; Mannino, S.; Escarpa, A., Nanoparticle-Based Assays of Antioxidant Activity. *Analytical Chemistry* **2006**, *78*, (6), 2060-2063.
27. Willner, I.; Baron, R.; Willner, B., Growing metal nanoparticles by enzymes. *Advanced Materials (Weinheim, Germany)* **2006**, *18*, (9), 1109-1120.
28. Burda, C.; Chen, X.; Narayanan, R.; El-Sayed, M. A., Chemistry and Properties of Nanocrystals of Different Shapes. *Chemical Reviews (Washington, DC, United States)* **2005**, *105*, (4), 1025-1102.
29. Nikoobakht, B.; El-Sayed, M. A., Preparation and growth mechanism of gold nanorods (NRs) using seed-mediated growth method. *Chemistry of Materials* **2003**, *15*, (10), 1957-1962.
30. Murphy, C. J.; Jana, N. R., Controlling the aspect ratio of inorganic nanorods and nanowires. *Advanced Materials* **2002**, *14*, (1), 80-82.
31. Ji, X.; Song, X.; Li, J.; Bai, Y.; Yang, W.; Peng, X., Size Control of Gold Nanocrystals in Citrate Reduction: The Third Role of Citrate. *Journal of the American Chemical Society* **2007**, *129*, (45), 13939-13948.
32. Jana, N. R.; Gearheart, L.; Murphy, C. J., Seeding growth for size control of 5-40 nm diameter gold nanoparticles. *Langmuir* **2001**, *17*, (22), 6782-6786.
33. Kimling, J.; Maier, M.; Okenve, B.; Kotaidis, V.; Ballot, H.; Plech, A., Turkevich Method for Gold Nanoparticle Synthesis Revisited. *J. Phys. Chem. B* **2006**, *110*, (32), 15700-15707.
34. Frens, G., Controlled nucleation for the regulation of the particle size in monodisperse gold suspensions. *Nature (London), Physical Science* **1973**, *241*, (105), 20-2.
35. Chow, M. K.; Zukoski, C. F., Gold sol formation mechanisms: role of colloidal stability. *Journal of Colloid and Interface Science* **1994**, *165*, (1), 97-109.
36. Turkevich, J.; Stevenson, P. C.; Hillier, J., The formation of colloidal gold. *Journal of Physical Chemistry* **1953**, *57*, 670-3.
37. Ojea-Jimenez, I.; Romero, F. M.; Bastus, N. G.; Puentes, V., Small Gold Nanoparticles Synthesized with Sodium Citrate and Heavy Water: Insights into the Reaction Mechanism. *Journal of Physical Chemistry C* **2010**, *114*, (4), 1800-1804.
38. Henglein, A.; Giersig, M., Formation of colloidal silver nanoparticles. Capping action of citrate. *J. Phys. Chem. B* **1999**, *103*, (44), 9533-9539.
39. Kumar, S.; Gandhi, K. S.; Kumar, R., Modeling of formation of gold nanoparticles by citrate method. *Industrial & Engineering Chemistry Research* **2007**, *46*, (10), 3128-3136.
40. Sau, T. K.; Murphy, C. J., Room Temperature, High-Yield Synthesis of Multiple Shapes of Gold Nanoparticles in Aqueous Solution. *Journal of the American Chemical Society* **2004**, *126*, (28), 8648-8649.

41. Nadagouda, M. N.; Varma, R. S., Green synthesis of silver and palladium nanoparticles at room temperature using coffee and tea extract. *Green Chemistry* **2008**, *10*, (8), 859-862.
42. Perrault, S. D.; Chan, W. C. W., Synthesis and Surface Modification of Highly Monodispersed, Spherical Gold Nanoparticles of 50–200 nm. *Journal of the American Chemical Society* **2009**, *131*, (47), 17042-17043.
43. Ziegler, C.; Eychmüller, A., Seeded Growth Synthesis of Uniform Gold Nanoparticles with Diameters of 15–300 nm. *The Journal of Physical Chemistry C* **2011**, *115*, (11), 4502-4506.
44. Anastas, P. T.; Warner, J. C., *Green chemistry: theory and practice*. Oxford University Press, USA: 2000.
45. Pati, P.; McGinnis, S.; Vikesland, P. J., Life Cycle Assessment of “Green” Nanoparticle Synthesis Methods. *Environmental Engineering Science* **2014**.
46. Walser, T.; Demou, E.; Lang, D. J.; Hellweg, S., Prospective Environmental Life Cycle Assessment of Nanosilver T-Shirts. *Environmental Science & Technology* **2011**, *45*, (10), 4570-4578.
47. Bauer, C.; Buchgeister, J.; Hischer, R.; Poganietz, W. R.; Schebek, L.; Warsen, J., Towards a Framework for Life Cycle Thinking in the Assessment of Nanotechnology. *Journal of Cleaner Production* **2008**, *16*, (8–9), 910-926.
48. Kim, H. C.; Fthenakis, V., Life Cycle Energy and Climate Change Implications of Nanotechnologies. *Journal of Industrial Ecology* **2013**, *17*, (4), 528-541.
49. Li, Q.; McGinnis, S.; Sydnor, C.; Wong, A.; Rennecker, S., Nanocellulose Life Cycle Assessment. *ACS Sustainable Chem. Eng.* **2013**, *1*, (8), 919-928.
50. Upadhyayula, V. K. K.; Meyer, D. E.; Curran, M. A.; Gonzalez, M. A., Evaluating the Environmental Impacts of a Nano-Enhanced Field Emission Display Using Life Cycle Assessment: A Screening-Level Study. *Environmental Science & Technology* **2013**.
51. Chen, H.; Kou, X.; Yang, Z.; Ni, W.; Wang, J., Shape- and Size-Dependent Refractive Index Sensitivity of Gold Nanoparticles. *Langmuir* **2008**, *24*, (10), 5233-5237.
52. Liu, X.; Atwater, M.; Wang, J.; Huo, Q., Extinction coefficient of gold nanoparticles with different sizes and different capping ligands. *Colloids and Surfaces, B: Biointerfaces* **2007**, *58*, (1), 3-7.
53. Haiss, W.; Thanh, N. T. K.; Aveyard, J.; Fernig, D. G., Determination of size and concentration of gold nanoparticles from UV-Vis spectra. *Analytical Chemistry* **2007**, *79*, (11), 4215-4221.
54. Bastus, N. G.; Comenge, J.; Puentes, V., Kinetically Controlled Seeded Growth Synthesis of Citrate-Stabilized Gold Nanoparticles of up to 200 nm: Size Focusing versus Ostwald Ripening. *Langmuir* **2011**, *27*, (17), 11098-11105.

55. Guinée, J. B.; Heijungs, R.; Huppes, G.; Zamagni, A.; Masoni, P.; Buonamici, R.; Ekvall, T.; Rydberg, T., Life Cycle Assessment: Past, Present, and Future†. *Environmental Science & Technology* **2011**, *45*, (1), 90-96.
56. Frischknecht, R.; Jungbluth, N.; Althaus, H.-J.; Doka, G.; Dones, R.; Heck, T.; Hellweg, S.; Hischer, R.; Nemecek, T.; Rebitzer, G., The ecoinvent database: Overview and methodological framework (7 pp). *The International Journal of Life Cycle Assessment* **2005**, *10*, (1), 3-9.
57. Pati, P.; McGinnis, S.; Vikesland, P. J., Life Cycle Assessment of "Green" Nanoparticle Synthesis Methods. *Environ. Eng. Sci.* **2014**, *31*, (7), 410-420.
58. Frischknecht, R.; Jungbluth, N.; Althaus, H. J.; Bauer, C.; Doka, G.; Dones, R.; Hischer, R.; Hellweg, S.; Humbert, S.; Köllner, T. *Implementation of life cycle impact assessment methods*; 3; EcoInvent Report: 2007, 2007.
59. Machesky, M. L.; Andrade, W. O.; Rose, A. W., Adsorption of gold(III)-chloride and gold(I)-thiosulfate anions by goethite. *Geochimica et Cosmochimica Acta* **1991**, *55*, (3), 769-76.
60. Goia, D. V.; Matijevic, E., Tailoring the particle size of monodispersed colloidal gold. *Colloids and Surfaces, A: Physicochemical and Engineering Aspects* **1999**, *146*, (1-3), 139-152.
61. Wang, S.; Qian, K.; Bi, X.; Huang, W., Influence of Speciation of Aqueous HAuCl<sub>4</sub> on the Synthesis, Structure, and Property of Au Colloids. *Journal of Physical Chemistry C* **2009**, *113*, (16), 6505-6510.
62. Brown, K. R.; Walter, D. G.; Natan, M. J., Seeding of colloidal Au nanoparticle solutions. 2. Improved control of particle size and shape. *Chemistry of Materials* **2000**, *12*, (2), 306-313.
63. Brown, K. R.; Walter, D. G.; Natan, M. J., Seeding of colloidal Au nanoparticle solutions. 2. Improved control of particle size and shape. *Chemistry of Materials* **2000**, *12*, (2), 306-313.
64. Thomas, J. C., The determination of log normal particle size distributions by dynamic light scattering. *Journal of Colloid and Interface Science* **1987**, *117*, (1), 187-92.
65. Khlebtsov, B. N.; Khlebtsov, N. G., On the measurement of gold nanoparticle sizes by the dynamic light scattering method. *Colloid Journal* **2011**, *73*, (1), 118-127.
66. Hull, M. S.; Chaurand, P.; Rose, J.; Auffan, M.; Bottero, J.-Y.; Jones, J. C.; Schultz, I. R.; Vikesland, P. J., Filter-Feeding Bivalves Store and Biodeposit Colloidally Stable Gold Nanoparticles. *Environmental Science and Technology* **2011**, *45*, (15), 6592-6599.
67. Leng, W.; Vikesland, P. J., MGITC Facilitated Formation of AuNP Multimers. *Langmuir* **2014**, *30*, (28), 8342-8349.
68. Liz-Marzan, L. M., Tailoring Surface Plasmons through the Morphology and Assembly of Metal Nanoparticles. *Langmuir* **2006**, *22*, (1), 32-41.

69. Murphy, C. J.; San, T. K.; Gole, A. M.; Orendorff, C. J.; Gao, J. X.; Gou, L.; Hunyadi, S. E.; Li, T., Anisotropic metal nanoparticles: Synthesis, assembly, and optical applications. *Journal of Physical Chemistry B* **2005**, *109*, (29), 13857-13870.
70. Kelly, K. L.; Coronado, E.; Zhao, L. L.; Schatz, G. C., The Optical Properties of Metal Nanoparticles: The Influence of Size, Shape, and Dielectric Environment. *J. Phys. Chem. B* **2003**, *107*, (3), 668-677.
71. Wilcoxon, J. P.; Martin, J. E.; Provencio, P., Optical properties of gold and silver nanoclusters investigated by liquid chromatography. *The Journal of Chemical Physics* **2001**, *115*, (2), 998-1008.
72. Kuyper, A. C., Oxidation of citric acid. *Journal of the American Chemical Society* **1933**, *55*, 1722-7.
73. Munro, C. H.; Smith, W. E.; Garner, M.; Clarkson, J.; White, P. C., Characterization of the Surface of a Citrate-Reduced Colloid Optimized for Use as a Substrate for Surface-Enhanced Resonance Raman Scattering. *Langmuir* **1995**, *11*, (10), 3712-3720.
74. Tang, B.; Tao, J.; Xu, S.; Wang, J.; Hurren, C.; Xu, W.; Sun, L.; Wang, X., Using hydroxy carboxylate to synthesize gold nanoparticles in heating and photochemical reactions and their application in textile coloration. *Chemical Engineering Journal (Amsterdam, Netherlands)* **2011**, *172*, (1), 601-607.
75. Iosin, M.; Baldeck, P.; Astilean, S., Study of tryptophan assisted synthesis of gold nanoparticles by combining UV-Vis, fluorescence, and SERS spectroscopy. *Journal of Nanoparticle Research* **2010**, *12*, (8), 2843-2849.
76. Turkevich, J., Colloidal gold. Part I. Historical and preparative aspects, morphology and structure. *Gold Bulletin (Geneva)* **1985**, *18*, (3), 86-91.
77. Turkevich, J., Colloidal gold. Part II. Color, coagulation, adhesion, alloying and catalytic properties. *Gold Bulletin (Geneva)* **1985**, *18*, (4), 125-31.
78. Hull, J. M.; Provorse, M. R.; Aikens, C. M., Formylxoyl Radical-Gold Nanoparticle Binding: A Theoretical Study. *Journal of Physical Chemistry A* **2012**, *116*, (22), 5445-5452.
79. Pei, L.; Mori, K.; Adachi, M., Formation Process of Two-Dimensional Networked Gold Nanowires by Citrate Reduction of AuCl<sub>4</sub><sup>-</sup> and the Shape Stabilization. *Langmuir* **2004**, *20*, (18), 7837-7843.
80. Chang, X.; Vikesland, P. J., Uncontrolled Variability in the Extinction Spectra of C60 Nanoparticle Suspensions. *Langmuir* **2013**, *29*, (31), 9685-9693.
81. Peng, S.; McMahon, J. M.; Schatz, G. C.; Gray, S. K.; Sun, Y., Reversing the size-dependence of surface plasmon resonances. *Proceedings of the National Academy of Sciences of the United States of America* **2010**, *107*, (33), 14530-14534.

82. Peck, J. A.; Tait, C. D.; Swanson, B. I.; Brown Jr, G. E., Speciation of aqueous gold(III) chlorides from ultraviolet/visible absorption and Raman/resonance Raman spectroscopies. *Geochimica et Cosmochimica Acta* **1991**, *55*, (3), 671-676.
83. Talley, C. E.; Jackson, J. B.; Oubre, C.; Grady, N. K.; Hollars, C. W.; Lane, S. M.; Huser, T. R.; Nordlander, P.; Halas, N. J., Surface-Enhanced Raman Scattering from Individual Au Nanoparticles and Nanoparticle Dimer Substrates. *Nano Letters* **2005**, *5*, (8), 1569-1574.
84. Huijbregts, M. A. J.; Hellweg, S.; Frischknecht, R.; Hendriks, H. W. M.; Hungerbühler, K.; Hendriks, A. J., Cumulative Energy Demand As Predictor for the Environmental Burden of Commodity Production. *Environmental Science & Technology* **2010**, *44*, (6), 2189-2196.
85. Huijbregts, M. A. J.; Rombouts, L. J. A.; Hellweg, S.; Frischknecht, R.; Hendriks, A. J.; van de Meent, D.; Ragas, A. M. J.; Reijnders, L.; Struijs, J., Is Cumulative Fossil Energy Demand a Useful Indicator for the Environmental Performance of Products? *Environmental Science & Technology* **2006**, *40*, (3), 641-648.
86. Shibasaki, M.; Fischer, M.; Barthel, L., Effects on Life Cycle Assessment — Scale Up of Processes. In *Advances in Life Cycle Engineering for Sustainable Manufacturing Businesses*, Takata, S.; Umeda, Y., Eds. Springer London: 2007; pp 377-381.
87. Shibasaki, M.; Warburg, N.; Eyerer, P. In *Upscaling effect and Life Cycle Assessment*, 2006, 2006; 2006.
88. Caduff, M.; Huijbregts, M. A. J.; Althaus, H.-J.; Hendriks, A. J., Power-Law Relationships for Estimating Mass, Fuel Consumption and Costs of Energy Conversion Equipments. *Environmental Science & Technology* **2011**, *45*, (2), 751-754.
89. Caduff, M.; Huijbregts, M. A. J.; Koehler, A.; Althaus, H.-J.; Hellweg, S., Scaling Relationships in Life Cycle Assessment. *Journal of Industrial Ecology* **2014**, *18*, (3), 393-406.



## Chapter 6

### Summary

Novel approaches for nanomaterial synthesis that employ renewable, bio-based reagents may intuitively seem *green*. However, these methods must be analyzed from a life cycle perspective to identify hidden environmental costs. LCA of green synthesis of AuNPs showed that the main driver of environmental burdens associated with AuNP synthesis is the large embodied energy of gold. Moreover, reaction yield, which is seldom reported in the literature for green synthesis of nanomaterials, greatly influenced the life cycle impacts of the overall synthesis. The large embodied energy of gold hinted at the potential for reducing the life cycle impacts of AuNP synthesis through recycling. To achieve this objective, host-guest inclusion complex formation facilitated by  $\alpha$ -cyclodextrin (recently reported by Liu *et al.*, (2013)) was employed to successfully recover gold from nanomaterial waste. A major advantage offered by this approach for selective gold recovery over conventional approaches is that the recovery does not involve the use of toxic cyanide or mercury. LCA modeling showed that recycling gold from nanomaterial waste can substantially reduce the life cycle environmental impact of AuNP synthesis. With regard to citrate-reduced AuNPs, conducting the synthesis at room temperature instead of boiling reduced the energy footprint. Moreover, the slow growth of AuNPs at room temperature provided new opportunities for tuning and controlling AuNP size and morphology.

The research presented in this dissertation is an effort to combine laboratory techniques with life cycle modeling to gain new insights into the sustainability of nanotechnology. However, both aspects – laboratory techniques and LCA modeling - have limitations that pose challenges for assessing the life cycle impacts of nanotechnologies. A major challenge in conducting LCAs of nanomaterials is the difficulty in defining appropriate functional units for comparative studies,

because nanomaterials and their synthesis methods are often tailored for unique functionalities that cannot be compared readily. In Chapter 2 and 5, the LCA models for AuNP synthesis excluded the use phase, and were limited to cradle-to-gate analyses. The use phase was also excluded in the LCA studies on AuNP recycling (Chapter 3). This limitation was due to the lack of a single, well-established large-scale use of AuNP, in which the enhanced functionality enabled by AuNPs could be compared with technologies that did not employ AuNPs. Therefore mass was used as the functional unit in the LCA studies reported in Chapter 2, 3 and 5. Indeed, several researchers have conducted cradle-to-gate LCAs for nanotechnologies using mass as a functional unit<sup>1-10</sup>. Mass has also been used as a functional unit even for products from mature industries (e.g., margarine and butter<sup>11</sup>) in comparative LCAs. As a baseline, mass does not capture the functionality associated with the use of nanomaterials. Nonetheless, by using mass as a functional unit, a screening-level, cradle-to-gate LCA of a novel product (e.g., AuNPs) with wide-ranging applications downstream can be a valuable initial step towards more comprehensive LCAs in the future. In addition to defining functional units, compiling the inventories for LCAs on nanomaterials is another challenge. Information about nanomaterial synthesis methods is often proprietary, which makes quantification of the material and energy flows involved in nanomaterial production difficult.<sup>12</sup> Therefore substantial uncertainties exist in the production and release estimates for nanomaterials. While such uncertainties exist due to data gaps, another factor that introduces uncertainty in LCAs is the natural process-to-process and product-to-product variability in the inventory, as well as due to effects of scale-up, improved process efficiencies and the maturing of technologies.

Laboratory and field studies are required to determine the fate and transport, as well as toxicity of nanomaterials in order to inform LCA studies. This information is necessary for

developing nano-specific characterization factors to be used in life cycle impact assessment. However, given the unique properties of nanomaterials, standardized fate and transport studies and toxicological assessments for nanomaterials have not been developed. It is important to note that the LCA studies presented in this dissertation do not account for nano-specific toxicity of gold, because that information is currently not available in impact assessment methods. However, the lack of nano-specific toxicity information in impact assessment methods is not a limitation of LCA, which was originally developed as a framework for studying mature technologies. As nanotechnology matures and the data about the toxicity of different nanomaterials becomes more robust through laboratory and field experiments, nano-specific characterization factors can be developed and integrated in life cycle impact assessment.

Life cycle thinking needs to be a part of nanotechnology, and research efforts should be focused on developing nano-specific characterization factors and impact assessment methods. However, it is not enough to tailor nanotechnology research findings to fit into the traditional LCA framework. Traditional LCAs are retrospective. In addition to streamlining nanotechnology research findings to fit into environmental systems analysis framework, a key research challenge is the development of new life cycle modeling and decision analysis approaches that are adaptive, nimble and anticipatory<sup>13</sup> in order to meet the challenges of emerging nanotechnologies.

Lessons from costly environmental mistakes made in the past urge us to consider the unforeseen implications of promising new technologies. Innovations in regulations and policy measures, however, have been outstripped by technological progress. Given the data gaps and uncertainties related to nanotechnology, it may be tempting to rely on intuition when making decisions or policies. However, intuitions about what is 'green' and sustainability may prove to

be wrong. The research presented in this dissertation shows that life cycle thinking to be an effective inoculation against intuitive, but sometimes faulty notions about sustainability. Regulations and policy measures informed by LCAs are therefore required for the continued growth of nanotechnology and its stewardship along sustainable paths.

## REFERENCES

1. Osterwalder, N.; Capello, C.; Hungerbühler, K.; Stark, W. J., Energy Consumption During Nanoparticle Production: How Economic is Dry Synthesis? *Journal of Nanoparticle Research* **2006**, *8*, (1), 1-9.
2. Joshi, S., Can Nanotechnology Improve the Sustainability of Biobased Products? *Journal of Industrial Ecology* **2008**, *12*, (3), 474-489.
3. Şengül, H.; Theis, T. L., An Environmental Impact Assessment of Quantum Dot Photovoltaics (QDPV) from Raw Material Acquisition Through Use. *Journal of Cleaner Production* **2011**, *19*, (1), 21-31.
4. Deorsola, F. A.; Russo, N.; Blengini, G. A.; Fino, D., Synthesis, characterization and environmental assessment of nanosized MoS<sub>2</sub> particles for lubricants applications. *Chemical Engineering Journal* **2012**, *195–196*, 1-6.
5. Tellaetxe, A.; Blázquez, M.; Arteché, A.; Egizabal, A.; Ermini, V.; Rose, J.; Chaurand, P.; Unzueta, I., Life cycle assessment of the application of nanoclays in wire coating. *IOP Conf. Ser.: Mater. Sci. Eng.* **2012**, *40*, (1), 012014.
6. Weil, M.; Dura, H.; Shimon, B.; Baumann, M.; Zimmermann, B.; Ziemann, S.; Lei, C.; Markoulidis, F.; Lekakou, T.; Decker, M., Ecological assessment of nano-enabled supercapacitors for automotive applications. *IOP Conf. Ser.: Mater. Sci. Eng.* **2012**, *40*, (1), 012013.
7. de Figueirêdo, M. C. B.; Rosa, M. d. F.; Ugaya, C. M. L.; Souza Filho, M. d. S. M. d.; Silva Braid, A. C. C. d.; Melo, L. F. L. d., Life Cycle Assessment of Cellulose Nanowhiskers. *Journal of Cleaner Production* **2012**, *35*, 130-139.
8. LeCorre, D.; Hohenthal, C.; Dufresne, A.; Bras, J., Comparative Sustainability Assessment of Starch Nanocrystals. *J Polym Environ* **2013**, *21*, (1), 71-80.
9. Li, Q.; McGinnis, S.; Sydnor, C.; Wong, A.; Renneckar, S., Nanocellulose Life Cycle Assessment. *ACS Sustainable Chem. Eng.* **2013**, *1*, (8), 919-928.
10. Gao, T.; Jelle, B. P.; Sandberg, L. I.; Gustavsen, A., Monodisperse hollow silica nanospheres for nano insulation materials: Synthesis, characterization, and life cycle assessment. *ACS applied materials & interfaces* **2013**, *5*, (3), 761-7.
11. Nilsson, K.; Flysjö, A.; Davis, J.; Sim, S.; Unger, N.; Bell, S., Comparative Life Cycle Assessment of Margarine and Butter Consumed in the UK, Germany and France. *The International Journal of Life Cycle Assessment* **2010**, *15*, (9), 916-926.

12. Hendren, C. O.; Mesnard, X.; Dröge, J.; Wiesner, M. R., Estimating Production Data for Five Engineered Nanomaterials As a Basis for Exposure Assessment. *Environmental Science & Technology* **2011**, *45*, (7), 2562-2569.
13. Wender, B.; Foley, R. W.; Prado-Lopez, V.; Eisenberg, D. A.; Ravikumar, D.; Hottle, T. A.; Sadowski, J.; Flanagan, W. P.; Fisher, A.; Laurin, L.; Seager, T.; Bates, M. E.; Fraser, M. P.; Linkov, I.; Guston, D. H., Illustrating Anticipatory Life Cycle Assessment for Emerging Photovoltaic Technologies. *Environmental Science & Technology* **2014**.

## Appendix A

### Supplementary materials for Chapter 2

#### Life cycle assessment of “green” nanoparticle synthesis methods

*Paramjeet Pati<sup>1,2,3</sup>, Sean McGinnis<sup>2,4</sup>, and Peter J. Vikesland<sup>1,2,3\*</sup>*

<sup>1</sup>Department of Civil and Environmental Engineering, Virginia Tech, Blacksburg, Virginia

<sup>2</sup>Virginia Tech Institute of Critical Technology and Applied Science (ICTAS) Sustainable Nanotechnology Center (VTSuN), Blacksburg, Virginia

<sup>3</sup>Center for the Environmental Implications of Nanotechnology (CEINT), Duke University, Durham, North Carolina

<sup>4</sup>Department of Materials Science and Engineering and Virginia Tech Green Engineering Program, Virginia Tech, Blacksburg, Virginia

\*Corresponding author. Phone: (540) 231-3568, Email: [pvikes@vt.edu](mailto:pvikes@vt.edu)

*Environmental Engineering Science* 31.7 (2014): 410-420

DOI: 10.1089/ees.2013.0444.

Reprinted (adapted) with permission from Mary Ann Liebert, Inc.

**Table A 1** - Environmental impacts across all impact categories for 1 mg AuNP synthesized using borohydride, citrate, hydrazine, soybean seeds and sugarbeet pulp. (The errors show 95% interval. The source of the error in each case is the combined effect of the uncertainty due to energy use and gold salt (chloroauric acid) model.)

Impact category	Unit	borohydride	citrate	Hydrazine	soybean seed	sugarbeet pulp
<b>Agricultural land occupation</b>	m <sup>2</sup> a	$5.89 \times 10^{-4} \pm 3.10 \times 10^{-4}$	$7.21 \times 10^{-4} \pm 3.40 \times 10^{-5}$	$8.07 \times 10^{-4} \pm 3.86 \times 10^{-4}$	$3.01 \times 10^{-3} \pm 8.90 \times 10^{-4}$	$1.46 \times 10^{-3} \pm 7.04 \times 10^{-4}$
<b>Climate change</b>	kg CO <sub>2</sub> eq	$2.88 \times 10^{-2} \pm 5.4 \times 10^{-3}$	$3.14 \times 10^{-2} \pm 5.35 \times 10^{-3}$	$3.45 \times 10^{-2} \pm 6.30 \times 10^{-3}$	$3.64 \times 10^{-2} \pm 5.95 \times 10^{-3}$	$4.75 \times 10^{-2} \pm 7.15 \times 10^{-3}$
<b>Fossil depletion</b>	kg oil eq	$7.99 \times 10^{-3} \pm 2.36 \times 10^{-3}$	$8.78 \times 10^{-3} \pm 2.27 \times 10^{-3}$	$9.68 \times 10^{-3} \pm 2.86 \times 10^{-3}$	$1.02 \times 10^{-2} \pm 2.56 \times 10^{-3}$	$1.36 \times 10^{-2} \pm 3.20 \times 10^{-3}$
<b>Freshwater ecotoxicity</b>	kg 1,4-DB eq	$1.38 \times 10^{-4} \pm 1.10 \times 10^{-4}$	$1.38 \times 10^{-4} \pm 1.07 \times 10^{-4}$	$1.49 \times 10^{-4} \pm 1.18 \times 10^{-4}$	$1.39 \times 10^{-4} \pm 1.03 \times 10^{-4}$	$1.37 \times 10^{-4} \pm 1.09 \times 10^{-4}$
<b>Freshwater eutrophication</b>	kg P eq	$1.15 \times 10^{-3} \pm 1.38 \times 10^{-3}$	$1.23 \times 10^{-3} \pm 1.40 \times 10^{-3}$	$1.33 \times 10^{-3} \pm 1.64 \times 10^{-3}$	$1.20 \times 10^{-3} \pm 1.37 \times 10^{-3}$	$1.19 \times 10^{-3} \pm 6.73 \times 10^{-3}$
<b>Human toxicity</b>	kg 1,4-DB eq	$1.13 \times 10^{-2} \pm 6.99 \times 10^{-3}$	$1.16 \times 10^{-2} \pm 6.82 \times 10^{-3}$	$1.26 \times 10^{-2} \pm 8.26 \times 10^{-3}$	$1.15 \times 10^{-2} \pm 7.01 \times 10^{-3}$	$1.20 \times 10^{-2} \pm 1.45 \times 10^{-3}$
<b>Ionizing radiation</b>	kBq U-235 eq	$5.25 \times 10^{-3} \pm 7.57 \times 10^{-3}$	$7.86 \times 10^{-3} \pm 1.25 \times 10^{-2}$	$8.82 \times 10^{-3} \pm 1.50 \times 10^{-2}$	$1.16 \times 10^{-2} \pm 1.85 \times 10^{-2}$	$2.16 \times 10^{-2} \pm 3.69 \times 10^{-2}$
<b>Marine ecotoxicity</b>	kg 1,4-DB eq	$1.75 \times 10^{-4} \pm 1.07 \times 10^{-4}$	$1.75 \times 10^{-4} \pm 9.90 \times 10^{-5}$	$1.88 \times 10^{-4} \pm 1.11 \times 10^{-4}$	$1.77 \times 10^{-4} \pm 1.02 \times 10^{-4}$	$1.79 \times 10^{-4} \pm 1.04 \times 10^{-4}$
<b>Marine eutrophication</b>	kg N eq	$6.99 \times 10^{-5} \pm 4.49 \times 10^{-5}$	$7.10 \times 10^{-5} \pm 4.51 \times 10^{-5}$	$7.65 \times 10^{-5} \pm 4.54 \times 10^{-5}$	$8.11 \times 10^{-5} \pm 4.89 \times 10^{-5}$	$7.23 \times 10^{-5} \pm 4.60 \times 10^{-5}$
<b>Metal depletion</b>	kg Fe eq	$1.0 \times 10^{-1} \pm 2.02 \times 10^{-2}$	$9.99 \times 10^{-2} \pm 2.10 \times 10^{-2}$	$1.10 \times 10^{-1} \pm 2.59 \times 10^{-2}$	$9.99 \times 10^{-2} \pm 2.09 \times 10^{-2}$	$1.00 \times 10^{-1} \pm 2.06 \times 10^{-2}$
<b>Natural land transformation</b>	m <sup>2</sup>	$1.36 \times 10^{-5} \pm 8.65 \times 10^{-6}$	$1.38 \times 10^{-5} \pm 8.70 \times 10^{-6}$	$1.52 \times 10^{-5} \pm 1.04 \times 10^{-5}$	$1.40 \times 10^{-5} \pm 9.11 \times 10^{-6}$	$1.46 \times 10^{-5} \pm 1.07 \times 10^{-5}$
<b>Ozone depletion</b>	kg CFC-11 eq	$2.97 \times 10^{-9} \pm 1.48 \times 10^{-9}$	$3.15 \times 10^{-9} \pm 1.42 \times 10^{-9}$	$3.37 \times 10^{-9} \pm 1.55 \times 10^{-9}$	$3.57 \times 10^{-9} \pm 1.48 \times 10^{-9}$	$4.51 \times 10^{-9} \pm 1.80 \times 10^{-9}$
<b>Particulate matter formation</b>	kg PM <sub>10</sub> eq	$1.01 \times 10^{-4} \pm 3.13 \times 10^{-5}$	$1.06 \times 10^{-4} \pm 3.25 \times 10^{-5}$	$1.16 \times 10^{-4} \pm 3.65 \times 10^{-5}$	$1.14 \times 10^{-4} \pm 3.16 \times 10^{-5}$	$1.33 \times 10^{-4} \pm 4.07 \times 10^{-5}$
<b>Photochemical oxidant formation</b>	kg NMVOC	$3.07 \times 10^{-4} \pm 1.17 \times 10^{-4}$	$3.11 \times 10^{-4} \pm 1.16 \times 10^{-4}$	$3.40 \times 10^{-4} \pm 1.35 \times 10^{-4}$	$3.21 \times 10^{-4} \pm 1.12 \times 10^{-4}$	$3.42 \times 10^{-4} \pm 1.20 \times 10^{-4}$
<b>Terrestrial acidification</b>	kg SO <sub>2</sub> eq	$2.73 \times 10^{-4} \pm 7.85 \times 10^{-5}$	$2.92 \times 10^{-4} \pm 8.35 \times 10^{-5}$	$3.22 \times 10^{-4} \pm 9.65 \times 10^{-5}$	$3.29 \times 10^{-4} \pm 9.45 \times 10^{-5}$	$4.13 \times 10^{-4} \pm 1.48 \times 10^{-4}$
<b>Terrestrial ecotoxicity</b>	kg 1,4-DB eq	$9.09 \times 10^{-6} \pm 7.20 \times 10^{-6}$	$9.25 \times 10^{-6} \pm 7.30 \times 10^{-6}$	$1.01 \times 10^{-5} \pm 8.29 \times 10^{-6}$	$9.15 \times 10^{-6} \pm 6.67 \times 10^{-6}$	$9.51 \times 10^{-6} \pm 7.19 \times 10^{-6}$
<b>Urban land occupation</b>	m <sup>2</sup> a	$3.26 \times 10^{-3} \pm 1.51 \times 10^{-3}$	$3.27 \times 10^{-3} \pm 1.51 \times 10^{-3}$	$3.60 \times 10^{-3} \pm 1.77 \times 10^{-3}$	$3.30 \times 10^{-3} \pm 1.56 \times 10^{-3}$	$3.35 \times 10^{-3} \pm 1.52 \times 10^{-3}$
<b>Water depletion</b>	m <sup>3</sup>	$6.66 \times 10^{-2} \pm 1.35 \times 10^{-2}$	$1.07 \times 10^{-1} \pm 1.73 \times 10^{-2}$	$1.24 \times 10^{-1} \pm 2.10 \times 10^{-2}$	$1.76 \times 10^{-1} \pm 3.25 \times 10^{-2}$	$3.46 \times 10^{-1} \pm 7.40 \times 10^{-2}$



**Table A 2 - AuNP morphology, reaction conditions, CEDs for the different synthesis methods (assuming 100% reaction yield).**

Source of reducing agent	AuNP morphology and size distribution	Reaction Time	Temp (° C)	Yield (%)	% Contribution to CED					
					Gold salt	Reducing agent	Energy	Cleaning solvent	DI water	Tap water
Sodium borohydride <sup>1</sup>	Particle size information was not reported	< 5 min	RT	NR	83.6%	0.29%	0.80%	13.3%	1.98%	0.32%
Citrate <sup>2</sup>	Near spherical particles, 13 ± 5 nm.	15 min	100° C, 15 min	> <b>99.9%</b>	72.2%	0.04%	14.68%	11.5%	1.64%	0.03%
Grape pomace <sup>3</sup>	Nearly spherical in (a) 10 -30 nm and (c) 5-10 nm. Anisotropic aggregates in (b) 40 – 50 nm. Microwaved for 60s (Power = 50 W)	3–48 h	-	<b>80%</b>	86.9%	-	0.52%	11%	1.57%	0.03%
Hydrazine <sup>4</sup>	Multi-branched nanoparticles with sizes between 20 – 130 nm	40 min	RT	NR	69.5%	<0.01%	17.70%	11%	1.63%	0.03%
Cypress leaf extract <sup>5</sup>	Nearly-spherical particles and agglomerates. Standard deviations not provided. Mean diameter increased from 5 nm to 94 nm as extract concentration increased.	10 min	RT	<b>94%</b>	27.9%	-	67.29%	4.16%	0.61%	0.01%
<i>C. camphora</i> leaf extract <sup>6</sup>	Near spherical, with some large nanotriangle aggregates. 15 to 25 nm with mean dia 23.4 nm for 0.5 g biomass, 21.5 nm for 1 g biomass	1 hour	30° C	NR	79.5%	-	6.09%	12.6%	1.81%	0.03%
Vitamin B <sub>2</sub> <sup>7</sup>	Spheres, rods and nanowires. Controlled morphology by varying solvent density. 5–12 nm size range (8.1± 0.1 nm) in ethylene glycol. 6–16 nm size range(11.54 ± 0.1 nm) in acetic acid,	30 min	RT	NR	78.3%	-	7.51%	12.4%	1.78%	0.03%
Cinnamon <sup>8</sup>	AuNPs appear near spherical with some anisotropy. Reported dia 13 ± 5 nm The sizes and morphologies are difficult to interpret from the TEM image provided.	30 min	25° C	NR	71.1%	-	15.9%	11.3%	1.61%	0.03%
<i>C. album</i> leaf extract <sup>9</sup>	Near spherical shapes. 10nm-30nm for 1mM HAuCl <sub>4</sub> , 50-100 nm for 5 mM HAuCl <sub>4</sub>	15 min – 2h	RT	NR	52.2%	-	34.78%	8.76%	1.26%	0.02%
Soybean seed <sup>10</sup>	Spherical nanoparticles, 15 ± 4 nm in dia	4 h	RT	NR	58.7%	0.58%	30%	9.31%	1.33%	0.02%
Mushroom <sup>11</sup>	Anisotropic AuNPs with dodecahedral triangular, hexagonal and near-spherical 20 - 150 nm AuNPs were more spherical as extract concentration was increased. No standard deviations/ size ranges provided.	2.5 h,	RT	NR	56%	-	33.8%	8.88%	1.29%	0.02%
Ginseng <sup>12*</sup>	Mostly spherical nanoparticles ranging from ranging from 2 to 40 nm. Mean dia 16.2 ± 3 nm	3 h	RT	NR	62%	-	26.7%	9.84%	1.41%	0.02%
D-Glucose <sup>13</sup>	Discrete, near-spherical AuNPs with narrow size distribution, 5.6 nm sd = 1.37, 6.7 nm sd = 1.24, 8.8nm sd = 1.39 nm	~60 min**	RT	NR	46.7%	-	44.8%	7.41%	1.06%	0.02%
Sugarbeet pulp <sup>14</sup>	Nanowires of 10 – 50 nm diameter, depending upon pH	5 h	RT	NR	40.2%	<0.01%	52.4%	6.38%	0.94%	0.02%
Soybean seed extract <sup>10</sup>	Spherical nanoparticles, 15 ± 4 nm in dia	70 min	95° C for 10 min	NR	30.9%	<0.01%	63.60%	4.9%	0.7%	0.01%
Coriander leaf extract <sup>15</sup>	Spherical, triangle, truncated triangles and decahedral morphologies. 6.75 nm to 57.91 nm with an average size of 20.65±7.09 nm	12 h	RT	NR	16.2%	-	80.76%	2.58%	0.37%	<0.01 %

Glossary shown below **Table A 3**

**Table A 3 - AuNP reaction conditions, Freshwater Ecotoxicity and Agricultural Land Occupation for the different synthesis methods.**

Source of reducing agent	Reaction Time	Temp (° C)	Yield (%)	% Contribution to Freshwater Ecotoxicity						% Contributions to Agricultural Land Occupation					
				Gold salt	Reducing agent	Energy	Cleaning solvent	DI water	Tap water	Gold salt	Reducing agent	Energy	Cleaning solvent	DI water	Tap water
Sodium borohydride <sup>1</sup>	< 5 min	RT	NR	98.5%	<0.01%	<0.01%	0.57%	0.88%	0.04%	76.3%	0.26%	1.1%	18.4%	3.81%	0.09%
Citrate <sup>2</sup>	15 min	100° C, 15 min	> <b>99.9%</b>	98.5%	0.01%	0.07%	0.56%	0.84%	0.04%	62.4%	0.49%	19.1%	15%	2.99%	0.08%
Grape pomace <sup>3</sup>	3–48 h	-	<b>80%</b>	98.8%	-	<0.01%	0.45%	0.67%	0.03%	80.6%	-	0.73%	15.5%	3.07%	0.08%
Hydrazine <sup>4</sup>	40 min	RT	NR	98.3%	0.13%	0.09%	0.56%	0.87%	0.04%	59.3%	<0.01%	22.8%	14.2%	2.92%	0.07%
Cypress leaf extract <sup>5</sup>	10 min	RT	<b>94%</b>	97.7%	-	0.89%	0.53%	0.80%	0.03%	20.4%	-	74%	4.61%	0.93%	0.02%
<i>C. camphora</i> leaf extract <sup>6</sup>	1 hour	30° C	NR	98.5%	-	0.03%	0.56%	0.84%	0.04%	71.2%	-	8.22%	17.1%	3.41%	0.09%
Vitamin B <sub>2</sub> <sup>7</sup>	30 min	RT	NR	98.5%	-	0.04%	0.56%	0.84%	0.04%	69.7%	-	10.1%	16.8%	3.34%	0.09%
Cinnamon <sup>8</sup>	30 min	25° C	NR	98.5%	-	0.08%	0.56%	0.84%	0.04%	61.5%	-	20.7%	14.8%	2.93%	0.08%
<i>C. album</i> leaf extract <sup>9</sup>	15 min – 2h	RT	NR	98.3%	-	0.23%	0.56%	0.84%	0.04%	44.7%	-	42.4%	10.8%	2.14%	0.06%
Soybean seed <sup>10</sup>	4 h	RT	NR	98.3%	0.08%	0.19%	0.56%	0.84%	0.04%	15%	69%	11.6%	3.62%	0.72%	0.02%
Mushroom <sup>11</sup>	2.5 h,	RT	NR	98.3%	-	0.23%	0.56%	0.85%	0.04%	45.4%	-	41.4%	10.9%	2.21%	0.06%
Ginseng <sup>12*</sup>	3 h	RT	NR	98.4%	-	0.16%	0.56%	0.84%	0.04%	51.6%	-	33.4%	12.4%	2.46%	0.06%
D-Glucose <sup>13</sup>	~60 min**	RT	NR	98.2%	-	0.34%	0.56%	0.84%	0.04%	36.6%	-	52.8%	8.8%	1.74%	0.05%
Sugarbeet pulp <sup>14</sup>	5 h	RT	NR	98.1%	<0.01%	0.48%	0.561%	0.86%	0.04%	30.7%	<0.01%	60.3%	7.4%	1.51%	0.04%
Soybean seed extract <sup>10</sup>	70 min	95° C for 10 min	NR	97.8	<0.01%	0.76%	0.56%	0.84%	0.04%	22.6%	0.83%	70%	5.44%	1.08%	0.03%
Coriander leaf extract <sup>15</sup>	12 h	RT	NR	96.8%	-	1.82%	0.55%	0.83%	0.03%	11.4%	-	85.3%	2.74%	0.55%	0.01%

NR – Not Reported (Assumed to be 100%), RT – Room temperature.

\* Using ICP-MS, the authors reported residual gold content in the pellet obtained after centrifugation. Reaction yield was not reported.

\*\* Actual duration for stirring was not reported. These values were estimated based on the description and data reported in the literature. References: **1** Lows and Bansal (2010), **2**- Actual measurements, **3**, Baruwati and Varma (2009), **4** – Jeong *et al.* 2009, **5**. Noruzi *et al.* 2012, **6**. Huang *et al.* 2007, **7**. Nadagouda and Varma (2006), **8**. Chanda *et al.* (2009), **9**. Dwivedi and Gopal (2010), **10**. Shukla *et al.* (2008), **11**. Philip (2009), **12**. Leonard *et al.* (2011), **13**. Raveendran *et al.* (2006), **14** Castro *et al.* (2011). **15**. Narayan and Sakthivel (2008)

## COMPARATIVE LCA OF GREEN AND CONVENTIONAL SYNTHESIS METHODS FOR AuNPs

For eleven out of the sixteen methods shown in **Table A 2**, greater than 60% of the CED can be attributed to the gold salt used for synthesizing AuNPs. We note that although the energy cost embedded in precious metals (e.g., gold) cannot be mitigated by green chemistry approaches, the overall CED can be reduced by choosing the appropriate synthesis method. As shown in **Tables A2 and A3**, when the green synthesis methods involve energy intensive processes (e.g., sonication; (“ginseng” - <sup>1</sup> and long reaction times (“coriander” - <sup>2</sup>, the energy used during the reaction (i.e., electricity) becomes increasingly important compared to the embodied energy in the gold salt.

In all sixteen methods, greater than 96% of the freshwater ecotoxicity is due to gold salt (**Table A 3**). Even for the methods that use toxic chemicals such as hydrazine and sodium borohydride, the contributions of these chemicals to freshwater ecotoxicity were less than 0.15%. The impacts on agricultural land occupation were an order of magnitude higher for soybean and sugarbeet pulp compared to those from sodium borohydride. In the case of sugarbeet pulp (an agricultural waste), the energy requirement for stirring accounted for over 60% of the agricultural land occupation, while the contribution from sugarbeet pulp itself was negligible. In contrast, for the synthesis method using soybean seed as reductant, the energy for stirring accounted to less than 12% of the agricultural land occupation potential, while soybean seed itself accounted for 69% (**Table A 2 and A 3**). These results show the substantial impact of upstream agricultural processes in the case of plant-derived chemicals.

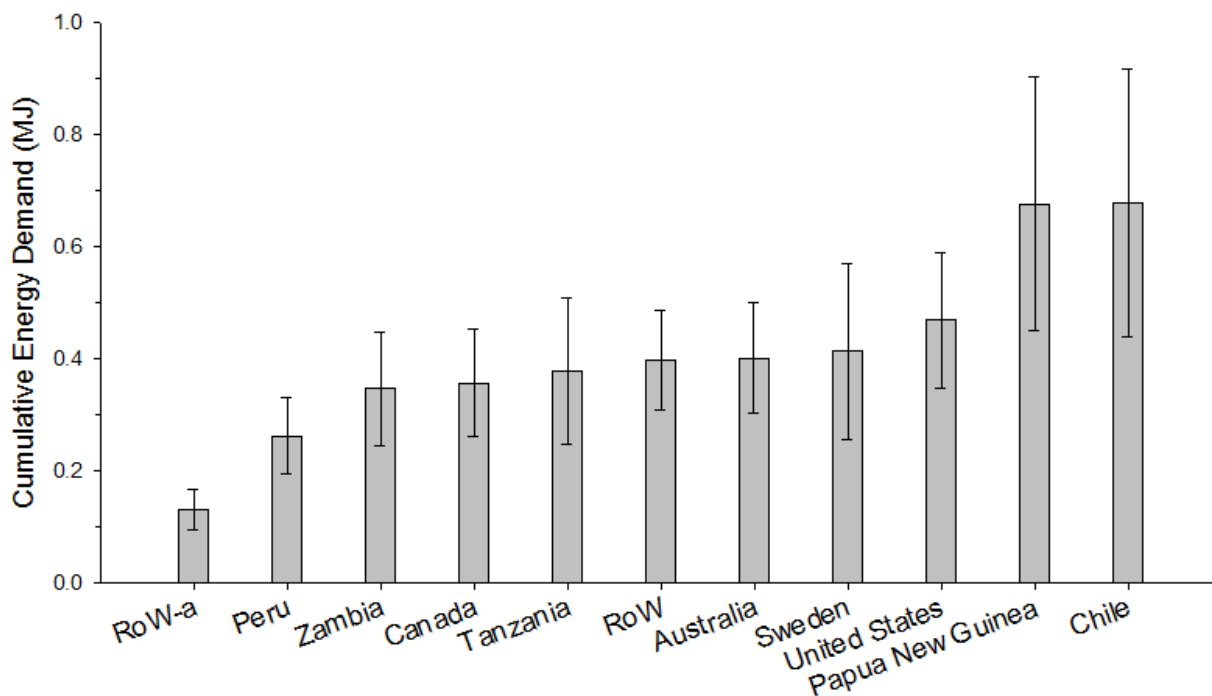


**Figure A 1** - The effect of different gold sources on the cumulative energy demand for citrate-reduced AuNPs. (RoW: Rest of the world. RoW-a: Rest of the world (precious metals from electronic scrap.) Error bars represent 95% confidence intervals for the combined uncertainties in the chloroauric acid and citric acid models, energy use and uncertainties in the EcoInvent unit processes.

## AuNP SYNTHESIS USING SPENT COFFEE AND BANANA PEEL EXTRACT

To investigate the quality (heterodispersity, colloidal stability) of AuNPs using plant-derived chemicals, we developed synthesis protocols that used coffee ground (reductant) and banana peel extract (stabilizer). AuNPs were prepared using spent coffee grounds as reductant and aqueous banana peel extract as stabilizer. 5 g of spent coffee grounds and 20 g of scrapings from banana peel were extracted using 100 mL and 200 mL (respectively) of deionized water at room temperature for 30 minutes under constant stirring. The stirring was then stopped and the heavier fractions were allowed to settle for 30 minutes. The lighter fractions of the extracts were then decanted and filtered through 0.22  $\mu\text{m}$  polyethersulfone (PES) filter (Millipore, Catalog # SCGPT01RE) and stored at 4° C. 4 mL of the spent coffee grounds extract was added to a reaction mixture containing 10 mL of 1 mM gold chloride trihydrate and 2.5 mL of the extract of scrapings from banana peel. The synthesis reactions were conducted at 22° C, 40° C, 60° C and

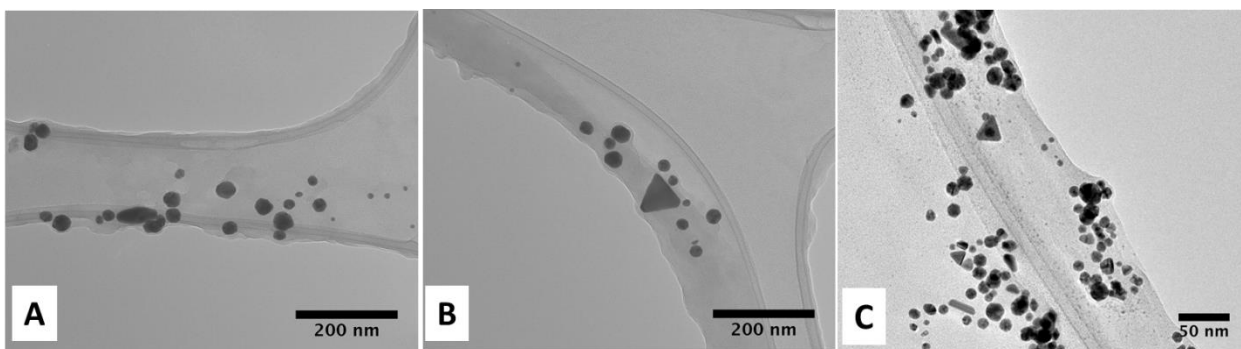


**Figure A 2** - Heterodispersity in AuNP synthesis using plant-derived chemicals. **A)** and **B)** AuNPs prepared using tea **C)** AuNPs prepared using coffee and banana peel extract at 80° C.

80° C.

AuNPs were also prepared using tea as reductant and stabilizer as per the methods reported by<sup>3</sup>. AuNP samples were analyzed by transmission electron microscopy (JEOL 2100 and Philips EM420), Figure A2 shows the heterodispersity in AuNPs prepared using “green” synthesis

methods. Figure S2 **A)** and **B)** AuNPs prepared using tea **C)** AuNPs prepared using coffee and banana peel extract at 80° C.

## REFERENCES

1. Leonard, K.; Ahmmad, B.; Okamura, H.; Kurawaki, J., In situ green synthesis of biocompatible ginseng capped gold nanoparticles with remarkable stability. *Colloids and surfaces. B, Biointerfaces* 2011, 82, (2), 391-6.
2. Narayanan, K. B.; Sakthivel, N., Coriander leaf mediated biosynthesis of gold nanoparticles. *Materials Letters* 2008, 62, (30), 4588-4590.
3. Nune, S. K.; Chanda, N.; Shukla, R.; Katti, K.; Kulkarni, R. R.; Thilakavathi, S.; Mekapothula, S.; Kannan, R.; Katti, K. V., Green Nanotechnology from Tea: Phytochemicals in Tea as Building Blocks for Production of Biocompatible Gold Nanoparticles. *J Mater Chem* 2009, 19, (19), 2912-2920.

## Appendix B

### Supplementary materials for Chapter 3

# Waste Not Want Not: Life Cycle Implications of Gold Recovery and Recycling from Nanowaste

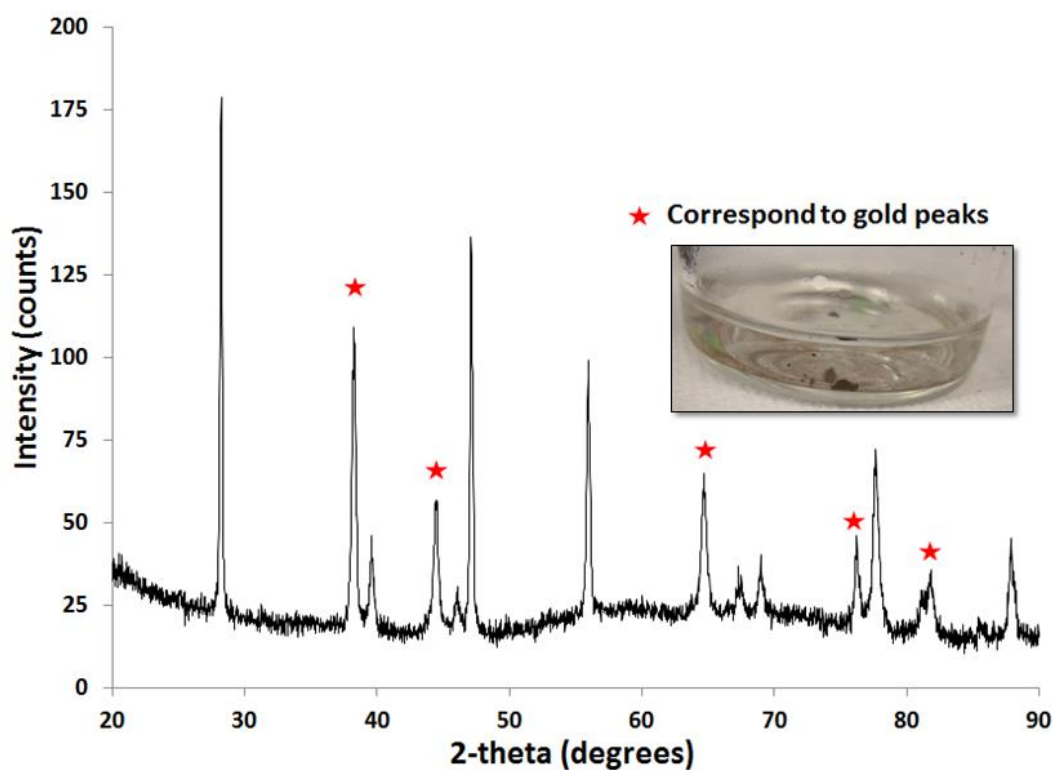


**Figure B 1** - Powder X-ray diffraction of recovered gold. The highlighted peaks correspond to gold peaks. The unidentified peaks are presumably due to impurities. XRD measurements were performed on a Rigaku MiniFlex II instrument (Rigaku Americas, The Woodlands, TX, USA).

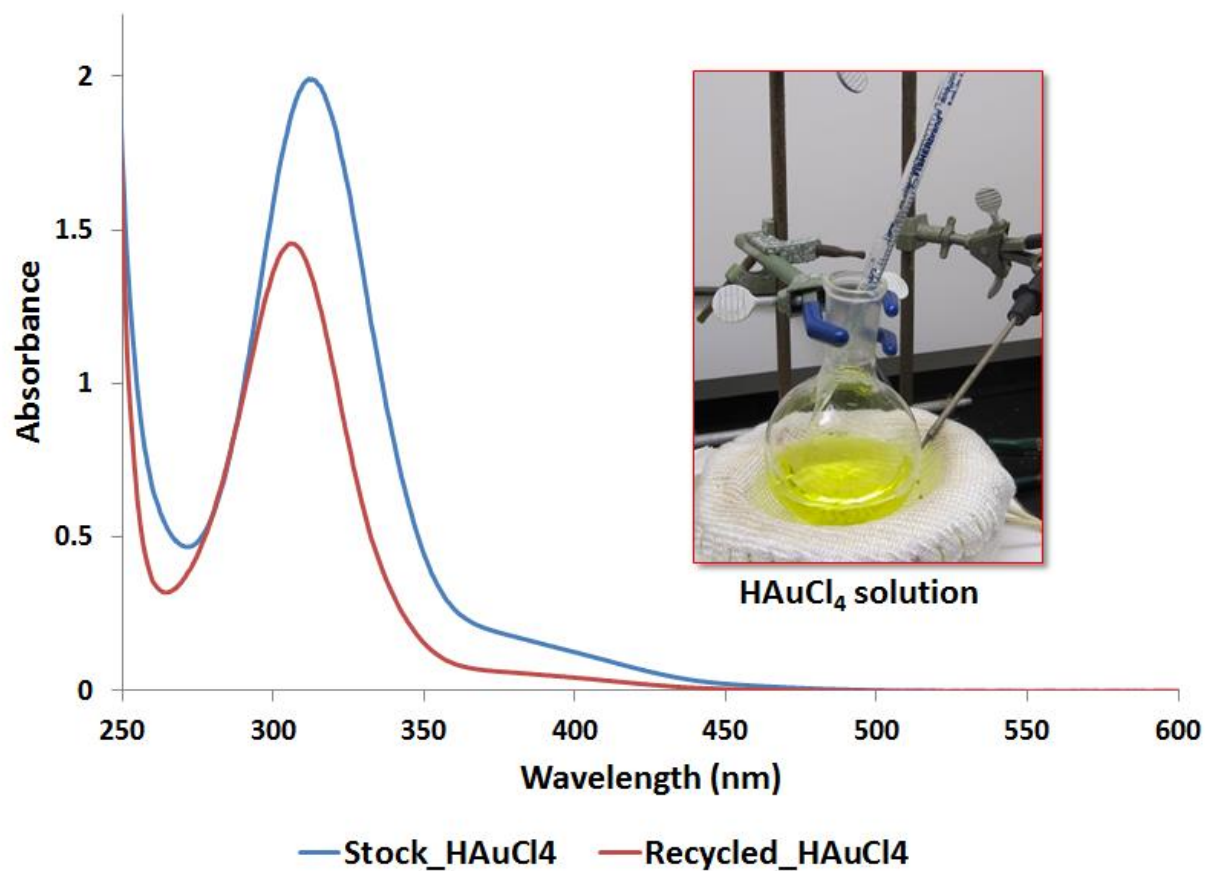
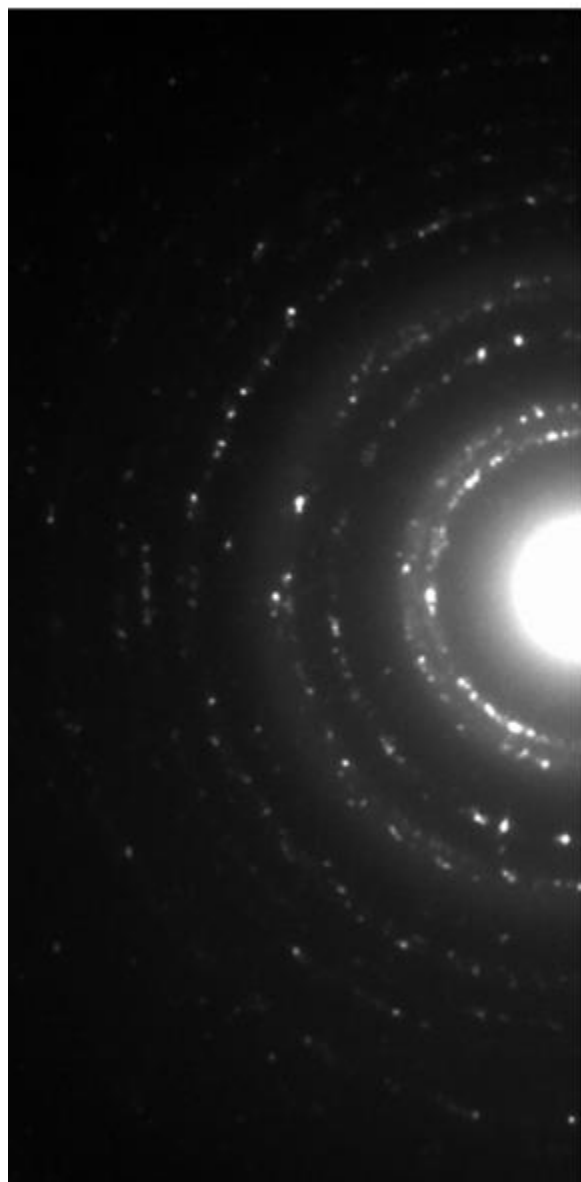


**Figure B 2** - UV-vis spectra of recovered gold chloride and chloroauric acid standard. All measurements were using a Cary 5000 UV-Vis-NIR spectrophotometer (Agilent, Santa Clara, CA). All samples were scanned in quartz cuvettes (Starna, model# 1-Q-10) with 10 mm path length.





Calculated d-spacing (Å) from recovered gold	d-spacing for gold (Å) reported in the literature
1.25, 1.19	1.23, 1.18
1.46	1.44
2.06	2.04
2.39	2.36

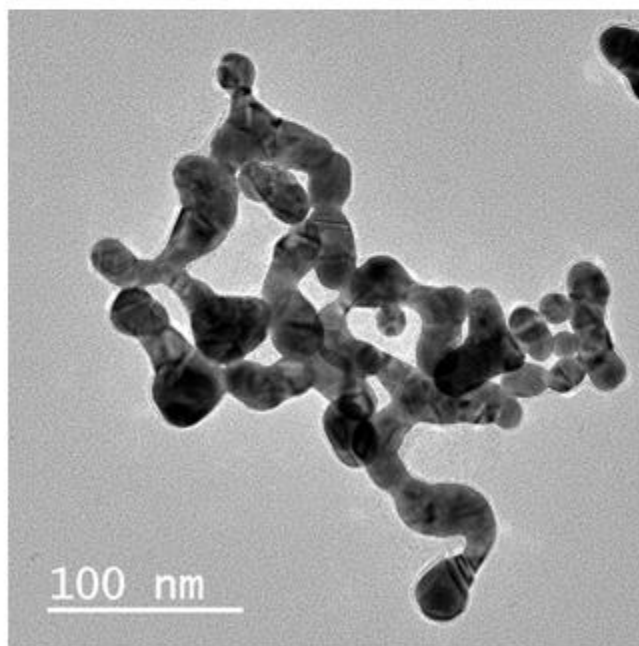


**Figure B 3** - Crystal structure information from SAED measurements confirms that the recovered precipitate is gold. TEM image shows highly aggregated citrate-reduced AuNPs produced by this approach. The existence of 'throats' between individual AuNPs provides evidence of AuNP coalescence. All TEM and SAED measurements were performed on a JEOL 2100 (JEOL, Peabody, MA, USA)

**Table B 1** - Life cycle inventories for custom defined chemicals AuNP synthesis and recovery steps.

<b>[Custom defined] Chloroauric acid (1 mg)</b>		
Gold {US}  production   Alloc Def, S	0.72	mg
Hydrochloric acid, without water, in 30% solution state {RER}  hydrochloric acid production, from the reaction of hydrogen with chlorine   Alloc Def, S	0.13	mg
Chlorine, gaseous {RER}  sodium chloride electrolysis   Alloc Def, S	0.39	mg
<b>[Custom defined] Trisodium citrate (1 mg)</b>		
Citric acid {GLO}  market for   Alloc Def, S	0.51	mg
Soda ash, light, crystalline, heptahydrate {GLO}  market for   Alloc Def, S	0.66	mg
<b>[Custom defined] Hydrobromic acid (1 mg)</b>		
Phosphorus, white, liquid {GLO}  market for   Alloc Def, S	0.13	mg
Bromine {GLO}  market for   Alloc Def, S	0.99	mg
Water, deionised, from tap water, at user {GLO}  market for   Alloc Def, S	0.22	mg
<b>[Custom defined] <math>\alpha</math>-cyclodextrin (1 mg)</b>		
Potato starch {GLO}  market for   Alloc Def, S	1.67	mg
Water, deionised, from tap water, at user {GLO}  market for   Alloc Def, S	16.67	mg
<b>[Stirring]</b> Electricity, medium voltage {NPCC, US only}  market for   Alloc Def, S	0.02	MJ
<b>[Heating]</b> Electricity, medium voltage {NPCC, US only}  market for   Alloc Def, S	0.18	MJ

**Table B 2** - Life cycle inventories for AuNP synthesis steps.

<b>Citrate-reduced gold nanoparticles (1 mg)</b>		
[Custom defined] Chloroauric acid	1.73	mg
[Custom defined] Trisodium citrate	5.08	mg
Water, deionised, from tap water, at user {CH}  production   Alloc Def, S	505.08	g
Tap water {CH}  market for   Alloc Def, S	30.00	g
<i>Cleaning solvents</i>		
Hydrochloric acid, without water, in 30% solution state {RER}  hydrochloric acid production, from the reaction of hydrogen with chlorine   Alloc Def, S	1.81	mg
Nitric acid, without water, in 50% solution state {RER}  nitric acid production, product in 50% solution state   Alloc Def, S	0.72	mg
<b>[Stirring]</b> Electricity, medium voltage {NPCC, US only}  market for   Alloc Def, S	0.01	MJ
<b>[Heating]</b> Electricity, medium voltage {NPCC, US only}  market for   Alloc Def, S	0.08	MJ

**Table B 3 - Life cycle inventories for AuNP recovery steps to treat 1 mg of gold nanowaste**

<b>AuNP precipitation using NaCl</b>		
Sodium chloride, powder {RER}  production   Alloc Def, S	7.42	mg
<b>Dissolution of precipitate using HBr and HNO<sub>3</sub>, followed by pH adjustment using KOH</b>		
[Custom defined] Hydrobromic acid	680.81	mg
Nitric acid, without water, in 50% solution state {GLO}  market for   Alloc Def, S	216.28	mg
Potassium hydroxide {GLO}  market for   Alloc Def, S	148.45	mg
Water, deionised, from tap water, at user {GLO}  market for   Alloc Def, S	1015.38	mg
<b>Gold : <math>\alpha</math>-cyclodextrin complex formation</b>		
[Custom defined] $\alpha$ -cyclodextrin	9.88	mg
<b>Gold : <math>\alpha</math>-cyclodextrin complex resuspension using sonication</b>		
Water, deionised, from tap water, at user {GLO}  market for   Alloc Def, S	5076.92	mg
Electricity, medium voltage {NPCC, US only}  market for   Alloc Def, S	4.21	kJ
<b>Gold precipitation from gold : <math>\alpha</math>-cyclodextrin complex</b>		
Sodium hydrogen sulfite {GLO}  market for   Alloc Def, S	138.95	mg
[Note: Sodium metabisulfite (Na <sub>2</sub> S <sub>2</sub> O <sub>5</sub> ) was not available in the EcoInvent inventory. Instead, we used sodium hydrogen sulfite (NaHSO <sub>3</sub> ) in the LCA models]		
<b>Dissolution of recovered gold in aqua regia</b>		
Hydrochloric acid, without water, in 30% solution state {RER}  hydrochloric acid production, from the reaction of hydrogen with chlorine   Alloc Def, S	452.99	mg
Nitric acid, without water, in 50% solution state {RER}  nitric acid production, product in 50% solution state   Alloc Def, S	180.35	mg
<b>HNO<sub>3</sub> boil-off , HCl addition and pH adjustment using KOH to obtain chloroauric acid for AuNP synthesis from recovered gold</b>		
Hydrochloric acid, without water, in 30% solution state {RER}  hydrochloric acid production, from the reaction of hydrogen with chlorine   Alloc Def, S	604.15	mg
Water, deionised, from tap water, at user {GLO}  market for   Alloc Def, S	10153.83	mg
Potassium hydroxide {GLO}  market for   Alloc Def, S	7.42	mg
Electricity, medium voltage {NPCC, US only}  market for   Alloc Def, S	0.07	MJ

## UNCERTAINTY ANALYSIS IN LCA

LCA results typically involve correlated uncertainties. For example, the 90%-recycle and no-recycle models use chemicals and processes from the life cycle inventories (such as gold, water, electricity, etc.) that are common to both scenarios. In such cases, the uncertainty in the LCA inventory for a chemical (say, gold) is common to all recycle scenarios, and is therefore

correlated. In the case of correlated uncertainties, differences in results may be statistically significant, even if the error bars at the 95% confidence level overlap (**Figure B4**, left). Therefore, we have chosen to represent uncertainty by comparing the actual Monte Carlo simulations. As seen from the tabulated results in **Figure B4** (right), of the 1000 runs performed during Monte Carlo simulation, the majority show that recycling has lower environmental burdens in the key impact categories (ecotoxicity, eutrophication, and metal depletion).

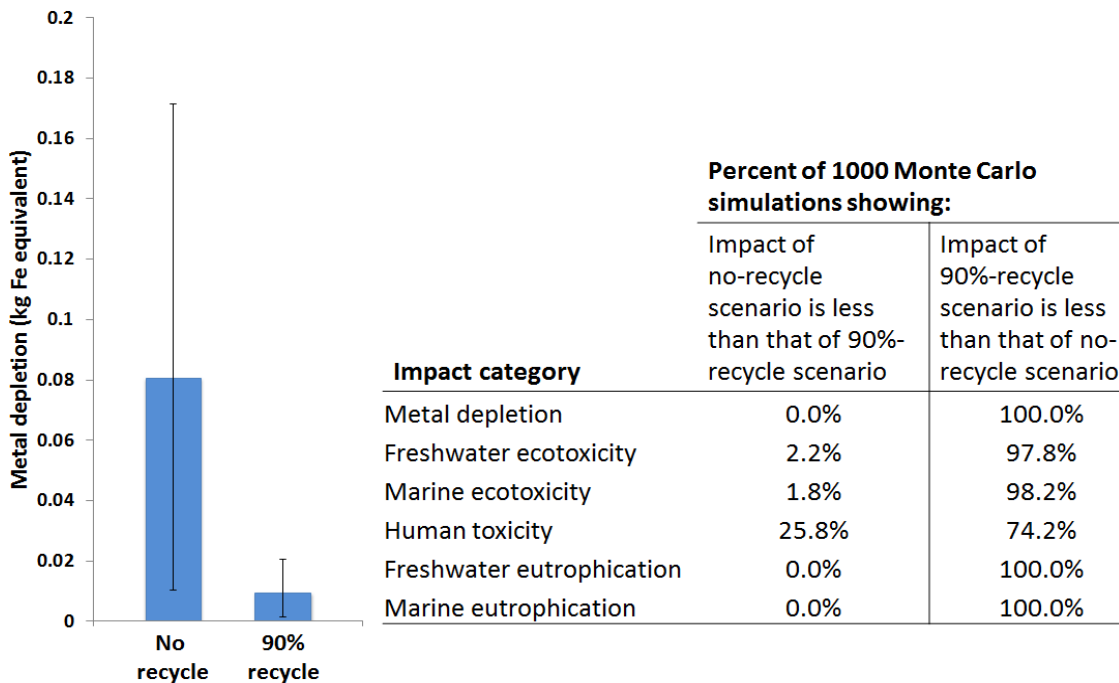


**Figure B 4** - (Left) The overlapping error bars for 95% confidence intervals should not be interpreted as statistically insignificant differences, because these LCA models involve correlated uncertainties. (Right) The majority of the Monte Carlo simulations showed that 90%-recycle scenario has lower impact than no-recycle scenario in terms of metal depletion, toxicity and eutrophication.

In **Figure B5**, **B6** and **B7**, we show the percentage of the Monte Carlo simulations for different recycle scenarios. For each of the impact categories, longer hatched bars indicate that for the majority of Monte Carlo simulations, recycling has lower impact than the no-recycle scenario. Longer solid bars, on

the other hand, indicate that no-recycle scenarios have lower impact in those impact categories (as seen, for example, in the Climate Change category).

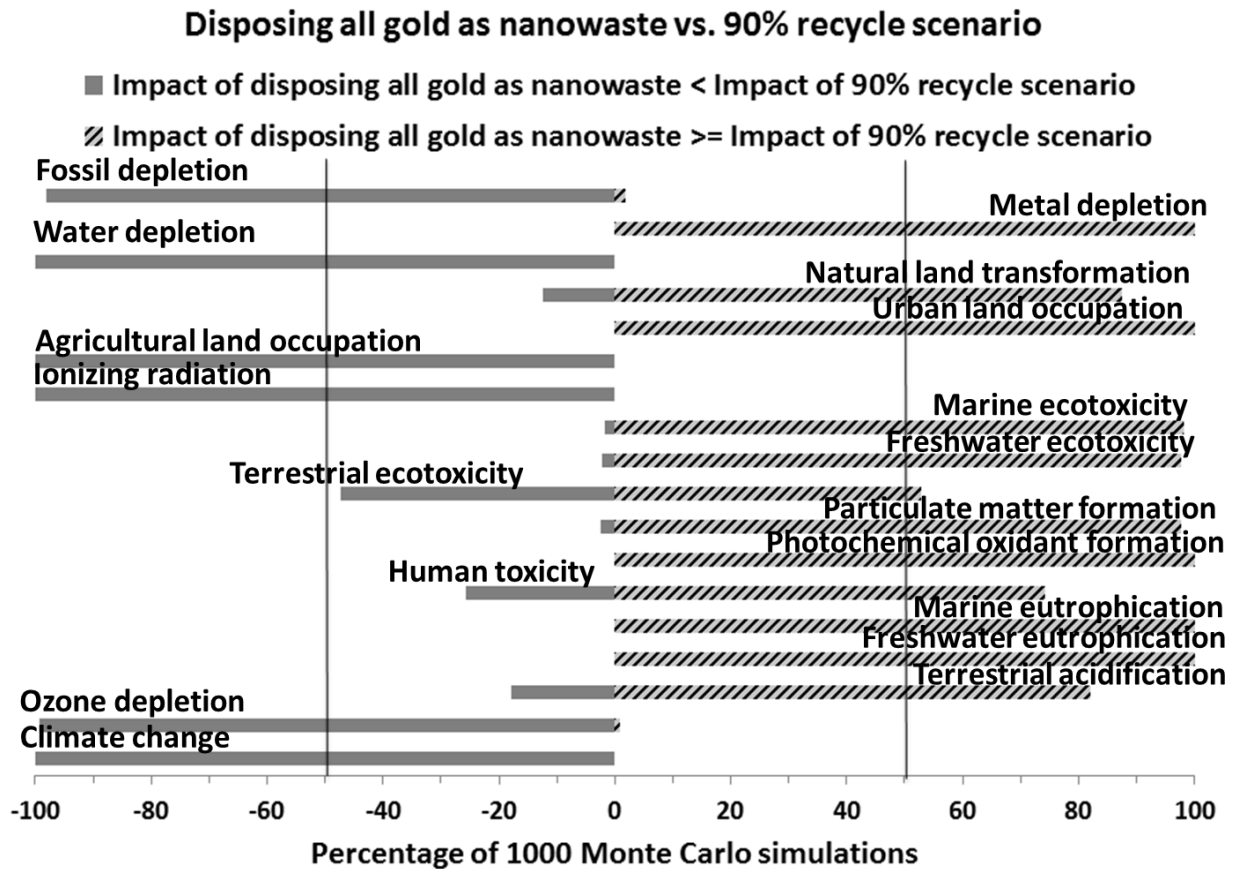


**Figure B 5** - Uncertainty analysis for 90% recycle scenario vs. no-recycle scenario.

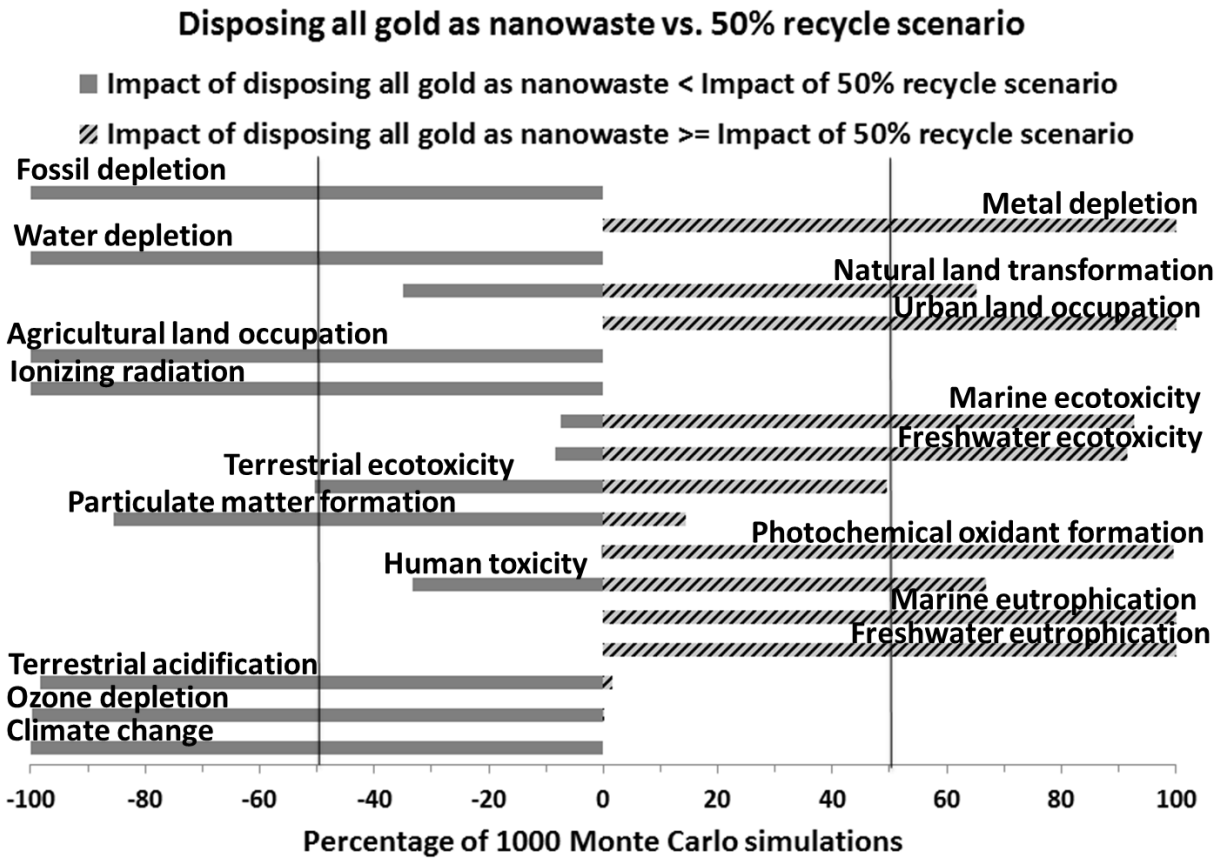


Figure B 6 - Uncertainty analysis for 50% recycle scenario vs. no-recycle scenario.

### Disposing all gold as nanowaste vs. 10% recycle scenario

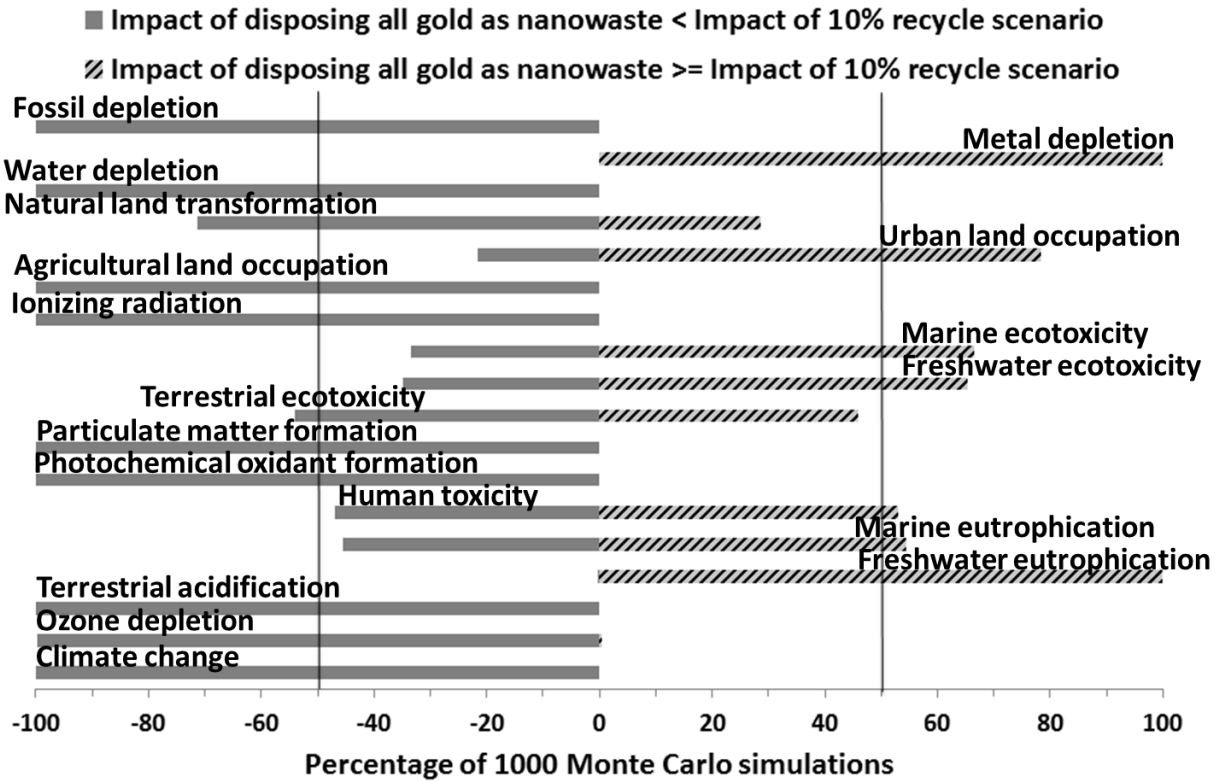


Figure B 7 - Uncertainty analysis for 10% recycle scenario vs. no-recycle scenario.

## Appendix C

### Supplementary materials for Chapter 4

# Bleeding from a Thousand Paper Cuts: Avoiding Dissipative Losses of Critical Elements by Recycling Nanomaterial Waste Streams

*Paramjeet Pati,<sup>1,2,3</sup> Sean McGinnis,<sup>2,4</sup> and Peter J. Vikesland<sup>1,2,3\*</sup>*

<sup>1</sup>Civil and Environmental Engineering, Virginia Tech

<sup>2</sup>Virginia Tech Institute of Critical Technology and Applied Science (ICTAS) Sustainable Nanotechnology Center (VTSuN)

<sup>3</sup>Center for the Environmental Implications of Nanotechnology (CEINT), Duke University

<sup>4</sup>Department of Material Science and Engineering, Virginia Tech

\*Corresponding author. Phone: (540) 231-3568, Email: [pvikes@vt.edu](mailto:pvikes@vt.edu)

**Table C 1** - Recycling approaches for critical materials

Critical material	Applications in nanotechnology	Recycling approaches
<b>Indium</b>	Photoelectrodes applications for solar energy conversion <sup>1</sup> Optoelectric applications <sup>2</sup> Biological imaging <sup>3</sup> molecular-specific spectroscopy, Gas sensors (e.g., for CO, NO <sub>2</sub> <sup>4</sup> , NH <sub>3</sub> <sup>5</sup> etc.)	Pyrometallurgical recovery <sup>6</sup> Anion exchange <sup>7</sup> Air-classification of sputtering waste <sup>8</sup> Acid-resistant nanofiltration followed by selective liquid–liquid extraction <sup>9</sup>
<b>Neodymium</b>	Nano-scale bacterial magnetic particles for biotechnological applications <sup>10</sup> Non-contact <sup>11</sup> and subtissue <sup>12</sup>	Gas phase extraction <sup>14, 15</sup> Hydrogen decrepitation <sup>16, 17</sup> Selective leaching from nitric acid medium



	<p>temperature sensing</p> <p>photonic applications (Infrared cameras, remote controls)<sup>13</sup></p>	<p>using functionalized ionic liquid trioctylmethylammonium dioctyl diglycolamate<sup>18</sup></p> <p>Hydrogenation disproportionation reaction<sup>19</sup></p> <p>Selective acid leaching followed solvent extraction and precipitation<sup>20</sup></p> <p>Precipitation from electroplating wastewater<sup>21</sup></p>
<b>Yttrium</b>	<p>Lasers and luminescent materials<sup>22</sup></p> <p>Magneto-optical materials<sup>23</sup></p> <p>Fuel cells<sup>24</sup></p> <p>Neuroprotective agent against oxidative stress damage<sup>25</sup></p>	<p>Acid leaching followed by, solvent extraction and thermal reduction<sup>26</sup></p> <p>Extraction from chloride solution using an extraction mixture comprised of 2-ethylhexyl phosphonic acid mono-(2-ethylhexyl) ester, Cyanex272, with kerosene as a diluent<sup>27</sup></p> <p>Acid leaching from computer monitor scrap<sup>28</sup></p> <p>Acid leaching from spent fluorescent tubes followed by precipitation using oxalic acid<sup>29</sup></p>
<b>Dysprosium</b>	<p>Light emitting devices (e.g., ceramics<sup>30</sup> and nano-garnets<sup>31</sup>)</p> <p>Dopant in magnetic nanoparticles<sup>32</sup></p> <p>Fingerprint detection<sup>33</sup></p> <p>Solid oxide fuel cells<sup>34</sup></p> <p>High strength corrosion resistant ceramics and catalyst supports<sup>35</sup></p>	<p>Hydrometallurgical recovery from magnetic waste sludge<sup>36</sup></p> <p>Selective volatilization followed by carbochlorination<sup>37</sup></p>
<b>Europium</b>	<p>Biological imaging<sup>38</sup></p> <p>Drug delivery<sup>39</sup></p> <p>Pathogen detection<sup>40</sup></p>	<p>Extraction using quaternary ammonium based ionic liquids<sup>41</sup></p> <p>Recovery from red lamp phosphor by selective reduction of Eu(III) to Eu(II) followed by precipitation of Eu as EuSO<sub>4</sub>, using isopropanol as radical scavenger<sup>42</sup></p>
<b>Terbium</b>	<p>Molecular switches (based on</p>	<p>Solid-liquid extraction phosphoric acid medium</p>

	reversible chiral switching) <sup>43</sup> Incorporation into glass-ceramics for laser applications <sup>44</sup> Fluorescence imaging <sup>45</sup> Phosphors <sup>46</sup>	using a bifunctional phosphinic acid resin Tulsion CH-96 <sup>47</sup>
<b>Thorium</b>	Ion-selective electrodes <sup>48, 49</sup> Photoluminescence <sup>50</sup>	Recovery of Th from acid leaching solutions using poly(styrene-co-maleic anhydride) (PSMA) as adsorbent <sup>51</sup> Extraction from sulfuric acid medium using 2-ethylhexyl phosphoric acid mono 2-ethylhexyl ester in kerosene <sup>52</sup> Extraction from sulfuric acid medium using tri-n-butyl phosphate (TBP) <sup>53</sup> Extraction from nitrate medium using diphenyl-N,N-dimethylcarbamoylmethylphosphine oxide in dichloromethane <sup>54</sup>
<b>Cerium</b>	Antioxidant <sup>55, 56</sup> Nanomedicine <sup>57</sup> Fuel additive <sup>58</sup>	Acid leaching <sup>59</sup> Leaching (using nitric acid liquor) followed by selective extraction using ionic liquid ([C <sub>8</sub> mim]PF <sub>6</sub> ) <sup>60</sup>
<b>Gold</b>	Pathogen detection <sup>61</sup> Cancer diagnostics <sup>62</sup> Drug delivery <sup>63</sup>	Cloud point extraction <sup>64</sup> Selective complexation <sup>65</sup> Magnetic recovery <sup>66</sup>
<b>Silver</b>	Antimicrobial properties <sup>67</sup> Electrochemical detection <sup>68</sup>	Cloud point extraction <sup>69</sup> Liquid-liquid phase separations <sup>70</sup>
<b>Platinum</b>	Fuel cells <sup>71</sup> Catalysis <sup>72</sup>	Biosorption using yeast-based biomass immobilized in polyvinyl alcohol cryogels <sup>73</sup> Selective leaching from automobile catalyst residue using chloride based leaching solutions <sup>74</sup> Selective recovery using thiourea modified

		magnetic nanoparticles <sup>75</sup>
<b>Palladium</b>	Hydrogen sensors <sup>76</sup> Fuel cells <sup>77</sup> Catalysis <sup>78</sup>	Smopex ® metal scavengers <sup>79</sup> Bioreduction <sup>80, 81</sup> Biosorption <sup>82</sup>

## REFERENCES

1. Wang, X.; Zhu, H.; Xu, Y.; Wang, H.; Tao, Y.; Hark, S.; Xiao, X.; Li, Q., Aligned ZnO/CdTe Core–Shell Nanocable Arrays on Indium Tin Oxide: Synthesis and Photoelectrochemical Properties. *ACS Nano* 2010, 4, (6), 3302-3308.
2. Lounis, S. D.; Runnerstrom, E. L.; Bergerud, A.; Nordlund, D.; Milliron, D. J., Influence of Dopant Distribution on the Plasmonic Properties of Indium Tin Oxide Nanocrystals. *Journal of the American Chemical Society* 2014, 136, (19), 7110-7116.
3. Zimmer, J. P.; Kim, S.-W.; Ohnishi, S.; Tanaka, E.; Frangioni, J. V.; Bawendi, M. G., Size Series of Small Indium Arsenide–Zinc Selenide Core–Shell Nanocrystals and Their Application to In Vivo Imaging. *Journal of the American Chemical Society* 2006, 128, (8), 2526-2527.
4. Soulantica, K.; Erades, L.; Sauvan, M.; Senocq, F.; Maisonnat, A.; Chaudret, B., Synthesis of Indium and Indium Oxide Nanoparticles from Indium Cyclopentadienyl Precursor and Their Application for Gas Sensing. *Advanced Functional Materials* 2003, 13, (7), 553-557.
5. Du, N.; Zhang, H.; Chen, B. D.; Ma, X. Y.; Liu, Z. H.; Wu, J. B.; Yang, D. R., Porous Indium Oxide Nanotubes: Layer-by-Layer Assembly on Carbon-Nanotube Templates and Application for Room-Temperature NH<sub>3</sub> Gas Sensors. *Advanced Materials* 2007, 19, (12), 1641-1645.
6. Terakado, O.; Saeki, T.; Irizato, R.; Hirasawa, M., Pyrometallurgical Recovery of Indium from Dental Metal Recycling Sludge by Chlorination Treatment with Ammonium Chloride. *Materials Transactions* 2010, 51, (6), 1136-1140.
7. Tsujiguchi, M., Indium Recovery and Recycling from an LCD Panel. In *Design for Innovative Value Towards a Sustainable Society*, Matsumoto, D. M.; Umeda, P. Y.; Masui, D. K.; Fukushima, D. S., Eds. Springer Netherlands: 2012; pp 743-746.
8. Hong, H. S.; Jung, H.; Hong, S.-J., Recycling of the indium scrap from ITO sputtering waste. *Res Chem Intermed* 2010, 36, (6-7), 761-766.
9. Zimmermann, Y.-S.; Niewersch, C.; Lenz, M.; Kül, Z. Z.; Corvini, P. F. X.; Schäffer, A.; Wintgens, T., Recycling of Indium From CIGS Photovoltaic Cells: Potential of Combining Acid-Resistant Nanofiltration with Liquid–Liquid Extraction. *Environmental Science & Technology* 2014.
10. Matsunaga, T.; Okamura, Y.; Tanaka, T., Biotechnological application of nano-scale engineered bacterial magnetic particles. *Journal of Materials Chemistry* 2004, 14, (14), 2099-2105.
11. Wawrzynczyk, D.; Bednarkiewicz, A.; Nyk, M.; Strek, W.; Samoc, M., Neodymium(III) doped fluoride nanoparticles as non-contact optical temperature sensors. *Nanoscale* 2012, 4, (22), 6959-6961.

12. Rocha, U.; Jacinto da Silva, C.; Ferreira Silva, W.; Guedes, I.; Benayas, A.; Martínez Maestro, L.; Acosta Elias, M.; Bovero, E.; van Veggel, F. C. J. M.; García Solé, J. A.; Jaque, D., Subtissue Thermal Sensing Based on Neodymium-Doped LaF<sub>3</sub> Nanoparticles. *ACS Nano* 2013, 7, (2), 1188-1199.
13. Lemański, K.; Gağor, A.; Kurnatowska, M.; Pażik, R.; Dereń, P. J., Spectroscopic properties of Nd<sup>3+</sup> ions in nano-perovskite CaTiO<sub>3</sub>. *Journal of Solid State Chemistry* 2011, 184, (10), 2713-2718.
14. Ozaki, T.; Miyazawa, T.; Murase, K.; Machida, K.-i.; Adachi, G.-y., Vapor phase extraction and separation of rare earths from bastnaesite concentrate mediated by vapor complexes. *Journal of Alloys and Compounds* 1996, 245, (1), 10-14.
15. Takeda, O.; Okabe, T. H.; Umetsu, Y., Recovery of neodymium from a mixture of magnet scrap and other scrap. *Journal of Alloys and Compounds* 2006, 408, 387-390.
16. Zakotnik, M.; Devlin, E.; Harris, I. R.; Williams, A. J., Hydrogen Decrepitation and Recycling of NdFeB-type Sintered Magnets. *Journal of Iron and Steel Research, International* 2006, 13, Supplement 1, 289-295.
17. Zakotnik, M.; Harris, I. R.; Williams, A. J., Possible methods of recycling NdFeB-type sintered magnets using the HD/degassing process. *Journal of Alloys and Compounds* 2008, 450, (1–2), 525-531.
18. Rout, A.; Binnemans, K., Solvent Extraction of Neodymium(III) by Functionalized Ionic Liquid Trioctylmethylammonium Dioctyl Diglycolamate in Fluorine-free Ionic Liquid Diluent. *Industrial & Engineering Chemistry Research* 2014, 53, (15), 6500-6508.
19. Miura, K.; Masuda, M.; Itoh, M.; Horikawa, T.; Machida, K.-i., Microwave absorption properties of the nano-composite powders recovered from Nd–Fe–B bonded magnet scraps. *Journal of Alloys and Compounds* 2006, 408–412, 1391-1395.
20. Hoogerstraete, T. V.; Blanpain, B.; Gerven, T. V.; Binnemans, K., From NdFeB magnets towards the rare-earth oxides: a recycling process consuming only oxalic acid. *RSC Adv.* 2014, 4, (109), 64099-64111.
21. Zhu, M.; Shi, Z. Method for extracting neodymium from neodymium-iron-boron electroplating pre-processing acid washing waste water. CN101186970 A, 2008/05/28/, 2008.
22. Srinivasan, R.; Yogamalar, N. R.; Elanchezhian, J.; Joseyphus, R. J.; Bose, A. C., Structural and optical properties of europium doped yttrium oxide nanoparticles for phosphor applications. *Journal of Alloys and Compounds* 2010, 496, (1–2), 472-477.
23. Kuroda, C. S.; Kim, T. Y.; Hirano, T.; Yoshida, K.; Namikawa, T.; Yamazaki, Y., Preparation of nano-sized Bi-YIG particles for micro optics applications. *Electrochimica Acta* 1999, 44, (21–22), 3921-3925.

24. Liang, F.; Chen, J.; Cheng, J.; Jiang, S. P.; He, T.; Pu, J.; Li, J., Novel nano-structured Pd+yttrium doped ZrO<sub>2</sub> cathodes for intermediate temperature solid oxide fuel cells. *Electrochemistry Communications* 2008, 10, (1), 42-46.
25. Schubert, D.; Dargusch, R.; Raitano, J.; Chan, S.-W., Cerium and yttrium oxide nanoparticles are neuroprotective. *Biochemical and Biophysical Research Communications* 2006, 342, (1), 86-91.
26. Rabah, M. A., Recyclables recovery of europium and yttrium metals and some salts from spent fluorescent lamps. *Waste Management* 2008, 28, (2), 318-325.
27. Zhang, C.; Wang, L.; Huang, X.; Dong, J.; Long, Z.; Zhang, Y., Yttrium extraction from chloride solution with a synergistic system of 2-ethylhexyl phosphonic acid mono-(2-ethylhexyl) ester and bis(2,4,4-trimethylpentyl) phosphinic acid. *Hydrometallurgy* 2014, 147-148, 7-12.
28. Resende, L. V.; Morais, C. A., Study of the recovery of rare earth elements from computer monitor scraps – Leaching experiments. *Minerals Engineering* 2010, 23, (3), 277-280.
29. De Michelis, I.; Ferella, F.; Varelli, E. F.; Vegliò, F., Treatment of exhaust fluorescent lamps to recover yttrium: Experimental and process analyses. *Waste Management* 2011, 31, (12), 2559-2568.
30. Ye, R.; Cui, Z.; Hua, Y.; Deng, D.; Zhao, S.; Li, C.; Xu, S., Eu<sup>2+</sup>/Dy<sup>3+</sup> co-doped white light emission glass ceramics under UV light excitation. *Journal of Non-Crystalline Solids* 2011, 357, (11-13), 2282-2285.
31. Haritha, P.; Martín, I. R.; Linganna, K.; Monteseuro, V.; Babu, P.; León-Luis, S. F.; Jayasankar, C. K.; Rodríguez-Mendoza, U. R.; Lavín, V.; Venkatramu, V., Optimizing white light luminescence in Dy<sup>3+</sup>-doped Lu<sub>3</sub>Ga<sub>5</sub>O<sub>12</sub> nano-garnets. *Journal of Applied Physics* 2014, 116, (17).
32. Karimi, Z.; Mohammadifar, Y.; Shokrollahi, H.; Asl, S. K.; Yousefi, G.; Karimi, L., Magnetic and structural properties of nano sized Dy-doped cobalt ferrite synthesized by co-precipitation. *Journal of Magnetism and Magnetic Materials* 2014, 361, 150-156.
33. Saif, M., Synthesis of down conversion, high luminescent nano-phosphor materials based on new developed Ln<sup>3+</sup>:Y<sub>2</sub>Zr<sub>2</sub>O<sub>7</sub>/SiO<sub>2</sub> for latent fingerprint application. *Journal of Luminescence* 2013, 135, 187-195.
34. Acharya, S. A., The effect of processing route on sinterability and electrical properties of nano-sized dysprosium-doped ceria. *Journal of Power Sources* 2012, 198, 105-111.
35. Hoffmann, M. M.; Young, J. S.; Fulton, J. L., Unusual dysprosium ceramic nano-fiber growth in a supercritical aqueous solution. *Journal of Materials Science* 2000, 35, (16), 4177-4183.
36. Rabatho, J. P.; Tongamp, W.; Takasaki, Y.; Haga, K.; Shibayama, A., Recovery of Nd and Dy from rare earth magnetic waste sludge by hydrometallurgical process. *J Mater Cycles Waste Manag* 2012, 15, (2), 171-178.

37. Mochizuki, Y.; Tsubouchi, N.; Sugawara, K., Selective Recovery of Rare Earth Elements from Dy containing NdFeB Magnets by Chlorination. *ACS Sustainable Chem. Eng.* 2013, 1, (6), 655-662.
38. Casanova, D.; Bouzigues, C.; Nguyễn, T.-L.; Ramodiharilafy, R. O.; Bouzahir-Sima, L.; Gacoin, T.; Boilot, J.-P.; Tharaux, P.-L.; Alexandrou, A., Single europium-doped nanoparticles measure temporal pattern of reactive oxygen species production inside cells. *Nature Nanotechnology* 2009, 4, (9), 581-585.
39. Chen, F.; Zhu, Y.-J.; Zhang, K.-H.; Wu, J.; Wang, K.-W.; Tang, Q.-L.; Mo, X.-M., Europium-doped amorphous calcium phosphate porous nanospheres: preparation and application as luminescent drug carriers. *Nanoscale research letters* 2011, 6, (67), 1-9.
40. Wu, J.; Ye, Z.; Wang, G.; Jin, D.; Yuan, J.; Guan, Y.; Piper, J., Visible-light-sensitized highly luminescent europium nanoparticles: preparation and application for time-gated luminescence bioimaging. *Journal of Materials Chemistry* 2009, 19, (9), 1258-1264.
41. Rout, A.; Venkatesan, K. A.; Srinivasan, T. G.; Vasudeva Rao, P. R., Ionic liquid extractants in molecular diluents: Extraction behavior of europium (III) in quaternary ammonium-based ionic liquids. *Separation and Purification Technology* 2012, 95, 26-31.
42. Bogaert, B. V. d.; Havaux, D.; Binnemans, K.; Gerven, T. V., Photochemical recycling of europium from Eu/Y mixtures in red lamp phosphor waste streams. *Green Chemistry* 2015.
43. Fu, Y.-S.; Schwöbel, J.; Hla, S.-W.; Dilullo, A.; Hoffmann, G.; Klyatskaya, S.; Ruben, M.; Wiesendanger, R., Reversible Chiral Switching of Bis(phthalocyaninato) Terbium(III) on a Metal Surface. *Nano Letters* 2012, 12, (8), 3931-3935.
44. Bocker, C.; Herrmann, A.; Loch, P.; Rüssel, C., The nano-crystallization and fluorescence of terbium doped Na<sub>2</sub>O/K<sub>2</sub>O/CaO/CaF<sub>2</sub>/Al<sub>2</sub>O<sub>3</sub>/SiO<sub>2</sub> glasses. *J. Mater. Chem. C* 2015, 3, (10), 2274-2281.
45. Chen, Y.; Chi, Y.; Wen, H.; Lu, Z., Sensitized Luminescent Terbium Nanoparticles: Preparation and Time-Resolved Fluorescence Assay for DNA. *Analytical Chemistry* 2007, 79, (3), 960-965.
46. Reisfeld, R.; Gaft, M.; Saridarov, T.; Panczer, G.; Zelner, M., Nanoparticles of cadmium sulfide with europium and terbium in zirconia films having intensified luminescence. *Materials Letters* 2000, 45, (3-4), 154-156.
47. Reddy, B. R.; Kumar, B. N.; Radhika, S., Solid-Liquid Extraction of Terbium from Phosphoric Acid Medium using Bifunctional Phosphinic Acid Resin, Tulsion CH-96. *Solvent Extraction and Ion Exchange* 2009, 27, (5-6), 695-711.
48. Khan, A. A.; Khan, A.; Inamuddin, Preparation and characterization of a new organic-inorganic nano-composite poly-o-toluidine Th(IV) phosphate: Its analytical applications as cation-exchanger and in making ion-selective electrode. *Talanta* 2007, 72, (2), 699-710.

49. Varshney, K. G.; Tayal, N.; Khan, A. A.; Niwas, R., Synthesis, characterization and analytical applications of lead (II) selective polyacrylonitrile thorium (IV) phosphate: a novel fibrous ion exchanger. *Colloids and Surfaces A: Physicochemical and Engineering Aspects* 2001, *181*, (1–3), 123-129.
50. Baranwal, B. P.; Fatma, T.; Varma, A.; Singh, A. K., Substitution reactions of thorium(IV) acetate to synthesize nano-sized carboxylate complexes. *Spectrochimica Acta Part A: Molecular and Biomolecular Spectroscopy* 2010, *75*, (4), 1177-1180.
51. Gui, W.; Zhang, H.; Liu, Q.; Zhu, X.; Yang, Y., Recovery of Th(IV) from acid leaching solutions of bastnaesite at low concentrations. *Hydrometallurgy* 2014, *147–148*, 157-163.
52. Wang, L.; Yu, Y.; Huang, X.; Hu, F.; Dong, J.; Yan, L.; Long, Z., Thermodynamics and kinetics of thorium extraction from sulfuric acid medium by HEH(EHP). *Hydrometallurgy* 2014, *150*, 167-172.
53. Sato, T., Extraction of uranium (VI) and thorium from nitric acid solutions by tri-n-butyl phosphate. *J. Appl. Chem.* 1965, *15*, (11), 489-495.
54. Yaftian, M. R.; Hassanzadeh, L.; Eshraghi, M. E.; Matt, D., Solvent extraction of thorium (IV) and europium (III) ions by diphenyl-N,N-dimethylcarbamoylmethylphosphine oxide from aqueous nitrate media. *Separation and Purification Technology* 2003, *31*, (3), 261-268.
55. Perez, J. M.; Asati, A.; Nath, S.; Kaittanis, C., Synthesis of Biocompatible Dextran-Coated Nanoceria with pH-Dependent Antioxidant Properties. *Small* 2008, *4*, (5), 552-556.
56. Karakoti, A. S.; Singh, S.; Kumar, A.; Malinska, M.; Kuchibhatla, S. V. N. T.; Wozniak, K.; Self, W. T.; Seal, S., PEGylated Nanoceria as Radical Scavenger with Tunable Redox Chemistry. *Journal of the American Chemical Society* 2009, *131*, (40), 14144-14145.
57. Das, S.; Dowding, J. M.; Klump, K. E.; McGinnis, J. F.; Self, W.; Seal, S., Cerium oxide nanoparticles: applications and prospects in nanomedicine. *Nanomedicine* 2013, *8*, (9), 1483-1508.
58. Wakefield, G.; Wu, X.; Gardener, M.; Park, B.; Anderson, S., Envirox™ fuel-borne catalyst: Developing and launching a nano-fuel additive. *Technology Analysis & Strategic Management* 2008, *20*, (1), 127-136.
59. Rumpold, R.; Antrekowitsch, J. In *Recycling of platinum group metals from automotive catalysts by an acidic leaching process*, 2012, 2012; 2012; pp 695-713.
60. Zuo, Y.; Liu, Y.; Chen, J.; Li, D. Q., The Separation of Cerium(IV) from Nitric Acid Solutions Containing Thorium(IV) and Lanthanides(III) Using Pure [C8mim]PF6 as Extracting Phase. *Industrial & Engineering Chemistry Research* 2008, *47*, (7), 2349-2355.
61. Rule, K. L.; Vikesland, P. J., Surface-Enhanced Resonance Raman Spectroscopy for the Rapid Detection of *Cryptosporidium parvum* and *Giardia lamblia*. *Environmental Science & Technology* 2009, *43*, (4), 1147-1152.



62. El-Sayed, I. H.; Huang, X. H.; El-Sayed, M. A., Surface plasmon resonance scattering and absorption of anti-EGFR antibody conjugated gold nanoparticles in cancer diagnostics: Applications in oral cancer. *Nano Letters* 2005, 5, (5), 829-834.
63. Dreaden, E. C.; Mwakwari, S. C.; Sodji, Q. H.; Oyelere, A. K.; El-Sayed, M. A., Tamoxifen-poly(ethylene glycol)-thiol gold nanoparticle conjugates: enhanced potency and selective delivery for breast cancer treatment. *Bioconjug Chem* 2009, 20, (12), 2247-53.
64. Akita, S.; Rovira, M.; Sastre, A. M.; Takeuchi, H., Cloud-Point Extraction of Gold(III) with Nonionic Surfactant—Fundamental Studies and Application to Gold Recovery from Printed Substrate. *Separation Science and Technology* 1998, 33, (14), 2159-2177.
65. Liu, Z.; Frasconi, M.; Lei, J.; Brown, Z. J.; Zhu, Z.; Cao, D.; Iehl, J.; Liu, G.; Fahrenbach, A. C.; Botros, Y. Y.; Farha, O. K.; Hupp, J. T.; Mirkin, C. A.; Fraser Stoddart, J., Selective isolation of gold facilitated by second-sphere coordination with  $\alpha$ -cyclodextrin. *Nature Communications* 2013, 4.
66. Oliveira, R. L.; Kiyohara, P. K.; Rossi, L. M., High performance magnetic separation of gold nanoparticles for catalytic oxidation of alcohols. *Green Chemistry* 2010, 12, (1), 144-149.
67. Panáček, A.; Kvítek, L.; Pucek, R.; Kolář, M.; Večeřová, R.; Pizúrová, N.; Sharma, V. K.; Nevěčná, T. j.; Zbořil, R., Silver Colloid Nanoparticles: Synthesis, Characterization, and Their Antibacterial Activity. *J. Phys. Chem. B* 2006, 110, (33), 16248-16253.
68. Chikae, M.; Idegami, K.; Nagatani, N.; Tamiya, E.; Takamura, Y., Highly Sensitive Method for Electrochemical Detection of Silver Nanoparticle Labels in Metalloimmunoassay with Preoxidation/Reduction Signal Enhancement. *Electrochemistry* 2010, 78, (9), 748-753.
69. Liu, J.-f.; Chao, J.-b.; Liu, R.; Tan, Z.-q.; Yin, Y.-g.; Wu, Y.; Jiang, G.-b., Cloud Point Extraction as an Advantageous Preconcentration Approach for Analysis of Trace Silver Nanoparticles in Environmental Waters. *Analytical Chemistry* 2009, 81, (15), 6496-6502.
70. Myakonkaya, O.; Guibert, C. m.; Eastoe, J.; Grillo, I., Recovery of Nanoparticles Made Easy. *Langmuir* 2010, 26, (6), 3794-3797.
71. Li, W.; Liang, C.; Zhou, W.; Qiu, J.; Zhou; Sun, G.; Xin, Q., Preparation and Characterization of Multiwalled Carbon Nanotube-Supported Platinum for Cathode Catalysts of Direct Methanol Fuel Cells. *J. Phys. Chem. B* 2003, 107, (26), 6292-6299.
72. Chen, J.; Lim, B.; Lee, E. P.; Xia, Y., Shape-controlled synthesis of platinum nanocrystals for catalytic and electrocatalytic applications. *Nano Today* 2009, 4, (1), 81-95.
73. Dimitriadis, S.; Nomikou, N.; McHale, A. P., Pt-based electro-catalytic materials derived from biosorption processes and their exploitation in fuel cell technology. *Biotechnology Letters* 2007, 29, (4), 545-551.

74. Harjanto, S.; Cao, Y.; Shibayama, A.; Naitoh, I.; Nanami, T.; Kasahara, K.; Okumura, Y.; Liu, K.; Fujita, T., Leaching of Pt, Pd and Rh from automotive catalyst residue in various chloride based solutions. *Materials transactions* 2006, *47*, (1), 129-135.
75. Lin, T.-L.; Lien, H.-L., Effective and Selective Recovery of Precious Metals by Thiourea Modified Magnetic Nanoparticles. *International Journal of Molecular Sciences* 2013, *14*, (5), 9834-9847.
76. Tittl, A.; Mai, P.; Taubert, R.; Dregely, D.; Liu, N.; Giessen, H., Palladium-Based Plasmonic Perfect Absorber in the Visible Wavelength Range and Its Application to Hydrogen Sensing. *Nano Letters* 2011, *11*, (10), 4366-4369.
77. Simões, M.; Baranton, S.; Coutanceau, C., Electro-oxidation of glycerol at Pd based nano-catalysts for an application in alkaline fuel cells for chemicals and energy cogeneration. *Applied Catalysis B: Environmental* 2010, *93*, (3-4), 354-362.
78. Das, P.; Sharma, D.; Shil, A. K.; Kumari, A., Solid-supported palladium nano and microparticles: an efficient heterogeneous catalyst for ligand-free Suzuki–Miyaura cross coupling reaction. *Tetrahedron Letters* 2011, *52*, (11), 1176-1178.
79. Phillips, S.; Kauppinen, P., Final Analysis: The Use of Metal Scavengers for Recovery of Palladium Catalyst from Solution. *Platinum Metals Review* 2010, *54*, (1), 69-70.
80. Yong, P.; Farr, J. P. G.; Harris, I. R.; Macaskie, L. E., Palladium recovery by immobilized cells of *Desulfovibrio desulfuricans* using hydrogen as the electron donor in a novel electrobioreactor. *Biotechnology Letters* 2002, *24*, (3), 205-212.
81. Yong, P.; Paterson-Beedle, M.; Mikheenko, I. P.; Macaskie, L. E., From bio-mineralisation to fuel cells: biomanufacture of Pt and Pd nanocrystals for fuel cell electrode catalyst. *Biotechnology Letters* 2007, *29*, (4), 539-544.
82. Dodson, J. R.; Parker, H. L.; García, A. M.; Hicken, A.; Asemave, K.; Farmer, T. J.; He, H.; Clark, J. H.; Hunt, A. J., Bio-derived materials as a green route for precious & critical metal recovery and re-use. *Green Chemistry* 2015.

## Appendix D

### Supplementary materials for Chapter 5

#### Seed Mediated Growth of Gold Nanoparticles at Room

#### Temperature: Mechanistic Investigation and Life Cycle Assessment

Weinan Leng, Paramjeet Pati, and Peter J. Vikesland

Department of Civil and Environmental Engineering, Virginia Polytechnic Institute and State University, 418 Durham Hall, Blacksburg, VA 24060-0246

**Table D 1** - Volumes (V) of nanopure water, H<sub>2</sub>AuCl<sub>4</sub>, seed suspension, and trisodium citrate (Ctr) used in the seed-mediated synthesis of the different sized nanoparticles.

AuNPs	intended particle size / nm	V <sub>water</sub> / mL	V <sub>H<sub>2</sub>AuCl<sub>4</sub></sub> <sup>a</sup> / mL (c = 44.7 mM)	V <sub>seed</sub> / mL (d = 14 nm, c = 6.54 × 10 <sup>12</sup> particles/ml)	Final seed conc. (µg/mL)	V <sub>Ctr</sub> / mL (c = 38.8 mM)
A	22.7	36.220	0.227	3.377	16.632	0.176
B	34.2	38.786	0.227	0.811	3.994	0.176
C	45.7	39.270	0.227	0.327	1.610	0.176
D	57.1	39.432	0.227	0.165	0.813	0.176
E	68.6	39.502	0.227	0.095	0.468	0.176
F	80.0	39.537	0.227	0.060	0.296	0.176
G	91.4	39.557	0.227	0.040	0.197	0.176
H	102.9	39.569	0.227	0.028	0.138	0.176
I	114.3	39.577	0.227	0.020	0.099	0.176

<sup>a</sup>Final mass concentration for gold is 50 µg/mL

**Table D 2** - Inputs for 1 mg of the following custom-defined processes in SimaPro: a) Chloroauric acid, b) Trisodium citrate, and c) AuNP 'seeds'

<b>[Custom defined] Chloroauric acid</b>		
Gold {US}  production   Alloc Def, S	0.72	mg
Hydrochloric acid, without water, in 30% solution state {RER}  hydrochloric acid production, from the reaction of hydrogen with chlorine   Alloc Def, S	0.13	mg
Chlorine, gaseous {RER}  sodium chloride electrolysis   Alloc Def, S	0.39	mg
<b>[Custom defined] Trisodium citrate</b>		
Citric acid {GLO}  market for   Alloc Def, S	0.51	mg
Soda ash, light, crystalline, heptahydrate {GLO}  market for   Alloc Def, S	0.66	mg
<b>[Custom defined] AuNP 'seeds'</b>		
[Custom defined] Chloroauric acid	1.73	mg
[Custom defined] Trisodium citrate	5.08	mg
Water, deionised, from tap water, at user {CH}  production   Alloc Def, S	505.08	g
Tap water {CH}  market for   Alloc Def, S	30.00	g
Sodium hydroxide, without water, in 50% solution state {GLO}  market for   Alloc Def, S	0.41	mg
<i>Cleaning solvents</i>		
Hydrochloric acid, without water, in 30% solution state {RER}  hydrochloric acid production, from the reaction of hydrogen with chlorine   Alloc Def, S	1.81	mg
Nitric acid, without water, in 50% solution state {RER}  nitric acid production, product in 50% solution state   Alloc Def, S	0.72	mg
<b>[Stirring]</b> Electricity, medium voltage {NPCC, US only}  market for   Alloc Def, S	0.01	MJ
<b>[Heating]</b> Electricity, medium voltage {NPCC, US only}  market for   Alloc Def, S	0.08	MJ

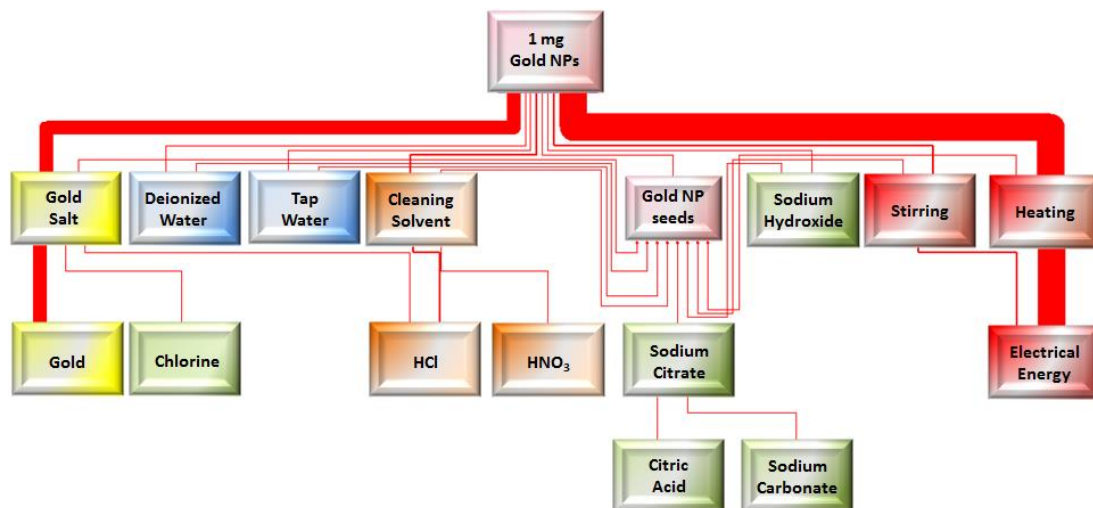


**Figure D 1** - Energy flows (cumulative energy demand) of 1 mg AuNP synthesis at 100 °C. (Flow lines show individual contributions of different inputs.)

**Table D 3** - Inputs for 1 mg of seed-mediated, citrate reduced AuNPs synthesized under boiling conditions

[Custom defined] Chloroauric acid	1.94	mg
Water, deionised, from tap water, at user {CH}  production   Alloc Def, S	444.13	g
Tap water {CH}  market for   Alloc Def, S	25.40	g
[Custom defined] AuNP 'seeds'	0.03	mg
Sodium hydroxide, without water, in 50% solution state {GLO}  market for   Alloc Def, S	0.03	mg
[Custom defined] Trisodium citrate	0.09	mg
<i>Cleaning solvents</i>		
Hydrochloric acid, without water, in 30% solution state {RER}  hydrochloric acid production, from the reaction of hydrogen with chlorine   Alloc Def, S	1.81	mg
Nitric acid, without water, in 50% solution state {RER}  nitric acid production, product in 50% solution state   Alloc Def, S	0.72	mg
<b>[Stirring]</b> Electricity, medium voltage {NPCC, US only}  market for   Alloc Def, S	0.08	kWh
<b>[Heating]</b> Electricity, medium voltage {NPCC, US only}  market for   Alloc Def, S	0.97	kWh

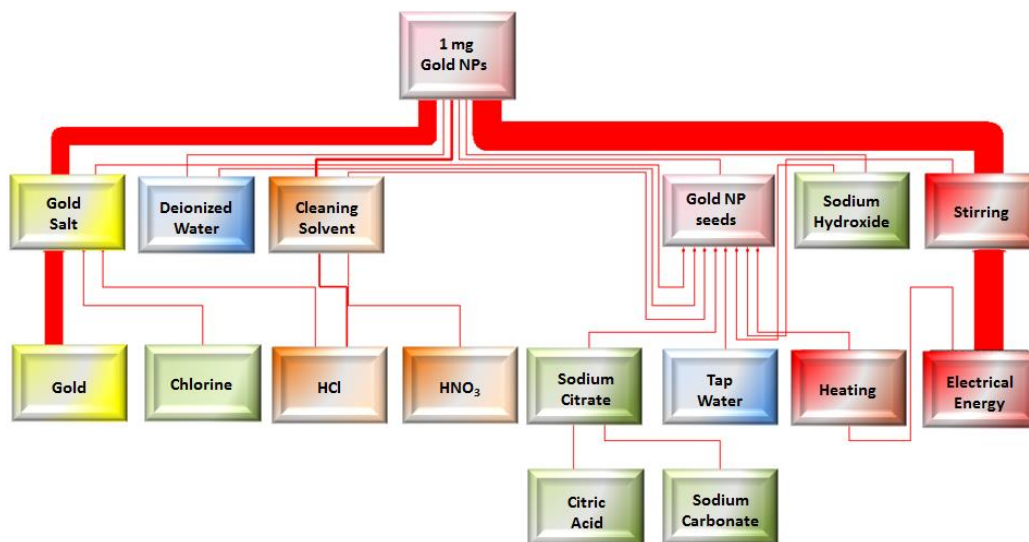


**Figure D 2** - Energy flows (cumulative energy demand) for 1 mg AuNP synthesis at room temperature. (Flow lines show individual contributions of different inputs.)

**Table D 4** - Inputs for 1 mg of seed-mediated, citrate reduced AuNPs synthesized at room temperature

[Custom defined] Chloroauric acid	1.94 mg
Water, deionised, from tap water, at user {CH}  production   Alloc Def, S	444.13 g
[Custom defined] AuNP 'seeds'	0.03 mg
Sodium hydroxide, without water, in 50% solution state {GLO}  market for   Alloc Def, S	0.03 mg
[Custom defined] Trisodium citrate	0.09 mg
<i>Cleaning solvents</i>	
Hydrochloric acid, without water, in 30% solution state {RER}  hydrochloric acid production, from the reaction of hydrogen with chlorine   Alloc Def, S	1.81 mg
Nitric acid, without water, in 50% solution state {RER}  nitric acid production, product in 50% solution state   Alloc Def, S	0.72 mg
[Stirring] Electricity, medium voltage {NPCC, US only}  market for   Alloc Def, S	0.76 kWh

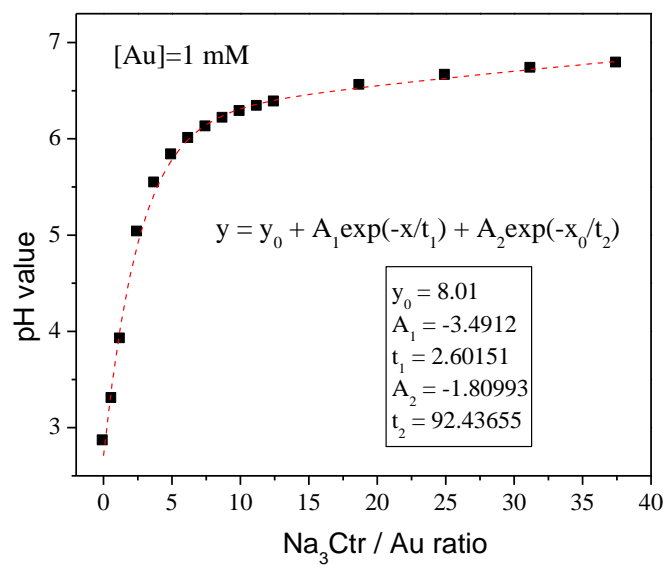


**Figure D 3** - pH value at room temperature against the concentration ratio of Na<sub>3</sub>Ctr and Au<sup>III</sup> for a fixed 1 mM Au<sup>III</sup> concentration.

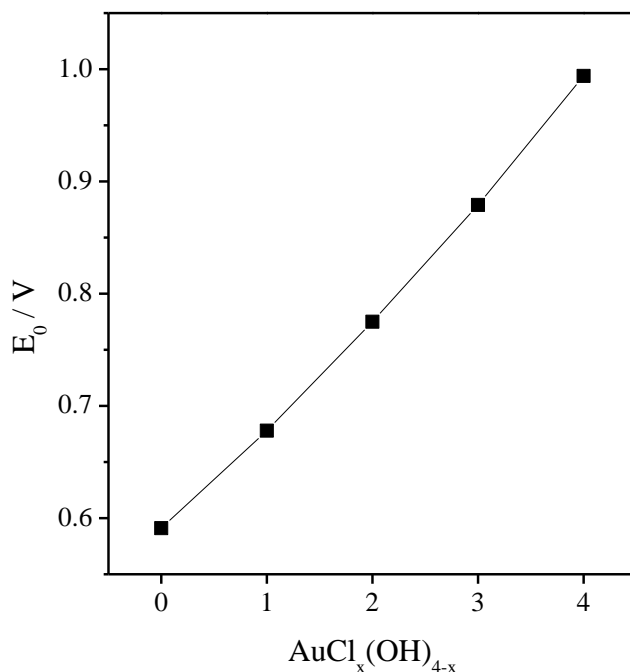


**Figure D 4** - The standard reduction potential ( $E^0$ ) for  $\text{Au}^{\text{III}} \rightarrow \text{Au}^0$  for the gold solution species  $\text{AuCl}_x(\text{OH})_{4-x}$  ( $x=0-4$ ).  $E^0$  was calculated using the Nernst equation of  $\Delta G^0 = -nFE^0$ , where Gibbs free energy ( $\Delta G^0$ ) of  $\text{AuCl}_x(\text{OH})_{4-x}$  ( $x=0-4$ ) was reported by Machesky et al.<sup>1</sup>

## FORMATION OF GOLD NANOPlates AND NANORODS

Gold nanoplates and nanorods were observed in the seeded growth approach, especially when seeds concentration was less than  $1.6 \times 10^{10}$  particles/mL (D – I). Under this condition, the growth tends to rely on the individual seeds, and the interaction between seeds decreases. It is different from the particles less than 50 nm, which includes two cluster formats in the early stage and around 1.5 hour during seeds mediated growth. Figure S5 shows the growth process of 111 nm gold nanoparticles. We cannot see these phenomena neither from UV-vis spectra or change of hydrodynamic size. The formation of rod or triangular-shaped nanoparticles is mostly due to the rod or triangular-shaped seeds.<sup>2</sup> Having the lowest surface energy of the (111) facet,<sup>3</sup> the nanoparticles will be gradually grown by adding Au atoms or ions onto more energetically



favorable faces other than (111). This will result in the formation of nanoplates, same as the nanorods and the hexagonally-arranged nanoparticles.<sup>2, 4</sup> On the other hand, citrate ions and its oxidation product – ACDC ions can also selectively adsorb on the (111) facets and hinder the crystal growth in those directions. The average numbers of particles with different shapes were counted and listed in **Table D5**.

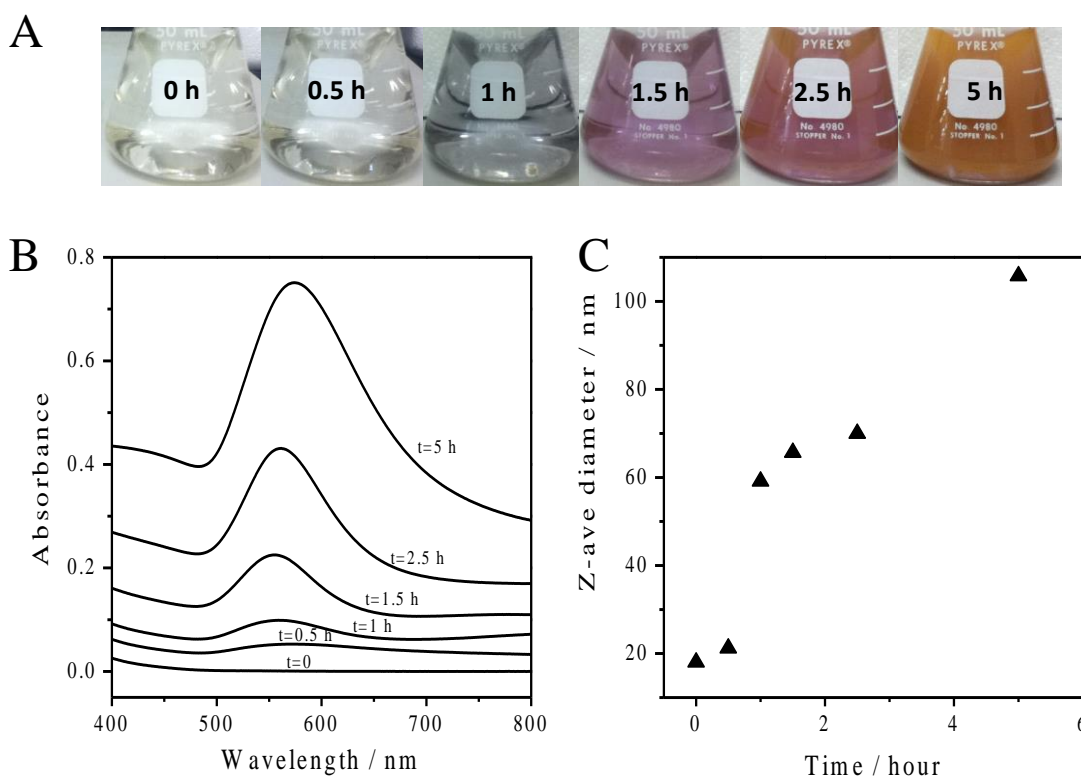


**Figure D 5** - Seed mediated growth with mixed solution of  $\text{HAuCl}_4$  (0.254 mM), Au seeds ( $3.3 \times 10^9$  particles/mL), and  $\text{Na}_3\text{Cit}$  (0.17 mM) at room temperature. (A) optical images, (B) absorption spectra and (C) hydrodynamic diameter of growth solutions in different times.

**Table D 5** - The percentage of nanoplates and nanorods in AuNP sample D – I.

Sample	D	E	F	G	H	I
n (# of nanoplates and nanorods)	21	14	15	32	16	17
N (# of particles counted)	216	148	156	343	126	213
Percentage / (100n/N)%	9.7	9.5	9.6	9.3	12.7	8.0

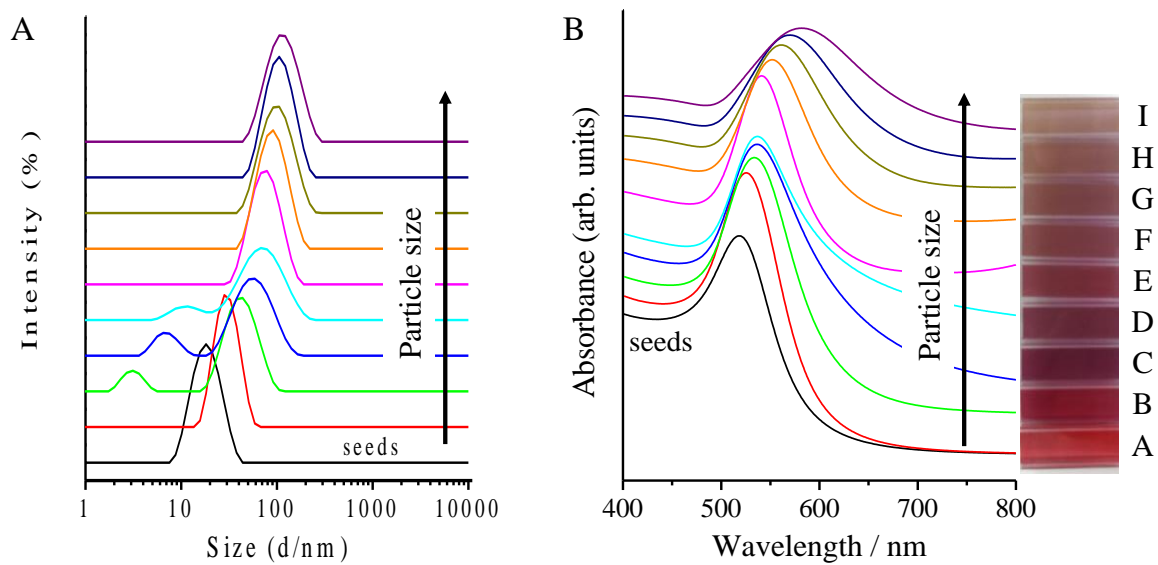


**Figure D 6** - (A) Size distributions by intensity (DLS) and (B) absorption spectra of a set of seeded growth prepared samples with increased size and shifted SPR.

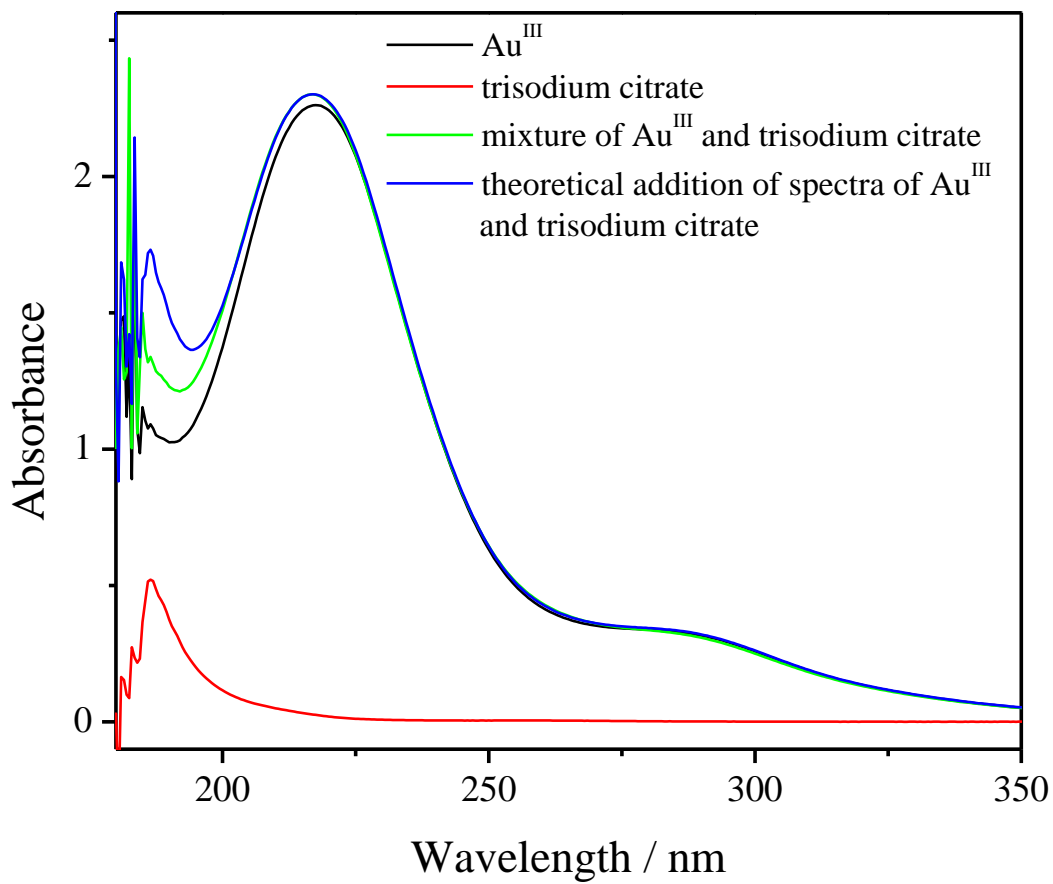


**Figure D 7** - UV absorption spectra of  $[\text{AuCl}_4]^-$  (0.127mM, black solid line),  $\text{Na}_3\text{Ctr}$  (0.088 mM, red line) and the mixture of same volume of  $[\text{AuCl}_4]^-$  and  $\text{Na}_3\text{Ctr}$  with final concentrations of 0.127 mM and 0.088 mM respectively (green line). Blue line is expected spectrum for the mixture based upon the combination of the spectra for  $[\text{AuCl}_4]^-$  and  $\text{Na}_3\text{Ctr}$ .

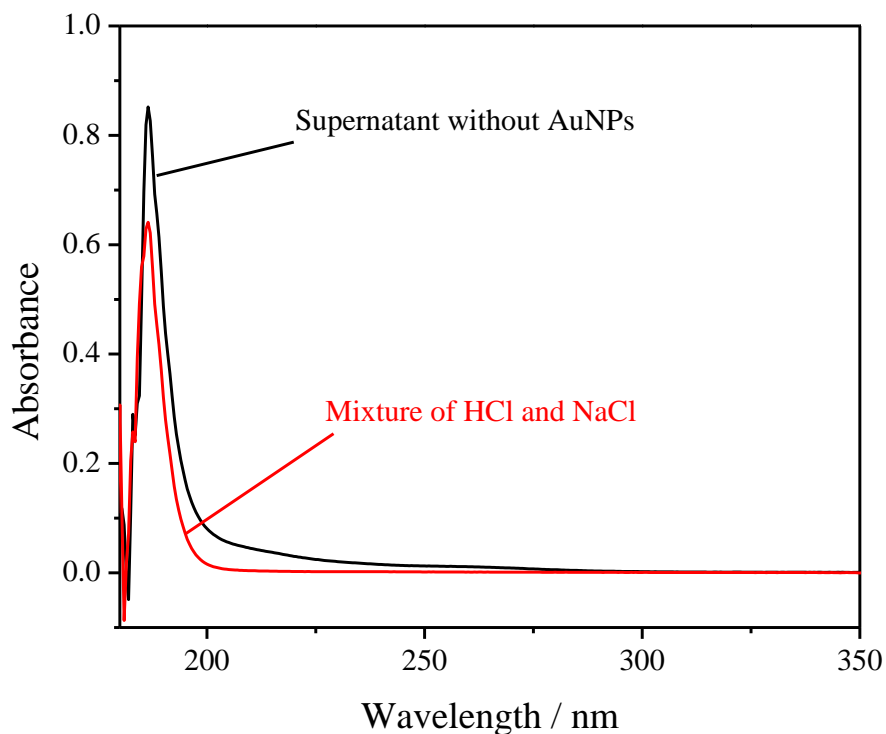


**Figure D 8** - Comparison of UV absorbance between supernatant from a completely reacted Au solution and a simulation mixture of HCl and NaCl. The final concentrations of HCl and NaCl are based on the stoichiometry of equation 11.

**46 nm seed mediated AuNPs prepared at 100 °C.** In brief, 0.818 mL seed suspension and 0.44 mL of 38.8 mM Na<sub>3</sub>Ctr were quickly added to a boiling solution of 100 mL of 0.254 mM HAuCl<sub>4</sub> under vigorous stirring. After a reaction period of 30 min, the AuNP suspension was cooled down at room temperature under stirring.

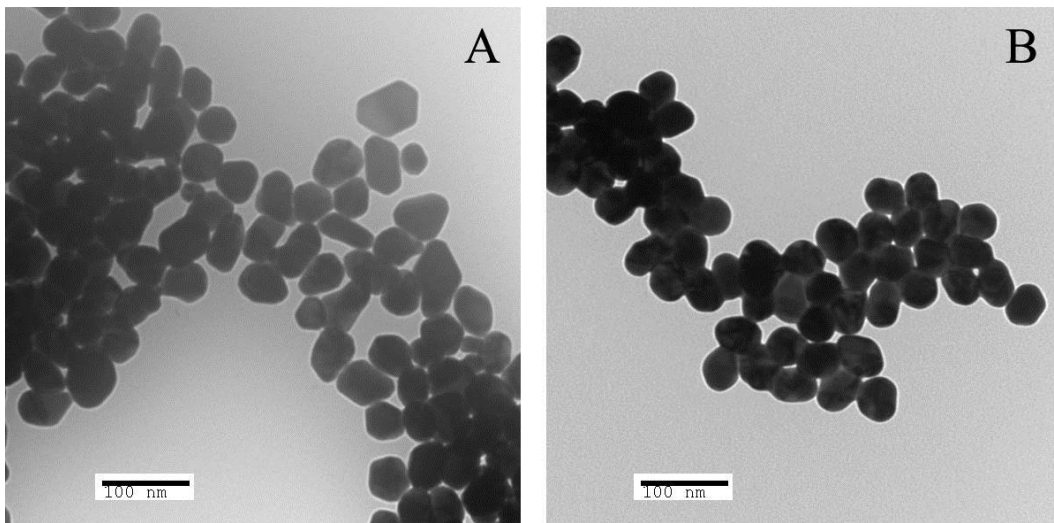


**Figure D 9** - TEM images of seed mediated 46 nm AuNPs produced at room temperature (A) and at 100 °C (B).

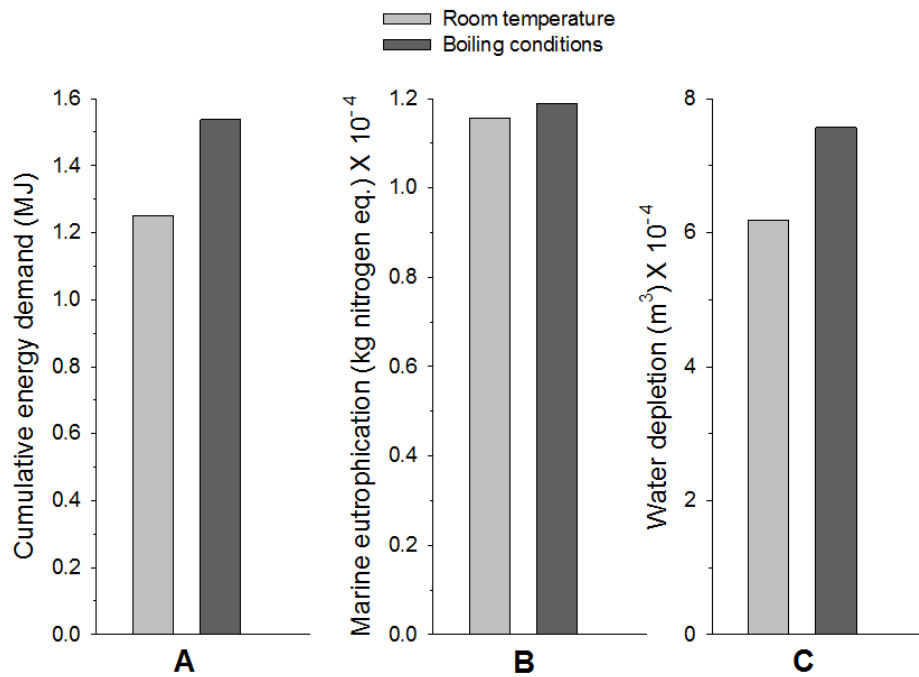


**Figure D 10**- Cumulative energy demand (CED), marine eutrophication and water depletion for 1 mg of 46 nm AuNP synthesis at 100 °C vs. room temperature. AuNP synthesis at room temperature has lower environmental impacts than synthesis under boiling conditions

## UNCERTAINTY ANALYSIS

LCA results typically involve *correlated* uncertainties. For example, some chemicals and processes from the life cycle inventories (such as gold, water, electricity etc.) are common to both synthesis methods - the room temperature AuNP synthesis and synthesis under boiling conditions. In such cases, the uncertainty for a chemical (say, gold) is common to both models, and therefore *correlated*<sup>5</sup>. In the case of correlated uncertainties, differences in results may be statistically significant, even if the error bars for 95% confidence interval overlap. Therefore, we have chosen to represent uncertainty in our LCA by comparing the actual Monte Carlo simulations instead of comparing 95% confidence intervals. As mentioned in the main manuscript, uncertainty analyses were performed using Monte-Carlo simulations for 1000 runs. As shown in Figure S7, most of those 1000 simulations showed that across all impact categories, AuNP synthesis at room temperature had lower impacts than previously reported methods that involved boiling conditions.

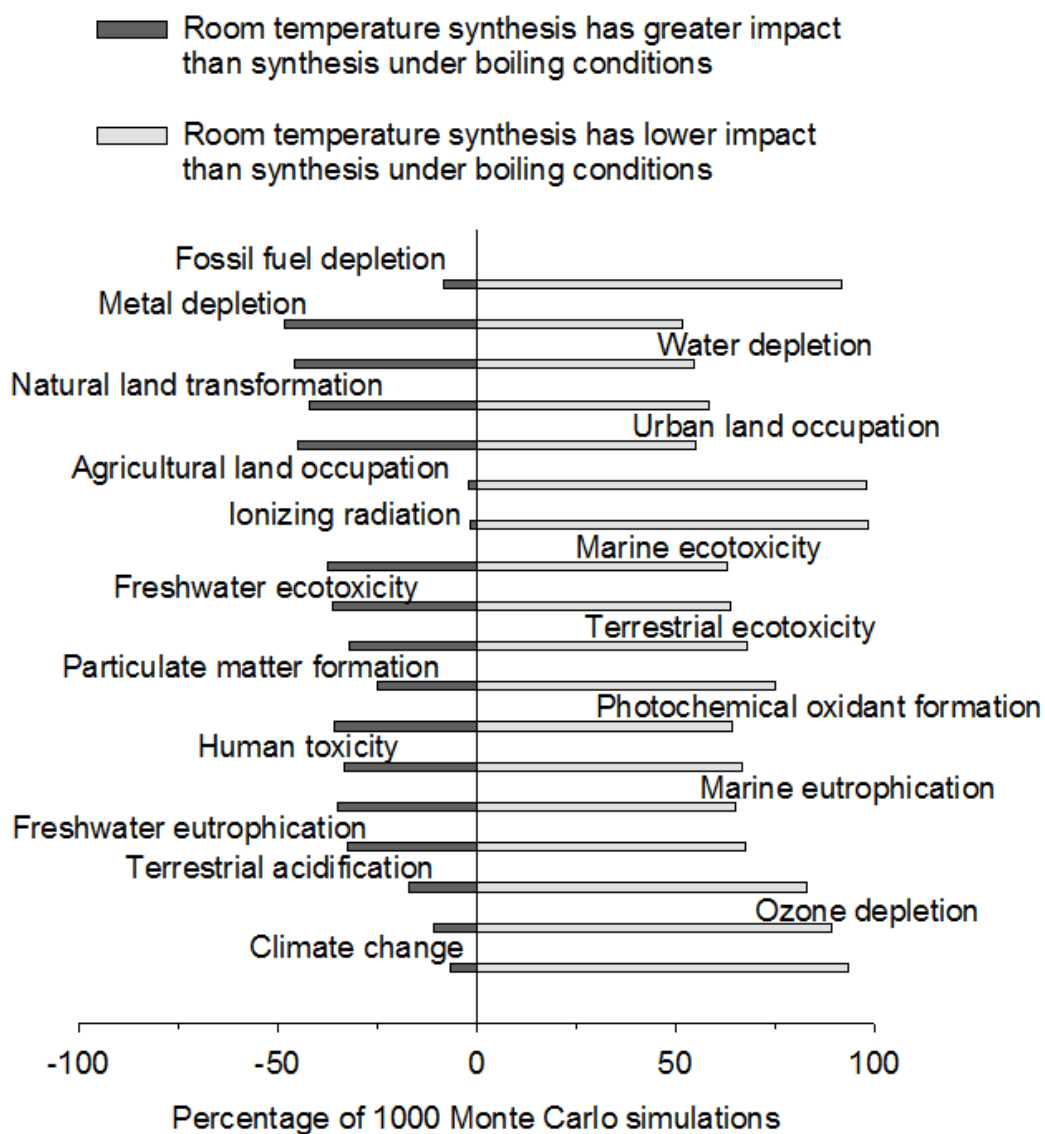


**Figure D 9** - The percentage of 1000 Monte Carlo simulations showing that across all impact categories, most simulations show that the environmental impacts for room temperature AuNP synthesis are lower than those for synthesis under boiling conditions.

## REFERENCES

1. Machesky, M. L.; Andrade, W. O.; Rose, A. W., Adsorption of gold(III)-chloride and gold(I)-thiosulfate anions by goethite. *Geochimica et Cosmochimica Acta* **1991**, *55*, (3), 769-76.
2. Xie, J.; Lee, J. Y.; Wang, D. I. C.; Ting, Y. P., Identification of active biomolecules in the high-yield synthesis of single-crystalline gold nanoplates in algal solutions. *Small* **2007**, *3*, (4), 672-682.
3. Brown, S.; Sarikaya, M.; Johnson, E., A Genetic Analysis of Crystal Growth. *J. Mol. Biol.* **2000**, *299*, (3), 725-735.
4. Shao, Y.; Jin, Y.; Dong, S., Synthesis of gold nanoplates by aspartate reduction of gold chloride. *Chemical Communications (Cambridge, United Kingdom)* **2004**, (9), 1104-1105.
5. Goedkoop, M.; Schryver, A. D.; Oele, M.; Roest, D. D.; Vieira, M.; Durksz, S., SimaPro 7 Tutorial. *PRé Consultants* **2010**.



# Appendix E

## Reprint Permission Letters

7/18/2015

Rightslink® by Copyright Clearance Center



# RightsLink®

Home

Create Account

Help



**Title:** Life Cycle Assessment of "Green" Nanoparticle Synthesis Methods

**Author:** Paramjeet Pati, Sean McGinnis, Peter J. Vikesland

**Publication:** Environmental Engineering Science

**Publisher:** Mary Ann Liebert, Inc.

**Date:** Jul 1, 2014

Copyright © 2014, Mary Ann Liebert, Inc.

**LOGIN**  
If you're a **copyright.com user**, you can login to RightsLink using your copyright.com credentials. Already a **RightsLink user** or want to [learn more?](#)

### Permissions Request

Mary Ann Liebert, Inc. publishers does not require authors of the content being used to obtain a license for their personal reuse of full article, charts/graphs/tables or text excerpt.

BACK

CLOSE WINDOW

Copyright © 2015 [Copyright Clearance Center, Inc.](#) All Rights Reserved. [Privacy statement.](#) [Terms and Conditions.](#) Comments? We would like to hear from you. E-mail us at [customercare@copyright.com](mailto:customercare@copyright.com)



**Title:** Recycling of Indium From CIGS Photovoltaic Cells: Potential of Combining Acid-Resistant Nanofiltration with Liquid-Liquid Extraction

**Author:** Yannick-Serge Zimmermann, Claudia Niewersch, Markus Lenz, et al

**Publication:** Environmental Science & Technology

**Publisher:** American Chemical Society

**Date:** Nov 1, 2014

Copyright © 2014, American Chemical Society

[LOGIN](#)

If you're a **copyright.com** user, you can login to RightsLink using your copyright.com credentials. Already a **RightsLink** user or want to [learn more?](#)

## PERMISSION/LICENSE IS GRANTED FOR YOUR ORDER AT NO CHARGE

This type of permission/license, instead of the standard Terms & Conditions, is sent to you because no fee is being charged for your order. Please note the following:

- Permission is granted for your request in both print and electronic formats, and translations.
- If figures and/or tables were requested, they may be adapted or used in part.
- Please print this page for your records and send a copy of it to your publisher/graduate school.
- Appropriate credit for the requested material should be given as follows: "Reprinted (adapted) with permission from (COMPLETE REFERENCE CITATION). Copyright (YEAR) American Chemical Society." Insert appropriate information in place of the capitalized words.
- One-time permission is granted only for the use specified in your request. No additional uses are granted (such as derivative works or other editions). For any other uses, please submit a new request.

If credit is given to another source for the material you requested, permission must be obtained from that source.

[BACK](#)[CLOSE WINDOW](#)



**Title:** Paper-based piezoresistive MEMS sensors  
**Author:** Xinyu Liu, Martin Mwangi, XiuJun Li, Michael O'Brien, George M. Whitesides  
**Publication:** Lab on a Chip  
**Publisher:** Royal Society of Chemistry  
**Date:** May 12, 2011  
Copyright © 2011, Royal Society of Chemistry

LOGIN

If you're a **copyright.com** user, you can login to RightsLink using your copyright.com credentials. Already a **RightsLink** user or want to [learn more?](#)

This reuse request is free of charge. Please review guidelines related to author permissions here: <http://www.rsc.org/AboutUs/Copyright/Permissionrequests.asp>

BACK

CLOSE WINDOW

Copyright © 2015 [Copyright Clearance Center, Inc.](#) All Rights Reserved. [Privacy statement](#). [Terms and Conditions](#). Comments? We would like to hear from you. E-mail us at [customercare@copyright.com](mailto:customercare@copyright.com)

**Title:** Paper-Based Device for Rapid  
Visualization of NADH Based on  
Dissolution of Gold Nanoparticles

**Author:** Pingping Liang, Haixiang Yu,  
Bhargav Guntupalli, et al

**Publication:** Applied Materials

**Publisher:** American Chemical Society

**Date:** Jul 1, 2015

Copyright © 2015, American Chemical Society

LOGIN

If you're a **copyright.com**  
user, you can login to  
RightsLink using your  
copyright.com credentials.  
Already a **RightsLink** user or  
want to [learn more?](#)

#### PERMISSION/LICENSE IS GRANTED FOR YOUR ORDER AT NO CHARGE

This type of permission/license, instead of the standard Terms & Conditions, is sent to you because no fee is being charged for your order. Please note the following:

- Permission is granted for your request in both print and electronic formats, and translations.
- If figures and/or tables were requested, they may be adapted or used in part.
- Please print this page for your records and send a copy of it to your publisher/graduate school.
- Appropriate credit for the requested material should be given as follows: "Reprinted (adapted) with permission from (COMPLETE REFERENCE CITATION). Copyright (YEAR) American Chemical Society." Insert appropriate information in place of the capitalized words.
- One-time permission is granted only for the use specified in your request. No additional uses are granted (such as derivative works or other editions). For any other uses, please submit a new request.

If credit is given to another source for the material you requested, permission must be obtained from that source.

BACK

CLOSE WINDOW



**Title:** What Gets Recycled: An Information Theory Based Model for Product Recycling  
**Author:** Jeffrey B. Dahmus, Timothy G. Gutowski  
**Publication:** Environmental Science & Technology  
**Publisher:** American Chemical Society  
**Date:** Nov 1, 2007

Copyright © 2007, American Chemical Society

LOGIN

If you're a [copyright.com](#) user, you can login to RightsLink using your [copyright.com](#) credentials. Already a [RightsLink](#) user or want to [learn more?](#)

## PERMISSION/LICENSE IS GRANTED FOR YOUR ORDER AT NO CHARGE

This type of permission/license, instead of the standard Terms & Conditions, is sent to you because no fee is being charged for your order. Please note the following:

- Permission is granted for your request in both print and electronic formats, and translations.
- If figures and/or tables were requested, they may be adapted or used in part.
- Please print this page for your records and send a copy of it to your publisher/graduate school.
- Appropriate credit for the requested material should be given as follows: "Reprinted (adapted) with permission from (COMPLETE REFERENCE CITATION). Copyright (YEAR) American Chemical Society." Insert appropriate information in place of the capitalized words.
- One-time permission is granted only for the use specified in your request. No additional uses are granted (such as derivative works or other editions). For any other uses, please submit a new request.

If credit is given to another source for the material you requested, permission must be obtained from that source.

[BACK](#)

[CLOSE WINDOW](#)